

Design and Synthesis of Polysilazanes

Mag. rer. nat. Amra Suljanović

2011

Institute of Inorganic Chemistry
TU Graz



*Ništa nije samo po sebi
dobro, ni loše,
ovisi samo
što o tome mislimo*

(W. Shakespeare)

Dedicated to my great parents and friends

Dank

Besonderer Dank gilt zuallererst den Betreuern meiner Dissertation, Professorin Michaela Flock und Dr. Roland Fischer für die Möglichkeit, das interessante Thema zu bearbeiten. Ich möchte ihnen danken für die anregenden Diskussionen und für den Freiraum, der es mir ermöglichte sowohl fachlich sowie persönlich mich weiterzuentwickeln.

Weiters danke ich dem Kristallographen Jörg Albering für das Messen und Lösen der kniffligen Kristallstrukturen.

Dank an den Vorstand des Institutes für Anorganische Chemie, Professor Frank Uhlig für die Bereitstellung von Ressourcen sowie für die Finanzierung des Projektes, der Frechen-Materie.

Ich möchte auch Dr. Rolan Feola danken, für das tolle Firmenpraktikum in seiner Forschungsgruppe.

Ich möchte speziell meinen Freunden und meiner Familie DANKE sagen, für die aufmunternden und motivierenden Worte, für die Geduld und die zahlreiche Unterstützung.

Kurzfassung

Diese Arbeit befasst sich mit der Synthese und Charakterisierung von Polymervorstufen. Die strukturellen Eigenschaften von Hexaphenylcyclotrisilazan und Tetrylen-Derivaten wurde experimentell sowie mit quantenchemischen Methoden untersucht.

Es zeigte sich, dass die Hexaphenylcyclotrisilazan Derivate vorwiegend in einer Boot Konformation vorliegen. Mit Hilfe von Dichtefunktional (DFT) Methoden durchgeführte Geometrieoptimierungen und Konformationsanalysen zeigten, dass die Boot-Konformation meistens tatsächlich die thermodynamisch stabilste Form ergibt.

Weiters zeigte sich auch, dass die Boot-Struktur des Si₃N₃-Rings sowohl von den Silizium als auch von den Stickstoff Substituenten beeinflusst wird. Dieser Umstand konnte experimentell und rechnerisch nachgewiesen werden. Hierzu wurden Kristallstrukturdaten mit Geometrie optimierten Strukturen verglichen.

Das Hexaphenylcyclotrisilazan Grundgerüst wurde ausschließlich am Stickstoff Atom funktionalisiert. Im Zuge dieses Syntheseprozesses ist es auch zur Darstellung von N-Heterozyklisch stabilisierten Ge, Sn, Pb Tetrylen-Derivaten gekommen. Verbindungen mit Metall-Zentralatomen der 14. Gruppe wurden mit organischen Bidentaten sowie monodentaten Liganden umgesetzt und die erhaltenen Produkte untersucht.

Nebst der Struktur wurden auch NMR-Verschiebungen und UV-Vis Spektren analysiert und simuliert. Somit wurde die Charakterisierung der synthetisierten Substanzen erheblich erleichtert. Die quantenchemisch generierten Daten sind konsistent mit den experimentell gemessenen Werten.

Abstract

Via quantum chemical and experimental methods hexaphenylcyclotrisilazanes and tetrylenes were analyzed. The astonishing result is that, the Si₃N₃-rings mostly appear in a boat conformation. The geometry optimizations were carried out using density functional theory (DFT). They confirmed that mostly the boat conformation represents the thermodynamically most stable conformation.

Further the conformational analysis showed, that the ring conformation is affected by both the substituents on the silicon and on the nitrogen atoms. The theoretical data were compared with solid state structures and spectroscopic data.

The hexaphenylcyclotrisilazane backbone was exclusively derivatized at the nitrogen atom. During this synthetical procedure we also generated N-heterocyclic Ge, Sn, and Pb tetrylene derivatives. These organo-metal substances were fully characterized and theoretically discussed.

Besides, the structural analysis also NMR and UV-Vis spectra were predicted. Consequently, full characterization of the synthesized compounds was made easier. Quantum chemical data and experimentally measured data are consistent. Via quantum chemical calculations it was possible to make predictions and to give explanations for some unusual compounds.

Contents

1	Introduction	1
2	Silazanes	3
2.1	Introduction	3
2.2	Substitution Pattern Analysis on the Silicon	5
2.3	Substitution Pattern Analysis on the Nitrogen	15
2.4	Derivatization Reactions with Hexaphenylcyclotrisilazane	19
2.4.1	N-H / N-D Hexaphenylcyclotrisilazane	31
2.4.2	N-Me Hexaphenylcyclotrisilazane	34
2.4.3	N-SiMe ₂ H Hexaphenylcyclotrisilazane	37
2.4.4	N-AlMe ₂ Hexaphenylcyclotrisilazane	41
2.4.5	N-PbCl Hexaphenylcyclotrisilazane	45
2.4.6	N-SnCl-Hexaphenylcyclotrisilazane	49
2.5	Dip-Coating and Solid-phase Pyrolysis	52
3	Tetrylenes	57
3.1	Introduction	57
3.2	Ge/Sn/Pb Divalent Derivatives	62
3.2.1	The Aminopyridin Ligand System	62
3.2.2	Chloro-Tetrylenes	66
3.2.3	Bis(TMS)amido-Tetrylenes	72
3.2.4	Reaction Conditions and Products	81
3.2.5	Di-amido Tetrylenes	87
4	Complexes with bidentate Ligand Systems	97
4.1	Introduction	97
4.2	Synthesis and Products	98
4.3	An aromatic Stannylene with special Geometry Features	108
4.3.1	Comparison of possible Products	115
4.3.2	BADER Analysis	117
5	Experimental	121
5.1	General Procedure	121
5.2	Synthesis	121
5.2.1	Hexaphenylcyclotrisilazane	121

5.2.2	1,3,5-deuterium-2,2,4,4,6,6-exaphenylcyclotrisilazane	122
5.2.3	1,3,5-trimethyl-2,2,4,4,6,6-hexaphenylcyclotrisilazane	123
5.2.4	1,3,-dimethyl-2,2,4,4,6,6-hexaphenylcyclotrisilazane	123
5.2.5	1-methyl-2,2,4,4,6,6-hexaphenylcyclotrisilazane	124
5.2.6	1-lithio-2,2,4,4,6,6-hexaphenylcyclotrisilazane	125
5.2.7	1,3,-dilithio-2,2,4,4,6,6-hexaphenylcyclotrisilazane	125
5.2.8	1,3,5-trilithio-2,2,4,4,6,6-hexaphenylcyclotrisilazane	126
5.2.9	1,3,5-tris(dimethylsilyl)-2,2,4,4,6,6-hexaphenylcyclotrisilazane . . .	127
5.2.10	1-potassium-2,2,4,4,6,6-hexaphenylcyclotrisilazane	127
5.2.11	1,3-di(potassium)-2,2,4,4,6,6-hexaphenylcyclotrisilazane	128
5.2.12	1,3,5-tris(Dimethylaluminum)-2,2,4,4,6,6-hexaphenylcyclotrisilazane	129
5.2.13	1,3,5-tris(SnCl)-2,2,4,4,6,6-hexaphenylcyclotrisilazane	129
5.2.14	1,3,5-tris(PbCl)-2,2,4,4,6,6-hexaphenylcyclotrisilazane	130
5.2.15	Tin(II)bis[bis(trimethylsilyl)amide]	131
5.2.16	Lead(II)bis[bis(trimethylsilyl)amide]	131
5.2.17	Germanium(II)bis[bis(trimethylsilyl)amide]	132
5.2.18	Lithium(I) N-(diisopropyl benzyl)(2-pyridylmethyl)amide	132
5.2.19	Chloro-tin(II) N-(diisopropyl)(2-pyridylmethyl)amide	133
5.2.20	Chloro-lead(II) N-(diisopropyl)(2-pyridylmethyl)amide	133
5.2.21	Chloro-Ge(II) N-(diisopropyl)(2-pyridylmethyl)amide	134
5.2.22	Bis(TMS)amidotin(II) N-(diisopropyl)(2-pyridylmethyl)amide . . .	135
5.2.23	Bis(TMS)amidolead(II) N-(diisopropyl)(2-pyridylmethyl)amide . . .	135
5.2.24	Bis(TMS)amidoGe(II) N-(diisopropyl)(2-pyridylmethyl)amide . . .	136
5.2.25	Ge(II)bis[N-(2,6-diisopropylphenyl)(2-pyridylmethyl)imide]	137
5.2.26	Sn(II)bis[N-(2,6-diisopropylphenyl)(2-pyridylmethyl)amide]	137
5.2.27	Pb(II)bis[N-(2,6-diisopropylphenyl)(2-pyridylmethyl)amide]	138
5.2.28	Ge(II)bis[N-(2,6-diisopropylphenyl)(2-pyridylmethyl)amide]	139
5.2.29	Dimethylpyridine-2,6-dicarboxylate	139
5.2.30	Pyridine-2,6-diylldimethanol	140
5.2.31	Pyridine-2,6-diylbis(methylene) bis(4-methylbenzenesulfonate) . .	141
5.2.32	N,N'-(pyridine-2,6-diylbis(methylene))bis(2,6-diisopropylaniline) .	141
5.2.33	Bisdiimino-Sn; Sn-N,N-(pyridine-diylbis(ethene))bis(2,6- diisopropylaniline)	142
5.2.34	N,N-tin(II)(NTMS)-N,N'-(pyridine-2,6-diylbis(methylene))bis(2,6- diisopropylaniline)	143
5.2.35	Ethene-bistirmethylsilyl-diamine-tin(II)	144
5.2.36	Tin(II) 2,6-Bis[1-(phenylimino)ethyl]pyridineTMS	144
5.2.37	2,6-diisopropyl-N-(pyridin-2-ylmethyl)aniline	145
5.2.38	(2,6-diisopropyl- benzyl)-pyridin-2-yl-amine	146
5.2.39	(N,N'E,N,N'E)-N,N'-(pyridine-2,6-diylbis(ethan-1-yl-1-ylidene))bis(2,6- diisopropylaniline)	146

6	Materials and Methods	147
6.1	NMR, XRD-measurements and Elemental Analysis	147

6.2	Quantum chemical methods	147
6.2.1	Geometry optimization and Frequencies	147
6.2.2	Nuclear Magnetic Resonance and NICS	148
6.2.3	Natural Bond Orbitals, UV-Spectra and BADER-Analysis	148
7	Appendix	150
7.1	Crystallographic Data	150
7.2	Geometry optimized Structures	155
	Bibliography	181

1 Introduction

This present work will report about synthesis, derivatization and characterization of polymer precursors. Particularly with regard to polymers derived from the 14th-group elements. Inorganic materials, especially inorganic polymers bear interesting abilities such as extreme thermal stability or photosensitive features.

For any type of polymer, monomer units and elemental composition are important.

Polymer and Material types:

- **C:** Polycarbosilanes and
- **Si:** Polysiloxanes, Silicones, Polycarbosiloxanes, Polysilazanes
- **Ge, Sn, Pb:** Metal functionalized polymers

Figure 1.1 shows some typical very common polymer types.

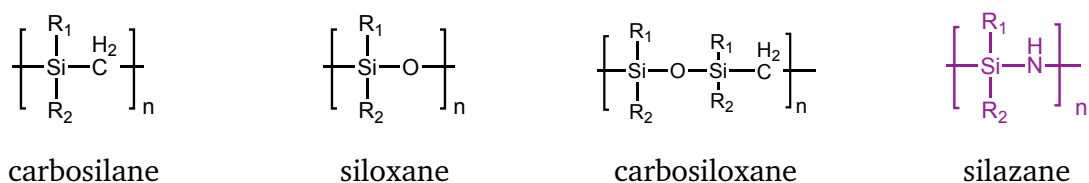
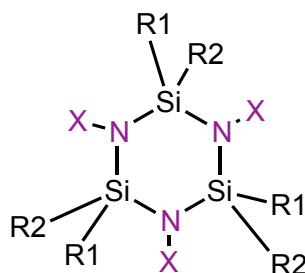


Figure 1.1: Common polymer types

Polycarbosilanes and silicones are already very common in our daily use as well as polysilazanes. Silazanes and polysilazanes have good abilities as high temperature ceramics. They are used for fire resistant materials or as dielectric coatings. The monomeric unit itself determines the polymer attributes at the end. The properties of the precursor molecules usually intensify in the corresponding polymer. Typical molecular precursors in ceramic and polymer chemistry are silazanes [1].

Therefore we modify cyclic silazanes, to generate functionalized monomeric units- see Figure 1.2. We especially focused our work on phenyl substituted derivatives (R1=R2=phenyl). Literature also reports about other modified types of cyclic silazanes [2].

The synthesized compounds will be experimentally analyzed and via DFT calculations we will confirm their parameters and attributes. Conformational studies and simulations of NMR and UV-Vis spectra will give more information about the new substances and facilitate the interpretation of the measured data.



R1,R2 = hydrogen, aliphatic, aromatic organic side groups
 X = Me, SiMe₂H, AlMe₂, SnCl, PbCl, Li, K,...

Figure 1.2: Simplified representation of a modified cyclic silazane

To build up such cyclic silazane systems it is proposed that silylenes are reactive intermediate species, which can occur during the synthesis [3]. Silylenes belong to the substance class called tetrylenes. These compounds are heavy carbene analogues with group 14 elements as metal centers [4].

Therefore it is also possible to use also tetrylenes as polymer precursor molecules. Smart ligand systems will be combined with Ge, Sn, and Pb as central atoms. The aim is to synthesize and to characterize these tetrylenes - maybe they can find use as potential precursors.

We will focus the work on nitrogen containing monodentate and bidentate ligand systems - see Figure 1.3. These ligands have the possibility to stabilize reactive divalent group 14 elements via their donor/acceptor interaction on the nitrogen atoms [4].

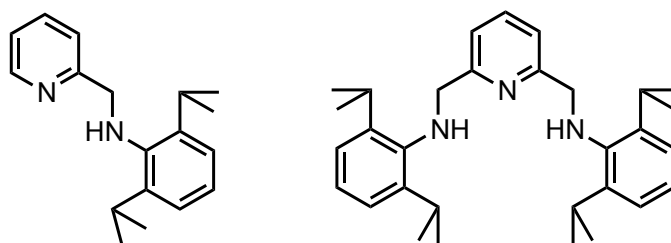


Figure 1.3: Aminopyridine ligands

The ligand system determines the reactivity and maybe the polymer characteristics at the end.

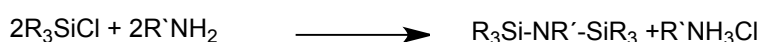
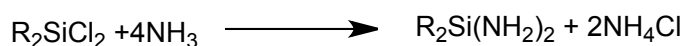
We hope to find new potential precursors for new useful materials.

2 Silazanes

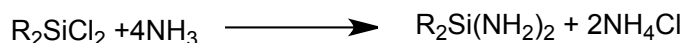
2.1 Introduction

Silazanes are known for a long time. Their use as high temperature ceramic precursors is a well investigated and discussed topic. The first preparation, classification, and characterization of silazanes and polysilazanes was reported already in 1885 [1]. Silazanes find application as silylating agents or as single source precursors for the preparation of ceramic materials by vapor-, liquid-, and solid-phase pyrolysis [5].

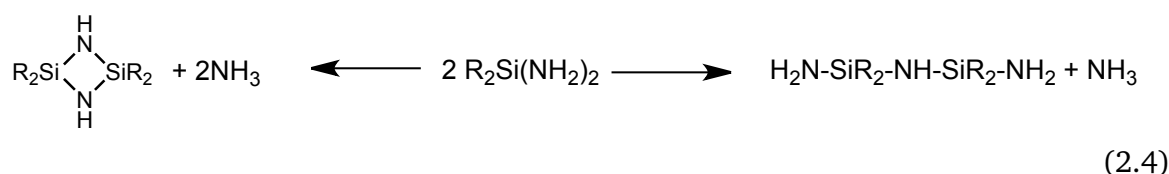
In general silazanes can be formed by ammonolysis of halogenosilanes [5] or by aminolysis with various primary amines. Equations 2.1 and 2.2 give the simplified general description of this synthesis. Variation of the starting materials leads to different products.



To generate alternating Si-N chains or rings the ammonolysis of dichlorosilanes R_2SiCl_2 is common. Reaction conditions determine the product distribution as well as the size of the used dichlorosilanes. Low temperatures and large substituents on the silicon lead to diaminosilazanes - see Equation 2.3 [6],[7] [8]



Upon heating, the diaminosilazanes condensate and form oligomeric silazanes. Possible products are linear disilazanes and cyclodisilazanes. Because of the ring strain of four-membered cyclodisilazanes a subsequent reaction follows and chains or cyclic tri- or tetramers are formed - see Equation 2.4



It has been reported by Klingebiel and Kliebisch [9] that cyclotrisilazanes can react further with two equivalents of dichlorosilane to form again cyclodisilazanes by ring contraction - see Figure 2.1.

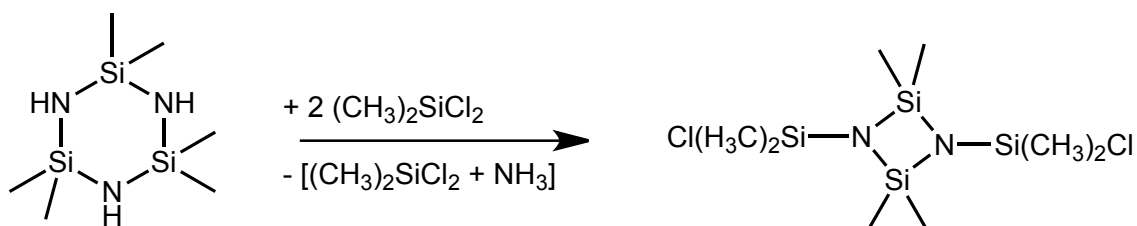


Figure 2.1: Ring contraction reaction of hexamethylcyclotrisilazane

The molecular structure and the type of the precursor molecules determine the microstructure of the final ceramic. Changing the functional groups (R1 and R2 on the silicon atom) influences the material content at the end as well as the functional groups on the nitrogen atoms (R3)- see Figure 2.2.



R1,R2 = hydrogen, aliphatic, aromatic organic side groups
 R3= hydrogen, metal, inorganic groups

Figure 2.2: General simplified representation of the molecular structure of cyclic precursor molecules

Via thermal treatment of the precursor molecules at elevated temperatures (300°C-1000°C), amorphous $\text{Si}_x\text{C}_y\text{N}_z$ ceramics can be obtained. The precursor-to-ceramic conversion leads to the decomposition or elimination of organic moieties (such as methyl, phenyl, vinyl groups) and Si-H, Si-OH, or Si-NH_a groups.

2.2 Substitution Pattern Analysis on the Silicon

Molecule geometry and chemical composition determine many attributes such as stability, reactivity and spectroscopic properties. Therefore it is important to analyze the influence of various substituents on the conformation of a molecule.

Via quantum chemical DFT (density functional theory) the influence of the substituents on the conformation of cyclic silazanes will be discussed. Six membered ring systems usually can appear in chair, boat or twist conformations -see Figure 2.3.

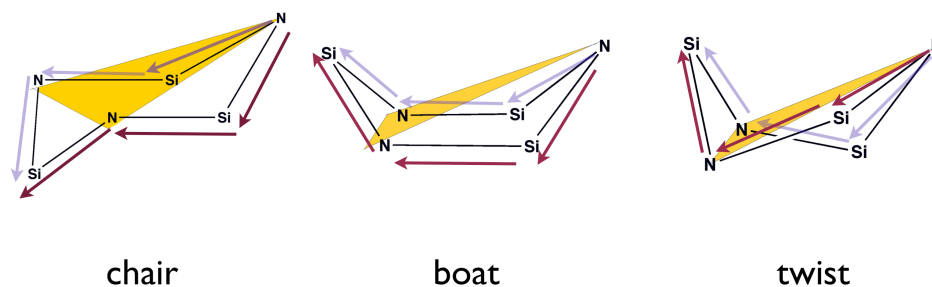
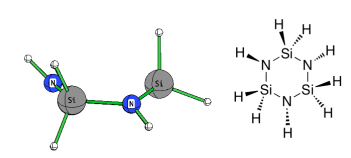
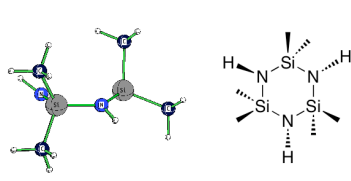
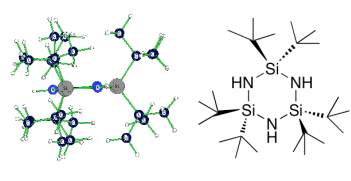
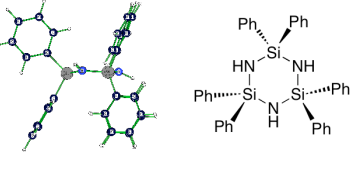


Figure 2.3: Chair, boat, and twist conformation of a six membered ring and definition of both N-Si-N-Si/Si-N-Si-N dihedral angles.

Which kind of conformation is favored depends on the substituents on the nitrogen and silicon atoms. Substituents can be sterically demanding as tertiary butyl groups or small as hydrogens or methyl groups. They can have an electronic effect on the ring system such as phenyl groups or metal substituents. For conformation analysis the four dihedral angles (2N-Si-N-Si and 2Si-N-Si-N) are a criterion. If all of them have the same value but two different signs than the ring conformation is a chair. If, respectively, two angles have the same values and opposite signs, than the conformation is a boat. The twist conformation is identified by different angles and different signs, with no further attributes[10].

Table 2.1 shows six membered Si-N rings with different substituents on the silicon atoms.

Table 2.1: Influence of the Si-substituents on the ring conformation calculated with mPW1PW91/6-31+G*.

structure	N-Si-N-Si angle Si-N-Si-N angle	Si-N [pm]	²⁹ Si shift [ppm]
	-8.57°	174.4	-37.68
	47.68°	173.4	-42.83
	-47.18°	174.3	
	8.73°		
	8.93°	175.0	-8.32
	-36.47°	173.9	-8.52
	36.47°	174.8	
	-8.64°		
	4.41°	175.0	-5.96
	-4.24°	175.3	-6.03
	4.56°	175.6	-6.21
	-4.44°		
	-14.76°	173.8	-23.93
	19.47°	173.7	-23.90
	-17.61°	174.3	-23.82
	11.67°		

The molecules were optimized using mPW1PW91 as functional with 6-31+G* basis sets. The chemical shifts were also calculated with mPW1PW91 and IGLO-II basis sets for all atoms.

Conformational analysis shows that small substituents such as methyl or hydride on the silicon atom have the same effect on the structure - they induce a boat conformation. The dihedral angles (N-Si-N-Si and Si-N-Si-N) of the methyl and hydrogen substituted Si₃N₃-rings are at similar value: 8.73°/ 47.68°/ -47.18°/ -8.57° for the per hydrated Si₃N₃-ring and 8.93°/ -36.47°/ 36.47°/ -8.64° for the methyl substituted Si₃N₃-ring - see Table 2.1. In contrast the dihedral angles for the tertiary butyl and phenyl substituted Si₃N₃-rings are: 4.41°/ -4.24°/ 4.56°/ -4.44° for the tertiary butyl substituted Si₃N₃-ring, which is a flattened boat-conformation and -14.76°/ 19.47°/ -17.61°/ 11.67° for the phenyl substituted ring. The phenyl substituted Si₃N₃-ring is in a slightly twisted boat-conformation. In Table 2.1 a trend is observable, the bulkier the substituents on the silicon atom are the more the structure of the Si₃N₃-ring is planarized. The Si-N bond distances in the ring are

not remarkably affected by the different substituents. The values for the Si-N distances are between 173.7 pm and 175.6 pm.

With the different substitution patterns at the silicon atoms also the ^{29}Si chemical shift changes. Tertiary butyl and methyl substituents give similar values for the ^{29}Si chemical shift, -8.32 ppm and -6.03 ppm. For the per-hydrogenated parent molecule a ^{29}Si chemical shift of -43.83 ppm was calculated. Further there is also a difference between the phenyl and tertiary butyl substituted structures. Both substituents are bulky but the phenyl group induces an electronic effect on the Si-N ring, and that is also mirrored in the ^{29}Si chemical shifts.

Several attempts to find other thermodynamically stable conformations for the methyl and hydrogen substituted Si-N rings failed, except for the hexamethylcyclotrisilazane.

In 1974 Mastryukov et.al. made electron diffraction studies on the molecular structure of $[(\text{CH}_3)_2\text{SiNH}]_3$ to determine the real Si₃N₃-ring conformation. They assumed that the Si₃N₃-ring is puckered but the deviation from planarity is relatively small [11]. We succeeded to get a solid state structure of $[(\text{CH}_3)_2\text{SiNH}]_3$ via a laser assisted crystallography method (COD). Figure 2.4 shows the structure of $[(\text{CH}_3)_2\text{SiNH}]_3$, with the Si₃N₃-ring in a twist conformation. According to the geometry optimization the $[(\text{CH}_3)_2\text{SiNH}]_3$ -boat conformation is a global minimum, while the twisted structure corresponds to a second thermodynamically stable conformer, (the energy difference ΔE is 5,05 kJ/mol) in the gas phase.

Furthermore, higher amounts of the slightly less stable structure may have been present due to the crystallographic method. (Fast cooling/freezing of the probe induces that the Si₃N₃ ring not able to get into the thermodynamically stable global minimum.)

In the solid state packaging forces can stabilize such geometries. In Table 2.2 calculated and experimental data are compared.

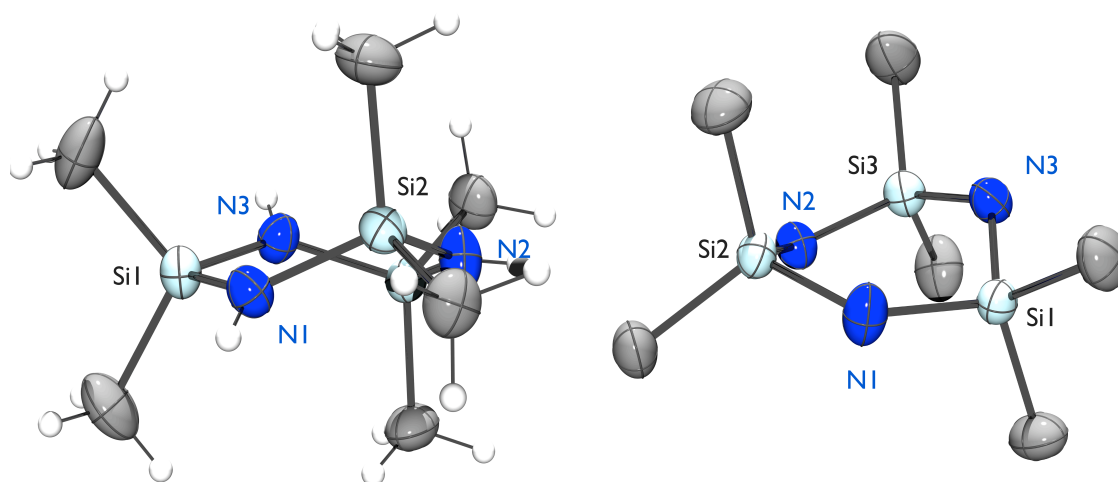


Figure 2.4: Solid state structure of hexamethylcyclotrisilazane in twist conformation.

The Si-N bond distances are as anticipated in the range of 172.0 pm - 172.7 pm for the geometry optimized molecule (boat conformation) and 173.9 pm - 175.0 pm in the solid

state structure. Only the N-Si-N-Si/Si-N-Si-N dihedral angles are different. For the predicted boat conformation values of $8.93^\circ / -8.64^\circ / -36.47^\circ / 36.47^\circ$ were measured and in the solid state structure the dihedral angles of $-47.29^\circ / -47.91^\circ / 13.69^\circ / 25.29^\circ$ are found. The fact that the two dihedral angles in the solid state structure are not the same indicates that the conformation is a twisted boat.

Table 2.2: Comparison of calculated (mPW1PW91/6-31+G*) and measured data of hexamethylcyclotrisilazane.

data	experimental	calculated boat	calculated twist
ΔE [kJ/mol]	-	0.00	5.05
Si-N [pm]	172.0	173.9	171.6
	172.3	174.8	172.6
	172.7	175.0	172.0
N-Si-N-Si angle	-47.29°	-36.47°	-47.27°
Si-N-Si-N angle	13.69°	8.93°	13.66°
N-Si-N-Si angle	25.29°	-8.64°	25.32°
Si-N-Si-N angle	-47.91°	36.47°	-47.92°
^{29}Si shift [ppm]	-5.64 [12]	-8.52	-

The influence of a sterically demanding Si-substituent can be best demonstrated by exchanging the methyl groups by tertiary butyl groups.

In 1984 Sheldrick et.al. analyzed the solid state structure of $[(\text{C}_4\text{H}_9)_2\text{SiNH}]_3$ hexatert-butylcyclotrisilazane. They reported about the strictly planar ring conformation and the reduced reactivity of $[(\text{C}_4\text{H}_9)_2\text{SiNH}]_3$. They substantiate these facts with the steric bulk of the tertiary butyl groups on the silicon atoms [13]. Usually, Si3N3-rings with smaller alkyl substituents readily undergo condensation reactions to give chain and ring silazanes [7]. Figure 2.6 displays the solid state structure of Sheldrick and our geometry optimized structure.

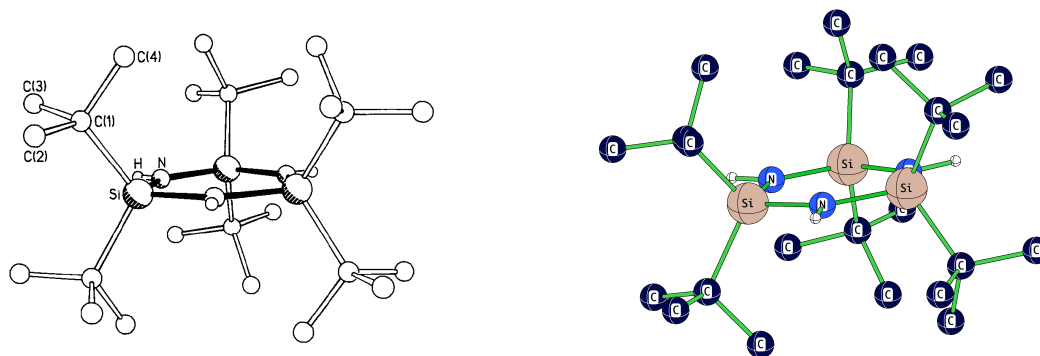


Figure 2.6: Solid state (planar conformation) and optimized (mPW1PW91/6-31+G*) structure (flattened boat conformation) of hexatertbutylcyclotrisilazane; hydrogens are omitted for clarity.

According to the solid state structure [13] the Si-N distances are 172.7 pm and the N-Si-N-Si / Si-N-Si-N dihedral angles are all indeed 0.00°. These values can be compared with the calculated figures (in Table 2.3), where Si-N distances of 175.0 pm to 175.6 pm are found and N-Si-N-Si/Si-N-Si-N dihedral angles of -4.44° / 4.41° / -4.24° / 4.56°. These calculated parameters indicate that the local minimum of hexatertbutylcyclotrisilazane is a flattened boat conformation. Via more detailed quantum chemical geometry analysis we found out that the completely planar Si₃N₃-ring conformation, as it was found in the crystal is definitely a transition state geometry, in the gas phase. The energy difference between the planar conformation and the flattened boat-conformation is only 0.16 kJ/mol. The measured ²⁹Si shift is at -1.59 ppm, and slightly deviates from the calculated value of -6.03 ppm.

Table 2.3: Comparison of calculated (mPW1PW91/ 6-31+G*) geometry and ²⁹Si chemical shift and experimental data of hexatertbutylcyclotrisilazane

data	experimental [13]	calculated
spacegroup	R-3c	-
Si-N [pm]	172.7	175.6
	172.7	175.3
	172.7	175.0
N-Si-N-Si angle	0.00°	4.41°
Si-N-Si-N angle	0.00°	-4.24°
N-Si-N-Si angle	0.00°	4.56°
Si-N-Si-N angle	0.00°	-4.44°
²⁹ Si shift [ppm]	-1.59	-6.03

The examples of methyl and tertiary butyl substituted Si₃N₃-rings show the trend that

bulky and sterically demanding groups induce a planarization of the ring.

Kroke and Wagler et.al. also observed that hexaphenylcyclotrisilazane (hpcts) appears in a planar conformation in the solid state[14] - see Figure 2.7. Remarkable is that the ellipsoids at the nitrogen atoms are distorted and at the other atoms, they are not well formed.

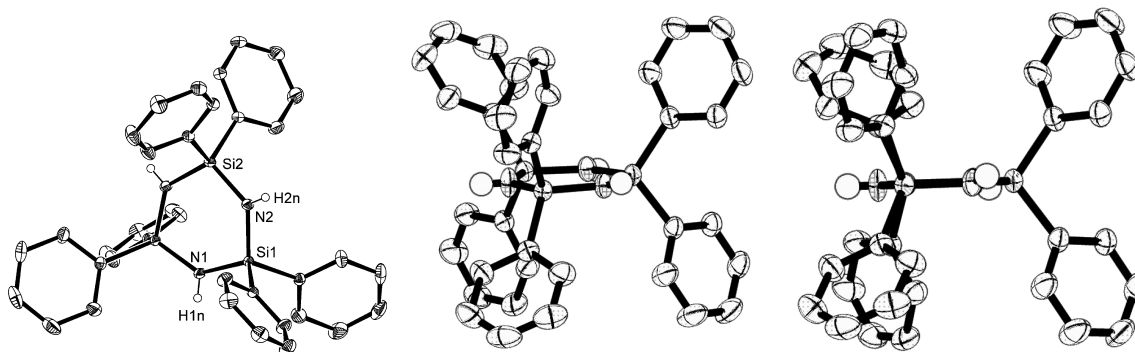


Figure 2.7: Molecular structure of hexaphenylcyclotrisilazane in the crystal [14], hydrogen atoms at the phenyl groups were omitted for clarity.

That is not further astonishing, because phenyl groups are bulky substituents and the effect can be compared with the tertiary butyl substituted silazane. However, our geometry optimization predicts a slight boat conformation as a global minimum for hpcts. There too the planar conformation is a transition structure in the gas phase. In Table 2.4 both geometry optimized structures are compared.

Table 2.4: Comparison of the mPW1PW91/6-31+G* optimized boat and planar conformation of hexaphenylcyclotrisilazane.

conformation	twisted boat	planar (TS)
ΔE [kJ/mol]	0	0.34
Si-N [pm]	173.8	170.8
Si-N [pm]	173.7	171.8
Si-N [pm]	174.3	171.9
N-Si-N-Si angle	-14.76°	0.00°
Si-N-Si-N angle	19.47°	0.00°
N-Si-N-Si angle	-17.61°	0.00°
Si-N-Si-N angle	11.67°	0.00°

According to the theoretical analysis the planar conformation is a transition structure and the twisted boat conformation represents the local minimum. The energy difference between these two conformations is only 0.34 kJ/mol. The two geometry optimized struc-

tures differ in dihedral N-Si-N-Si/Si-N-Si-N angles and also in the Si-N distances. The planar ring contains Si-N bond distances that are in average 2 to 3 pm shorter than those in the boat conformation- see Table 2.4.

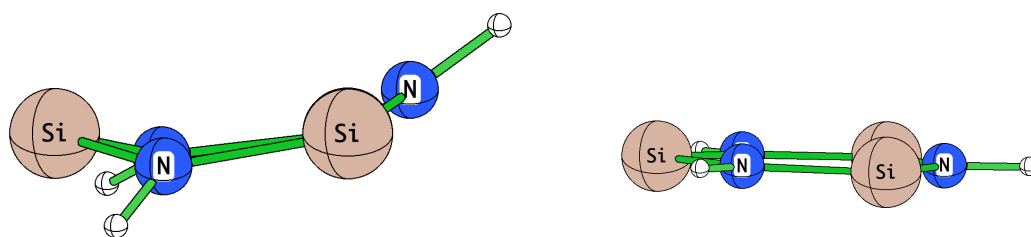


Figure 2.8: Geometry optimized structures (mPW1PW91/6-31+G*) of hpcts in slight twist and planar conformation; phenyl groups on the silicon atoms were omitted for clarity.

But how is it possible to find the planar ring in the crystal structure as Kroke and Wagler et.al. did [14]? Due to the low energy difference of only 0.34 kJ/mol between the transition structure and the local minimum, packaging forces in the solid state are enough to stabilize the planar geometry.

We made several attempts to crystallize hpcts under different conditions and with different solvents. Crystal-growth is dependent on temperature, solvent and time. Our result is that indeed there can be different conformations of the same compound in the solid state. The hpcts crystal cell geometry is special. Cell-constants and parameters have to be considered. Weak reflections during the measurement appear and can be explained by the fact that in one cell-unit there are actually two molecules - see Figure 2.9. Thereby, it is possible to find both, the slight boat and the planar conformation in the solid state.

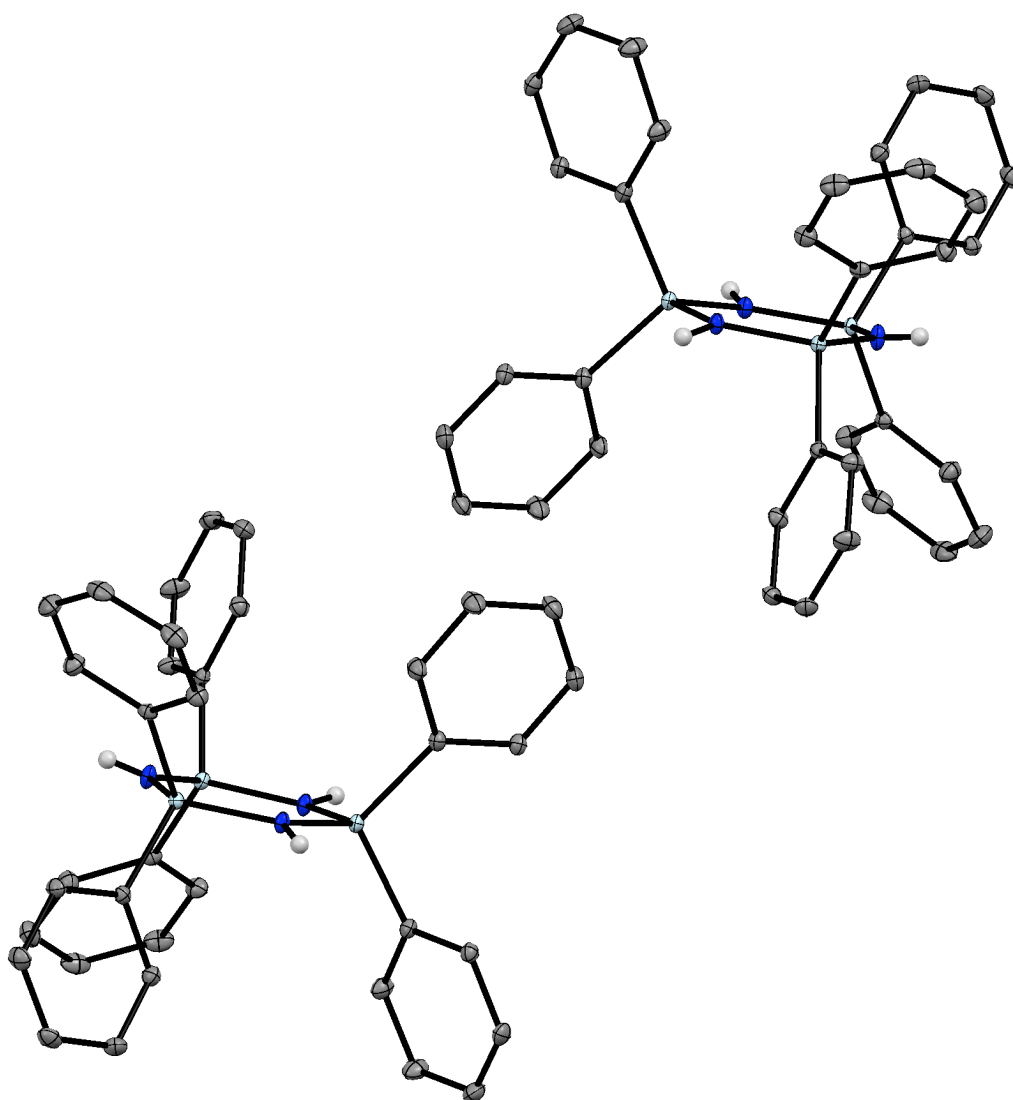
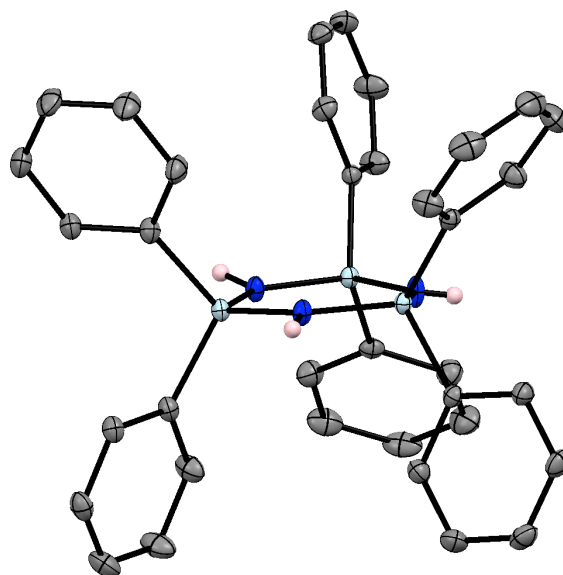


Figure 2.9: Solid state structure of hpcts, showing the slight boat conformation; hydrogen atoms at the phenyl groups were omitted for clarity.

Otherwise, if the cell-constants and dimensions are misinterpreted or if the crystal is too small, the result is a nearly planar Si₃N₃-ring with rather distorted ellipsoids. In Table 2.5 cell-parameters of the two different cell-types are displayed. Obviously the two different conformations of the hpcts-molecule have different space-groups, cell lengths and cell angles.

Table 2.5: Comparison of the two different solid state structures and the two different cell-units of hexaphenylcyclotrisilazane.

conformation	slight boat	planar
spacegroup	P21/n	C2/c
cell lengths [Å]	a 17.9258	a 17.931
	b 18.3731	b 9.1872
	c 18.7349	c 18.729
cell angle	a 90.00°	a 90.00°
	b 94.275°	b 94.324°
	c 90.00°	c 90.00°
Si-N [pm]	171.7	171.3
	171.9	171.4
	171.8	171.3
N-Si-N-Si angle	-7.88°	0.11°
Si-N-Si-N angle	8.29°	0.08°
N-Si-N-Si angle	-1.41°	0.08°
Si-N-Si-N angle	0.43°	0.11°

**Figure 2.10:** Solid state structure of the nearly planar boat conformation of the hpts molecule, showing distorted ellipsoids as Krote and Wagler observed.

The two solid state conformations only differ in the N-Si-N-Si/Si-N-Si-N angles. For the slight boat conformation angles of -1.41° / -7.88° / 8.29° / 0.43° were found and for the nearly planar conformation the angles are 0.08° / 0.11° / 0.08° / 0.11° .

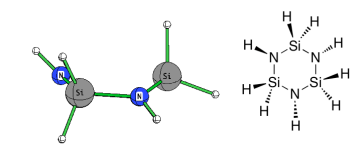
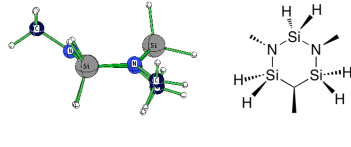
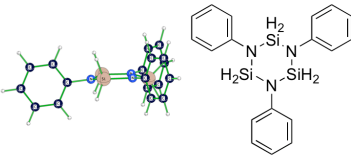
In sum, theoretical analysis of the Si-substitution pattern of six-membered SiN rings shows that small substituents, as methyl and hydride on the silicon atoms cause a boat conformation. For bulky, sterically demanding groups such as tertiary butyl or phenyl groups, we observed a flattened boat or a slightly twisted boat conformation.

The quantum chemical calculations were confirmed with the experimental data, gained from solid state structures. Further it can be maintained that the nearly planar Si₃N₃-ring in hexaphenylcyclotrisilazane is dominated by the steric effect of the phenyl groups and a little by the electronic effect. The ring geometry of hpcts is very similar to the ring geometry in the tertiary butyl substituted Si₃N₃-ring.

2.3 Substitution Pattern Analysis on the Nitrogen

How does the Si₃N₃-ring behave if different substituents are attached to the nitrogen atom? In Table 2.6 cyclotrisilazanes are displayed containing different substituents on the nitrogen atom.

Table 2.6: Influence of the N-substituents on the ring conformation calculated with mPW1PW91/6-31+G*.

structure	N-Si-N-Si angle Si-N-Si-N angle	Si-N [pm]	²⁹ Si shift [ppm]
	-8.57°	174.4	-37.68
	47.68°	173.4	-42.83
	-47.68°	174.3	
	8.73°		
	-48.76°	174.5	-17.66
	44.76°	173.3	-19.73
	48.41°	174.6	-20.13
	-44.31°		
	-13.39°	173.9	-33.80
	3.32°	174.0	-34.02
	10.98°	174.1	-34.62
	-11.22°		

On the first glance it seems that substituents on the nitrogen atom also induce a boat conformation in the Si₃N₃-ring. When a methyl group is attached on the nitrogen atoms the Si₃N₃-ring has got the very same conformation as the per-hydrogenated parent molecule. The N-Si-N-Si/Si-N-Si-N dihedral angles are in both cases similar; 8.73° / -47.68° / 47.68° / -8.57° in the parent molecule and 44.76° / -48.76° / 48.41° / -44.31° in the methyl substituted derivative. Also the Si-N distances do not change, but the ²⁹Si chemical shift is impaired. The methyl groups on the nitrogen atoms induce the effect that the ²⁹Si chemical shift goes to higher values; for the parent molecule -37.68 ppm were calculated and for the methyl derivative -17.66 ppm were obtained - see Table 2.6.

Comparison of the parent molecule with the phenyl substituted molecule gives the information that the Si₃N₃-ring is more affected by the sterically demanding phenyl substituents. The boat conformation turns into a slight twist conformation. According to the N-Si-N-Si angles (-13.39° / 3.32° / 10.98° / -11.22°) the ring is nearly planar. The Si-N bond distances remain constant as in the parent molecule - at an average value of 174.0

pm. Further the phenyl groups on the nitrogen atoms induce an electronic effect, so that the ^{29}Si chemical shift is at -34.02 ppm similar to the per-hydrogenated parent molecule. The Si3N3-rings are often substituted on the nitrogen atom as well as on the silicon atom. Thus the ring conformation is impaired by both substituents and the resulting ring geometry is a combination of both effects. These substituent effects can enforce or compensate each other.

Figure 2.11 displays the simplest example of a substituted cyclotrisilazane. The per-methylated Si3N3-ring contains Si-N bond distances at the average value of 174.0 pm, like all other derivatives. The N-Si-N-Si angles are not equal any more, this means that the boat conformation is turning into a slightly twisted boat conformation.

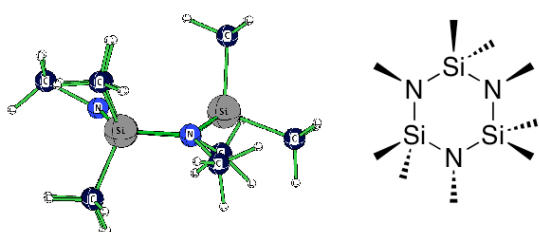


Figure 2.11: Geometry optimized (mPW1PW91/6-31+G*) slightly twisted boat structure of nonamethylcyclotrisilazane

Table 2.7: Parameter of $[(\text{CH}_3)_2\text{SiNCH}_3]_3$

data	
N-Si-N-Si angle	-44.75 °
Si-N-Si-N angle	4.04 °
N-Si-N-Si angle	44.37 °
Si-N-Si-N angle	-9.40 °
Si-N [pm]	175.3
	174.0
	175.6
^{29}Si shift [ppm]	+0.02
	-0.92
	-1.19

In the next example, we will discuss, how the the Si3N3-ring is affected by bulky and by small substituents.

Blake and Ebsworth analyzed hexamethyltriphenylcyclotrisilazane (see Figure 2.12). They found out that the six-membered Si3N3-ring is twisted and the deviation from planarity is rather large. Some trisilazane rings are planar or nearly so, and it has been suggested that small substituents (e.g. H or CH₃) on the nitrogen atoms favor planarity [15]. According to our conformational study, Si3N3-rings with bulky substituents on the nitrogen atoms tend to form flattened boat conformations. Further we found out that small substituents favor a boat structure in the Si3N3-ring. A relevant example is the hexatertbutylcyclotrisilazane (Figure 2.14).

For the molecule Blake and Ebsworth published, we expect a maybe twisted boat conformation. On the one hand there is the effect of the phenyl groups on the nitrogen atoms, which induce a twist conformation. On the other hand the methyl groups on the silicon atoms, usually induce a boat conformation. Both effects will determine the Si₃N₃-ring conformation.

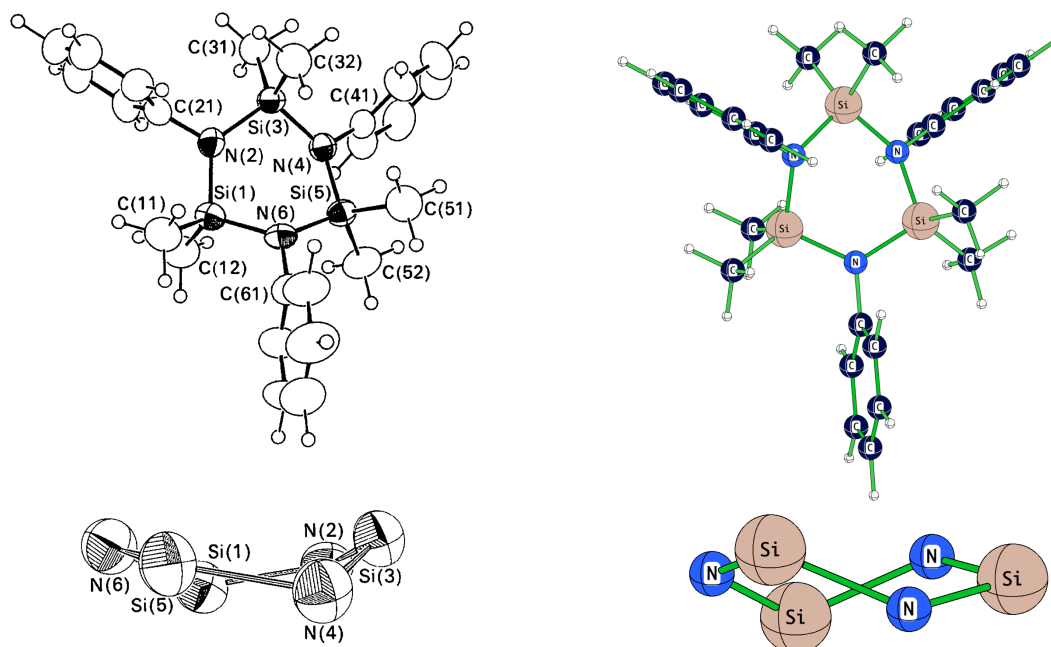


Figure 2.14: Solid state structure of hexamethyltriphenylcyclotrisilazane and optimized (mPW1PW91/6-31+G*) structure; phenyl groups and hydrogen atoms were omitted for clarity.

In Table 2.8 experimental [15] and our calculated data (mPW1PW91/6-31+G*) of hexamethyltriphenylcyclotrisilazane are compared. This molecule includes two different types of substituents, on the one hand the small methyl groups on the silicon atoms and on the other hand the bulky phenyl groups on the nitrogen atoms. It is obvious that the ring conformation is a twist, in the optimized structure (Figure 2.14) as well as in the solid state. Si-N distances are within the range of 176.3 pm for the geometry optimized molecule and 174.2 pm in the crystal. The N-Si-N-Si/Si-N-Si-N dihedral angles are -41.26°/ 26.94°/ -47.22°/ 22.69° in the solid state and -25.71°/ 52.06°/ -33.04°/ 56.26° in the geometry optimized molecule), this indicates that the Si₃N₃-ring is far away from being planar.

Table 2.8: Comparison of calculated (mPW1PW91/6-31+G*) and measured data[15] of hexamethyltriphenylcyclotrisilazane

data	experimental [15]	calculated
spacegroup	P1	-
Si-N [pm]	173.9	175.3
	174.2	176.3
	174.1	176.5
N-Si-N-Si angle	26.94°	33.05°
Si-N-Si-N angle	-41.26 °	-52.06°
N-Si-N-Si angle	-47.22 °	- 56.26°
Si-N-Si-N angle	22.69 °	25.71°
²⁹ Si shift [ppm]	-1.25	-4.80

Hence substituents on each atom in the Si₃N₃-ring influence the conformation. Our assumption about the Si₃N₃-ring conformation was confirmed by the measured and calculated data. It seems that the phenyl groups on the silicon atom have a greater effect on the conformation, than the substituents on the nitrogen atom. The hexamethyltriphenylcyclotrisilazane is in a twist conformation.

The combination of both effects, determines the geometry of the ring. Further we will see that the substituents also influence the reactivity and determine which kind of products can be obtained.

2.4 Derivatization Reactions with Hexaphenylcyclotrisilazane

As already mentioned in the introduction, hexamethylcyclotrisilazane undergoes a ring contraction reaction and forms cyclodisilazane as product - see Figure 2.1. This reaction behavior was also observed during attempts to functionalize the nitrogen atoms in the Si₃N₃-ring. Kroke, Wagler and Roewer tried the functionalization with silicon- and tin-agents. They report, that the reactions with hexamethylcyclotrisilazane led to a large variety of products due to the competition of substitution reactions and ring contraction [16]. It was possible to mono-functionalize hexamethylcyclotrisilazane via a metallization reaction with n-BuLi and a subsequent salt elimination reaction to provide the desired products - see Figure 2.15.

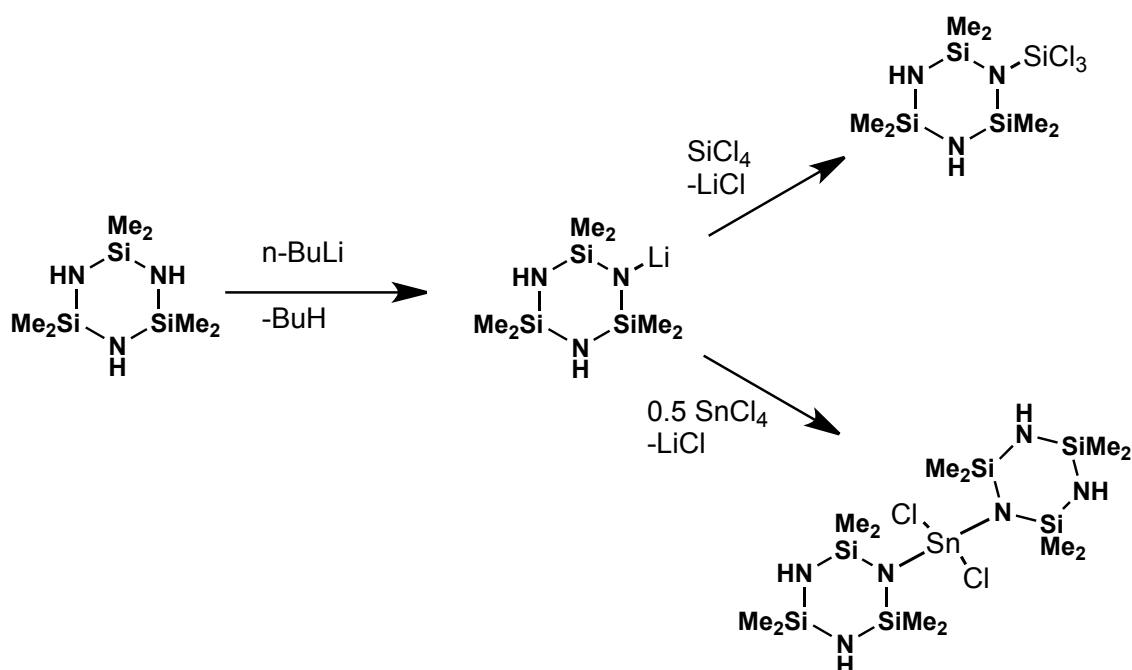


Figure 2.15: Lithiation reaction of hexamethylcyclotrisilazane and subsequent functionalization

In spite of attempts to generate also di- and tri- substituted hexamethylcyclotrisilazane by the same reaction pathway as shown in Figure 2.15, they could only establish that the ring contraction reaction is faster.

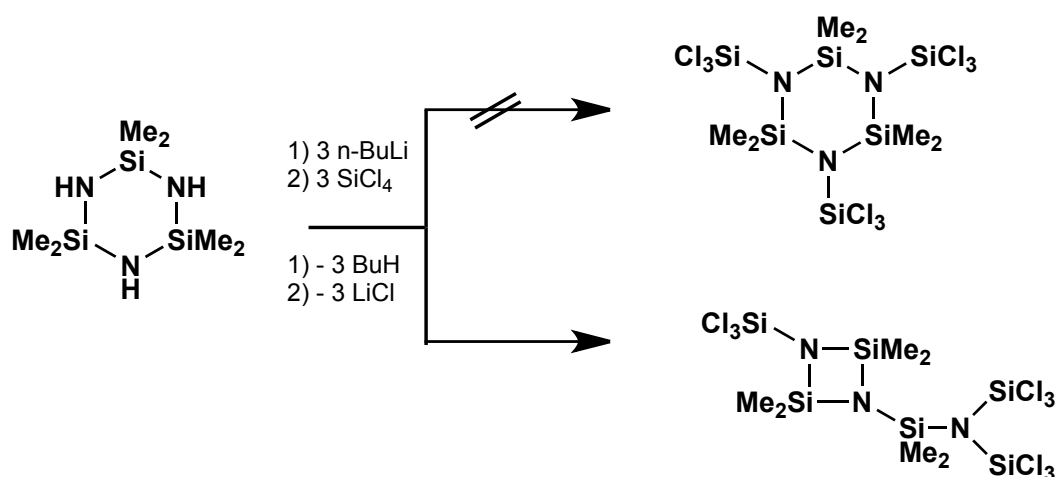


Figure 2.16: Tri-lithiation reaction of hexamethylcyclotrisilazane and subsequent functionalization.

They assume that an anionic rearrangement is accompanied by ring contraction and as product the disilazane is formed - Figure 2.16. Isomerizations of the cyclotrisilazane system depend on both, the extent of lithiation as well as the type of additional substituents. Also thermal effects are important [16], [17].

Besides these observations they also tried reactions of hexamethylcyclotrisilazane with SnCl_4 - see Figure 2.17.

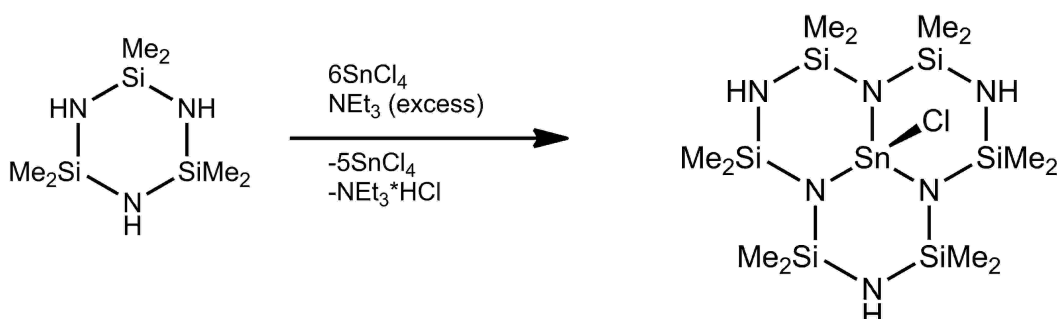


Figure 2.17: Formation of the tin cyclohexasilazane complex with tin as central atoms, by reaction of H_3 (HMCTS) with SnCl_4 and Et_3N

Kroke and Wagler proposed a reaction pathway. Via silicon NMR measurements they were able to assume cyclodisilazanes as intermediates in the formation of the dodecamethylcyclohexasilazane ring. A ring opening reaction of hexamethylcyclotrisilazane happens.

We tried the very same experiment with our hexaphenylcyclotrisilazane ring, and we only obtained starting material and tin-oxide as side product. No ring degradation or rearrangement reactions could be observed.

Detailed studies show that a variety of effects (*thermal effects, electronic effects, kinetic effects, type of additional substituent*) has to be considered, while derivatizing cyclotrisilazanes [18].

Cyclosilazanes with small substituents on the silicon atoms, tend to make smaller rings, but they can be cross-linked with different spacer groups [19]. But first of all it is necessary to activate the Si₃N₃-ring.

We carried out the very same experiments with hexaphenylcyclotrisilazane (see Figure 2.18) but obtained different results. The Si₃N₃-ring always stays intact during the metalation reaction. It is possible to mono-, di- and tri- functionalize the whole molecule. No byproducts or degradation reactions could be observed.

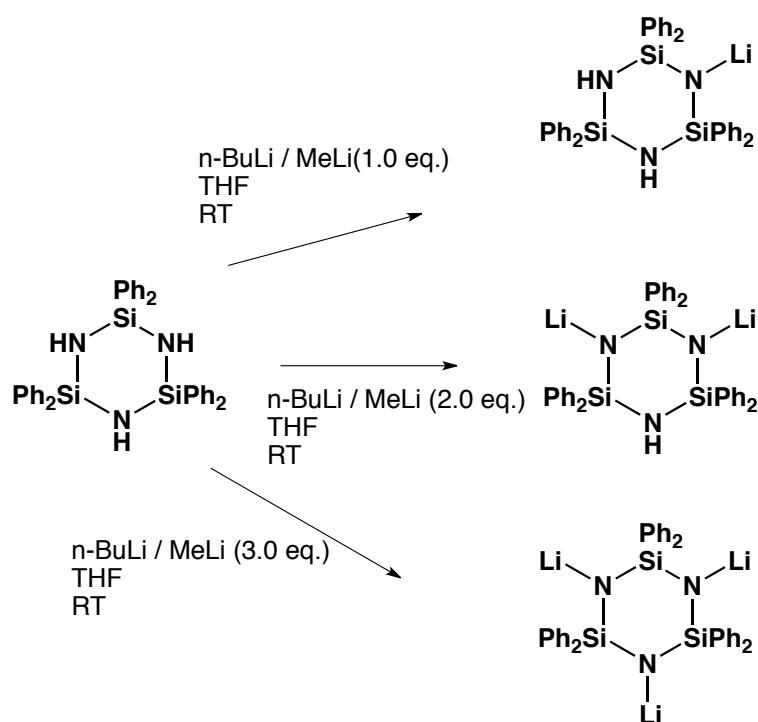


Figure 2.18: Lithiation reactions of hexaphenylcyclotrisilazane

The reaction conditions for the lithiation are very gentle, only stirring at room temperature in THF (tetrahydrofuran) and addition of the metallizing agent n-BuLi or MeLi are necessary. In contrast Fink [20] reported about very harsh conditions and mainly poor yields, during the attempt to functionalize the hexaphenylcyclotrisilazane rings. Attention should only be paid to the amount of the metallizing agent. It is necessary to use the exact stoichiometric amount of n-BuLi or MeLi. Otherwise an inseparable mixture of the products will be obtained.

The generated compounds are poorly soluble in organic solvents, hence the products crystallize easily. Figure 2.19 displays the solid state structures of the mono-, di-, and tri-lithiated hexaphenylcyclotrisilazane.

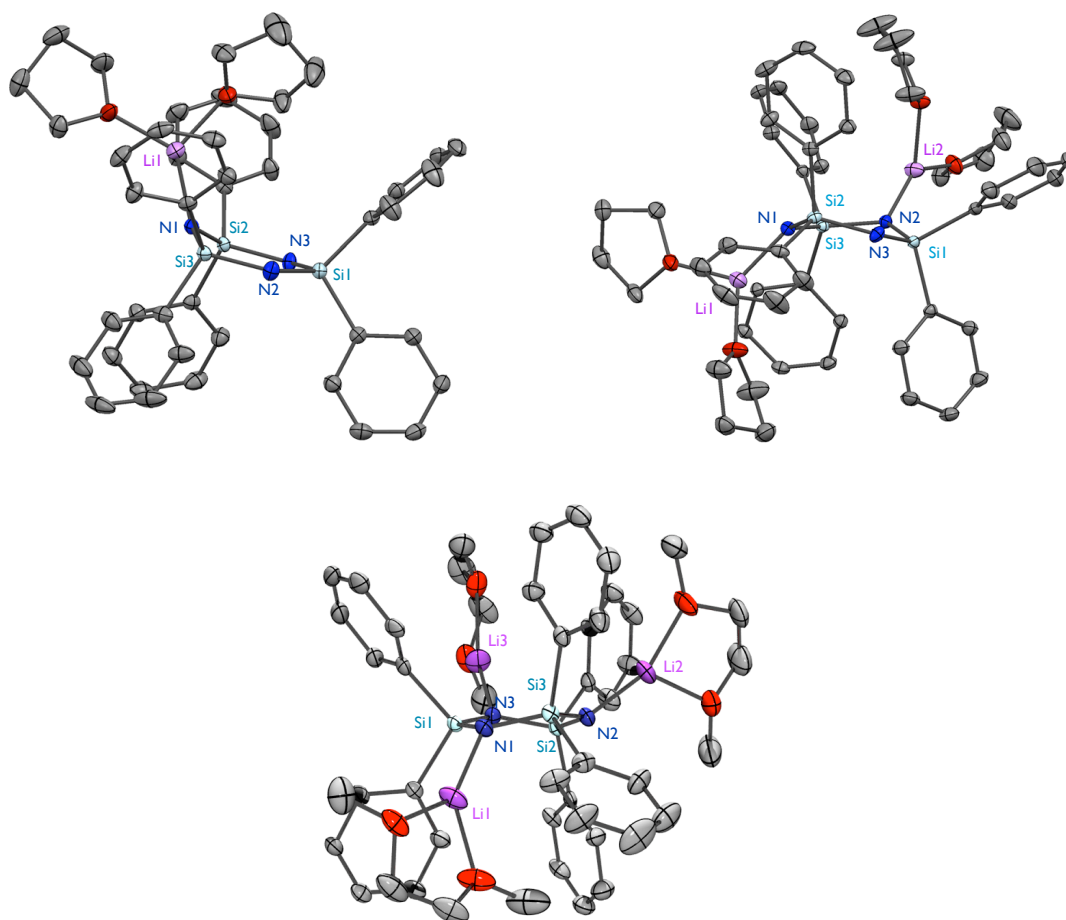


Figure 2.19: Solid state structures of the mono-, di-, and tri-lithiated hexaphenylcyclotrisilazane, showing a boat, twisted boat, and twist conformation. Hydrogens were omitted for clarity.

At first view it is obvious that the Li-derivatives of hexaphenylcyclotrisilazane have an unusual conformation, because they are more twisted the more the ring is lithiated. The lithium atoms on the nitrogen induce this conformation change. The same observation is made in the geometry optimized structures - see Figure 2.20. The more lithium ions are attached to the ring, the heavier is the twist in the Si3N3-ring.

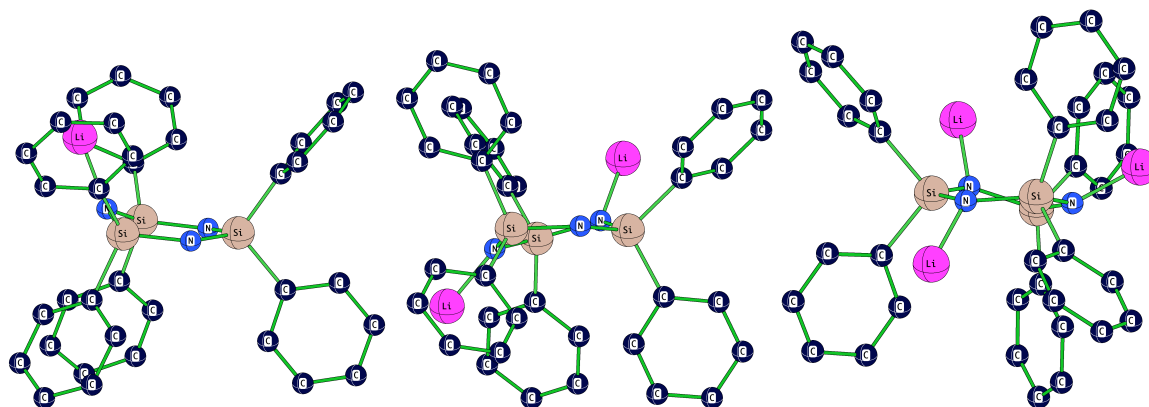


Figure 2.20: Geometry optimized structures (mPW1PW91/6-31+G*) of mono-, di-, and tri-lithiated hexaphenylcyclotrisilazane, showing a boat, twisted boat, and twist conformation. Hydrogens were omitted for clarity.

In Table 2.9 calculated and measured bond lengths and angles of lithiated-hexaphenylcyclotrisilazanes are displayed.

Table 2.9: Experimental and calculated (mPW1PW91/6-31+G*) data of mono-, di-, and tri-lithiated hexaphenylcyclotrisilazane

structure	experimental data			calculated data		
	1xLi	2xLi	3xLi	1xLi	2xLi	3xLi
spacegroup	P-1	P21/n	P21/n	-	-	-
Si-N [pm]	173.6	173.4	-	173.5	173.5	-
	171.6	173.6	-	171.6	173.4	-
	171.6	173.6	-	171.6	173.4	-
Si-NLi [pm]	167.2	167.0	169.0	167.5	169.6	168.7
	167.5	169.6	168.7	167.1	166.5	169.5
	-	169.6	169.2	-	-	169.6
angle						
N-Si-N-Si	-8.35°	-30.38°	19.05°	-8.35°	-31.21°	19.05°
Si-N-Si-N	32.55°	9.60°	-31.72°	-11.40°	18.49°	-31.71°
N-Si-N-Si	-32.55°	24.73°	-19.46°	11.40°	13.73°	-17.76°
Si-N-Si-N	8.25°	-33.19°	5.11°	8.22°	-27.53°	5.05°
Σ angle NLi	350.12°	354.60°	342.37°	349.50°	351.68°	351.12°
²⁹ Si [ppm]	-21.35	-21.35	-37.67	-24.81	-40.40	-48.88
	-32.24	-34.37	-	-39.14	-46.75	-47.08

First of all one trend is visible, the Si-N bond distances decrease from the original 173 pm to an average value of 167 pm. Resultant a Si₃N₃-ring-contraction happens when all hydrogens are replaced by lithium atoms. This ring contraction can be explained by the stronger electrostatic attraction between the nitrogen and silicon atoms. This effect is promoted by the lithium ions. Figure 2.24 illustrates the Si₃N₃-ring contraction. N-Si-N angles become smaller when the lithium-substituent is on the nitrogen atom (the original N-Si-N angle is at 127.42° and it decreases to 118.39° when all three hydrogen atoms are replaced by lithium ions).

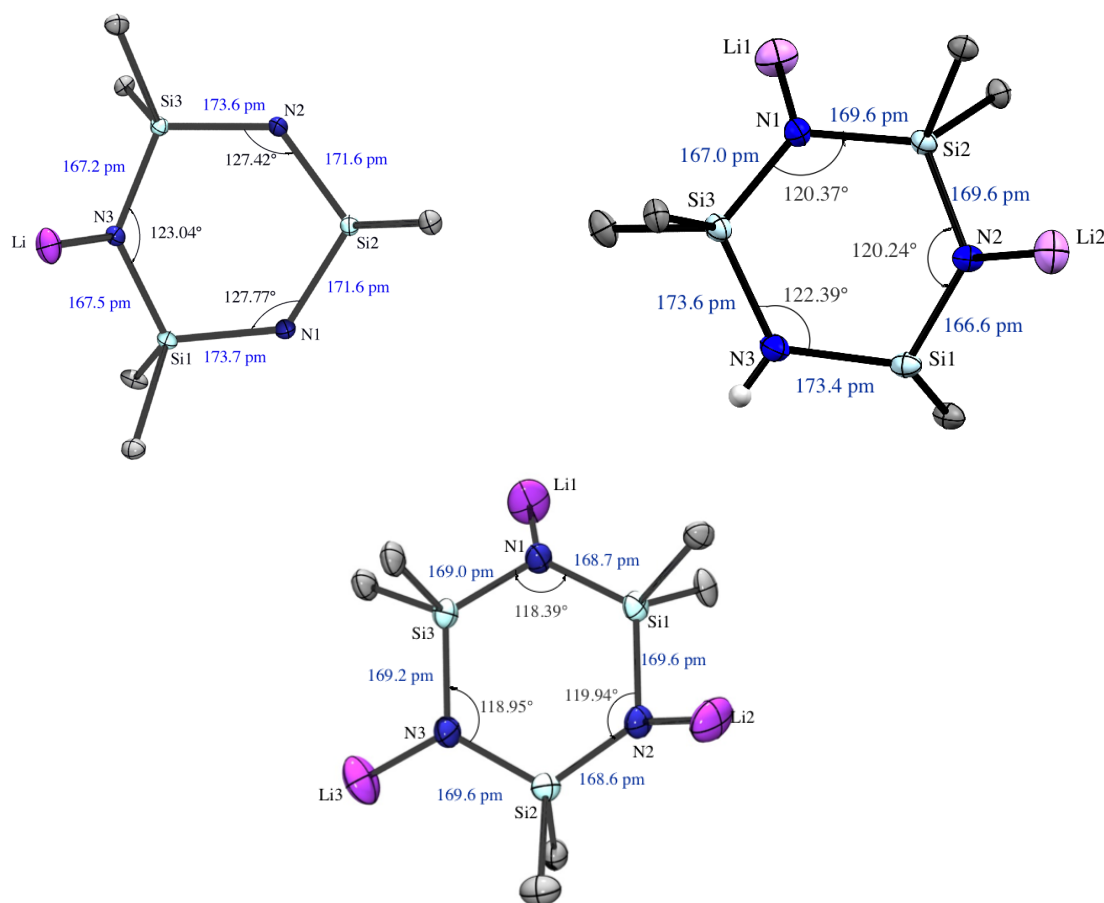


Figure 2.24: Top view of the solid state structures of the mono-, di-, and tri-lithiated hexaphenylcyclotrisilazane: hydrogens and phenyl groups were omitted for clarity.

Second, the N-Si-N-Si/Si-N-Si-N dihedral angles increase and consequently the ring conformation turns into a twist. This transformation becomes more obvious with more than one lithium atom on the Si₃N₃-ring. The twist is most apparent when all three hydrogens on the nitrogen atom are replaced by lithium atoms. In the tri-lithiated hexaphenylcyclotrisilazane different N-Si-N-Si/Si-N-Si-N angles were found: 19.05° / -31.72° / -19.46° / 5.11° (exp.) and 19.05° / -31.72° / -17.76° / 5.05° (calc.).

Further the nitrogen atoms in the six-membered Si-N heterocycle feature a trigonal pyramidal coordination sphere, containing an angular sum of 354.12° or smaller in the solid state data and 351.68° in the calculated gas phase data - see Table 2.9. Usually the nitrogen atom is in a trigonal planar coordination sphere in hexaphenylcyclotrisilazane with an average bond angle sum of 359° . The increasing pyramidal environment around the nitrogen atoms enables the twist conformation in the Si₃N₃-ring. This trend is found in both, the geometry optimized and in the solid state structures.

Third, the ^{29}Si chemical shifts are also affected by the lithium-substituents. The ^{29}Si signals tend to fall to lower values. In the ^{29}Si spectra the hexaphenylcyclotrisilazane signal appears at -21.14 ppm, in contrast signals for the lithiated-species can be measured at -34.24 ppm to -37.67 ppm. Influenced are only silicon atoms, which are directly neighboring to the lithium-substituted nitrogen atom.

Metallization steps with agents like *n*-BuLi, elemental metals like potassium, sodium or even lithium are usually used to activate a molecule for subsequent reactions. Therefore an investigation to modify the hexaphenylcyclotrisilazane ring with potassium was tried -see Figure 2.25.

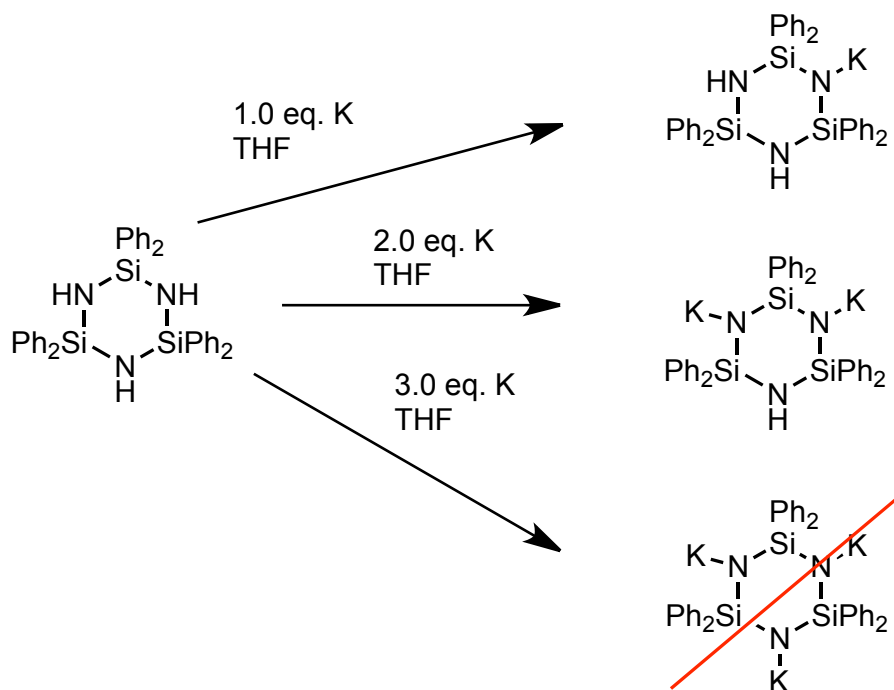


Figure 2.25: Derivatization reactions of hexaphenylcyclotrisilazane with potassium

Modifying the hexaphenylcyclotrisilazane molecule with potassium shows an interesting result. Quantitatively it is possible to generate mono-K-hexaphenylcyclotrisilazane and di-K-hexaphenylcyclotrisilazane but a species containing three potassium atoms could not be observed. Table 2.10 gives the experimental and calculated data of the mono- and di-potassium-hexaphenylcyclotrisilazanes.

Table 2.10: Comparison of the solid state structures and the geometry optimized (mPW1PW91/6-31+G*) structures of mono- and di-potassium-hexaphenylcyclotrisilazane

structure	experimental		calculated	
	1xK	2xK	1xK	2xK
spacegroup	-	P-1	-	-
Si-N [pm]	-	174.5	173.7	173.8
	-	173.0	175.9	173.7
	-	173.0	175.9	173.7
	-	173.0	175.9	173.7
Si-NK [pm]	-	168.9	-	168.2
	-	168.5	167.3	168.4
	-	165.7	167.2	166.3
	-	165.7	167.2	166.3
N-Si-N-Si angle	-	12.70°	6.18°	12.18°
Si-N-Si-N angle	-	-7.90°	-16.16°	-6.78°
N-Si-N-Si angle	-	1.57°	13.13°	-2.85°
Si-N-Si-N angle	-	-1.08°	-0.60°	5.19°
²⁹ Si [ppm]	-22.26	-38.28	-26.39	-44.40
	-35.76	-	-47.82	-46.75

The Si₃N₃-ring geometry is similarly affected by the potassium ions as by the lithium ions. The ring undergoes a ring contraction, the Si-N distances decrease (from originally 174 pm up to 165 pm). This can be also explained by the electrostatic attraction between the nitrogen and the silicon atoms, which is amplified by the potassium-substituents. Hence the Si₃N₃-ring changes the conformation - but still it can be described as a twist conformation. N-Si-N-Si/Si-N-Si-N angles are at 6.18° / -0.60° / 13.13° / -16.16° for the geometry optimized mono-potassium-hexaphenylcyclotrisilazane (Figure 2.27) and in the geometry optimized di-potassium-hexaphenylcyclotrisilazane (Figure 2.28) angles of 12.18° / 5.19° / -2.85° / -6.78° can be found. In the solid state structure of di-potassium-hexaphenylcyclotrisilazane (Figure 2.26) the N-Si-N-Si/Si-N-Si-N dihedral angles of 12.70° / -1.08° / -7.90° / 1.57° can be found - fitting the calculated data - see Table 2.10.

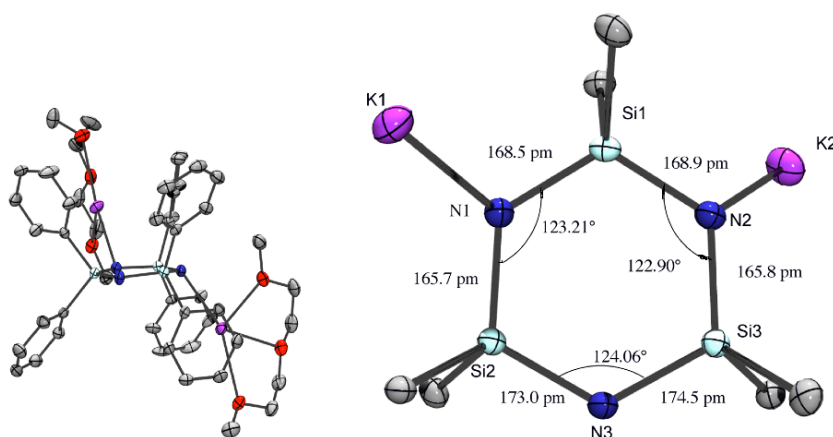


Figure 2.26: Solid state structure of di-K-hexaphenylcyclotrisilazane in a slight twist conformation; hydrogens were omitted for clarity; top view of the Si₃N₃-ring.

Unfortunately, the solid state structure of the mono-K-hexaphenylcyclotrisilazane could not be obtained, but the geometry optimized structure (see Figure 2.27) gives information about the Si₃N₃-ring conformation and the ²⁹Si chemical shift. The Si₃N₃-ring is in a slightly twisted boat conformation according to the calculated N-Si-N-Si/Si-N-Si-N dihedral angles. The Si-N distances decrease if the hydrogen atom is substituted by a potassium ion from 173.7 pm to 167.3 pm.

The simulation also gives an explanation why a second ²⁹Si signal in the NMR spectra of the di-K-hexaphenylcyclotrisilazane could not be observed. As a result of the calculation the two ²⁹Si signals are at -44.40 ppm and -46.75 ppm, and that is too small a difference to be detected. So in the experiment only a signal at -38.28 ppm could be measured for the di-K-hexaphenylcyclotrisilazane. The resolution of the 300 MHz NMR-machine is not high enough to split the ²⁹Si signal at -38.28 ppm into two.

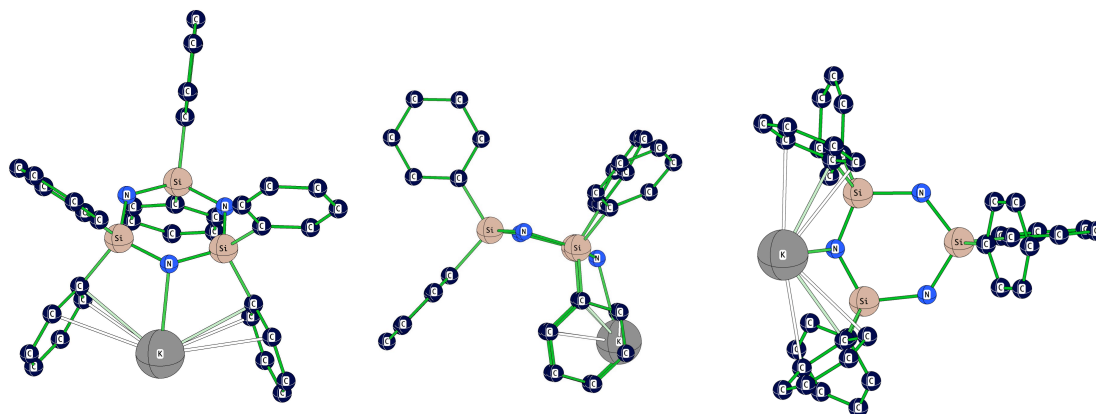


Figure 2.27: Geometry optimized structure (mPW1PW91/6-31+G*) of mono-K-hexaphenylcyclotrisilazane in slightly twisted boat conformation; hydrogens were omitted for clarity.

Additionally can be maintained that an interaction between the potassium and two phenyl groups occurs. The phenyl groups stabilize the huge potassium ion - see Figure 2.27 and Figure 2.28 . This stabilizing effect could not be observed with lithium, since the lithium atom has a much smaller coordination-sphere.

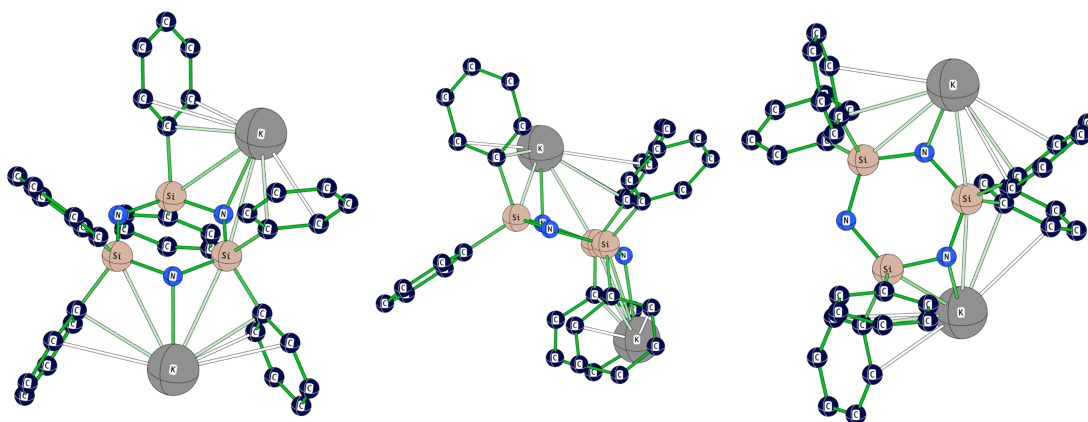


Figure 2.28: Geometry optimized structure (mPW1PW91/6-31+G*) of di-K-hexaphenylcyclotrisilazane; hydrogens were omitted for clarity; showing weak interactions between the potassium and two neighboring phenyl groups.

This might also explain why it is not possible to synthesize the tri-substituted potassium hexaphenylcyclotrisilazane. As there is not enough space to stabilize a third potassium atom on the ring with the two remaining phenyl groups. Further the tri-potassium species

is possibly too alkaline and reacts back to the starting material and potassium-crown ether- see Figure 2.29.

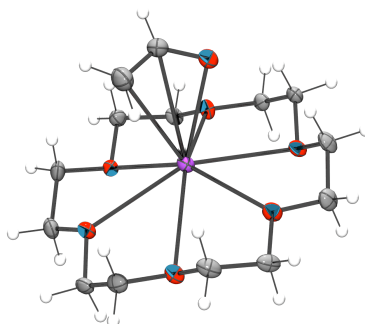


Figure 2.29: Solid state structure of the potassium-crown ether, with an ethenyl group attached to.

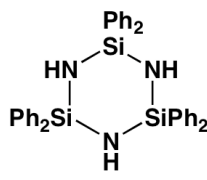
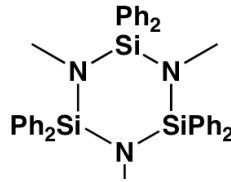
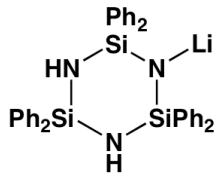
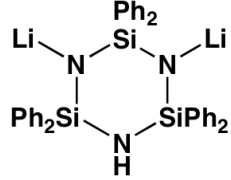
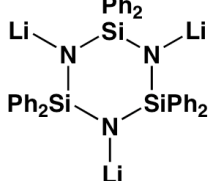
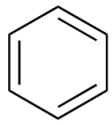
Because of the Si₃N₃-ring contraction of the hexaphenylcyclotrisilazane derivatized with potassium and n-BuLi the question comes up if the generated compounds could be π -aromatic. In accordance with the Hückel $(4n+2)$ -rule the hexaphenylcyclotrisilazane system could be aromatic.

Hückel says that, monocyclic planar (or almost planar) systems of trigonally hybridized atoms that contain $(4n + 2)\pi$ -electrons (where n is a non-negative integer) will exhibit aromatic character. The rule is generally limited to $n=1-5$ [21].

To prove this aspect some NICS-calculations were done, (results see Table 2.11). NICS stands for Nucleus-Independent Chemical Shifts and is a quantum chemical method to evaluate the aromaticity in a ring system. Schleyer et al. proposed the use of absolute magnetic shieldings, computed at ring centers with available quantum mechanics programs [22] as an aromaticity / antiaromaticity criterion [23].

Negative "nucleus-independent chemical shifts" denote aromaticity and positive NICSs anti-aromaticity.

Table 2.11: Calculated NICS values (mPW1PW91/IGLO-II) for selected hexaphenylcyclotrisilazane derivatives with benzene for comparison

structure	NICS [ppm]
	-1.06
	-1.82
	-1.64
	-0.90
	-0.35
	-8.36

The calculated NICS values in Table 2.11 show that the hexaphenylcyclotrisilazane derivatives are not aromatic. The compounds have values between -0.35 ppm and -1.82 ppm. This proves that the ring contraction occurs only due to electrostatics.

2.4.1 N-H / N-D Hexaphenylcyclotrisilazane

The simplest as well as most interesting derivatization reaction is to substitute the N-protons with deuterium atoms- see Figure 2.30. Already small changes in the molecule can cause effects, such as shifted infrared frequencies or missing ^1H chemical shifts. Hexaphenylcyclotrisilazane and deuterio-hexaphenylcyclotrisilazanes differ only in the three NH/ND groups, but it is possible to spot the difference in the adequate measurement. Reaction control as well as characterization can be done easily, by analyzing the N-H group via NMR or IR-measurements.

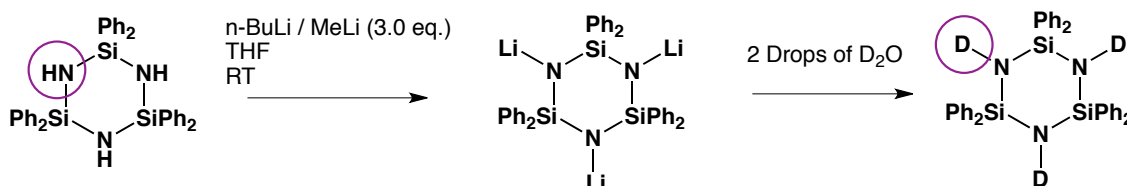


Figure 2.30: Synthesis of deuterio-hexaphenylcyclotrisilazane

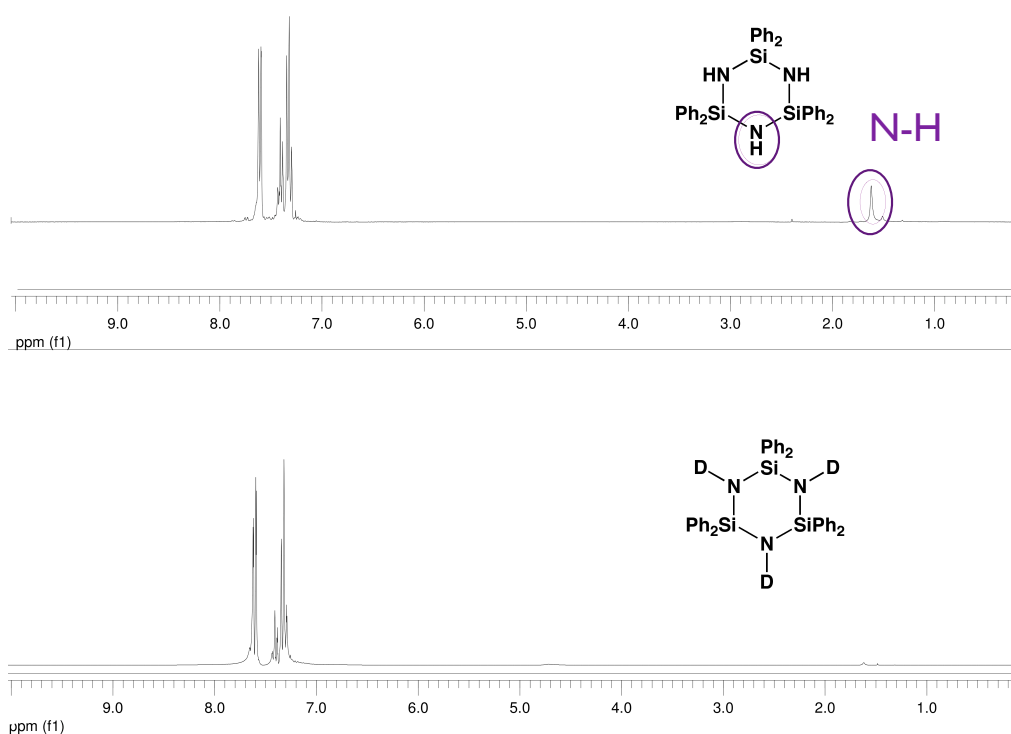


Figure 2.31: ^1H NMR spectra of hexaphenylcyclotrisilazane and the corresponding deuterio-hexaphenylcyclotrisilazane

Exercising ^1H NMR measurements with the two molecules shows that the typical NH signal at 1.68 ppm disappears when the N-hydrogens are replaced by deuterium atoms - see Figure 2.31. The rest of the signals remain the same.

An other effective and fast method to detect such differences is the infrared frequency measurement (IR-measurement). One of the major factors influencing the IR-absorption frequency of a bond is the identity of the two atoms involved. To be precise, it is the mass of the two atoms which is of importance. The greater the masses of the attached atoms are, the lower is the IR-frequency at which the bond will absorb. Figure 2.32 displays the IR-spectra.

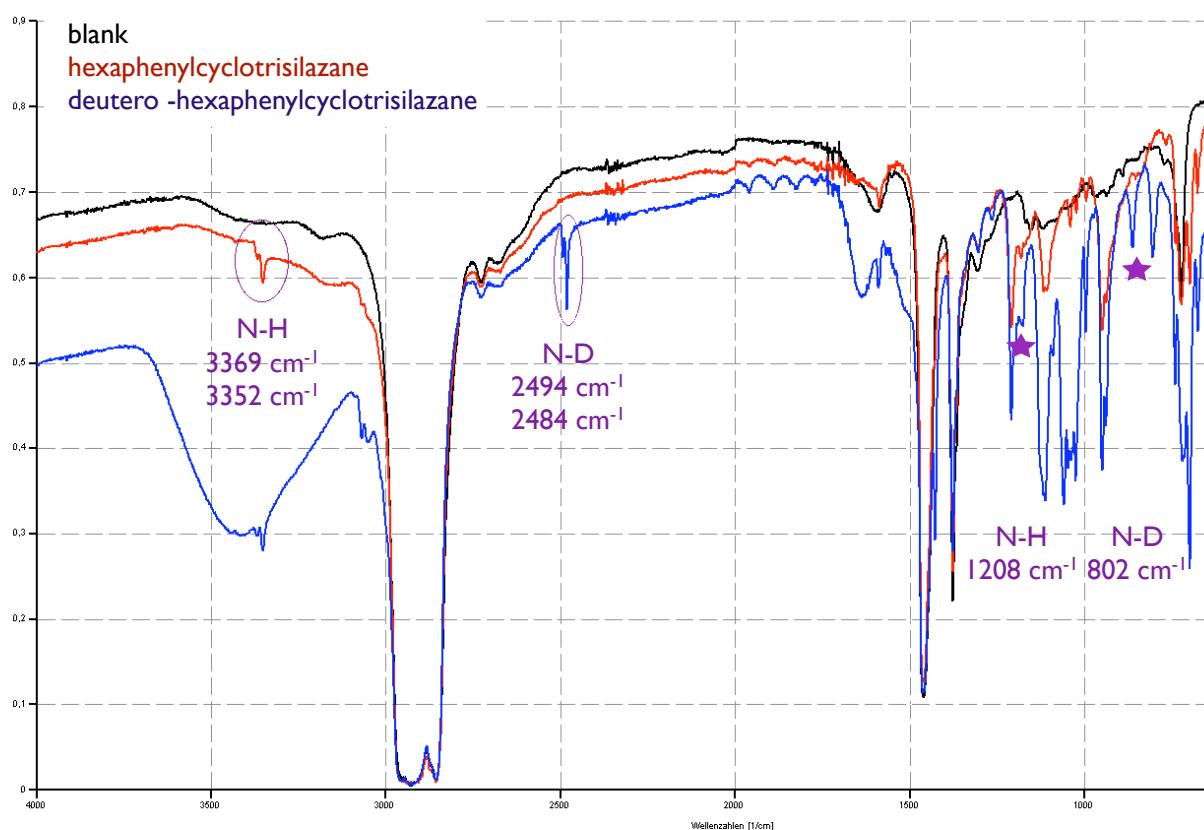


Figure 2.32: IR-spectra of hexaphenylcyclotrisilazane and the corresponding deuterio-hexaphenylcyclotrisilazane; spectra were measured in nujol

Table 2.12 displays the the calculated and the observed IR-frequencies of hexaphenylcyclotrisilazane and deuterio-hexaphenylcyclotrisilazane. The NH group can vibrate in five different modes: symmetric and antisymmetric stretching, rocking, wagging and twisting. Only four modes could be found in the calculation and three in the spectra. On complete deuteration of the NH-groups one should expect a shift of the stretching modes attributed to the NH vibrations by approximately 1000 cm^{-1} [24].

In the region appropriate to NH bond vibrations, between 3400-3200 cm^{-1} , two bands are observed. The most intense one in the hexaphenylcyclotrisilazane spectrum is at 3369 cm^{-1} , which is assigned to the antisymmetric stretching mode of NH. The second band is at 3352 cm^{-1} and belongs to the symmetric stretching mode. Calculated data fit well with the observed values - see Table 2.12. In general, they give a good trend for the interpretations of such IR-spectra.

In the deuterio-hexaphenylcyclotrisilazane spectrum also two intense bands are found, at 2494 cm^{-1} and 2484 cm^{-1} . They are assigned to the antisymmetric and symmetric ND stretching modes.

The remaining intense absorption at 1208 cm^{-1} is assigned to the rocking motion of the NH group and at 802 cm^{-1} of the ND group. According to the calculated spectra there should be an antisymmetric deformation mode at 1237 cm^{-1} for the NH groups and analog a band at 1080 cm^{-1} for the ND groups.

Table 2.12: Calculated (mPW1PW91/sdd) and measured IR frequencies in cm^{-1} of hexaphenylcyclotrisilazane and deuterio-hexaphenylcyclotrisilazane.

hexaphenylcyclotrisilazane			deuterio-hexaphenylcyclotrisilazane			
Mode	Obs.	Calc.	Obs.	Calc.		
(NH) _a st	ν	3369	3597	(ND) _a st	2494	2626
(NH) _s st	ν	3352	3554	(ND) _s st	2484	2600
(NH) _a ^{rock}	δ	1208	1254	(ND) _a ^{rock}	802	799
(NH) _a ^{def}	γ	-	1237	(ND) _a ^{def}	-	1080

2.4.2 N-Me Hexaphenylcyclotrisilazane

As already mentioned, Li-hexaphenylcyclotrisilazane is a reactive species and further experiments show that a second derivatization reaction can follow. For instance, the N-Me derivative of hexaphenylcyclotrisilazane was synthesized via the reaction pathway in Figure 2.33. The reaction is a one pot reaction and gives the product in good yields (>90%).

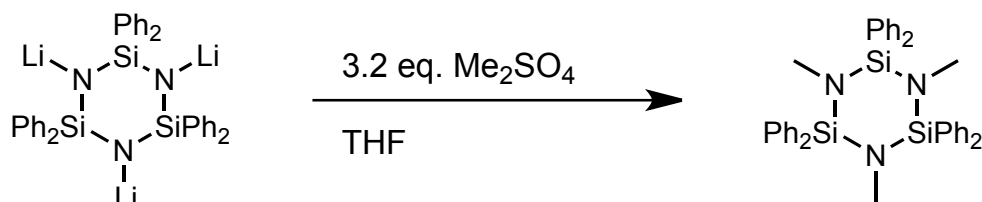


Figure 2.33: Synthesis of trimethyl-hexaphenylcyclotrisilazane starting from the tri-Li-hexaphenylcyclotrisilazane

Already in 1964 Breed and Elliott [25] found another method to synthesize the same compound-see Figure 2.34. They start as well with diphenyldichlorosilane, but instead of ammonia they use already functionalized methyl-amine for the reaction. Therefore, they get the desired compound in one step but only in a yield of 56%.

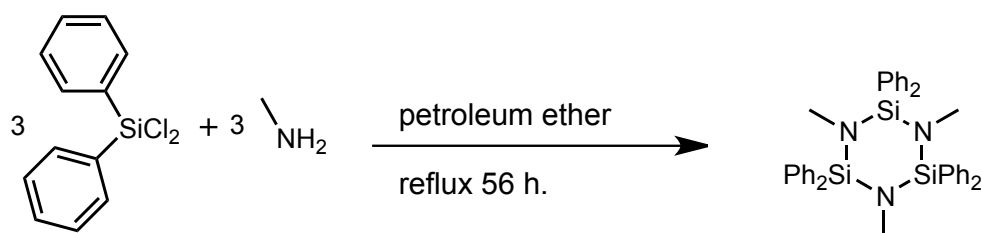


Figure 2.34: Synthesis of trimethyl-hexaphenylcyclotrisilazane according to Breed and Elliott [25]

Starting from the Li-hexaphenylcyclotrisilazanes offers more options to attach various substituents on the SiN-ring. First of all, it is easier to handle the amounts of the needed chemicals, second a better reaction control is possible, and last there is nearly no limitation concerning the starting materials.

Trimethyl-hexaphenylcyclotrisilazane is a rather stable compound and represents an analog of trimethyl-hexamethylcyclotrisilazane.

As mentioned before, according to DFT calculations, the nonamethylcyclotrisilazane appears in a boat conformation. In the case of trimethyl-hexaphenylcyclotrisilazane two different substituent-types have an effect on the Si₃N₃-ring, on the one hand the small CH₃-groups on the nitrogen atom and the bulky phenyl-groups on the silicon atom. Therefore

we expect that the Si₃N₃-ring conformation is a combination of the N-methyl-substituted and the Si-phenyl substituted cyclotrisilazane - a twist conformation.

Table 2.13 displays parameters of the geometry optimized and the solid state structure of tri-N-methyl-hexaphenylcyclotrisilazane and Figure 2.36 shows the simulated and the solid state structure.

Table 2.13: Experimental and calculated (mPW1PW91/sdd) geometry of trimethyl-hexaphenylcyclotrisilazane

data	experimental	calculated
spacegroup	Pb ca	-
Si-N [pm]	171.8	174.1
	172.5	174.0
	172.0	173.8
N-Si-N-Si angle	25.70°	28.61°
Si-N-Si-N angle	-24.50°	-22.07°
N-Si-N-Si angle	-11.05°	-9.29°
Si-N-Si-N angle	-19.02°	-14.82°
²⁹ Si shift [ppm]	-15.25	-20.46

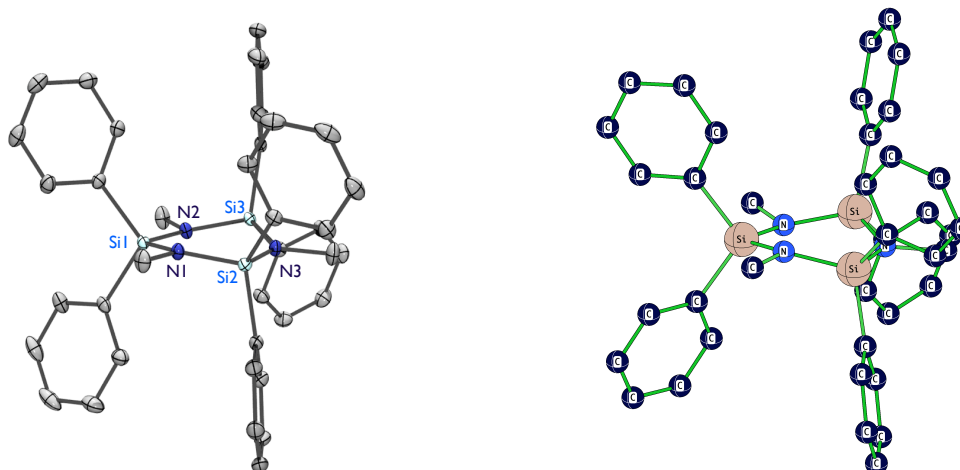


Figure 2.36: Solid state structure and mPW1PW91/6-31+G* optimized structure of trimethyl-hexaphenylcyclotrisilazane

The Si-N bond distances are not highly affected by the methyl-substituents. They remain in the range of 171 -174 pm in the solid state and in the geometry optimized structure.

The N-Si-N-Si/Si-N-Si-N dihedral angles indicate that the Si₃N₃-ring is in a slight twist conformation similar to hexaphenylcyclotrisilazane. In the solid state angles of $-19.02^\circ / -24.50^\circ / -11.05^\circ / 25.70^\circ$ can be found and in the geometry optimized Si₃N₃-ring angles of $-14.82^\circ / -22.07^\circ / -9.29^\circ / 28.61^\circ$ can be measured.

This conformation actually is a combination of the hexaphenylcyclotrisilazane (slightly twisted boat) and the N-methyl-cyclotrisilazane (boat). The two different substituents have both an effect on the Si₃N₃-ring. The two effects amplify each other and give a slight twist conformation of the ring backbone in the end.

Knowing what effect is induced by the different substituents it is possible to predict properties and geometries of the compound.

Similar predictions can be made for the ²⁹Si chemical shift. The ²⁹Si chemical shift of -15.25 ppm in the experiment and -20.46 ppm in the calculation, can be compared with N-methyl-cyclotrisilazane and hexaphenylcyclotrisilazane. For the N-methyl-cyclotrisilazane an average ²⁹Si shift of -19.73 ppm was calculated and for hexaphenylcyclotrisilazane a ²⁹Si shift value of -23.90 ppm was predicted. The impact of the Si-substituent is here higher than the impact of the N-substituent.

All in all the Si₃N₃-ring conformation is affected by both the N-methyl groups and by the Si-phenyl groups to the same extent. The resulting conformer is a combination of both effects.

2.4.3 N–SiMe₂H Hexaphenylcyclotrisilazane

Synthetic access to modified six-membered Si₃N₃-rings is not easy. Fink reports about their extreme air sensitivity, as well as their affinity to undergo rearrangement reactions and form four-membered SiN-rings, in the case of methyl substituted cyclotrisilazanes ((NHMe₂Si)₃) [26], [27]. Not all reaction conditions lead to a product mixture. In some cases it is possible to generate modified six-membered cylosilazane derivatives - see Figure 2.37 [26].

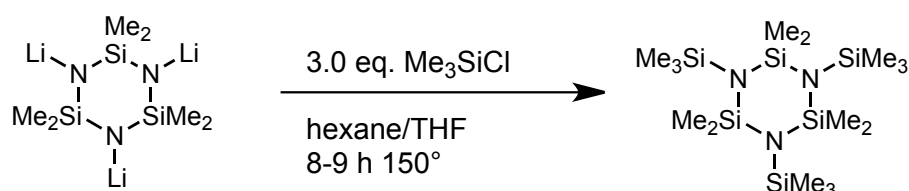


Figure 2.37: Synthesis of tris(trimethylsilyl)-hexamethylcyclotrisilazane according to Fink[26]

Table 2.14: Geometry data of 1,3,5-tris(trimethylsilyl)-2,2,4,4,6,6-hexamethylcyclotrisilazane, according to [28] and [29].

data	experimental
spacegroup	Pnma
Si ₁₋₃ -N [pm]	173.7
in the ring	174.2
	175.0
Si ₄₋₆ -N [pm]	175.4
out of the ring	176.2
	175.4
N-Si-N-Si angle	-57.37°
Si-N-Si-N angle	57.37°
N-Si-N-Si angle	-39.90°
Si-N-Si-N angle	39.90°
²⁹ Si ₁₋₃ shift [ppm]	-4.7
²⁹ Si ₄₋₆ shift [ppm]	-14.5

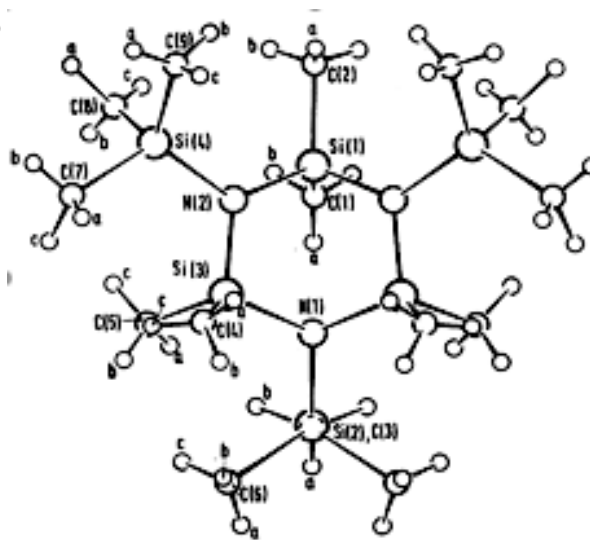


Figure 2.38: Solid state structure of 1,3,5-tris(trimethylsilyl)-2,2,4,4,6,6-hexamethylcyclotrisilazane[28]

Daly and Adamson determined the structure of hexamethyl-tris-(trimethylsilyl) cyclotrisilazane to provide accurate information on the ring geometry of a cyclotrisilazane - see Figure 2.38. Table 2.14 displays data from the solid state structure of hexamethyl-tris-(trimethylsilyl)cyclotrisilazane.

They describe the cyclotrisilazane ring to be in a boat form, where four of the ring atoms are coplanar [N2, Si3, N2' and Si3'] and the remaining two atoms lie on the same side of this plane [28]. The Si-N bond lengths are at an average value of 174.4 pm. The Si-N bond lengths outside the ring are slightly longer, mean 175.8 pm. They suggest that the boat conformation is favored because the three valences on each nitrogen atoms adopt a planar configuration.

We also made very similar observations for the hexaphenylcyclotrisilazane derivatives - see Figure 2.41. Two atoms are always on the same side of the N-Si-Si-N plane and that sometimes the three valences on the nitrogen atom adopt nearly planar configuration - see Table 2.15 .

Attempts were made to functionalize the hexaphenylcyclotrisilazane with Me_3SiCl , starting from tri-Li-hexaphenylcyclotrisilazane - see Figure 2.39. The reaction failed, only starting material could be obtained.

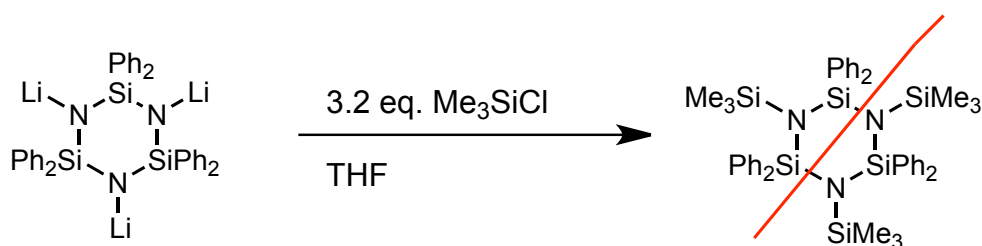


Figure 2.39: Synthesis of tris(trimethylsilyl)-hexaphenylcyclotrisilazane

Thus, an other derivatization reaction was chosen, to obtain a N-silyl substituted Si_3N_3 -ring. At gentle reaction conditions (0°C and 12h stirring) tris-(dimethylsilyl)-hexaphenylcyclotrisilazane could be obtained in 90% yield -see Figure 2.40.

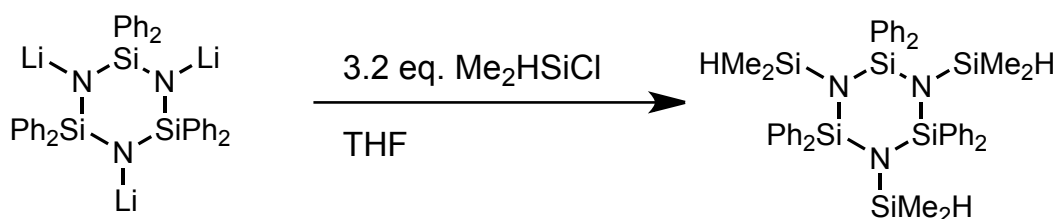


Figure 2.40: Synthesis of tris(dimethylsilyl)-hexaphenylcyclotrisilazane.

Obviously the trimethylsilyl group is too bulky to be attached to the nitrogen in the

(Ph₂SiN)₃-six membered ring. In contrast, a dimethylsilyl group can fit in the hexaphenylcyclotrisilazane frame. Figure 2.41 shows the solid state structure of tris(dimethylsilyl)-hexaphenylcyclotrisilazane.

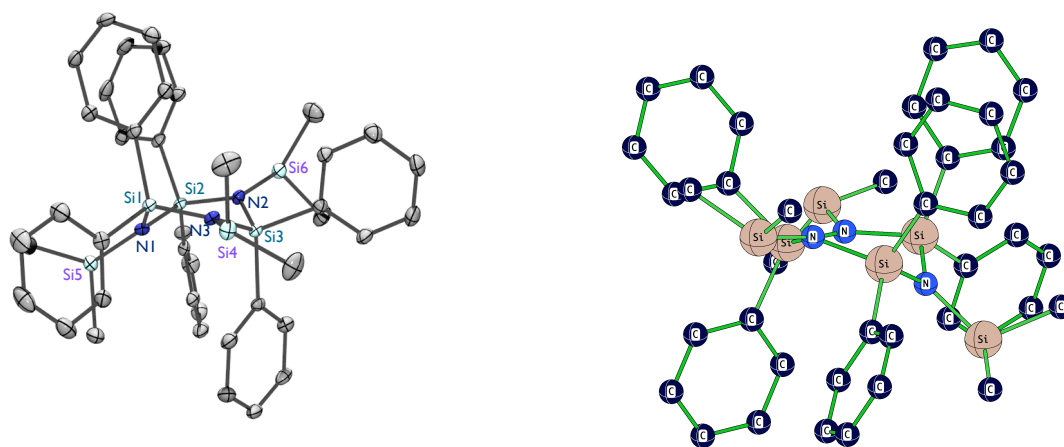


Figure 2.41: Solid state and optimized (mPW1PW91/6-31+G*) structure of tris(dimethylsilyl)-hexaphenylcyclotrisilazane; hydrogens were omitted for clarity.

Table 2.15 presents collected calculated and measured geometry and ²⁹Si NMR chemical shift data of tris(dimethylsilyl)-hexaphenylcyclotrisilazane.

Table 2.15: Experimental and calculated data of tris(dimethylsilyl)-hexaphenylcyclotrisilazane.

data	experimental	calculated
spacegroup	P-1	-
Si ₁₋₃ -N [pm]	174.9	176.2
in the ring	174.2	176.7
	175.2	176.4
Si ₄₋₆ -N [pm]	177.5	178.8
out of the ring	176.9	179.8
	177.2	178.3
N-Si-N-Si angle	-58.70°	-58.74°
Si-N-Si-N angle	19.08°	16.83°
N-Si-N-Si angle	-52.07°	-37.86°
Si-N-Si-N angle	17.34°	10.17°
²⁹ Si ₄₋₆ shift [ppm]	-10.90	-12.43
²⁹ Si ₁₋₃ shift [ppm]	-21.10	-24.71

Tris-(dimethylsilyl)-hexaphenylcyclotrisilazane appears in a slightly twisted boat conformation in the solid state structure as well as in the geometry optimized gas phase structure. The molecule contains exo-cyclic N-Si bonds ($\text{Si}_{4-6}\text{-N}$) and ring backbone N-Si ($\text{Si}_{1-3}\text{-N}$) bonds. The exo-cyclic Si-N bonds are in average 2 pm longer than the ring Si-N bonds, according to calculated and measured values- see Table 2.15. This circumstance was also reported by Daly e.al. [28], - see Table 2.14.

The N-Si-N-Si/Si-N-Si-N dihedral angles of $19.08^\circ / -58.70^\circ / -52.07^\circ / 17.34^\circ$ in the experiment and $-58.74^\circ / 16.83^\circ / -37.86^\circ / 10.17^\circ$ in the simulation, indicate the slightly twisted boat conformation of the Si_3N_3 -ring.

As expected the ^{29}Si shift shows two values. The ring silicon atoms appear at $^{29}\text{Si}_{1-3}$ -10.90 ppm and the exo-cyclic $\text{Si}(\text{CH}_3)_2\text{H}$ groups give the signal at $^{29}\text{Si}_{4-6}$ -21.10 ppm. The calculated ^{29}Si shifts help to assign the measured signals.

Attempts to generate other silyl substituted hexaphenylcyclotrisilazane compounds (like in Figure 2.42) failed. Only product mixtures could be obtained, because of the metallation step with n-Buli and the subsequent derivatization reaction.

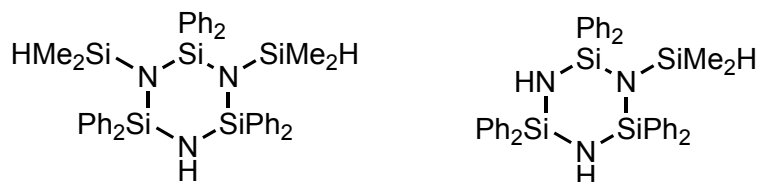


Figure 2.42: Miscellaneous substituted hexaphenylcyclotrisilazanes

Lithiation works well under smooth room temperature conditions, but it is important to work with exact equimolar ratios. If these circumstances are not taken in account, product mixtures of lithiated species are produced. The best is to do a subsequent lithiation and to proof the reaction stages via ^{29}Si NMR measurements.

In this case the subsequent derivatization step with $(\text{CH}_3)_2\text{HSiCl}$ makes problems, and gives the inseparable mixture of products. It is assumed that a Li-metal migration takes place. Identification of the generated product in the ^{29}Si spectra, can only be done by process of elimination.

2.4.4 N–AlMe₂ Hexaphenylcyclotrisilazane

The multitude and complexity of aluminum-nitrogen compounds has fascinated chemists for more than 30 years [30]. These aluminum-nitrogen compounds are used as precursors in material science. Wehmschulte et. al. published in 2001 a method to generate aluminum substituted cyclotrisilazane rings - see Figure 2.43

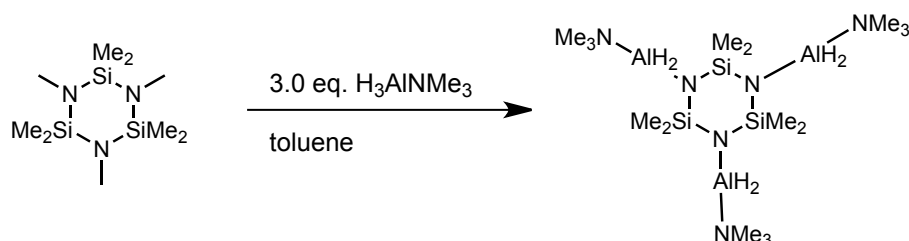


Figure 2.43: Synthesis of 1,3,5-(H₂AlNMe₃)₃(NSiMe₂)₃ [30]

Although the aluminum containing compounds are highly oxygen and moisture sensitive Wehmschulte et.al. reported crystal structures and geometry parameters. Figure 2.44 and Table 2.16 show the experimental data.

Table 2.16: Experimental data of 1,3,5-(H₂AlNMe₃)₃(NSiMe₂)₃ [30].

data	experimental
spacegroup	P21/c
Si-N [pm]	174.1
	172.5
	173.5
Al-N [pm]	182.2
	184.3
	182.3
N-Si-N-Si angle	-24.06°
Si-N-Si-N angle	63.94°
N-Si-N-Si angle	-42.44°
Si-N-Si-N angle	-12.29°
²⁷ Al shift [ppm]	140

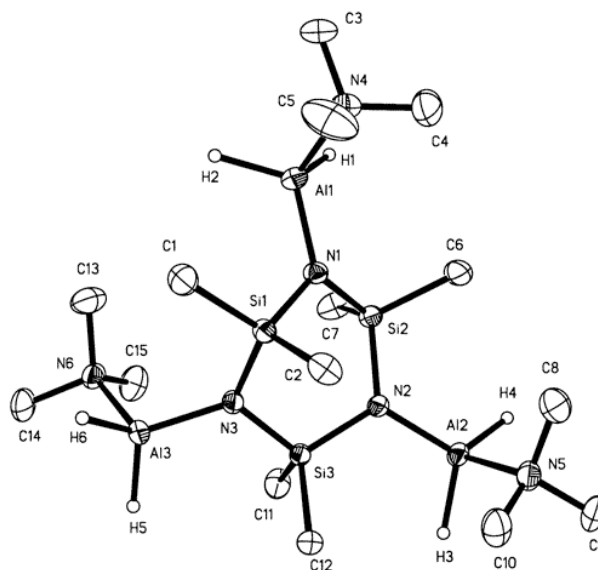


Figure 2.44: Solid state structure of 1,3,5-(H₂AlNMe₃)₃(NSiMe₂)₃ according to [30]

They observed that the ring displays a twisted-boat conformation and that the metric parameters are within the expected ranges for amine stabilized aluminum derivatives

with average Al-N(amide) distances of 182.3 pm-184.3 pm. Further they also observed that the amide nitrogen atoms (nitrogen atoms in the ring-skeleton) are basically planar, as is typical for a nitrogen atom bound to three electropositive atoms.

Very similar results could be obtained for our modified aluminum substituted hexaphenylcyclotrisilazane molecule. Figure 2.45 shows the reaction conditions. The reaction of AlMe_3 with hexaphenylcyclotrisilazane in a 3:1 molar ratio at elevated temperatures (70°C) provides the tri-aluminum-hexaphenylcyclotrisilazane via methane elimination.

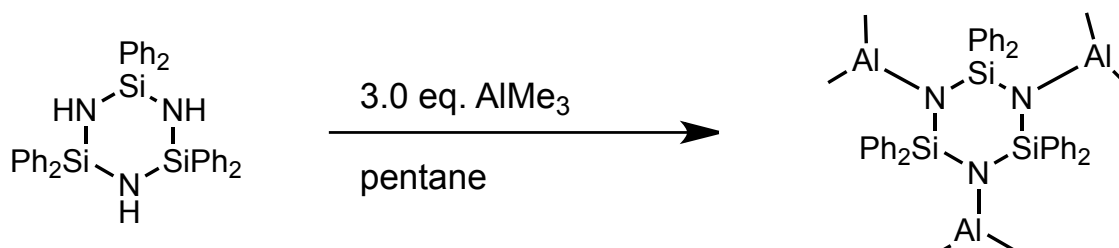


Figure 2.45: Synthesis of tri-aluminum-hexaphenylcyclotrisilazane

The structure of tris-aluminum-hpcts features a six-membered Si_3N_3 -ring, in which each nitrogen is bound to a AlMe_2 group. The Si_3N_3 -ring is in a twisted boat conformation. The AlMe_2 groups are rotated away from each other in such a way that two AlMe_2 groups are in plane and the third one out of plane when viewed with respect to the Si_3 plane - see Figure 2.46. The ring nitrogen atoms are planar ($\Sigma(\text{Si-N-Si,Al}) = 359.22^\circ, 359.75^\circ, 359.51^\circ$) as expected for a nitrogen atom bonded to tree electropositive atoms [31].

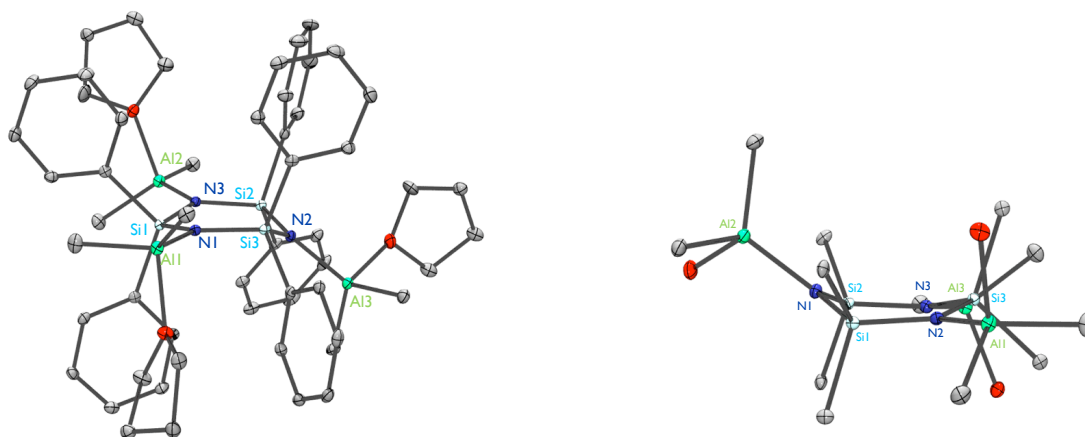


Figure 2.46: Solid state structure of tri-aluminum-hexaphenylcyclotrisilazane, showing the Si_3N_3 -ring conformation. Phenyl groups and hydrogens were omitted for clarity

In Table 2.17 parameters from the geometry optimized structure and the solid state structure are compared. The geometry optimized structure of tris-aluminum-hexaphenylcyclotrisilazane shows a twisted boat conformation. Si-N distances are in the average

range of 172.6 pm to 173.3 pm in the solid state structure and 173.8 pm to 174.7 in the geometry optimized molecule - see Figure 2.47. The N-Si-N-Si/Si-N-Si-N dihedral angles of 21.97° / -15.67° / -11.67° / 37.42° in the solid state and 57.64° / -25.65° / -28.74° / 58.67° in the geometry optimized structure both indicate a twisted boat conformation. ^{29}Si chemical shifts undergo an upfield shift to -27.03 ppm (experimental value) and -33.30 ppm (calculated value) which is induced by the AlMe_2 groups. Further the ^{27}Al chemical shift was measured with 189.10 ppm and calculated (mPW1PW91/IGLO-II) [32] with 187.03 ppm. Wehmschultes tris-aluminum-hexamethylcyclotrisilazane has a ^{27}Al chemical shift of 140 ppm.

Table 2.17: Experimental and simulated (mPW1PW91/sdd) data of tris-aluminum-hexaphenylcyclotrisilazane

data	experimental	calculated
spacegroup	P21/c	-
Si-N [pm]	173.3	173.8
	172.6	174.1
	173.0	174.7
Al-N [pm]	187.9	184.9
	187.1	182.7
	187.5	184.9
N-Si-N-Si angle	21.97°	57.64°
Si-N-Si-N angle	-15.67°	-25.30°
N-Si-N-Si angle	-11.67°	-28.74°
Si-N-Si-N angle	37.42°	58.67°
^{29}Si shift [ppm]	-27.03	-33.03
^{27}Al shift [ppm]	189.10	187.03

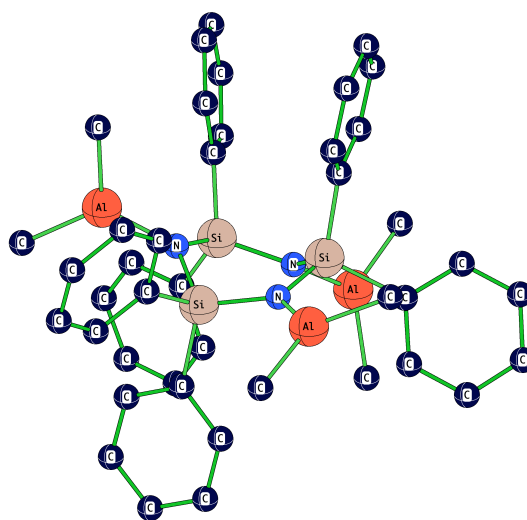


Figure 2.47: Geometry optimized structure of tri-aluminum-hexaphenylcyclotrisilazane

Interestingly, attempts to substitute only one or two of the three amine hydrogens of hexaphenylcyclotrisilazane were unsuccessful and only starting material and tris-aluminum hexaphenylcyclotrisilazane could be obtained. No further degradation or dimerization reactions could be observed.

In contrast, Wehmschulte reports about dimerization and condensation reactions, so that tri-cyclic aluminum-bridged compounds could be characterized. They propose some ligand exchange processes, which are rather typical for aluminum compounds [30]. This may be favored due to the small methyl substituents on the silicon atoms. As already

discussed before, cyclic silazanes with small substituents tend to undergo rearrangement reactions.

2.4.5 N–PbCl Hexaphenylcyclotrisilazane

During this work some attempts have been made to derivatize the hexaphenylcyclotrisilazane ring with heavier elements. The idea was to combine the Si₃N₃-ring with some divalent group 14 elements. Although a mass of compounds is known, which contain germanium(II), tin(II) or lead (II) in their ligand system [4] it has never been tried before to combine a cyclic phenyl substituted silazane with these metals.

Herein we present a lead(II) substituted hexaphenylcyclotrisilazane. The synthesis starts from tri-lithium-hexaphenylcyclotrisilazane (see Figure 2.48). The metal (II) is attached to the Si₃N₃-ring via a salt elimination of LiCl. The reaction conditions are gentle and the products can be obtained in quantitative yields.

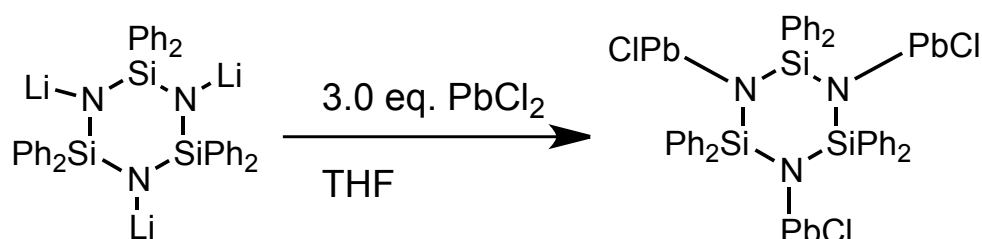


Figure 2.48: Synthesis of tris-(PbCl)-hexaphenylcyclotrisilazane.

The lead substituted Si₃N₃-ring can be viewed as a plumbylene. The metal is in the oxidation state (+II), consequently there is a lone-pair at the metal center. A special feature of the modified Si₃N₃-ring is that the molecule itself includes actually three metal(II)-chloride groups for further derivatization reactions.

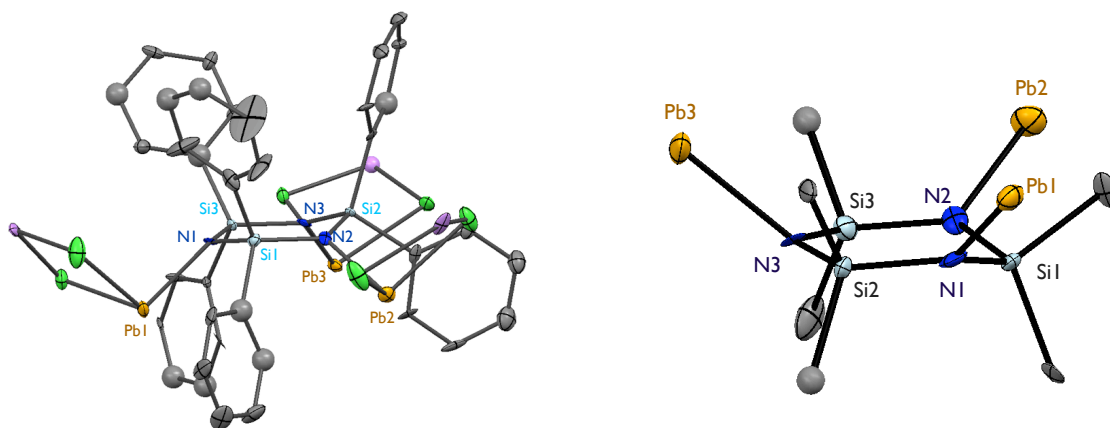


Figure 2.50: Solid state structure of tris-(PbCl)-hexaphenylcyclotrisilazane, in chair conformation; hydrogens were omitted for clarity.

Figure 2.51 shows the solid state structure of tri-(PbCl)-hexaphenylcyclotrisilazane. Apparently, the Si₃N₃-ring geometry is strongly affected by the lead-chloride substituent. The silazane ring appears in a classical chair conformation. The PbCl-groups point away from each other. The N-Si-N-Si/Si-N-Si-N-Si dihedral angles have opposite signs and are nearly all at the same value in the simulated chair conformation - see Table 2.18. The solid state structure is more flattened.

Table 2.18: Experimental and calculated data of tris-(PbCl)-hexaphenylcyclotrisilazane, chair conformation (TS)

data	experimental	calculated
spacegroup	P21/c	-
Si-N [pm]	171.5	174.9
	170.7	175.1
	173.3	175.0
Pb-N [pm]	226.0	225.6
	220.7	225.7
	223.9	225.5
N-Si-N-Si angle	-31.34°	-41.59°
Si-N-Si-N angle	-15.34°	-41.83°
N-Si-N-Si angle	30.92°	42.52°
Si-N-Si-N angle	14.29°	42.32°
²⁹ Si shift [ppm]	-30.71	-34.70
²⁰⁷ Pb shift [ppm]	2057	1740

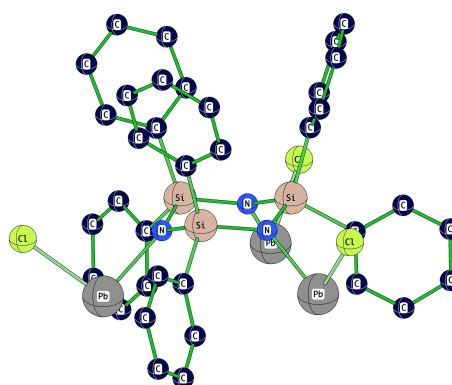


Figure 2.51: Geometry optimized (mPW1PW91/ZORA/TZP) structure of tris-(PbCl)-hexaphenylcyclotrisilazane in chair conformation

For tri-PbCl-hexaphenylcyclotrisilazane a second conformation was found- see Figure 2.52. The molecule can also appear in a twisted boat conformation, like most of the discussed hexaphenylcyclotrisilazane derivatives. Table 2.19 summarizes calculated and experimental data. According to the quantum chemical analysis the twisted boat conformation represents the global minimum and the chair conformation is a local minimum. The energy difference between chair and twisted boat conformation is 14 kJ/mol.

Further, the measured N-Si-N-Si/Si-N-Si-N dihedral angles in the solid state (-35.81°/ 45.67°/ -22.46°/ 30.66°) indicate that the Si₃N₃-ring is twisted and not completely in a clear boat conformation. This trend is confirmed by quantum chemical analysis -see Table 2.19.

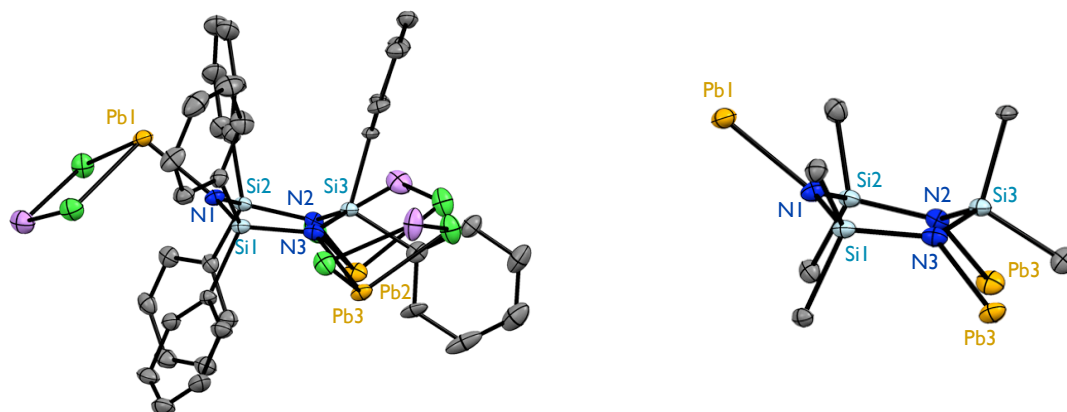


Figure 2.52: Solid state structure of tri-PbCl-hexaphenylcyclotrisilazane in twisted boat conformation; phenyl groups and hydrogens were omitted for clarity

Table 2.19: Experimental and calculated (mPW1PW91/sdd) data of tri-(PbCl)-hexaphenylcyclotrisilazane, twisted boat conformation.

data	experimental	calculated
space-group	P21/n	-
Si-N [pm]	171.5	174.9
	170.7	175.1
	173.3	175.0
Pb-N [pm]	226.0	225.6
	220.7	225.7
	223.9	225.5
N-Si-N-Si angle	-22.46°	-45.45°
Si-N-Si-N angle	-35.81°	-44.86°
N-Si-N-Si angle	45.67°	20.72°
Si-N-Si-N angle	30.66°	23.17°
²⁹ Si shift [ppm]	-30.71	-34.70
²⁰⁷ Pb shift [ppm]	2057.26	1790.59

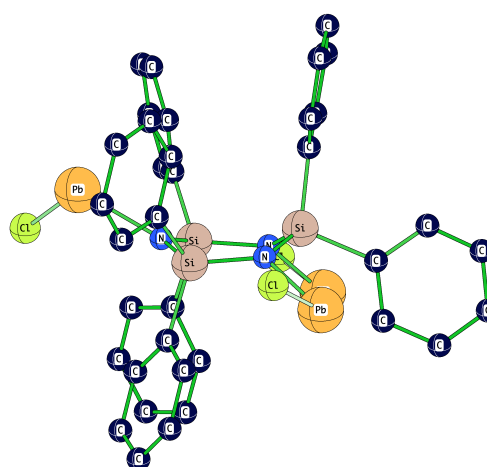


Figure 2.53: Geometry optimized (mPW1PW91/sdd) structure of tri-(PbCl)-hexaphenylcyclotrisilazane

According to the calculation the twisted boat conformation is the global minimum and the chair conformation is a second local minimum. Both of them can be found in the solid state. Possible explanation for this phenomenon is that the energy difference between the

two conformations is 14 kJ/mol. This energy barrier can be overcome by packaging forces in the crystal.

A slow crystallization process enables the system to get into the thermodynamically global minimum structure. Whereas, fast crystallization at reduced temperature can favor the thermodynamically stable local minimum as structure.

The twisted boat conformation is more stable than the chair conformation. As it seems that adequate crystal growth conditions can advance both possible conformations. Quantum chemical calculations confirm this assumption.

2.4.6 N–SnCl–Hexaphenylcyclotrisilazane

Besides the successful synthesis of the lead(II) functionalized hexaphenylcyclotrisilazane we also were able to generate and crystallize tris-SnCl-hexaphenylcyclotrisilazane. Reaction conditions are the same as for the lead derivative - see Figure 2.54.

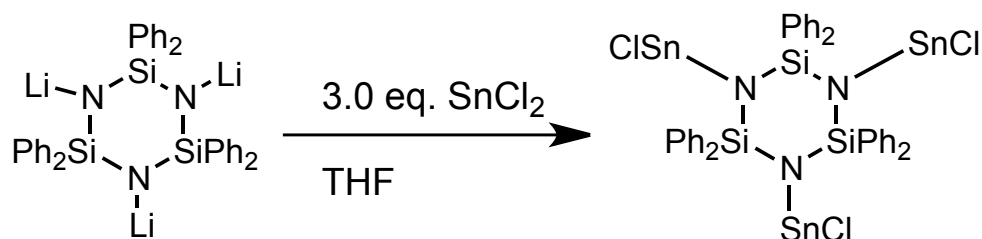


Figure 2.54: Synthesis of tris-(SnCl)-hexaphenylcyclotrisilazane.

Also this compound can be seen as a tetrylene. It also has got three functional Sn(II)Cl groups attached on the Si₃N₃-ring. These functional parts can be used for further derivatization.

In Figure 2.55 the solid state structure is shown. The crystal structure displays the Si₃N₃-ring in a typical boat conformation, with N–Si–N/Si–N–Si–N dihedral angles of -2.05° / -50.14° / 52.47° / -2.00° and in the geometry optimized (mPW1PW91/sdd) structure values of -3.45° / -46.60° / 53.13° / -7.98° were found. The SnCl-groups are rotated away from each other in such way that two SnCl-groups are equatorial. The third SnCl-group is placed on the opposite side of the plane.

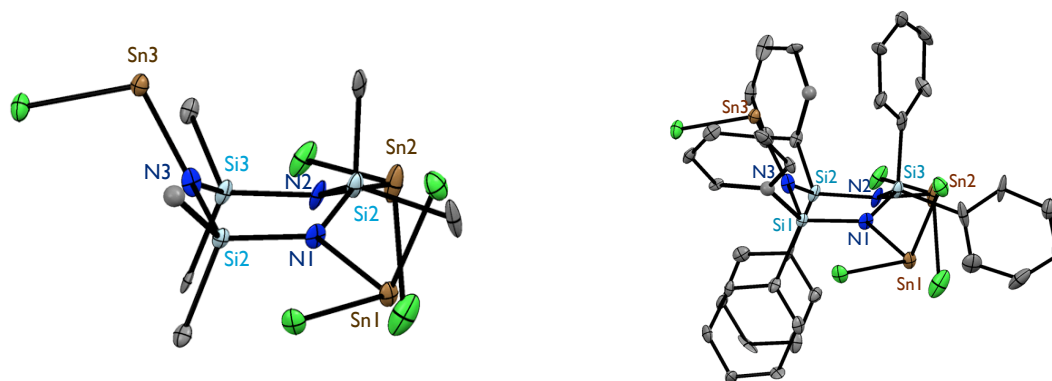


Figure 2.55: Solid state structure of tri-(SnCl)-hexaphenylcyclotrisilazane in boat conformation; hydrogens were omitted for clarity

In Table 2.21 measured and calculated data are compared. The Si–N distances are longer (up to 174 pm) in comparison to the Si–N distances of 171 pm in the hexaphenylcyclotrisi-

lazane molecule - see Table 2.21. This might come from the electrostatic interaction between the Sn-N-Si atoms.

At the Sn-center there is still an electron-lonepair and according to the ^{119}Sn chemical shift (of 94.98 ppm in the experiment and 138.45 ppm in the simulation) this molecule also behaves like a stannylene in solution, showing the typical very broad ^{119}Sn peaks in the NMR spectra. Broad signals in the NMR spectra indicate that anisotropy around the ^{119}Sn -core exists, caused by the electron-lonepair.

The compound is moisture and air sensitive. The SnCl-group is still reactive. A comparison with literature-known chloro stannylenes [33],[34] gives more information about potential subsequent derivatization reactions.

Table 2.20: Experimental and calculated (mPW1PW91/sdd) data of tri-(SnCl)-hexaphenylcyclotrisilazane

data	experimental	calculated
space-group	P21/n	-
Si-N [pm]	172.2	174.9
	170.7	175.1
	174.0	175.0
Sn-N [pm]	207.8	225.6
	213.7	225.7
	213.0	225.5
Sn-Cl [pm]	248.7	225.6
	250.3	225.7
	247.1	225.5
angle N-Sn-Cl	98.76°	100.95°
N-Si-N-Si angle	-2.05°	-3.45°
Si-N-Si-N angle	-50.14°	-46.60°
N-Si-N-Si angle	52.47°	53.13°
Si-N-Si-N angle	-2.00°	-7.98°
^{29}Si shift [ppm]	-28.85	-34.70
^{119}Sn shift [ppm]	94.98	138.45

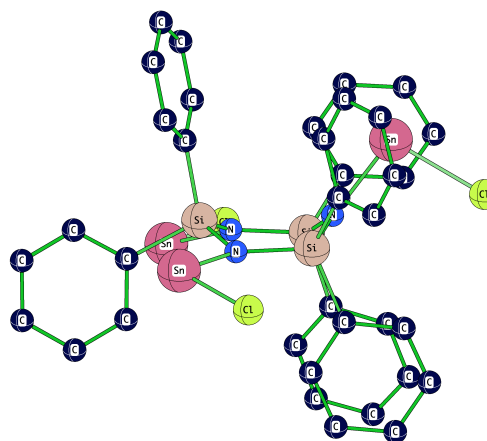


Figure 2.56: Optimized (mPW1PW91/sdd) structure of tri-(SnCl)-hexaphenylcyclotrisilazane; hydrogens were omitted for clarity

Roesky et al. synthesized monomeric divalent tin(II) compounds with terminal chlorine substituents ($[\text{PhC}-(\text{NtBu})_2\text{SnCl}]$) [35] - see Figure 2.57.

Table 2.21: Experimental data of $[\text{PhC}-(\text{NtBu})_2\text{SnCl}]$ according to [35].

data	experimental
spacegroup	P1
Sn-Cl [pm]	248.3
Sn-N [pm]	217.7
	219.2
angle N-Sn-Cl	94.16°
angle N-Sn-N	66.80°
^{119}Sn shift [ppm]	26.6

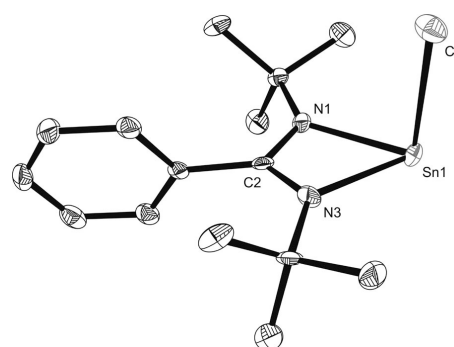


Figure 2.57: Solid state structure of $[\text{PhC}-(\text{NtBu})_2\text{SnCl}]$; hydrogens were omitted for clarity

The N-Sn-Cl unit in the tris-(SnCl)- hexaphenylcyclotrisilazane molecule can be easily compared to the corresponding unit in the $[\text{PhC}-(\text{NtBu})_2\text{SnCl}]$ molecule. The N-Sn distances are very similar (213 pm in the tris-(SnCl)- hexaphenylcyclotrisilazane and 217 pm for the $[\text{PhC}-(\text{NtBu})_2\text{SnCl}]$), as well as the Sn-Cl distances (250 pm and 248 pm). Even the geometry around the Sn - atom is pretty comparable, including the N-Sn-Cl angles of 98.76° (for tris-(SnCl)- hexaphenylcyclotrisilazane) and 94.16° (for $[\text{PhC}-(\text{NtBu})_2\text{SnCl}]$). Only the ^{119}Sn chemical shift differs, but that may come from solvent interactions and concentration effects and the different N-Sn-N angles. The tin(II) center in the $[\text{PhC}-(\text{NtBu})_2\text{SnCl}]$ molecule is three-coordinated. Also the coordination sphere makes a difference in the ^{119}Sn chemical shift.

Tin(II) halides can act as precursors for subsequent reactions with nucleophiles or they can be reduced to build up tin-clusters. There is plenty of room for new discoveries in tetrylene chemistry.

Stable tin(II) compounds and related tetrylenes are an abundant class of compounds. Therefore we studied N- and NN-substituted tetrylenes. The results will be discussed in the following chapters.

2.5 Dip-Coating and Solid-phase Pyrolysis

Hexaphenylcyclotrisilazane can be converted to an infusible polymer of exceptional and chemical stability. Polymerization of hexaphenylcyclotrisilazane can be described by equation 2.5.



Already in 1965 Lacey and Burks reported about their attempts to polymerize hexaphenylcyclotrisilazane by thermal treatment. They observed a loss of weight and assumed that benzene is eliminated during the polymerization reaction. Further they described the coating as smooth, colorless and transparent [36].

We also did a very similar experiment. First of all we made a suspension of hexaphenylcyclotrisilazane in THF. Second, glass stripes were coated with this solution and dried in vacuo for five minutes to remove the solvent. The crude coat was placed in an oven and heated over night (14 hours) at 500°C at atmospheric pressure. The result was that the glass stripes were covered with a colorless, transparent hard film.

To verify what happened during the pyrolysis process, ^1H , ^{13}C and ^{29}Si NMR measurements were done. Some pieces of the coating were dissolved in CDCl_3 . According to the NMR spectra no traces of the starting material could be found, only some polymer traces were detected in the ^{29}Si NMR. On the one hand this means that the polymerization was successful and on the other hand it indicates that the coat is not very soluble in CDCl_3 .

We also tried to melt the crude coat at atmosphere pressure and an open flame to generate an insoluble film (2 minutes heating until everything is liquid). The result is, that the hexaphenylcyclotrisilazane melts but it does not polymerize. It recrystallizes on the surface- see Figure 2.58.

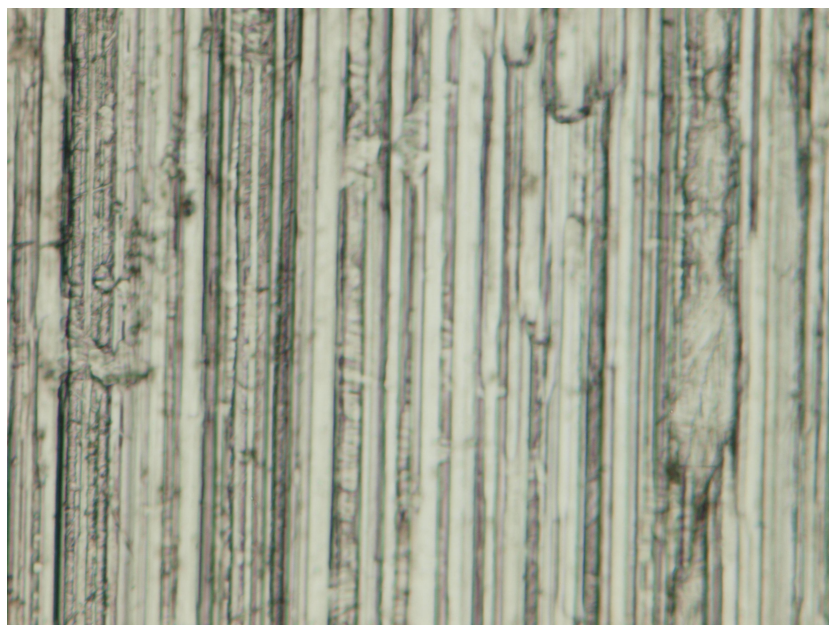


Figure 2.58: Hexaphenylcyclotrisilazane coat on a steel plate, showing the recrystallized starting material

Control measurements by NMR showed that, there is still starting material in the film. This means that temperatures above 450°C are necessary to initiate the polymerization reaction.

Figure 2.59 displays the Si-N coat on a glass plate and Figure 2.60 shows the coat on a steel plate. The two different surfaces are built due to the different underground. The steel plates are rough and the glass plates have a more glazed surface. Therefore the produced coat looks different - but it has the same composite.

To make a persistent film all over the glass or steel plate it is necessary to dip-coat the plates several times. During these experiments we found out that coatings on the glass plates are more glossy and have less gaps on the surface.

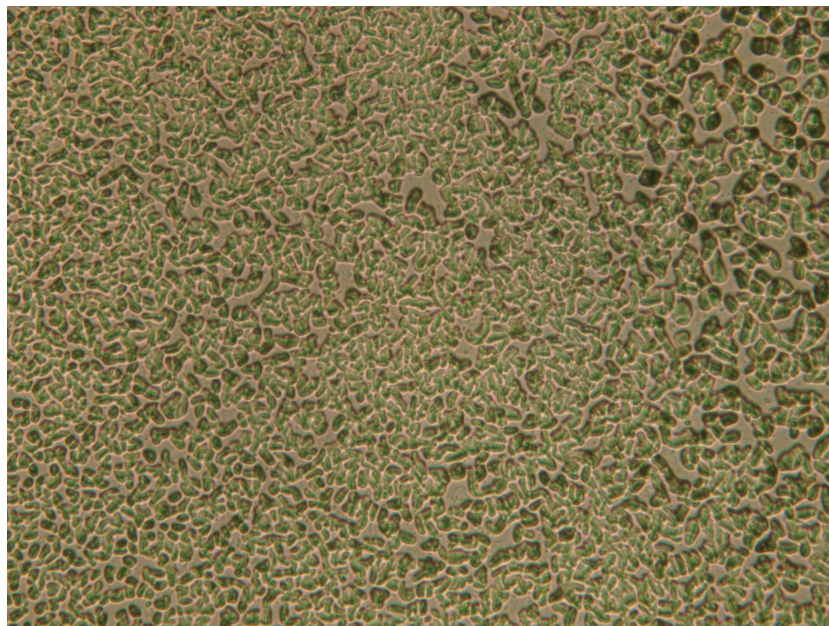
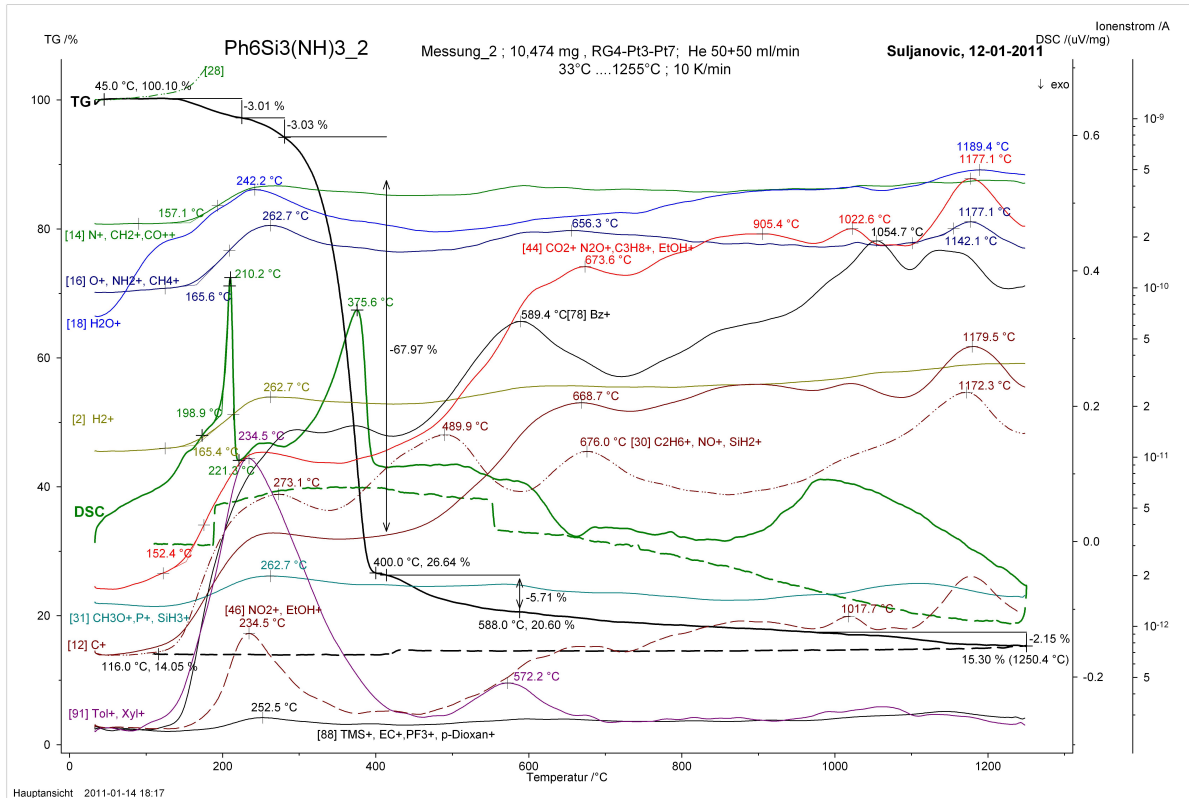


Figure 2.59: Finished hexaphenylcyclotrisilazane coat on a glass plate; resolution 1:50 000



Figure 2.60: Finished hexaphenylcyclotrisilazane coat on a steel plate; resolution 1:50 000

To prove the assumption that benzene is eliminated during the reaction we did a thermogravimetric measurement. Figure 2.61 displays the resulting curves and data.



mass loss of $\text{Ph}_6\text{Si}_3\text{N}_3$

formation of C_6H_6

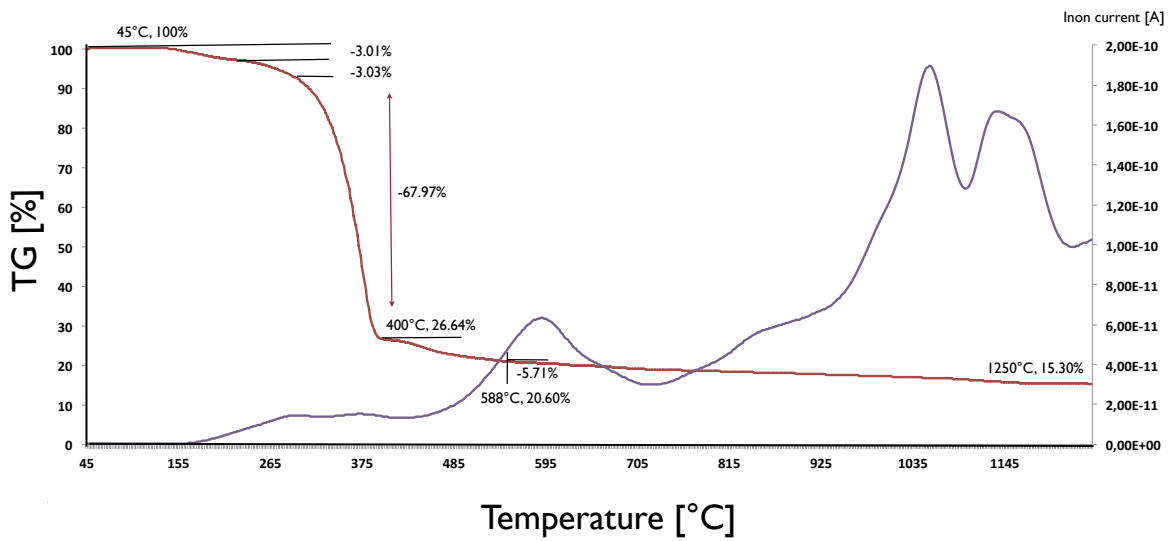


Figure 2.61: Thermogravimetric analysis of hexaphenylcyclotrisilazane.

The first map in Figure 2.61 shows the whole measurement and all generated data. The second map gives information about mass loss as a function of temperature. Obvious is, that at 400°C the mass decreases dramatically (-67.97%). At 400°C the reaction starts and at 450°C the reaction is getting faster.

This means that a transformation of the starting material happens. Simultaneously benzene is produced. The higher the temperature the more benzene is formed. At 588°C a big amount of benzene is produced and the mass losing process is getting slower. The formation to the Si-N coat takes places at temperatures between 588°C and 1250°C.

Benzene was detected in the mass analyzer. During the heating process a loss of mass happens at about 82% of the original amount of hexaphenylcyclotrisilazane.

It is also possible to put additives like PbO or some other oxides into the hexaphenylcyclotrisilazane mixture and to heat them up. We tried these kind of experiments with PbO, and we were able to produce a glasslike coat, but we were not able to fully characterize this material. However, NMR measurements showed, that there are no phenyl groups in the probe.

3 Tetrylenes

3.1 Introduction

During the last decades, tetrylenes were the focus of a wealth of research. [37], [4], [38].

Silylenes, germylenes, stannylenes and plumbylenes are analogues of the classical carbenes. These heavy analogues of the carbenes are so called metallylenes or tetrylenes. The oxidation state of the central atom of the tetrylenes is (+II), bearing an additional electron lone-pair at the metal center. In contrast to the carbenes the heavier analogues have exclusively singlet ground states, because two electrons remain in an ($3 sp^2$)-orbital - see Figure 3.1. It was stated, that heavier group 14 carbene analogs (as tin and lead) do not tend to form hybrid orbitals but instead remain in $(ns)^2(np)^2$ electron configuration due to the increasing s-p gap for larger elements [39]. In contrast silylenes and germylenes can form hybrid orbitals.

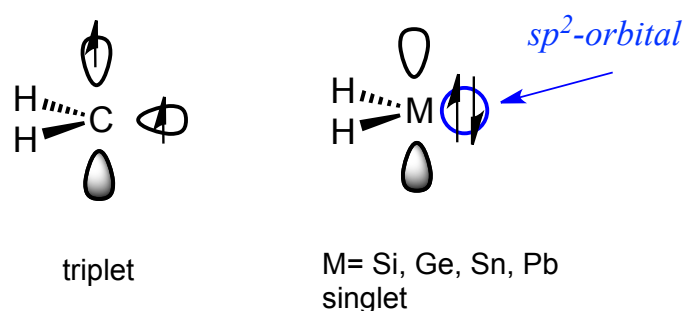


Figure 3.1: Difference between the ground states of carbenes and metallylenes

Further tetrylenes can act as Lewis-amphoteric species, where the acidic and basic center coincide at the metal center. The sp^2 -orbital (lone pair / mostly HOMO) is reactive for nucleophilic attack. The vacant p-orbital (mostly LUMO) is reactive for the electrophilic attack. Therefore these highly reactive species require stabilization.

The stabilization of the tetrylenes can be accomplished by kinetic or/and thermodynamic stabilization. This is by variation of the substituents on the the central atom - see Figure 3.2.

It is necessary to prevent the vacant p-like orbital from inter- and intramolecular reactions.

Therefore steric hindrance (bulky ligands) and electronic effects (hetero atoms as N, O, P) offer the possibility to isolate stable tetrylenes.

There are various ligand-designs, which can stabilize metallylenes. Ligands can be bulky, can feature π -donor/ σ -acceptor atoms or can have both attributes for successful stabilization of metallylenes.

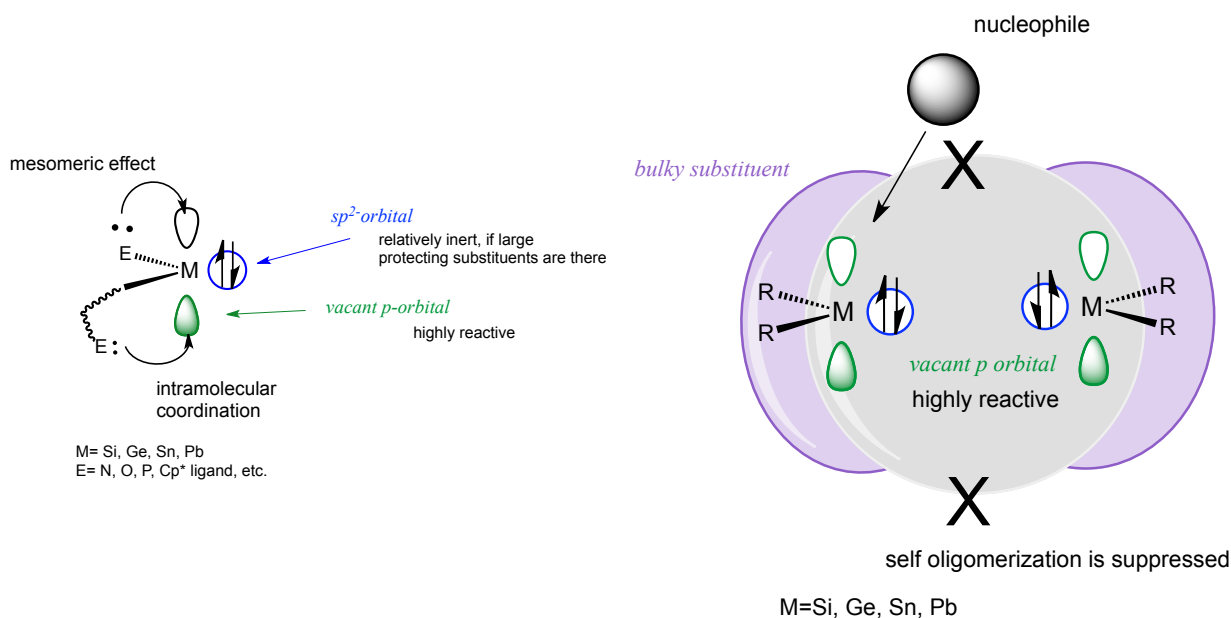


Figure 3.2: Thermodynamic and kinetic stabilization of tetrylenes

Otherwise these highly reactive species will undergo self-oligomerization and build the corresponding dimer, oligomer or even polymer. This is especially true for silylenes, which are believed to be the monomers of polysilanes [39].

On the basis of their ligand type and substitution pattern it is possible to differentiate homo-leptic and hetero-leptic tetrylenes. Homo-leptic tetrylenes have two same ligands or substituents on the metal center. In some cases the ligand system is symmetric. In contrast, hetero-leptic tetrylenes possess two different ligands or substituents on the metal center.

Kinetic stabilization can be achieved by sufficiently bulky substituents (R).

The first isolable and stable homo-leptic tetrylene ($\text{Sn}[\text{CH}(\text{SiMe}_3)_2]_2$ -Figure 3.3) was synthesized by Lappert et. al. in 1976. They found out that the stannylyene exists as a monomer in the gas phase and as a centro-symmetric dimer in the solid state. Whereas in solution a dimer-monomer equilibrium mixture was proposed [40].

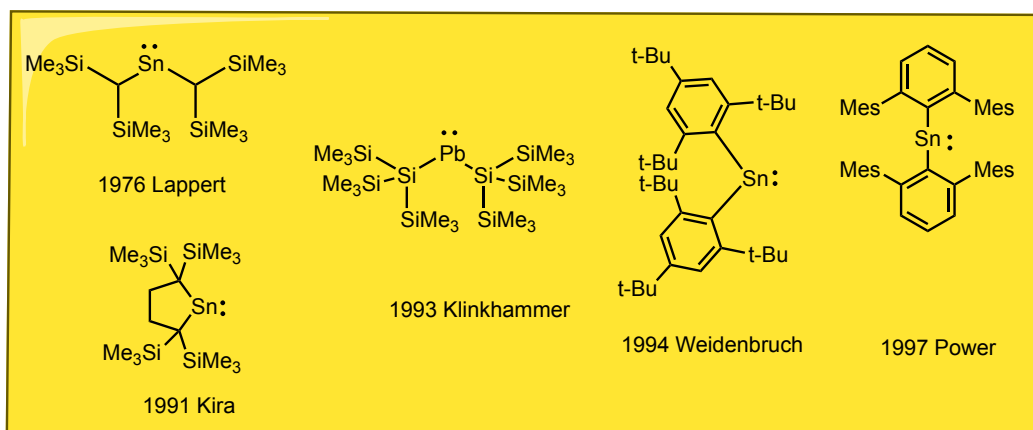


Figure 3.3: Kinetically stabilized tetrylenes $\text{Sn}[\text{CH}(\text{SiMe}_3)_2]_2$ [40], dialkylstannane [41] $\text{Sn}[\text{CH}(\text{SiMe}_3)_2]_2$ [42] and $\text{Sn}(2,6\text{-Mes}_2\text{C}_6\text{H}_3)_2$ [43]

Kira et al report about the first monomeric dialkylstannene (Figure 3.3) with coordination number 2 in the solid state. The dialkylstannylene involves a bulky cyclic bis(trimethylsilyl)-alkyl substituent on tin. The substituent works like a helmet, protecting the central atom much more efficient from dimerization, than Lapperts derivative [41].

In 1994 Weidenbruch et. al. introduced the first diarylstannylene ($\text{Sn}[\text{CH}(\text{SiMe}_3)_2]_2$ - Figure 3.3) which also exists without intramolecular donor-stabilization. They proposed that the bulky ortho-tert-butyl groups in $\text{Sn}[\text{CH}(\text{SiMe}_3)_2]_2$ not only hinder cyclotristannene formation, but also destabilize a possible distannene [42].

Another similar example of a donor-free stabilized diarylstannylene ($\text{Sn}(2,6\text{-Mes}_2\text{C}_6\text{H}_3)_2$ - Figure 3.3) was reported by P. Power et. al. in 1997. In the solid state the compound exists as a monomer, having an extremely large C-Sn-C angle of 120° [43].

Very similar observations were made by Klinkhammer et. al. in 1995. They synthesized and crystallized a hypersilyl substituted plumbylene, ($\text{Pb}[\text{Si}(\text{SiMe}_3)_3]_2$), where the sterically demanding hypersilyl-substituents protect the lead central atom. In the solid state they observed the compound as a monomer [44].

All these examples of metallylenes bear a bulky ligands for their stabilization. There is no further π -donor atom in the ligand system. They are exclusively kinetically stabilized.

Stabilizing tetrylenes by bulky substituents works very well - but it is also possible to offer an additional π -donor / σ -acceptor (N, O) in the ligand system.

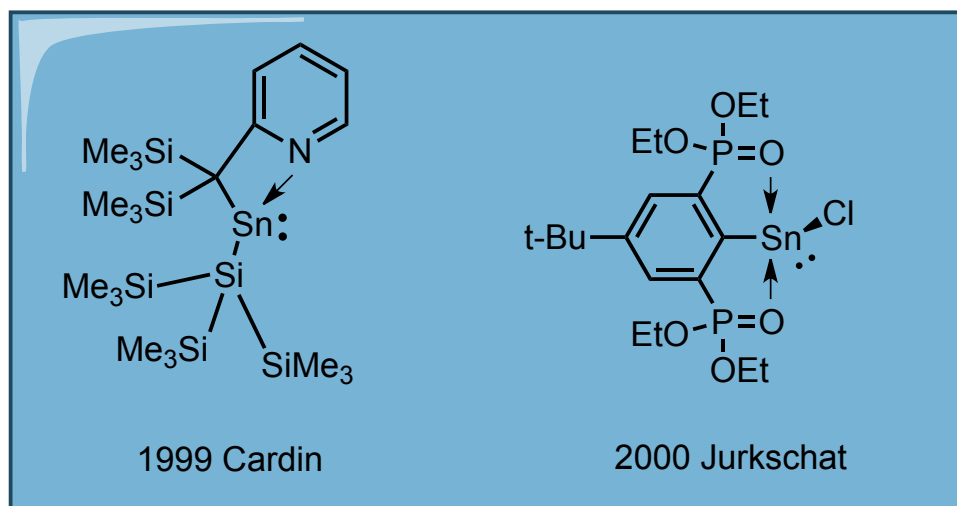


Figure 3.4: Exclusively thermodynamically stabilized tetrylenes, $\text{Sn}[2-(\text{Me}_3\text{Si})_2\text{C}](\text{C}_5\text{H}_4\text{N})[\text{Si}(\text{SiMe}_3)_3]$ [45], $2,6-[(\text{P}(\text{O})(\text{OEt})_2)_2-4\text{-tert-BuC}_6\text{H}_2]\text{SnCl}$ [46].

Intramolecular stabilization of a tetrylene can be provided by coordinating ligands, containing nitrogen, phosphorous or oxygen atoms in their system. These are only examples for a variety of ligand systems and coordinating hetero-atoms.

For instance in 1999, Cardin and coworkers prepared and characterized monomeric heteroleptic derivatives of divalent Sn (Figure 3.4). Stabilization of the tetrylene $\text{Sn}[2-(\text{Me}_3\text{Si})_2\text{C}](\text{C}_5\text{H}_4\text{N})[\text{Si}(\text{SiMe}_3)_3]$ is provided by intramolecular interaction of Sn with the pyridine-nitrogen. The nitrogen electron lonepair donates electrons into the vacant p-like orbital of the central metal atom [45].

In 2000, Jurkschat et. al. demonstrated the versatility of the O,C,O-coordinating ligand in stannylene chemistry. They showed that the ring backbone of the ligand including the coordinating $\text{P}=\text{O}$ donor groups stabilize the tin(II) center [46].

These type of thermodynamic stabilization Jurkschat et.al. already accomplished with oxygen-pincer complexes [46]. But there are more examples of smart ligand systems - see Figure 3.5

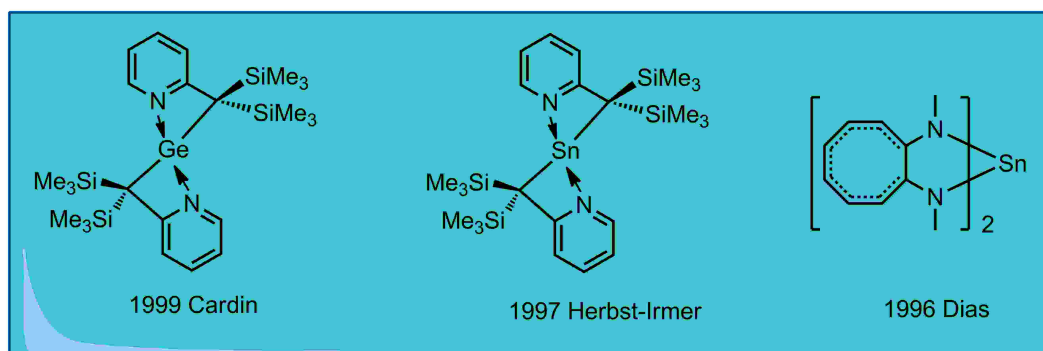


Figure 3.5: Thermodynamically and kinetically stabilized tetrylenes with additional σ -acceptor and π -donor atoms, bis[(2-pyridyl)bis(trimethylsilyl)methyl]germanium(II) [47] and di[2-pyridylbis(trimethylsilyl)methyl]tin(II) [45], [33], and $[(\text{Me})_2\text{ATI}]_2\text{Sn}$ [48]

Meller and coworkers analyzed bis[(2-pyridyl)bis(trimethylsilyl)methyl]germanium(II) already in 1997. They found out that the Ge-N bond interaction (mean value 227.3 pm) possesses a dative character, while the Ge-C bonds (mean value 212.7 pm) correspond to long Ge-C single bonds [47].

The analog tin(II) compound (bis[2-pyridylbis(trimethylsilyl)methyl]tin(II)) was crystallized and analyzed by C.L. Raston and coworkers. They report, that the C,N-ligands chelate the tin(II) atom. They also observe a longer Sn-C bond (237.7 pm) and a dative character of the Sn-N bond (244.9 pm). Further they found out, that the variation of the ^{119}Sn chemical shift with temperature is consistent with a weak dative pyridyl N-Sn bond. Therefore an equilibrium ^{119}Sn value is measured of the possible coordination number (2 to 4) of the tin(II) atom [33].

In 1996 Dias and Jin published a troponinimide complex with tin(II) as metal center - see Figure 3.5. They describe their structure of the $[(\text{Me})_2\text{ATI}]_2\text{Sn}$ compound as a monomeric structure with a pseudo trigonal bi-pyramidal arrangement at the Sn(II) center.

These tetrylenes are on the one hand stabilized by directly neighboring hetero atoms and on the other hand they have additional donation of the hetero atom placed somewhere in the smart ligand system. The ligand systems are bulky but also include additional donor atoms [49], [50], [48]

Via a combination of bulky and coordinating ligands it should be possible to generate quite stable tetrylenes. So that these compounds can be precursors for further reactions.

We focused this work on hetero-leptic and homo-leptic tetrylenes (M= Ge, Sn, Pb) bearing aminopyridine ligand systems.

3.2 Ge/Sn/Pb Divalent Derivatives

3.2.1 The Aminopyridin Ligand System

For this type of N,N and N,N,N-stabilized tetrylenes, two already common ligand systems have been used- 2,6-diisopropyl-N-(pyridin-2-ylmethyl)aniline and 2,6-bis[[2,6-diisopropylphenyl) amino]methyl]pyridine. The organic amino-pyridine ligands (see Figure 3.6 below) are well reviewed and often applied in transition metal chemistry. They are di- and monohaptic ligands with an additional (N)-coordination center, which can act as a σ -acceptor and π -donor.

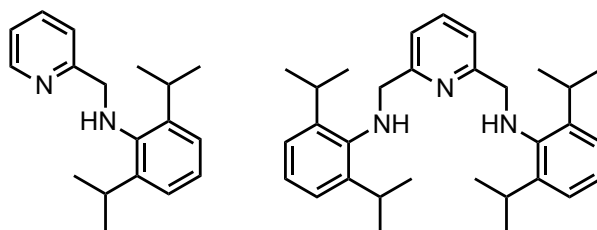


Figure 3.6: 2,6-Bis[[2,6-diisopropylphenyl)amino]methyl]pyridine and 2,6-diisopropyl-N-(pyridin-2-ylmethyl)aniline

In 2003, Gibson et. al. published a complex containing an iron metal as active catalytic center [51]. These iron(II) complexes are good catalysts for electron transfer radical polymerization. A notable feature of these imino-pyridine /amino-pyridine systems is, that the catalyst activity is dependent of the substituents on the nitrogen position - see Figure 3.7; which shows the iron (II) catalyst .

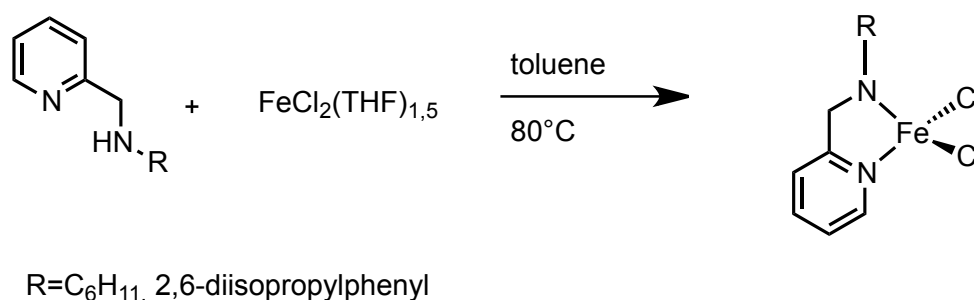


Figure 3.7: Synthesis of the iron(II) aminopyridine catalyst according to [51]

Also other transition metals have been used such as thorium [52] or vanadium [53] . The generated complexes are used in ring opening or closing metathesis as well as catalysts for polymerization reactions. Figure 3.8 below shows applications of the amino-pyridine ligand.

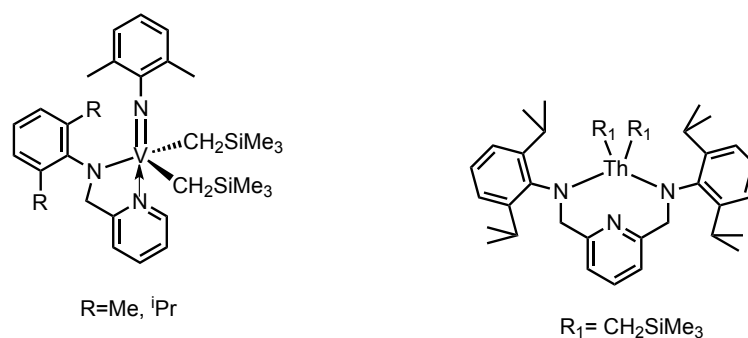


Figure 3.8: Examples of transition metal complexes with amino-pyridine ligands [52], [53]

There are more examples of transition metal complexes using this type of amino-pyridine ligands [54][55]. However only a few complexes with group 14 elements, such as tin or lead, as central atom are known. Westerhausen et. al. built complexes with tin(II) as central atom using bis[N-(diphenylphosphanyl)(2-pyridylmethyl)amide] as organic ligand (see Figure 3.9)[56]. They synthesized homoleptic and heteroleptic stannylenes, which have the feature to be stabilized by additional donor/acceptor atoms.

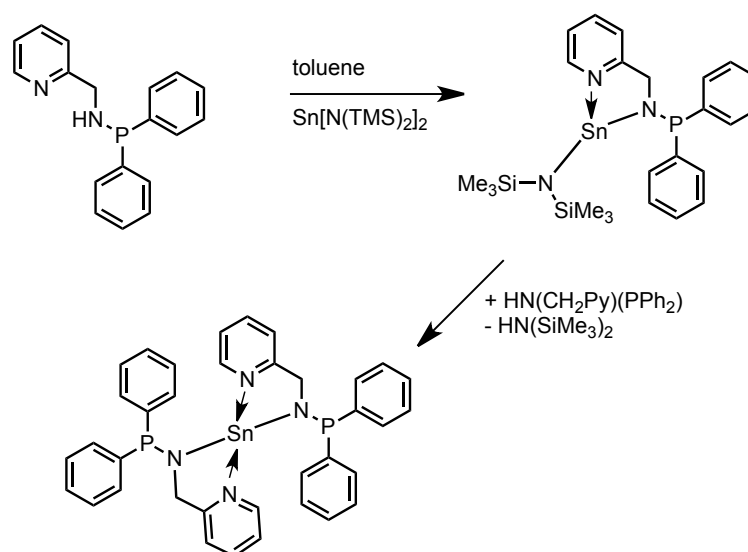


Figure 3.9: Synthesis of homo and hetero-leptic tin(II) complexes with a phosphanyl-2-pyridylmethyl-amide ligand [56]

In these complexes the N-(diphenylphosphanyl)(2-pyridylmethyl)amido groups act as bidentate ligands through the nitrogens. The tin (II) atom lies in a pyramidal environment and the hetero-leptic stannylene can be transformed to the homo-leptic analog via a transamination reaction[56].

Synthesis

How to generate homo-leptic and hetero-leptic tetrylenes? How to treat the ligand system so that it stays intact during the reaction? In general, there are two possible ways to accomplish synthesis. Pathway number one is to make a transamination reaction with a soft metallation reagent, such as $\text{Sn}[\text{N}(\text{SiMe}_3)_2]_2$. This is a very elegant and easy method. The other pathway is a common metallation with some hard organo-metal agents like $n\text{-BuLi}$ followed by a salt elimination reaction with some adequate metal salts, such as SnCl_2 , PbCl_2 , and GeCl_2 . Figure 3.10 illustrates both synthesis methods.

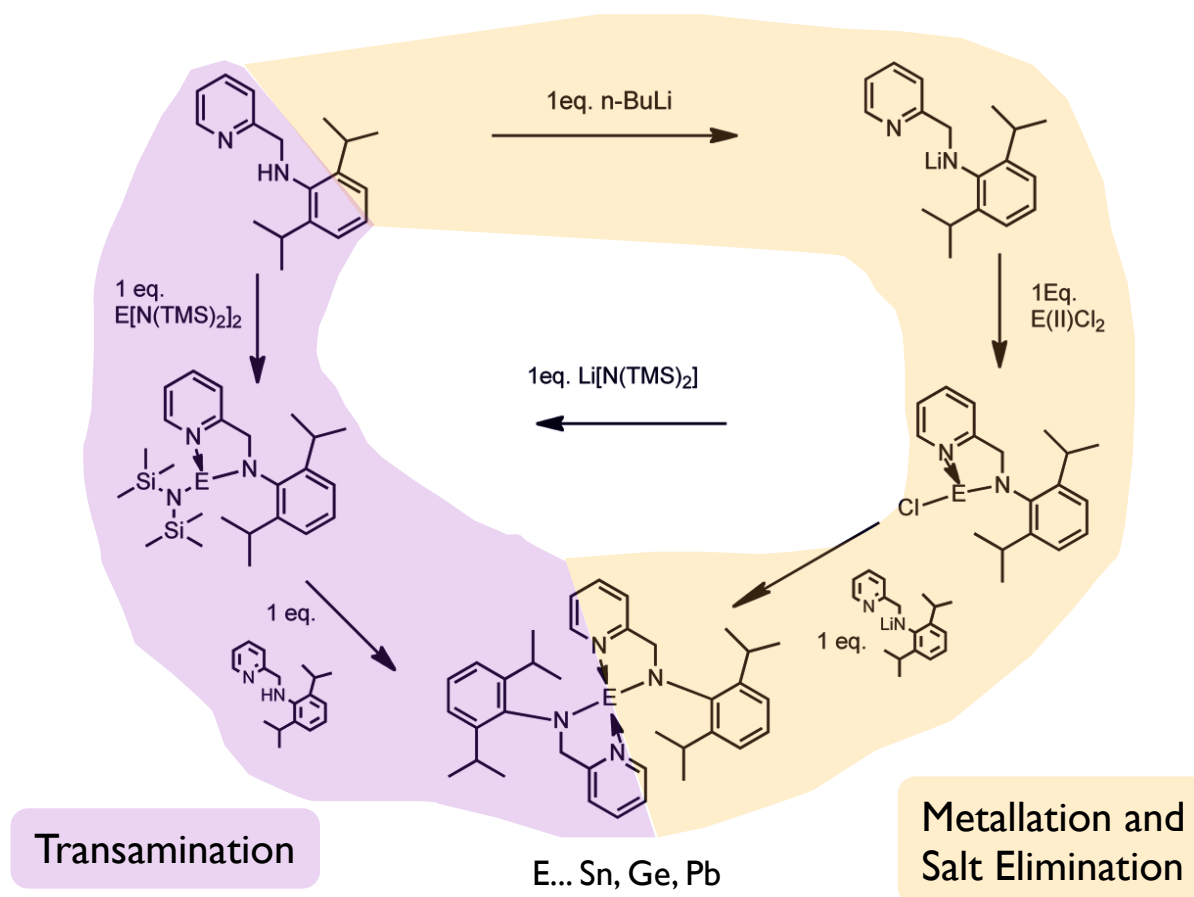


Figure 3.10: Reaction pathways for tetrylene synthesis

With this reaction pattern it is possible to catch all intermediate products and to characterize them. Treatment of the 2,6-diisopropyl-N-(pyridin-2-ylmethyl)aniline ligand with $n\text{-BuLi}$ leads to the lithiated ligand - Figure 3.11.

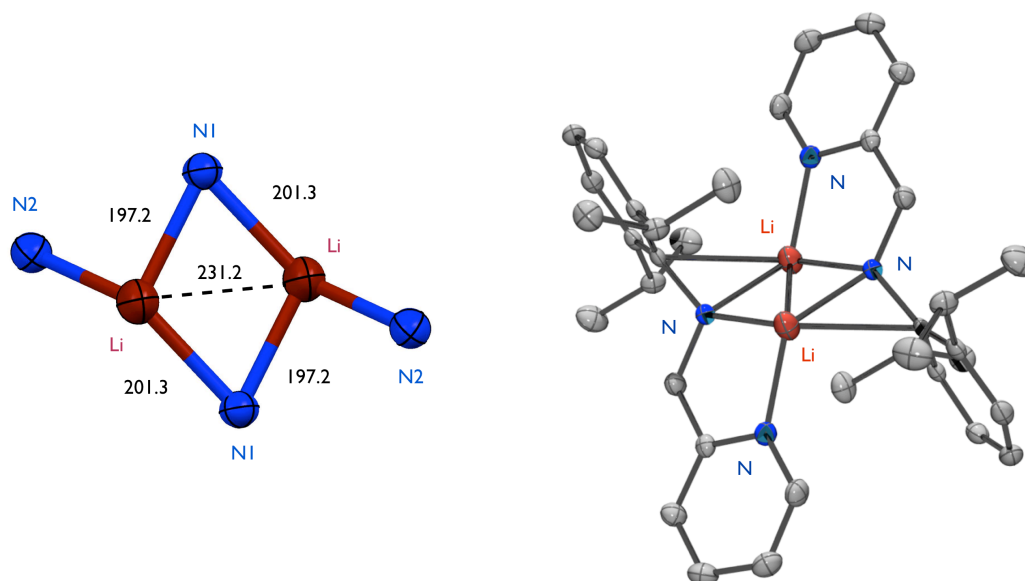


Figure 3.11: Solid state structure of lithium 2,6-diisopropyl-N-(pyridin-2-ylmethyl)aniline with distances in [pm]

The structural motif of Li_2N_2 rings is very common in lithium chemistry [57][58][59]. Literature reports about Li-N bond distances of 199.0 pm - 204.5 pm. The observed Li-N distances for lithium 2,6-diisopropyl-N-(pyridin-2-ylmethyl)aniline are similar (from 197.2 pm to 201.3 pm). Remarkable is the quite short inter-atomic Li-Li distance of only 231.2 pm. This is shorter than in the literature reported (248.1pm) [58]. Although there are many variations of such Li-N compounds, this structure is new for this type of ligand system. It is dimeric in the solid state and gives a deep red solution in THF as solvent.

3.2.2 Chloro-Tetrylenes

During the reaction it was possible to isolate stable chloro tetrylene derivatives of the amino-pyridine ligand system. This type of compounds is not so common. They usually appear as intermediates and precursors for other reactions [45].

Using the mono-dentate amino-pyridine ligand it was possible to built up chloro derivatives with Ge, Sn, and Pb - see Figure 3.12 . Some of the compounds crystallized others could only be characterized by ^1H , ^{13}C and hetero atom NMR measurements.

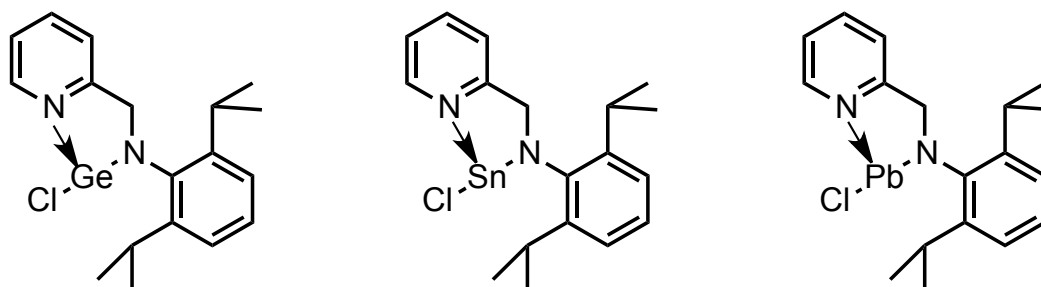


Figure 3.12: Chloro-tin(II)N-(diisopropyl)(2-pyridylmethyl)amide, chloro-germanium(II)N-(diisopropyl)(2-pyridylmethyl)amide, chloro-lead(II)N-(diisopropyl)(2-pyridylmethyl)amide

In literature it has already been reported about chloro-germylenes [45], [60]. These compounds are stabilized by an additional nitrogen σ -acceptor, π -donor atom. Very interesting is the N-Ge-Cl structure motif in these compounds - Table 3.1 shows selected data from the literature.

We also were able to find this special structural motif in our tetrylenes.

Table 3.1: Data from the solid state structures of dipp-NacNac-Ge(II)-chloride[60] and [Ge(2-((Me₃Si)₂C)-C₅H₄N)Cl][45]

distances [pm]		
Ge-Cl	229.5	229.4
Ge-N2	199.3	-
Ge← N1	-	208.2
N1-Ge-Cl angle	95.00°	91.89°

There are two types of Ge-N bonds. One represents a covalent single bond (199.3 pm) and the other one (208.2 pm) represents a stabilizing donor interaction. Obviously the dative bond has got a longer bond length (204.1 pm[61]) than the common Ge-N bond. The chlorine atom is normal on the N-Ge-C/N plane. This is indicated by the N-Ge-Cl angle (95.00° and 91.89°).

These literature known parameters can be compared with our chloro-germylene. In Table 3.2 parameters from the geometry optimized (mPW1PW91/SDD) and the solid state structure are displayed.

Table 3.2: Experimental and optimized (mPW1PW91/SDD) data from Cl-germanium(II)N-(diisopropyl)(2-pyridylmethyl)amide

distances [pm]	experimental	calculated
Ge-Cl	235.8	245.3
Ge-N2	185.9	191.0
Ge← N1	206.0	215.3
N2-Ge-Cl angle	99.01°	101.00°
N1-N2-Ge-Cl angle	85.05°	82.00°

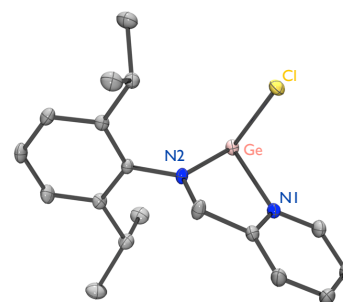


Figure 3.13: Solid state structure of Cl-germanium(II) N-(diisopropyl)(2-pyridylmethyl)amide. Hydrogens were omitted for clarity.

Calculated and measured data show the same trend. The covalent Ge-N bond is at the expected value (185.9 pm observed and 191.0 pm calculated). The N-Ge dative bond is longer (206.0 pm observed and 215.3 pm calculated) and again as expected the chlorine atom is normal to the N1-N2-Ge layer with a dihedral angle of 85.05° and 82.00°.

In the solid state structure (see Figure 3.13) the nitrogen atoms (N1 and N2) are in a trigonal planar environment with a bond angle sum of 359.89°(N1) and 359.81°(N2) as well as in the geometry optimized structure (359.99°(N1) and 359.89°(N2)). The compound crystallizes as a monomer.

Unfortunately, not all intermediate chloro-tetrylenes crystallize. Therefore, quantum chemical calculations were done to get some information about the geometry of these compounds. Figure 3.14 displays the geometry optimized (mPW1PW91/SDD) chloro-tetrylenes.

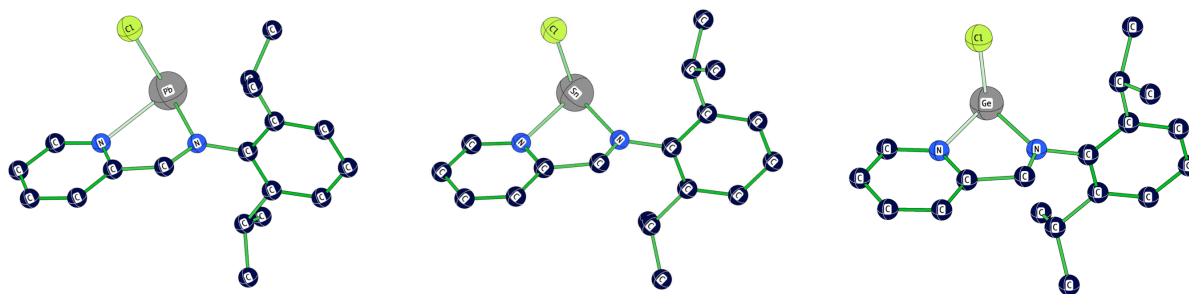


Figure 3.14: Geometry optimized structures of (Chloro-lead(II)N-(diisopropyl)(2-pyridylmethyl)amide, Chloro-tin(II)N-(diisopropyl)(2-pyridylmethyl)amide, Chloro-germanium(II)N-(diisopropyl)(2-pyridylmethyl)amide

The three structures in Figure 3.14 have similar geometry characteristics. In Table 3.3 the calculated geometry data are displayed.

Table 3.3: Calculated (mPW1PW91/SDD) data of the Cl-E(II)N-(diisopropyl)(2-pyridylmethyl)amides

distances [pm]	E=Ge	E=Sn	E=Pb
E-Cl	245.3	257.6	264.1
E-N2	191.0	208.1	217.7
E← N1	215.3	< 233.1	< 244.6
N2-E-Cl angle	101.00°	98.02°	99.04°
N1-N2-E-Cl angle	82.00°	> 79.51°	> 79.09°
HOMO-LUMO gap	4.03 eV	3.29 eV	2.09 eV
	307 nm	376 nm	593 nm
ΔE [kJ/mol]	67	62	58
NICS Bq1 [ppm]	-0.71	-0.75	-0.8
NICS Bq2 [ppm]	-6.9	-6.4	-7.0

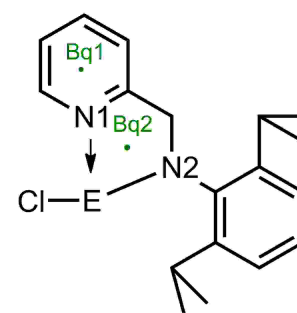


Figure 3.15: Substitution pattern.

The ΔE values are the energy differences between the open and closed conformation.

All E-N1/N2, E-Cl bond distances become longer the heavier the central atom becomes - see Table 3.3, due to the growing size of the atom radii of the elements within the group. There is not much difference in the N2-E-Cl angle. The chlorine atom is always more or less normal to the N1-N2-E layer. This is also confirmed by the calculated dihedral angles 82.00°, 79.51° and 79.09°.

In Table 3.4 common dative and common E-N single bonds are summarized, for comparison with our calculated data. As already discussed for the chloro-germylene derivative, calculated and experimental data fit to literature known values.

The same result we observed for the tin(II) and lead(II) chloro-tetrylene compound. The common experimental Sn-Cl single bond is at 248.3 pm [35], and we found 257.6 pm in our geometry optimized structure. Here as well we can observe the dative Sn-N1 bond, 233.1 pm in the simulation and 236.6 pm from literature [62].

The geometry optimized data for the chloro-plumbylene can also be compared with data from literature. For the Pb-N2 single bond literature reports values of 227.5 pm and we found 217.7 pm. Also the dative Pb-N1 bond can be identified, we found 244.6 pm and in literature values at about 243.6 were reported [63].

Table 3.4: Literature known E-N distances

distances [pm]	E-Cl	E-N2	E← N1	literature
E=Ge	229.5	199.3	208.2	[60],[45]
E=Sn	248.3	210.1	236.6	[35],[62]
E=Pb	-	227.5	243.6	[63]

Analysis of the aromaticity of these chloro-tetrylenes shows that the pyridine backbone is not aromatic. The calculated NICS values are nearly at zero ppm. In contrast the N1-C-C-N2-E five membered ring is aromatic, showing NICS values at -6 ppm.

The stabilizing effect of the N1-pyridyl nitrogen atom becomes smaller the heavier the central atom is - mirrored in the falling ΔE values. The ΔE values are the energy differences between the open and closed conformation. The closed conformation represents the global minimum, as we found in the solid state structure for the chloro-germylene.

Remarkable is also that the HOMO-LUMO gap is becoming smaller- see energy-level diagram, Figure 3.16. According to literature [64] it should grow, but in our case it is making the triplet state easier accessible.

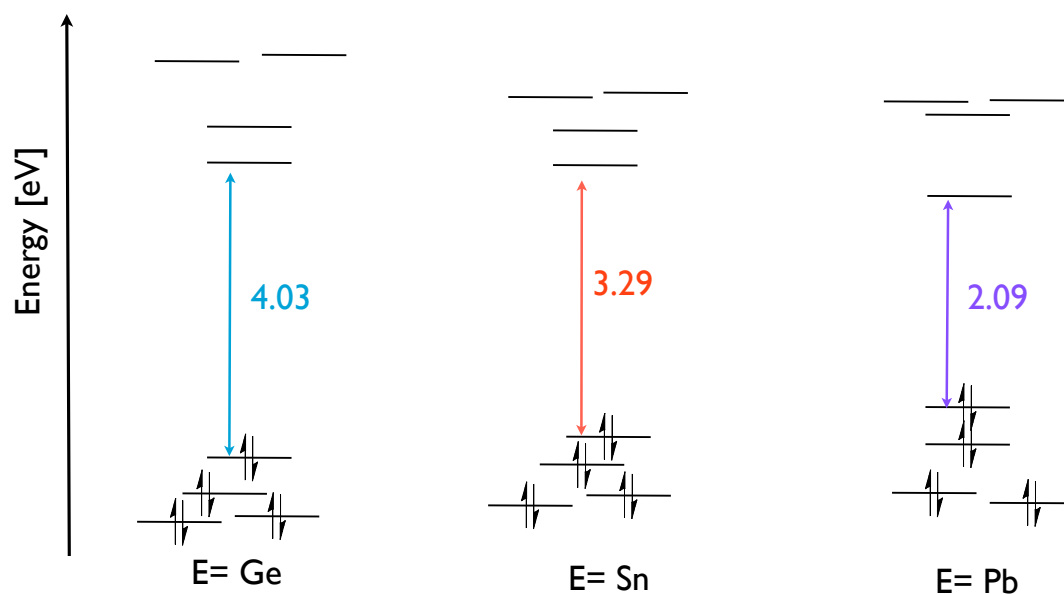


Figure 3.16: Energy-level diagram of Cl-E(II)N-(diisopropyl)(2-pyridylmethyl)amides

The heavier E becomes, the more the HOMO rises in energy and the LUMO orbital decreases in energy. Therefore the gap becomes smaller the heavier the metal center is. This also can be observed in the experiment. The solutions of these compounds are typically colored yellow-orange (Ge), yellow-green (Sn), and yellow (Pb).

NBO analysis will show how the pyridyl-nitrogen and the chlorine ion influence the metal center - see Figure 3.17

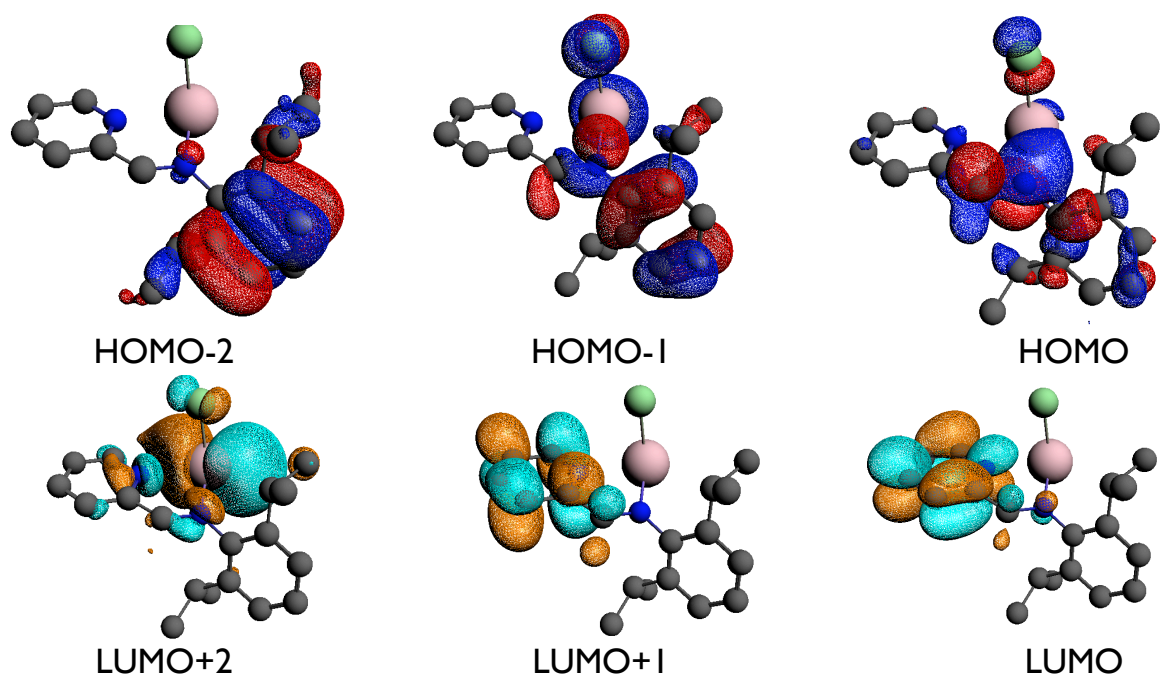


Figure 3.17: Natural bond orbitals of Cl-E(II)N-(diisopropyl)(2-pyridylmethyl)amides

The HOMO orbital shows the nitrogen-carbon bond and one lone-pair of the chlorine as well as the electron lone pair at the pyridyl-nitrogen. The corresponding anti-bonding orbital is the LUMO+1, showing π^* -orbitals at the pyridyl backbone. In the HOMO-1 orbital the electron lone pair at the metal center is displayed and the σ -bond between the metal center and the amine nitrogen atom. Additionally there are also the π -orbitals of the diisopropyl containing six-membered carbon ring displayed. The corresponding anti-bonding orbitals are displayed in the LUMO orbital. And last the HOMO-2 orbitals again displays π -orbitals at the diisopropyl containing six-membered carbon ring and the corresponding anti-bonding orbitals is the LUMO+2. In the LUMO+2 orbital the anti-bonding pyridyl-nitrogen and metal center interaction is visible.

These chloro-tetrylenes are thermodynamically stabilized by the pyridine-nitrogen and additionally the bulky Dip-substituent on the second nitrogen atom protects the molecule from dimerization.

We used the chloro-tetrylenes (already asymmetric tetrylenes) as intermediates for further reactions, to synthesize homo-leptic and hetero-leptic tetrylenes.

3.2.3 Bis(TMS)amido-Tetrylenes

These compounds can be generated directly via a transamination reaction of the ligand and a soft reagent such as $\text{Sn}[\text{N}(\text{SiMe}_3)_2]_2$. Alternatively, these substances can be synthesized by a three step reaction. First the desired ligand is metallized with *n*-BuLi, second a metal(II)salt is added and third an additional salt elimination is done with an accordant organo-metal reagent - see Figure 3.10.

There are nearly no examples of hetero-leptic tetrylenes, which include three nitrogen atoms in the immediate vicinity of the metal atom. Here we want to present some examples of these hetero-leptic tetrylenes.

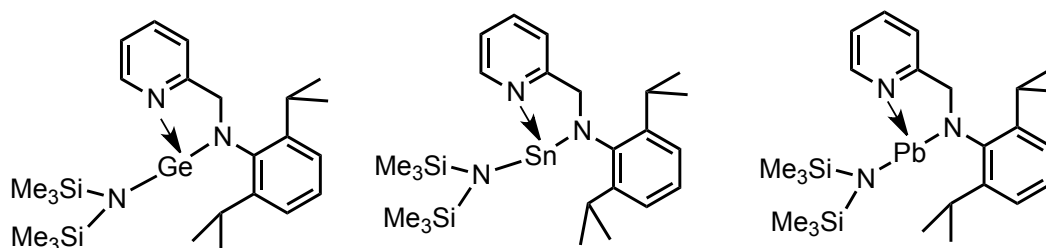


Figure 3.18: Bis(TMS)amidotin(II)N-(diisopropyl)(2-pyridylmethyl)amide, bis(TMS)amidolead(II)N-(diisopropyl)(2-pyridylmethyl)amide, bis(TMS)amidogermanium(II)N-(diisopropyl)(2-pyridylmethyl)amide

These three substances are stabilized by a donor atom (the pyridyl nitrogen) and they are covalently bond to two nitrogen atoms. In 2009, Westerhausen and coworkers published a stannylene, which also was stabilized by a nitrogen as electron donor atom [56] - see Figure 3.19

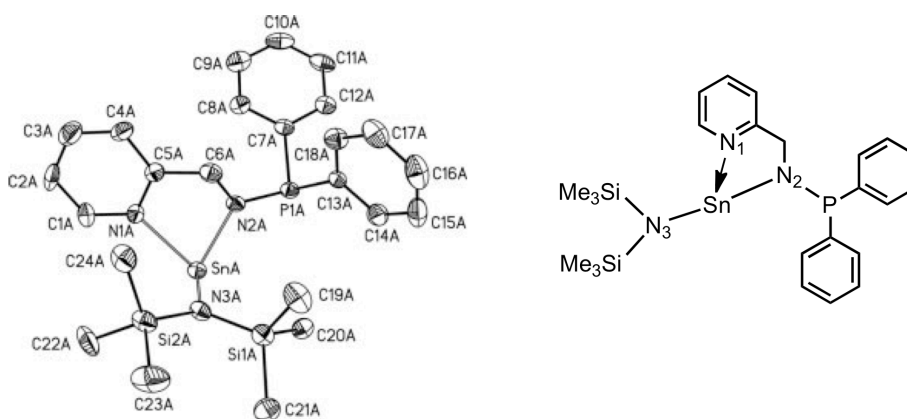


Figure 3.19: Solid state structure of bis(trimethylsilyl)amidotin(II)N-(diphenylphosphanyl)(2-pyridylmethyl)amide. Hydrogen atoms are neglected for clarity reasons [56]

of bis(trimethylsilyl)amidotin(II)N-(diphenylphosphanyl)(2-pyridylmethyl)amide. Hydrogen atoms are neglected for clarity reasons [56]

Westerhausen et.al. mentioned that all Lewis bases can act as donor atoms. They found out that the Sn-N bonds on the anionic amido functionalities are much shorter than on the pyridyl unit-see Table 3.19. The tin(II) atom lies in a trigonal pyramidal environment, with an angular sum of 347.97° [56]. Further the N-(TMS) group is normal to the N1-Sn-N2 layer. That is similar to the geometric arrangement in the chloro derivatives. In Table 3.5 the measured and calculated data are displayed.

Table 3.5: Calculated (BP86/RI/TZVP; Turbomole [65]) and experimental data from the bis(trimethylsilyl)amido tin(II)N-(diphenylphosphanyl)(2-pyridylmethyl)amide [56]

distances [pm]	experimental	calculated
Sn← N1	232.8	242.6
Sn-N2	212.9	220.4
Sn-N3	215.2	216.6
N2-Sn-N3 angle	90.05°	94.30 °
N1-N2-Sn-N3 angle	107.52°	104.74°
¹¹⁹ Sn shift [ppm]	59	-177

Their experimental and calculated data fit quite well, except for the ¹¹⁹Sn chemical shift. The deviation of 118 ppm between the simulated and measured value is too large. This may come from the circumstance that solvent interactions and conformation change were not taken into account for the simulation.

As already mentioned we were also able to synthesize and analyze a hetero-leptic stan-nylene, with a similar bonding situation as in the compound of Westerhausen. Figure 3.20 displays the solid state structure of bis(TMS)amidotin(II)N-(diisopropyl)(2-pyridylmethyl)-amide. According to the crystallographic data the tin(II) atom is in a trigonal pyramidal environment as the compound of Westerhausen. The N[SiMe₃]₂ substituent is normal to the N1-N2-Sn plane.

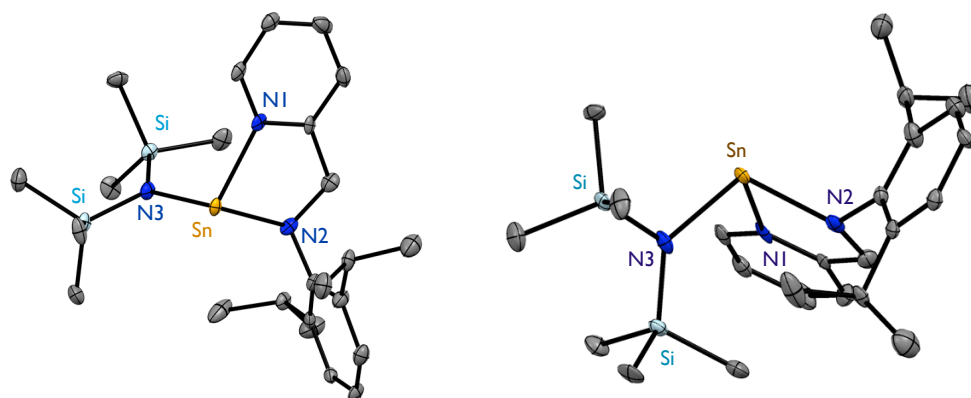


Figure 3.20: Solid state structure of bis(TMS)amidotin(II) N-(diisopropyl)(2-pyridylmethyl)amide; hydrogens were omitted for clarity

In Table 3.6 theoretical and experimental data of the new bis(TMS)amidotin(II) N-(diisopropyl)(2-pyridylmethyl)amide are summarized. Comparison of calculated and experimental data show that in the molecule there are two covalent Sn-N bonds (Sn-N2 212.6 pm in the experiment and 213.8 pm in the calculation and Sn-N3 with 214.5 pm versus 215.7 pm). The third coordination Sn-N1 is a so called σ -acceptor π -donor interaction. This Sn-N1 distance is much longer than the other two bonds, with 226.8 pm in the solid state and 235.7 pm in the simulation - see Table 3.6.

Table 3.6: Calculated (mPW1PW91/SDD) and experimental data of the Bis(TMS)amidotin(II) N-(diisopropyl)(2-pyridylmethyl)amide

distances [pm]	experimental	calculated
Sn← N1	226.8	235.7
Sn-N2	212.6	213.8
Sn- N3	214.5	215.7
N2-Sn-N3 angle	90.00°	79.84 °
angular Σ Sn	277.27°	270.98°
N1-N2-Sn-N3 angle	107.08°	98.76°
^{119}Sn shift [ppm]	80	-114
^{29}Si shift [ppm]	1.89	3.54
	-2.97	-2.48

Calculations confirm, that the tin(II) atom is in a pyramidal trigonal environment. The angular sum at the tin(II) metal center is 277.27° (in the experiment) and 270.98° according to the calculation. Further the N[SiMe₃]₂ group is almost normal to the N1-N2-Sn plane. The N1-N2-Sn-N3 dihedral angle is 107.08°/98.76°.

The quantum chemical simulation did not only give information about bond distances and angles but as well about the ^{119}Sn and ^{29}Si chemical shifts, and the UV-spectra. The quantum chemical calculation confirmed that bis(TMS)amidotin(II)N-(diisopropyl)(2-pyridylmethyl)amide can have at least two different conformations - see Figure 3.21

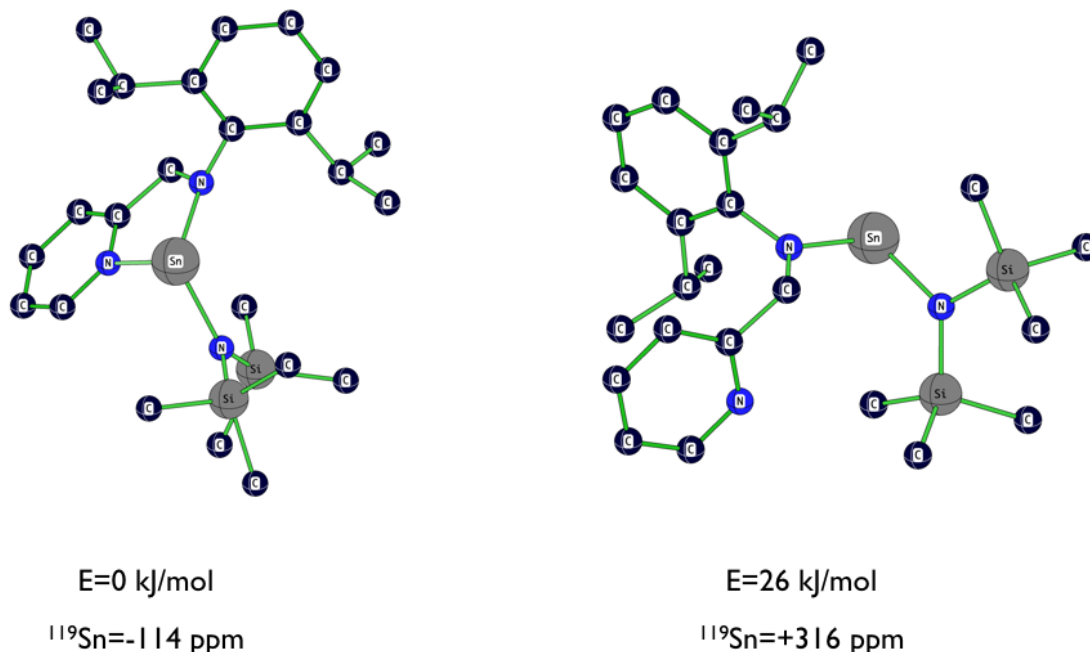


Figure 3.21: Optimized (mPW1PW91/SDD) conformers, energies and ^{119}Sn chemical shifts of bis(TMS)amidotin(II) N-(diisopropyl)(2-pyridylmethyl)amide. Hydrogen atoms were omitted for clarity.

The three-coordinated tin structure represents the global minimum and the two-coordinated (open conformation) is a local minimum. The energy difference between these two structures is 26 kJ/mol. The energetic difference is the reason why in the solid state only one conformation is found and why in the measured NMR spectra only one signal in the ^{119}Sn spectra is observed. Obvious is that the ^{119}Sn chemical shift is heavily influenced by the conformation. For the two-coordinated tin compound a value of 316 ppm was calculated and for the three co-ordinated compound a value of -114 ppm was predicted. Using a Boltzmann distribution[66] correction, the calculated ^{119}Sn chemical shift was assigned with -114 ppm. So the Boltzmann distribution was not the proper explanation for this deviation of values.

Solvent interactions in the experiment have to be taken into account. The ^{119}Sn NMR measurements were carried out in THF as solvent and C_6D_6 -capillary as reference. Calculations with an solvent continuum were carried out, but did not lead to any conclusive results. Because the ^{119}Sn value decreased to -113 ppm, and that is not much. Therefore it would be necessary to place solvent molecules around the substance-molecule.

This calculation would show the influence of the solvent molecules on the ^{119}Sn chemical shift.

As mentioned before, besides geometry optimization, calculation of UV-Vis-spectra is also possible. Organo-metal compounds tend to be colored in solid state and in solution. For instance bis(TMS)amidotin(II) N-(diisopropyl)(2-pyridylmethyl)amide is yellow-greenish in crystal and in heptane solution. Figure 3.22 shows the simulated and measured UV-Vis spectra. The simulation was done with the ADF [67], [68] program using the mPW1PW91 hybrid functional in combination with ZORA for the relativistic effects and TZ2P basis sets.

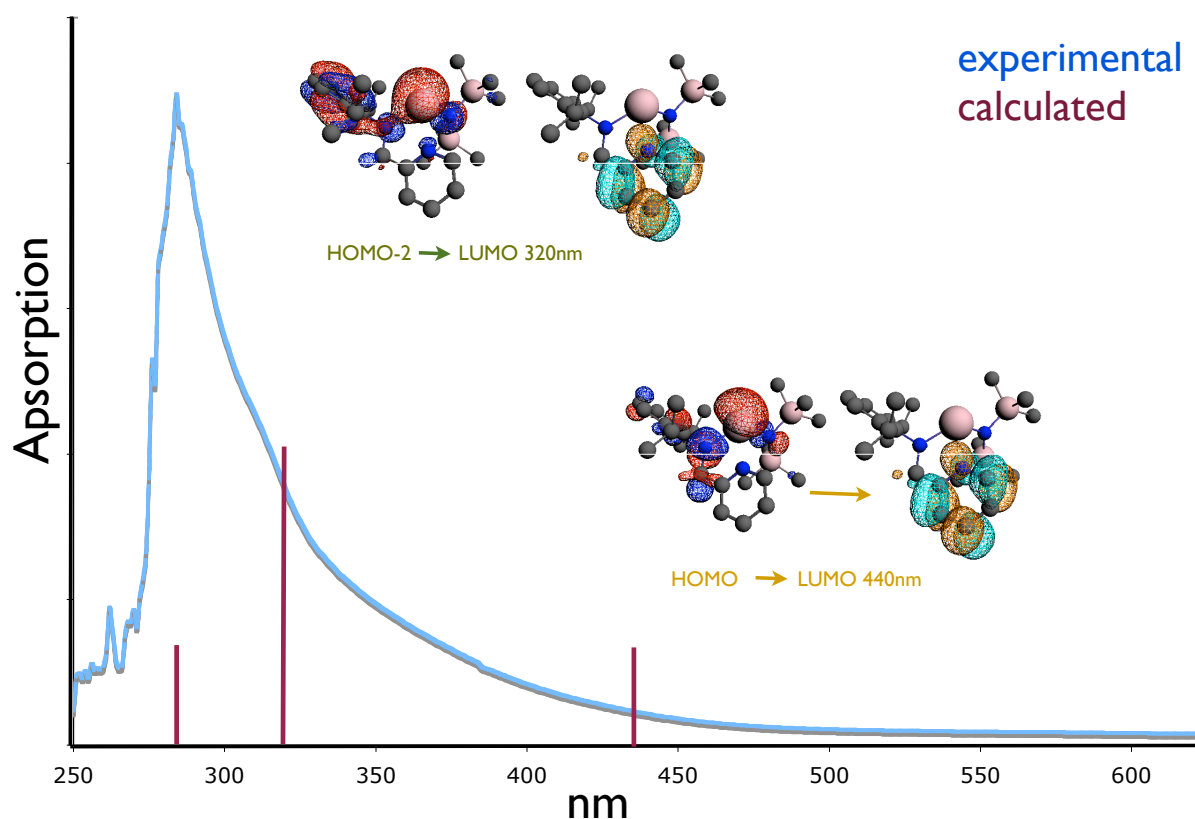


Figure 3.22: Calculated (mPW1PW91/ZORA/TZ2P) and experimental UV-Vis spectrum of bis(TMS)amidotin(II) N-(diisopropyl)(2-pyridylmethyl)amide

Obvious is that the color of the solution and in the crystal comes from the HOMO to LUMO transition. Figure 3.23 displays the molecular orbitals of bis(TMS)amidotin(II) N-(diisopropyl)(2-pyridylmethyl)amide.

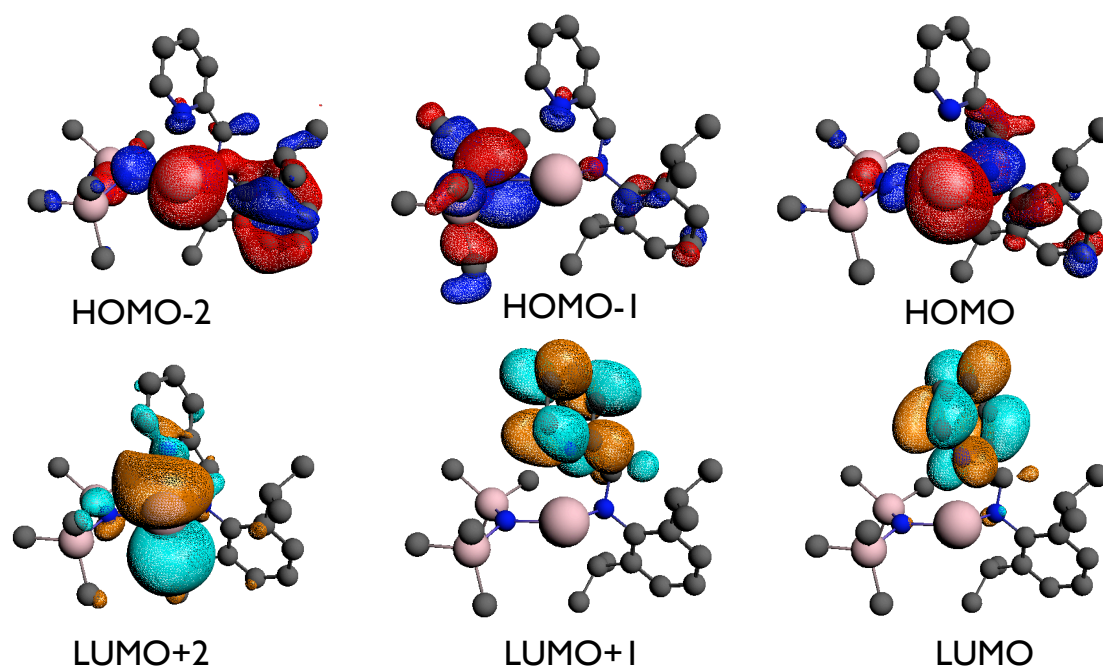


Figure 3.23: Natural bond orbitals of bis(TMS)amidotin(II) N-(diisopropyl)(2-pyridylmethyl)amide, calculated with mPW1PW91/SDD

The HOMO orbital contains the electron lone-pair at the tin(II) center and the corresponding anti-bonding orbital is the LUMO. The LUMO is the anti-bonding π^* of the system at the pyridyl backbone. Further it also contains the lone pair at the bonding nitrogen atom. HOMO-1 is the π -orbital at the nitrogen atom (N-TMS) and the corresponding anti-bonding is the LUMO+1 orbital. And last the HOMO-2 orbital is the π -orbital at the diisopropyl containing six-membered carbon ring and a part of the electron lone-pair at the pyridyl nitrogen atom with the corresponding LUMO+2 orbital. In the LUMO+2 also the anti-bonding combination of the electron lone-pair is visible as well as the p-orbitals at the tin atom.

In this case the tin(II) derivative has a HOMO-LUMO transition at 440 nm. A second band was calculated at 320 nm - in the ultra violet region and corresponds to the HOMO-2 to LUMO transition. Experimental molar extinction coefficient were identified: 320 nm ($\epsilon = 3024$); 440 ($\epsilon = 706$). Table 3.7 summarizes the calculated data from the UV-Vis simulation.

Table 3.7: Calculated (mPW1PW91/ZORA/TZ2P) and experimental UV-Vis transitions of the bis(TMS)amidotin(II N-(diisopropyl) (2-pyridylmethyl)amide.

	experimental	calculated
nm	280	320
transition		$\pi-\pi^*$
orbitals		HOMO-2 to LUMO
nm	400	440
transition		$n-\pi^*$
orbitals		HOMO to LUMO

Unfortunately for the germanium and lead derivative of the bis(TMS)amido N-(diisopropyl)-(2-pyridylmethyl)amide ligand no crystal structures could be obtained. Therefore quantum chemical calculations were made to get an idea of the molecule structure. Figure 3.24 displays the geometry optimized molecules in the three coordinated form. Of course also the open two-coordinated form exists in these cases

For bis(TMS)amidogermanium(II)N-(diisopropyl) (2-pyridylmethyl)amide the energy difference between the open and closed conformation is 21 kJ/mol. This value is in the same range as for the tin(II) derivative (26 kJ/mol) and the lead derivative (27 kJ/mol).

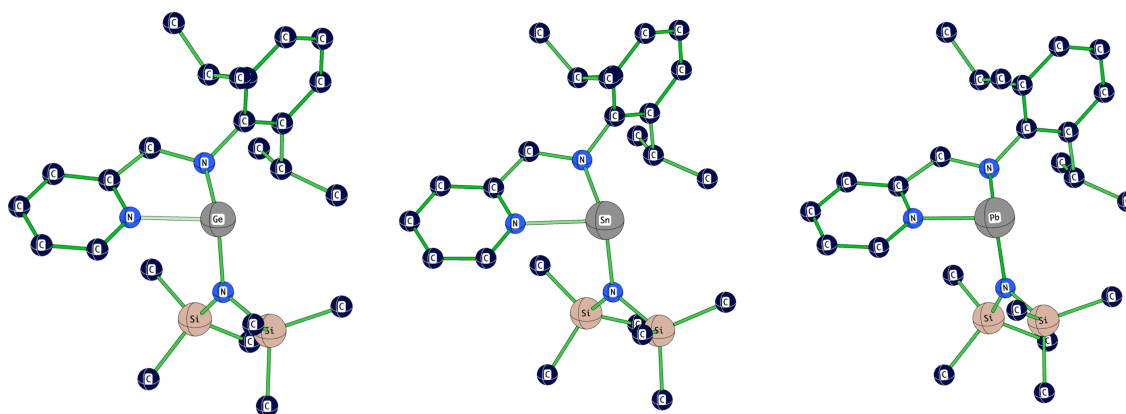
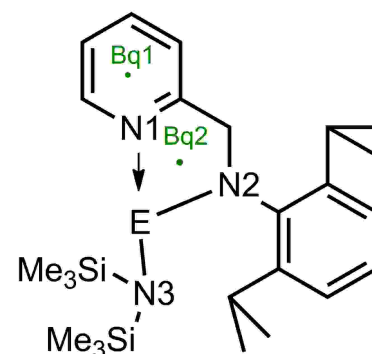


Figure 3.24: Optimized (mPW1PW91/SDD) structures of bis(TMS)amido tin(II)N-(diisopropyl) (2-pyridylmethyl)amide, bis(TMS)amido lead(II)N-(diisopropyl) (2-pyridylmethyl)amide, and bis(TMS)amido germanium(II)N-(diisopropyl) (2-pyridylmethyl)amide.

Table 3.8 summarizes the calculated values of the germanium and tin derivative of the hetero-leptic tetrylenes.

Table 3.8: Calculated (mPW1PW91/SDD) geometry data for bis(TMS)amidoE(II) N-(diisopropyl)(2-pyridylmethyl)amide

distances [pm]	E=Ge	E=Sn	E=Pb
E← N1	218.3	235.7	240.7
E-N2	196.8	215.7	222.2
E- N3	197.1	213.6	223.6
N2-E-N3 angle	112.08°	112.97°	113.54°
N1-N2-E-N3 angle	89.08°	85.52°	84.93°
angular Σ E	284.43°	270.98°	276.32°
HOMO-LUMO gap	3.28 eV 377 nm	3.36 eV 368 nm	3.52 eV 352 nm
Δ E [kJ/mol]	21	26	27
NICS Bq1 [ppm]	-0.9	-0,9	-0,8
NICS Bq2 [ppm]	-5.0	- 5.5	-5.4



The ΔE value is the, energy difference between the open and the closed conformation.

Obvious is that again as at the chloro-tetrylene derivatives, the bond lengths became larger the heavier the metal atom becomes. As expected for the germanium and the lead compound the $N[\text{SiMe}_3]_2$ residue is normal to the N1-N2-E plane, according to the angular sum at the metal center 284.43° (Ge), 276.32° (Pb) and the N1-N2-E-N3 angle 89.08° (Ge), 84.93° (Pb). The same we observed for the simulated structures of the chloro-tetrylene derivatives.

Again two E-N bonds are covalent bonds and the third E-N1 bond is an electron donor-interaction between the nitrogen and the metal atom. The stabilizing effect becomes stronger the heavier the central atom is. This is obvious at the ΔE values- see Table 3.8. The ΔE values are gained form the relative energy difference between the open and closed conformation. In both cases for the lead and the germanium derivative the closed conformation represents the global minimum.

The HOMO-LUMO gap is rising, the heavier the central atom becomes as already mentioned in the introduction. This is also can be observed experimentally. The germanium compound is more yellow, the tin derivative is more greenish and the lead compound is green. The energy-level diagram gives the explanation why the HOMO-LUMO gap is

becoming larger- see Figure 3.25

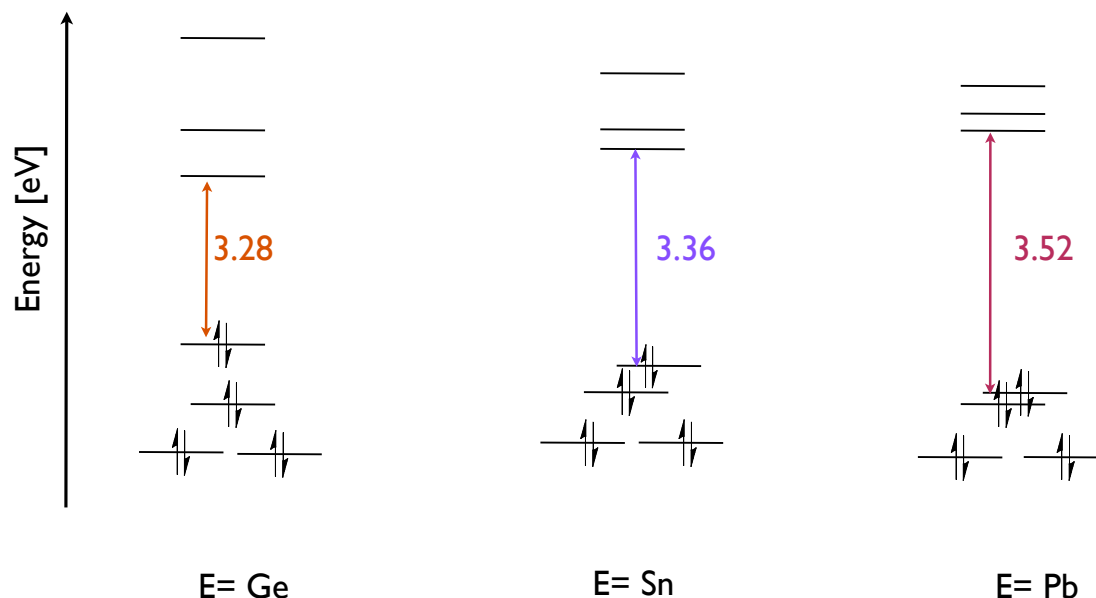


Figure 3.25: Energy level diagram of bis(TMS)amidoE(II)N-(diisopropyl)(2-pyridylmethyl)amide calculated with mPW1PW91/SDD.

According to the energy level diagram the HOMO orbital is getting lower in energy and the LUMO orbital is simultaneously getting higher in energy, the heavier the central atom is. Also the gap between the HOMO and the HOMO-1 is getting smaller, the same effect is calculated for the LUMO to LUMO+1 and LUMO+2 gap. In sum the HOMO to LUMO gap is growing.

NICS calculations show that the N1-E-N2-C-C five membered ring is aromatic, because the calculated NICS values (Bq2) are at -5 ppm. In contrast the pyridine ring is non-aromatic, having NICS values (Bq1) at about -1 ppm. This observation we already made at the chloro tetrylene derivatives.

These type of tetrylenes have got on the one hand bulky protecting substituents as the diisopropyl-aniline side chain, and on the other hand the metal center is directly bonded to two nitrogen atom. Additionally a stabilization via the pyridyl nitrogen is enabled via a π -donor, σ -acceptor interaction. That is a perfect thermodynamic and kinetic protection.

3.2.4 Reaction Conditions and Products

During our experimental work to generate hetero-leptic tetrylenes we observed a very interesting circumstance. Same reaction conditions and chemically the same type of metal - precursor (as $\text{Ge}[\text{N}(\text{TMS})_2]_2$, $\text{Sn}[\text{N}(\text{TMS})_2]_2$, $\text{Pb}[\text{N}(\text{TMS})_2]_2$) do not always lead to the chemically same type of product - see Figure 3.26.

Derivatives of germanium and lead tend to undergo rearrangement reactions and build up homo-leptic and aromatic tetrylenes as end products. Figure 3.26 displays one and the same type of transamination reaction with different metal(II) precursors and the resulting products.

Reaction conditions were the same for all three experiments. The mixture was stirred at room temperature for 24 hours in diethyl ether. The products crystallized after a few days storage at -30°C .

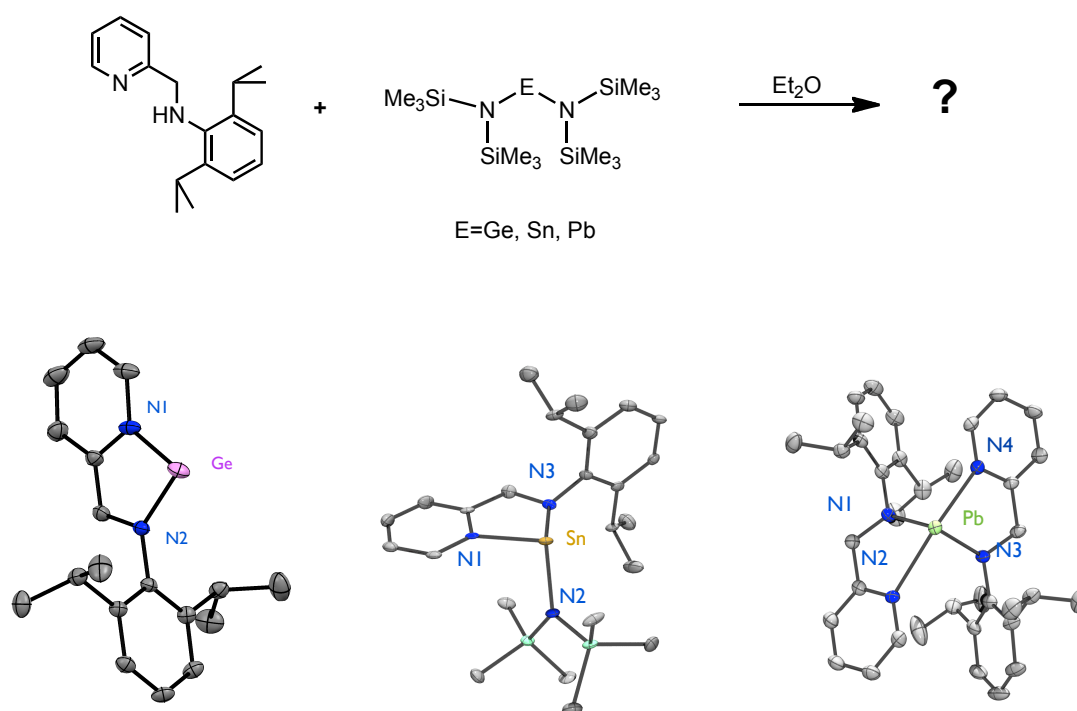


Figure 3.26: Transamination reaction of 2,6-diisopropyl-N-(pyridin-2-ylmethyl)aniline with metal(II) precursors. Solid state structures of Ge-2,6-diisopropyl-N-(pyridin-2-ylmethyl)amide, bis(TMS)amidotin(II)N-(diisopropyl)(2-pyridylmethyl)amide, and bis[N-(2,6-diisopropylphenyl)(2-pyridylmethyl)amid]Pb(II).

It seems that during the reaction some rearrangement and side reactions take place and the thermodynamically stable product is built. Obvious is that the coordination state is growing from two (Ge) to three (Sn) to four (Pb) the heavier the central atoms becomes.

Some enthalpy change analysis were done for all possible products. Therefore we calculated (mPW1PW91/SDD) all enthalpies of the starting materials and the products - illustrated in Figure 3.26.

Equation 3.1 describes if the reaction is exothermic or endothermic. If $\Delta H_{\text{reaction}}$ is positive, the reaction is endothermic, that means that heat is absorbed by the system due to the products of the reaction having a greater enthalpy than the reactants. On the other hand if $\Delta H_{\text{reaction}}$ is negative, the reaction is exothermic, that is the overall decrease in enthalpy is achieved by the generation of heat [69].

$$\Delta H_{\text{reaction}} = \sum \Delta H_{\text{products}} - \sum \Delta H_{\text{educts}} \quad (3.1)$$

According to the enthalpy change during the reaction, it makes sense why these compounds are formed. The more energy is released, the more stable is the product.

Figures 3.27 and 3.28, display reaction enthalpies of the predicted products for the germanium and the tin derivatives. All reactions show opportune thermodynamic conditions, bearing negative signs at the $\Delta H_{\text{reaction}}$ values. But only the stannylene as product (as asymmetric stannylene) was formed.

In the case of the germylene a subsequent reaction step formed the aromatic germylene as product. This circumstance can be explained by the fact that in this case the aromatic germylene is most stable.

And in the case of the plumbylene also a subsequent elimination reaction formed a homo-leptic plumbylene. To give information about this product - formation is difficult.

This simple reaction enthalpy pattern can only explain some aspects of the product distribution and can give trends, why specific different products may be formed at similar reaction conditions.

To gain a closer insight we investigated the formation of the aromatic germylene in more detail. We also tried to make the same simulation for the stannylene.

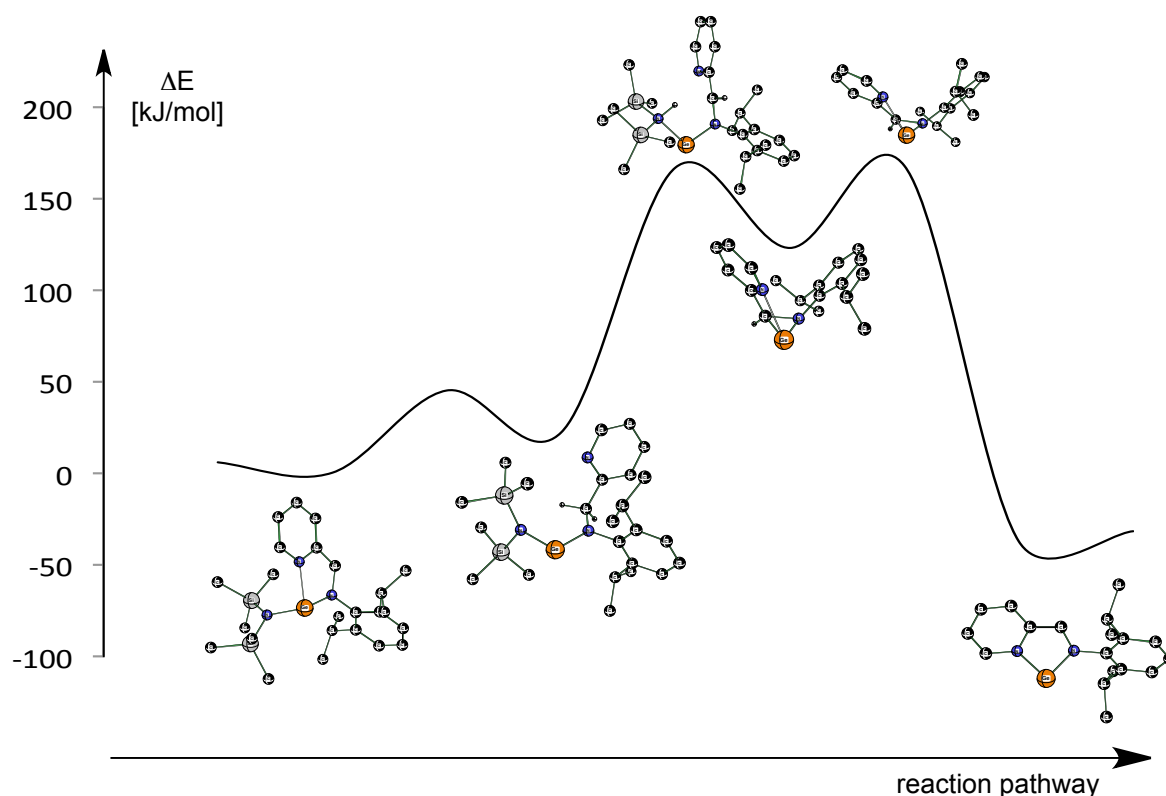


Figure 3.27: Reaction pathway of bis[N-(2,6-diisopropylphenyl)(2-pyridylmethyl)amid]Ge(II)

The product distribution for the different germanium derivatives shows that the aromatic germylene is thermodynamically most stable. We propose two different products and the aromatic germylene is 33 kJ/mol more stable than the hetero-leptic germylene. The reaction pathway shows that formation of the aromatic germylene goes within different transition state geometries.

According to our proposed reaction pathway, the hetero-leptic germylen undergoes a rearrangement reaction, where the $\text{N}(\text{TMS})_2$ group leaves the molecule within a proton abstraction. Activation energy for the last step is only approximated, but the energy gain is in the end higher. We also were able to simulate the transition state for the proton transfer to form $\text{HN}(\text{TMS})_2$. At the same time the germanium atom is exactly placed between the nitrogen-carbon double bond.

For the last step a high energy gain is proposed. For exact data a multi configuration calculation would be needed.

The reaction mechanism is not completely clear yet, but this is the first step to give some information about the product distributions and intermediate structures (TS).

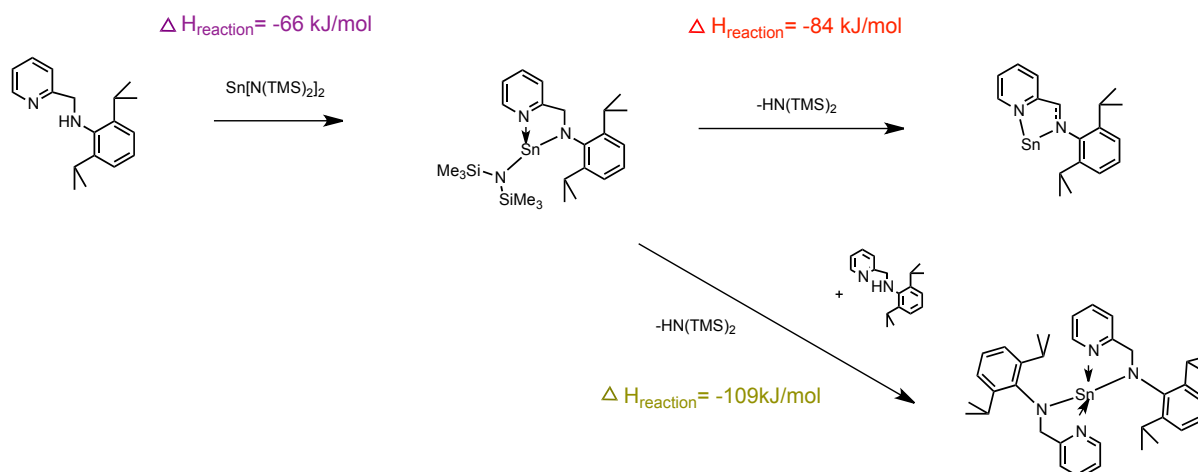


Figure 3.28: Proposed reaction enthalpies of bis[*N*-(2,6-diisopropylphenyl)(2-pyridylmethyl)amid]Sn(II)

In the case for the hetero-leptic tin derivative we only can give an assumption of the reaction pathway- see Figure 3.28 . According to the energy values here also the aromatic tin derivative would be thermodynamically most stable. We found some possible transition states, but a completely clear mechanism could not be established. Here we also assume a proton transfer during the reaction. However, it seems that the energy barrier is too high to provide the aromatic stannylene as product. Further work will be needed on this topic.

A reaction with exact a one to one molar ratio leads to the heteroleptic tetrylene as product. We also found out that more ligand in the reaction mixture always leads to the homoleptic derivative as product. It can be assumed, that in this case the energy gain favors the symmetric product.

For the last product distribution (the lead derivative) analysis we can say that the homoleptic structure for the lead(II) derivative is more stable. The enthalpy differences between the homo and hetero-leptic plumbylene is rather small - only 2 kJ/mol. This may also indicate that the hetero-leptic plumbylene is formed, but it undergoes easily a rearrangement reaction and forms the homo-leptic product. Until now we can not say how this mechanism is working and why always the hetero-leptic plumbylene is formed. Further work on this interesting topic will be done.

Reaction of the amino ligand with the $\text{Ge}[\text{N}(\text{TMS})_2]_2$ metal precursor, leads to an aromatic germylene. Figure 3.29 displays solid state and optimized structure and Table 3.9 summarizes geometry data.

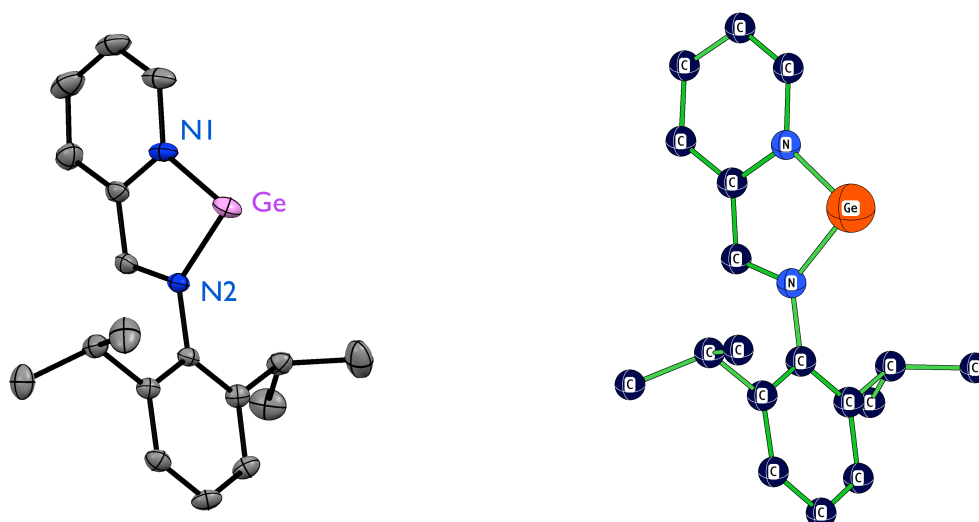


Figure 3.29: Solid state and optimized (mPW1PW91/SDD) structure of bisiminoGe(II) N-(diisopropyl)(2-pyridylmethyl)amide. Hydrogen atoms were omitted for clarity.

The Ge-N1 and Ge-N2 distances are quite at the same value (190.6 pm/187.3 pm in solid state and 191.7pm/188.2 pm in the simulation)- see Table 3.9. So the two nitrogen atoms are equal in their function and both of them built a bond to the metal center. The dihedral angle (C-N1-Ge-N2) is at -0.76° in the crystal and 0.00° in the simulation, consequently the five-membered ring is nearly planar in the solid state and completely planar in the gas phase.

Table 3.9: Calculated (mPW1PW91/SDD) data from the bisimino-Ge(II)N-(diisopropyl)(2-pyridylmethyl)amide

distances [pm]	experimental	calculated
Ge-N1	190.6	191.7
Ge-N2	187.3	188.2
N2-Ge-N1 angle	82.59°	81.85°
C-N1-Ge-N2 angle	-0.76°	0.00°

Because of the nearly planar environment around the germanium metal center, some NICS (mPW1PW91/IGLO-II) calculations can give information about aromaticity. The system is indeed π -aromatic, having a NICS value of -11.3 ppm. The dummy molecule was placed in the center of the five membered ring. A second dummy was placed in the pyridine ring and gave the NICS value nearly at zero. The aromaticity at the pyridine ring is lost. Further the aromaticity of the compound could be confirmed by NBO analysis. The HOMO, HOMO-2 and the LUMO orbitals show that the whole system is conjugated - see Figure 3.30.

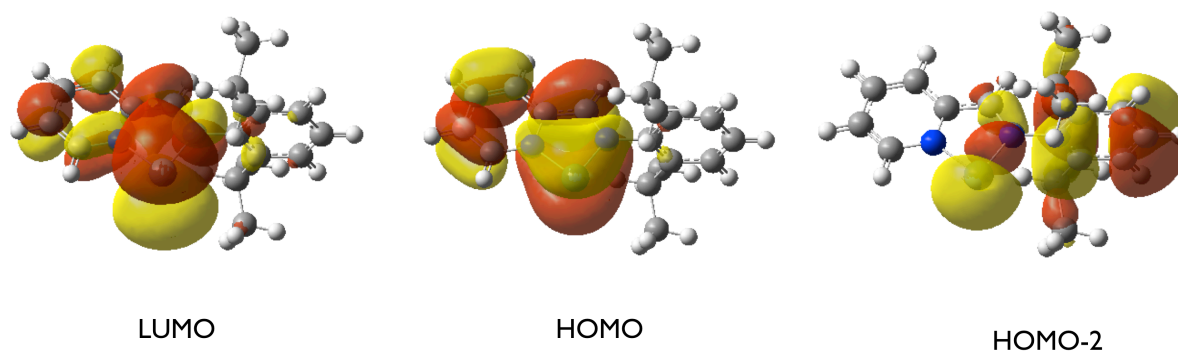


Figure 3.30: LUMO, HOMO, and HOMO-2 orbitals of bisiminoGe(II) N-(diisopropyl)(2-pyridylmethyl)amide

According to quantum chemical analysis and enthalpy comparison of the aromatic germylene is more stable than the predicted hetero-leptic compound. Energy gain from the aromatic germylene is -32 kJ/mol - as already explained.

Doing the very same reaction with $\text{Sn}[\text{N}(\text{TMS})_2]_2$ as metal precursor with the amino ligand leads to the hetero-leptic stannylene. The product and its properties were already discussed.

And last, the amino ligand was tried out with the $\text{Pb}[\text{N}(\text{TMS})_2]_2$ precursor. The astonishing result was, that the yellow crystalline product was not as expected maybe an aromatic plumbylene or hetero-leptic blumbylene. According to the NMR measurement and the solid state structure, one lead (II) atom is surrounded by two ligand molecules. Other attempts to synthesize the hetero-leptic plumbylene also failed.

The metal center is protected by two ligand molecules and further the lead center is stabilized by two π -donor pyridyl nitrogen atoms. These type of substance represents a homo-leptic tetrylene. In the next chapter homo-leptic tetrylenes and their properties will be discussed.

3.2.5 Di-amido Tetrylenes

As already mentioned in the introduction, tetrylenes can be stabilized by bulky substituents and by additional donor hetero atoms in the ligand system. Herein we present three new derivatives, which are stabilized by two diamino ligands.

In literature only a few examples of twice-bonded and two-coordinated nitrogen tetrylenes are known. In 1996 Dias and Jin published a troponimidate complex with tin(II) as metal center - see Figure 3.31. They suggest, according to the very simple ^1H spectra, that the molecule may be fluxional in solution at room temperature and that the metal center is in a trigonal pyramidal surroundig [48].

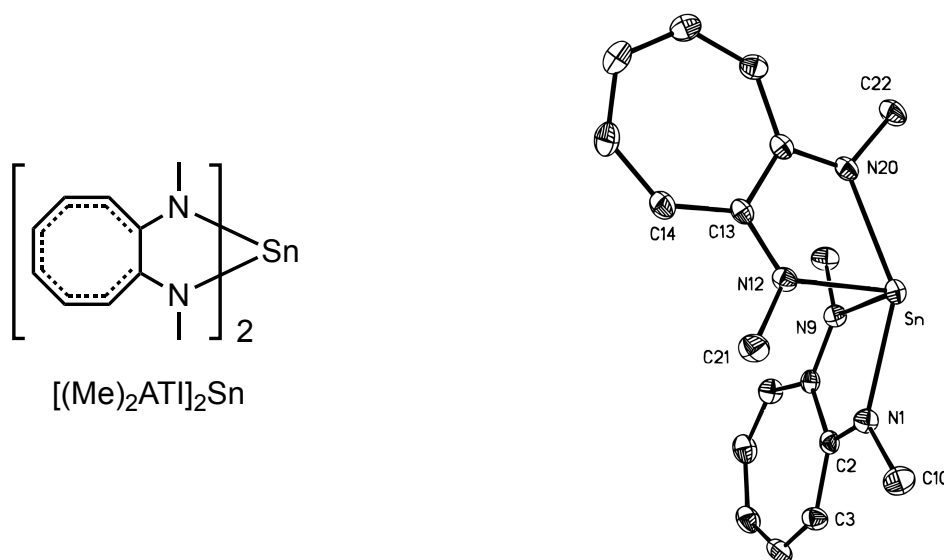


Figure 3.31: Structure scheme for $[(\text{Me})_2\text{ATI}]_2\text{Sn}$; hydrogens have been omitted for clarity[48]

Regrettably there is a lack of publications about lead(II) species containing two stabilizing donor atoms in the ligand system. Nevertheless, we have been able to synthesize and analyze a rare representative of these compounds. Besides a lead(II) derivative also a germanium(II) and tin(II) compound were generated. These three compounds are isostructural and they only deviate in their central atom, which determines most of the molecules properties. We also have found out that these homo-leptic tetrylenes are more stable than the hetero-leptic derivatives. As already reported in the chapter before, hetero-leptic tetrylenes tend to undergo rearrangement reactions and form the more stable homo-leptic derivative (especially in the case of the lead derivative). Besides that, direct reaction pathways (see Figure 3.32) are possible to generate selectively these tetrylenes.

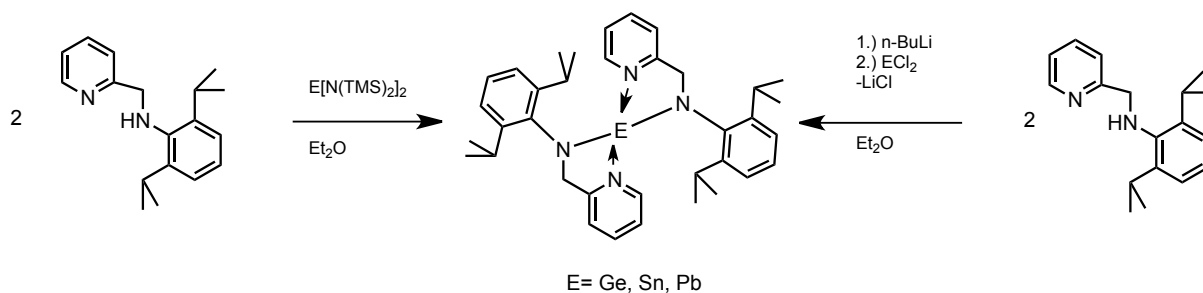


Figure 3.32: Direct synthesis of bis[N-(2,6-diisopropylphenyl)(2-pyridylmethyl)amid]E(II).

Very unusual about these new tetrylenes is that the metal center is surrounded by four nitrogen atoms - see Figure 3.34. Two nitrogen atoms build covalent E-N bond and the other two nitrogen atoms stabilize the tetrylene via donor-interaction.

The N,N coordinated tetrylenes were analyzed by single crystal diffraction, UV-Vis measurements, ^{119}Sn , ^{13}C , ^{207}Pb and 1H NMR.

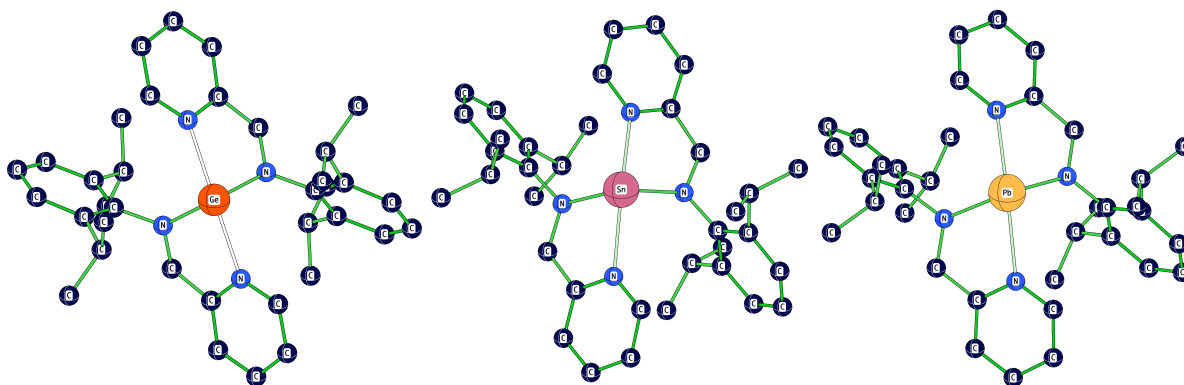


Figure 3.33: Optimized (mPW1PW91/SDD) structures of bis[N-(2,6-diisopropylphenyl)(2-pyridylmethyl)amid]Ge(II), bis[N-(2,6-diisopropylphenyl)(2-pyridylmethyl)amid]Sn(II), bis[N-(2,6-diisopropylphenyl)(2-pyridylmethyl)amid]Pb(II)

In Table 3.10 the observed and calculated (mPW1PW91/SDD) data of the homo-leptic tetrylenes are collected.

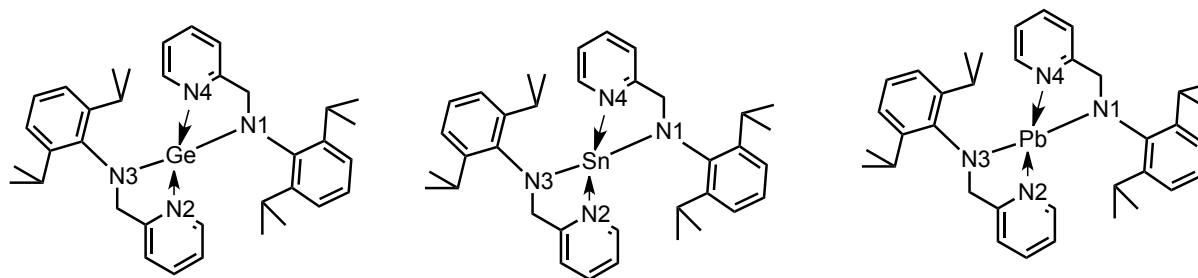


Figure 3.34: Bis[N-(2,6-diisopropylphenyl)(2-pyridylmethyl)amid]Ge(II), bis[N-(2,6-diisopropylphenyl)(2-pyridylmethyl)amid]Sn(II), bis[N-(2,6-diisopropylphenyl)(2-pyridylmethyl)amid]Pb(II)

Table 3.10: Calculated (mPW1PW91/SDD) and experimental data from the bis[N-(2,6-diisopropylphenyl)(2-pyridylmethyl)amid]E(II); hydrogen atoms were omitted for clarity

distances [pm]	experimental			calculated		
	E=Ge	E=Sn	E=Pb	E=Ge	E=Sn	E=Pb
E-N1	195.0	214.7	224.5	199.6	216.2	228.1
E← N2	238.1	247.1	254.2	234.6	246.5	258.9
E-N3	197.3	215.0	223.9	199.6	216.8	228.1
E← N4	229.4	244.3	252.7	234.6	246.4	258.8
N4-E-N1 angle	76.18 °	71.62°	69.25 °	75.05 °	71.78°	68.98°
N1-E-N2 angle	88.08 °	86.18°	86.59 °	88.73 °	87.96°	88.75°
N2-E-N3 angle	74.83 °	71.18°	69.34 °	75.05 °	71.48°	68.98°
N3-E-N4 angle	88.82 °	86.75°	86.07 °	88.73 °	87.95°	88.74°
N4-E-N2 angle	154.63 °	151.62°	143.38 °	153.46 °	146.14°	142.28°
N1-E-N3 angle	96.70 °	99.82°	101.66 °	104.82 °	105.32°	107.91°
Σ angle at E	327.56 °	315.73°	311.25 °	327.56 °	319.17°	315.45°

Experimental and calculated data show consistent trends. First of all, as already mentioned [47], there are two E-N bond types in the molecules. The shorter E-N1/E-N3 bonds (E=Ge: 195.0 pm, 197.3 pm exp. and 199.6 pm, calc.), are common covalent bonds and the two larger E-N2/E-N4 bonds (E=Ge: 238.1 pm, 229.4 pm exp. and 234.6 pm calc.), can be described as interactions of the nitrogen electron lone pair with the vacant p-orbital of the metal center - see Table 3.10. Further the trend is obvious, that these bonds become larger, the heavier the metal center becomes, due to the growing van der Waals radii of the heavy metals (Ge, Sn, Pb).

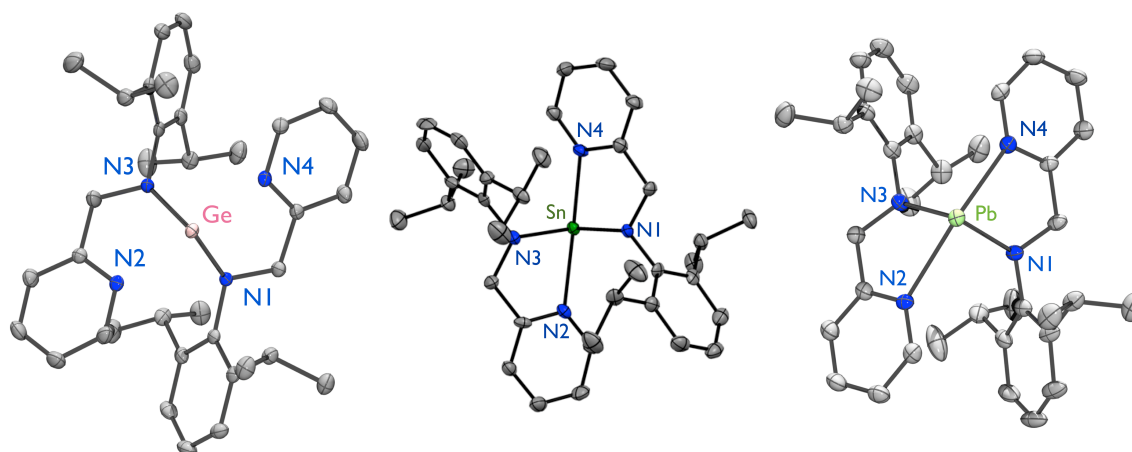


Figure 3.35: Solid state structures of bis[N-(2,6-diisopropylphenyl)(2-pyridylmethyl)amid]Ge(II), bis[N-(2,6-diisopropylphenyl)(2-pyridylmethyl)amid]Sn(II), bis[N-(2,6-diisopropylphenyl)(2-pyridylmethyl)amid]Pb(II); hydrogen atoms were omitted for clarity

According to the solid state and the geometry optimized structure, the metal center is in a trigonal bi-pyramidal environment. N1, N3 and electron lone-pair build the trigonal surrounding, where the metal center is placed in the middle. N2 and N4 are above and below the metal center. The N2-E-N4 angles are smaller than 180° (Ge $154^\circ/153^\circ$, Sn $151^\circ/146^\circ$, Pb $143^\circ/142^\circ$), the bi-pyramide is distorted. The distortion is caused by the too small spacers between the pyridyl-nitrogen (N4 or N2) and the amine-nitrogen (N1 or N3).

Hence the metal center is only twice covalently bonded and two bonds are just σ -acceptor/ π -donor interactions, the molecule is flexible. The weak electron lone-pair interactions can open and close in solution. Dias et.al. also reported this observations for their compounds. They noticed, that the NMR-spectra for these quite complex substances are very simple [48].

In the chapter before we found a connection between the ^{119}Sn chemical shift and the conformation. Herein for the stannylene we found five different thermodynamically stable conformations with five different ^{119}Sn chemical shifts-see Figure 3.36.

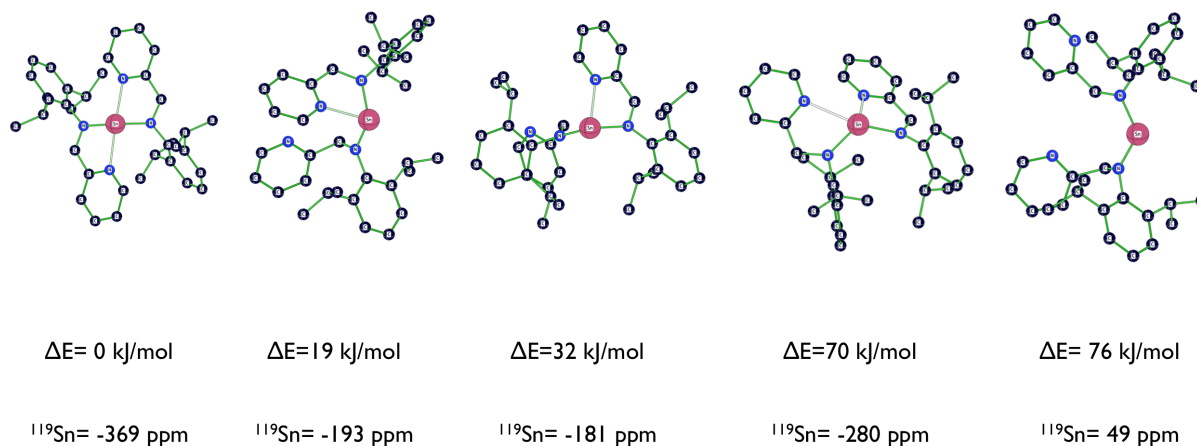


Figure 3.36: Calculated ^{119}Sn chemical shifts (mPW1PW91/ IGLO-II) and energy differences to the global minimum of bis[N-(2,6-diisopropylphenyl)(2-pyridylmethyl)amid]Sn(II); optimized (mPW1PW91/SDD) structures are displayed without hydrogen atoms for clarity.

The chemical shift is strongly affected by the conformation. The ^{119}Sn shift range is from -369 ppm to +49 ppm in the calculation. The most stable conformation is the four coordinated stannylene, which was also found in the solid state structure, having a theoretical ^{119}Sn chemical shift of -369 ppm. In contrast the least stable conformation is the free stannylene, with a theoretical ^{119}Sn chemical shift of +49 ppm. The energy difference between these two extremes is 76 kJ/mol. Using a Boltzmann-distribution[66], enables to weight the calculated ^{119}Sn chemical shift with the calculated energy difference. The energy difference is a barrier and according to the Boltzmann distribution the average calculated ^{119}Sn chemical shift is -300 ppm. Therefore the measured ^{119}Sn chemical shift is -143 ppm (a broad signal of 7 ppm range) does not fit. The measured ^{119}Sn chemical shift, can be compared to an calculated value of -181 ppm for the three coordinated stannylene.

The experimental ^{119}Sn chemical shift deviates from the calculated data, because solvent interactions have to be taken into account. The solvent interactions can stabilize the three-coordinated conformations.

Besides the calculations of the chemical shift it is also possible to simulate UV-Vis spectra. These homo-leptic tetrylenes are colored. The color becomes less intensive the heavier the central atom is. In general, mostly the color comes from the visible HOMO to LUMO transition in the molecule [70]. In Figure 3.37 the natural bond orbitals are displayed.

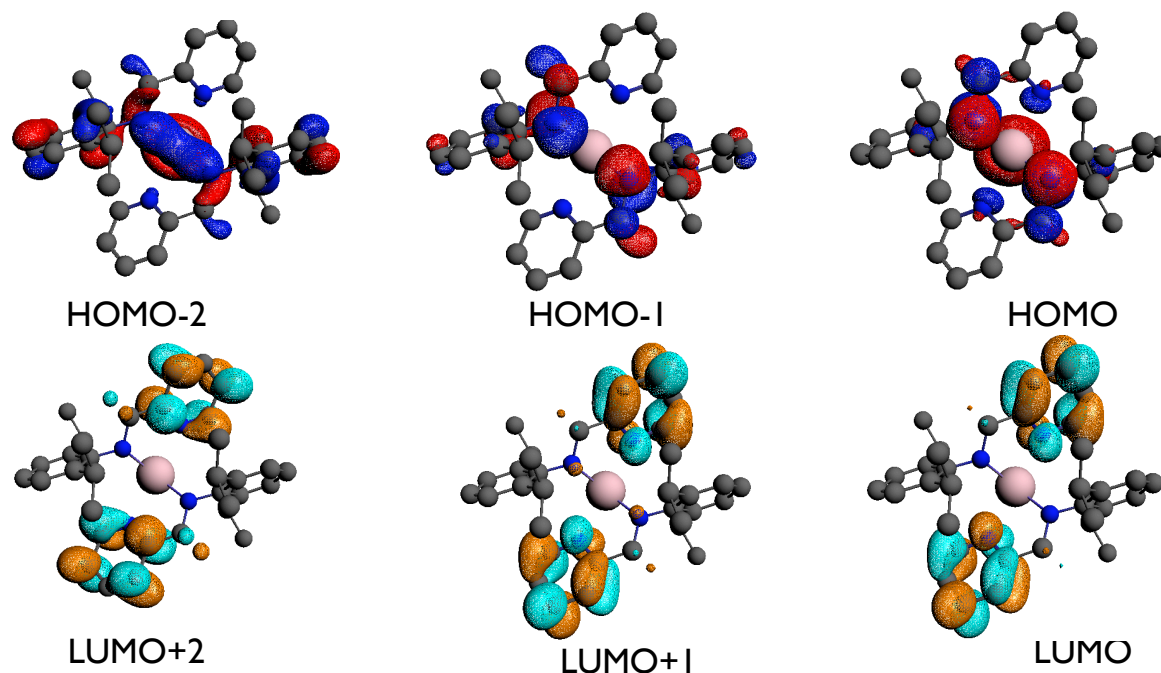


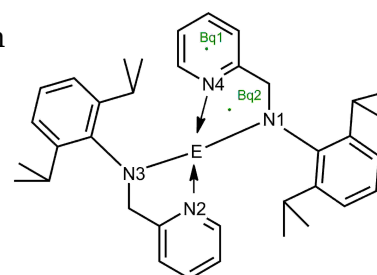
Figure 3.37: Natural bond orbitals of bis[N-(2,6-diisopropylphenyl)(2-pyridylmethyl)amid]Sn(II) (mPW1PW91/SDD).

The HOMO orbital shows the electron lone-pair at the metal(II) center and the p-orbitals at the neighboring nitrogen atoms. The corresponding anti-bonding orbital is the LUMO+1. Further the electron lone-pairs at the pyridine nitrogens are visible in the HOMO orbital.

The HOMO-2 orbital displays the sigma bond between the tin and the neighboring nitrogen atoms, and the corresponding anti-bonding orbital is the LUMO. According to the natural bond orbitals there is no π -conjugation in the system. To proof this assumption NICS calculations were carried out - results see in Table 3.11.

Table 3.11: Calculated NICS (mPW1PW91/SDD) from bisimino-E(II)N-(diisopropyl)(2-pyridylmethyl)amide

	E=Ge	E=Sn	E=Pb
NICS Bq2 [ppm]	0.9	-0.8	0.8
NICS Bq1 [ppm]	-6.1	-6.0	-5.9



As already observed before for the case of the chloro tetrylenes and the bis-amino tetrylenes, we can say that the N1-E-N4-C-C ring is not aromatic. The calculated NICS (Bq1) values are between 0.9 and -0.8 ppm. The pyridine ring stays intact and aromatic, showing NICS (Bq2) values between -5.9 and -6.1 ppm.

In Table 3.12 absorption maxima and molar extinction coefficients are collected of the homo-leptic tetrylenes. Figure 3.38 displays the experimental UV-Vis spectra of the homo-leptic tetrylenes. Spectra were recorded in heptane as solvent. The listed bands in the spectra are observed in the measurement, but via quantum chemical calculations it is possible to find out where these transitions come from.

Table 3.12: Calculated (mPW1PW91/ZORA/TZ2P;) data from the bis(TMS)amidoE(II)N-(diisopropyl)(2-pyridylmethyl)amide

	E=Ge	E=Sn	E=Pb
Absorption max.	experimental		
	427nm	401nm	412nm
	323nm	337nm	346nm
	280nm	296nm	309nm
ϵ [L/(mol cm)]			
	758 _{ϵ_{427}}	5792 _{ϵ_{337}}	6623 _{ϵ_{309}} 2268 _{ϵ_{412}}
Transitions	calculated		
HOMO to LUMO n- π^*	471nm	425nm	-
HOMO-1 to LUMO+1 π - π^*	392nm	378nm	-
HOMO-2 to LUMO π , n- π^*	312nm	311nm	-
HOMO to LUMO gap	3.45 eV	3.34 eV	-

The experimental HOMO-LUMO transitions are at 427 nm (Ge), 401 nm (Sn), and 412 nm (Pb). These transitions are mainly responsible for the color of the compounds. All three of them have a yellow-greenish color in a heptane solution.

The calculated data verify this trend for the HOMO to LUMO transitions. Additionally, according to the TD-DFT simulations there are also other transitions, and we also could find them in the experiment. The other transitions are from the HOMO-2 to the LUMO orbital and from the HOMO-1 to the LUMO+1 orbital- details see Table 3.12. Figure 3.38 displays the experimental UV-Vis spectra of all three homo-leptic tetrylenes, and in Figure 3.39 experimental and calculated spectra of bis[N-(2,6-diisopropylphenyl)(2-pyridylmethyl)amid]Pb(II) are displayed.

UV-Vis calculations of the lead derivative did not finish, because the generated basis sets may be too large. All in all this type of simulations need long time to finish.

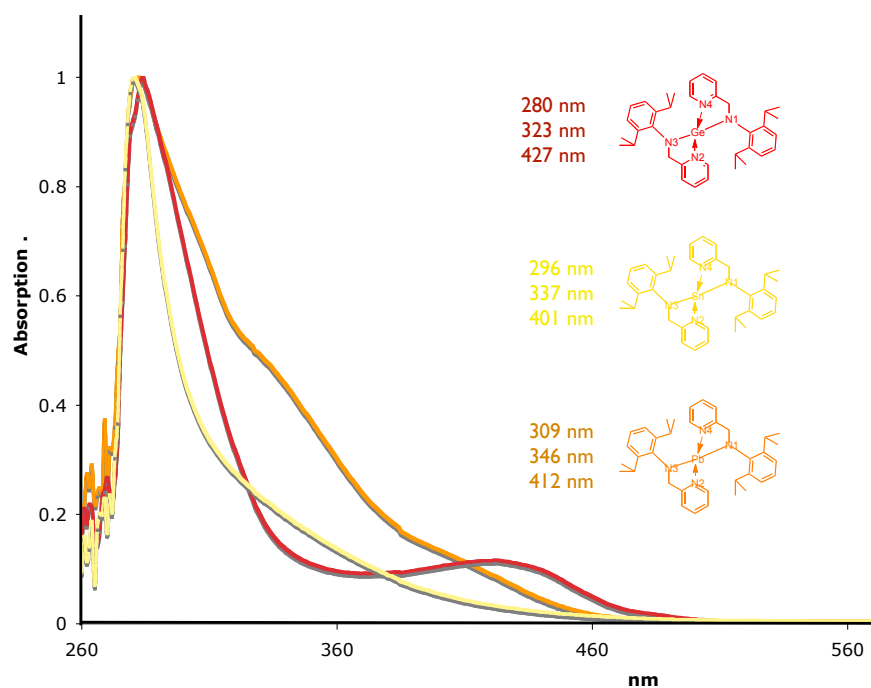


Figure 3.38: Experimental UV-Vis spectra of bis[N-(2,6-diisopropylphenyl)(2-pyridylmethyl)amid]Ge(II), bis[N-(2,6-diisopropylphenyl)(2-pyridylmethyl)amid]Sn(II), bis[N-(2,6-diisopropylphenyl)(2-pyridylmethyl)amid]Pb(II)

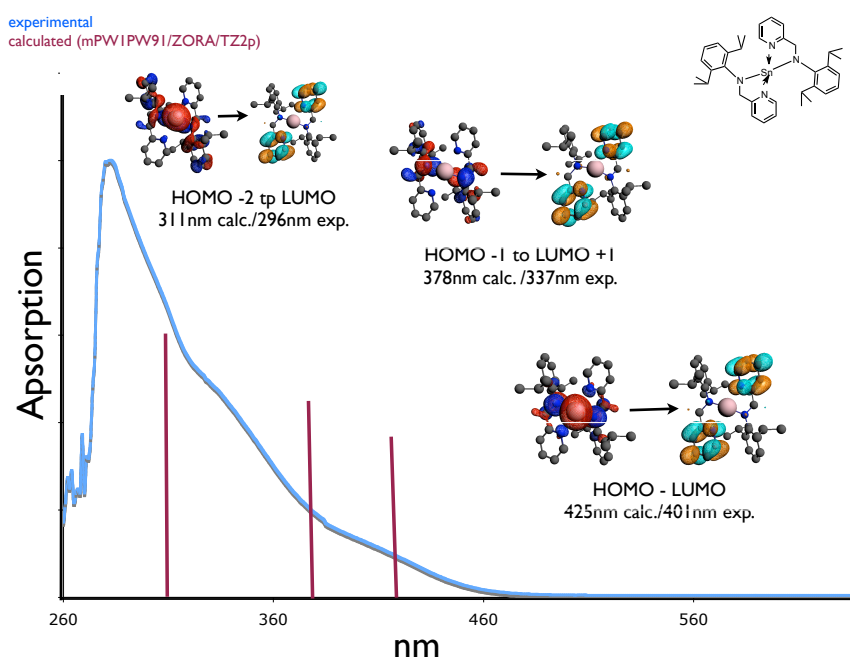


Figure 3.39: Experimental and calculated (mPW1PW91/ZORA/TZ2p) spectra of bis[N-(2,6-diisopropylphenyl)(2-pyridylmethyl)amid]Sn(II)

According to the experimental UV-Vis spectra it is obvious that the absorption maximum is shifting to higher values, the heavier the metal center is. This effect can be explained by the growing HOMO-LUMO gap. Literature reports that the HOMO-LUMO gap is becoming larger the heavier the metal center is, for the case of tetrylenes [64]. But in the case of the diamino-tetrylenes we can observe they the HOMO-LUMO gap is not constantly growing.

Figure 3.40 displays the energy level diagram, showing the changing gap between the highest occupied and lowest unoccupied orbital.

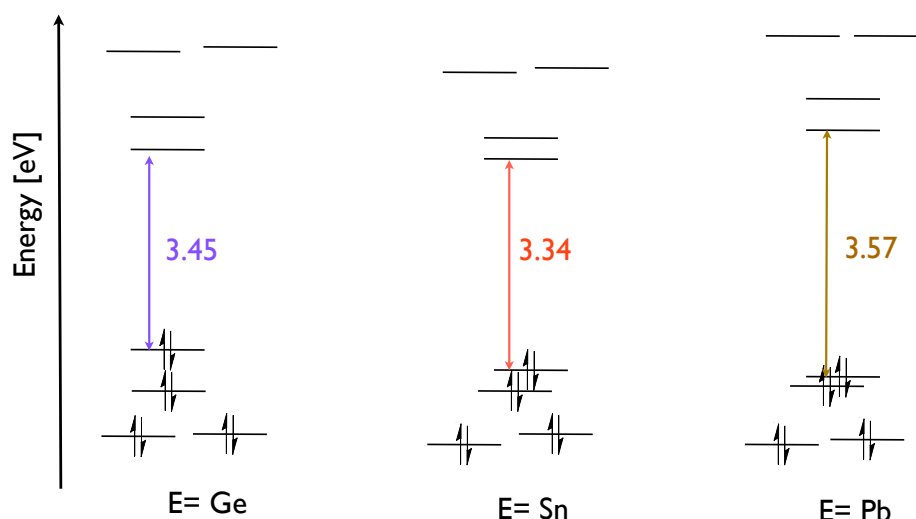


Figure 3.40: Calculated (mPW1PW91/ZORA/TZp) energy level diagram of bis[N-(2,6-diisopropylphenyl)(2-pyridylmethyl)amid]E(II)

Analysis of the energy level diagram shows, that the HOMO and HOMO-1 orbitals are becoming lower in energy and that the gap between the HOMO and HOMO-1 is decreasing. Simultaneously the LUMO and LUMO+1 orbital are becoming higher in energy and the gap between these two orbitals is increasing. In the end the HOMO-LUMO gap is changing. The HOMO-LUMO gap of the stannylene is a little bit smaller (0.11 eV) than of the germylene. And for the plumbylene we calculated a HOMO-LUMO gap of 3.57 eV. These calculated values can thoroughly be compared with the experimental spectra. In the experimental spectra we see the the maximum of the stannylene is the lowest as the smallest gap.

These symmetric tetrylenes are stabilized by two sterically demanding ligands. Additionally they are kinetically stabilized by two directly bonded hetero atoms (N) and by two additional σ -acceptor / π -donor nitrogen atoms. In the solid state they appear in a trigonal bi-pyramidal surrounding. The UV-Vis attributes are highly affected by the central atom, obvious at the energy level diagram and the UV-Vis spectra.

The ligand strongly affects the stability of a tetrylene.

As already mentioned in the introduction we also did experiments with some bidentate ligand. The DAMPY ligand bears two nitrogen atoms as possible reactive sites and a third nitrogen atom, which can act as an additional donor in the ligand system.

In the next chapter we will discuss how the bidentate ligand system and the metal(II) precursors react.

4 Complexes with bidentate Ligand Systems

4.1 Introduction

In the chapter before we introduced tetrahylenes bearing an amino-pyridin ligand system. Two ligand parts act as kinetic and thermodynamic stabilizers for the highly reactive metallylene species. We used a special ligand system, which can stabilize the metal center in both ways - see Figure 4.1. We analyzed the bonding situation and we also characterized some tin-derivatives via single crystal diffractometry, NMR and quantum chemical calculations (DFT).

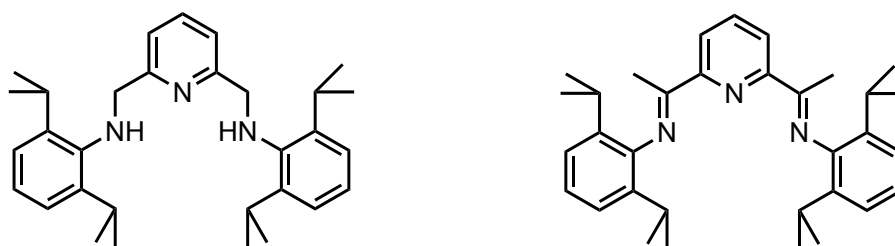


Figure 4.1: Diaminopyridine ligand (DAMPY[71]) and diiminopyridine ligand(DIMPY)

The diiminopyridine and diaminopyridine ligands (DIMPY and DAMPY) have become omnipresent ligands in transition-metal chemistry, as they can stabilize reactive metal centers that have shown great utility in catalysis [72], [73]. These ligands are also remarkable in stabilizing metals in a wide variety of oxidation states, which is related to their capacity to act as both σ -acceptors and π -donors [74].

In this context we combined these two ligands with tin(II) precursors.

4.2 Synthesis and Products

Reaction pathway number one is to lithiate the N-H functionalities of the DAMPY ligand and to follow a subsequent salt elimination reaction with SnCl_2 - see Figure 4.2. This attempt failed, because the lithiation step with n-BuLi makes problems.

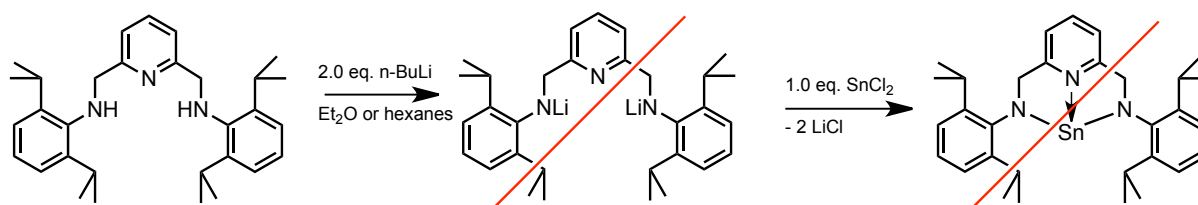


Figure 4.2: Unsuccessful attempt to lithiate the DAMPY ligand.

Robertson et.al. reported that the reaction of DAMPY with two equivalents of an alkyl lithium reagent in hexane at -78°C results in a precipitation of the base-free lithiated ligand. This compound is unusually temperature sensitive and decomposes in minutes at room temperature [52]. Therefore, we dismissed this idea and found another reaction pathway - see Figure 4.3. Instead of lithiating the ligand system we decided to use an active metal(II)-precursor, like $\text{Sn}[\text{N}(\text{TMS})_2]_2$ [75].

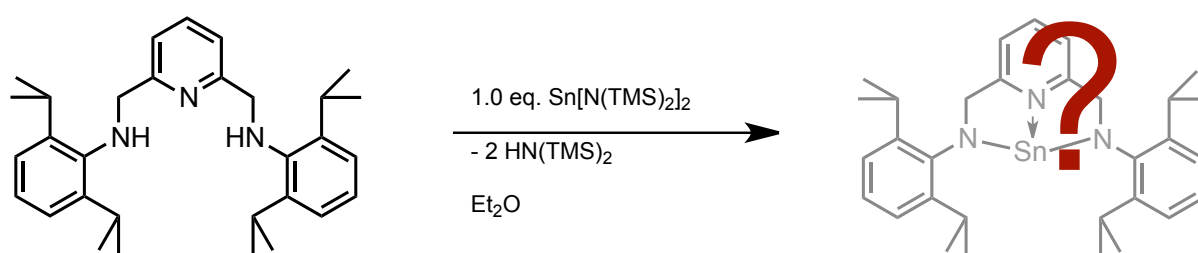


Figure 4.3: Transamination reaction of DAMPY with $\text{Sn}[\text{N}(\text{TMS})_2]_2$.

Indeed this reaction conditions were opportune. No degradation reactions or appearance of elemental tin could be observed. After two to three weeks brown crystals were formed.

Besides that, we also tried same reactions with an two to one ratio of tin(II)precursor and ligand as well as reactions with and without additional base $\text{HN}(\text{TMS})_2$ - see Figure 4.4.

Reaction conditions, have been the same for all three experiments. First, stirring at room temperature for two days. Second, storage at -30°C for one week, so that crystals were formed. As expected the amount of tin(II)precursor is important, because it determines the product. The reaction is base catalyzed and extra base in the reaction mixture causes the ligand system to dimerize, or two precursor molecule share one ligand.

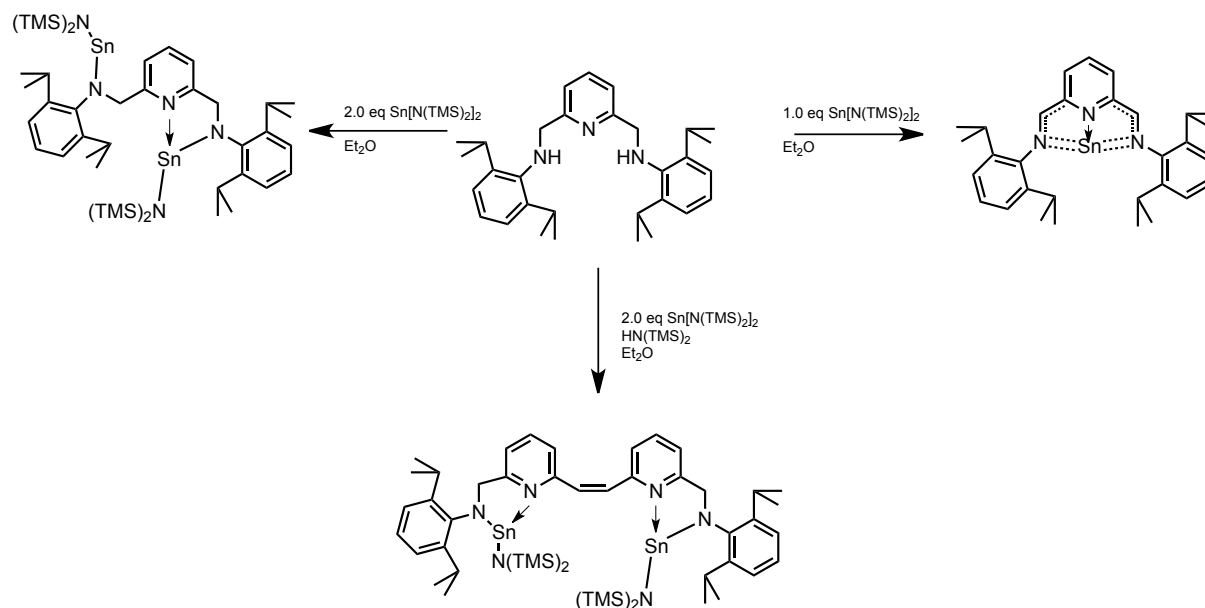


Figure 4.4: Reaction pattern of the DAMPY ligand with various combinations of tin(II) precursor and base

If the double amount of tin(II) precursor is used, two metal centers are coordinated to one ligand molecule. The compound is a di-stannylene - see Figure 4.5. No double bond is formed between the nitrogen and the carbon atoms and according to the solid state structure one tin(II)-center is two-coordinated and the other one is three-coordinated.

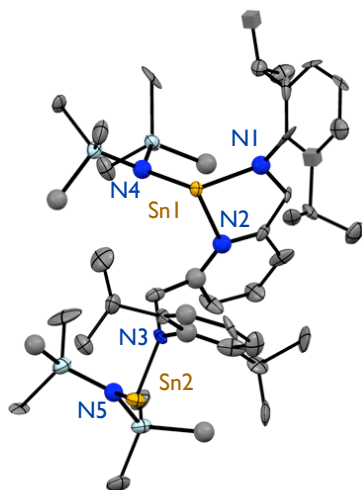


Figure 4.5: Solid state structure of $\text{N,N-tin(II)(NTMS)-N,N'-(pyridine-2,6-diylbis(methylene))bis(2,6-diisopropylaniline)}$. Hydrogen atoms were omitted for clarity.

Geometry optimization of this molecule confirms the crystal structure - see Figure 4.6. The two coordinated tin(II) center (Sn2) has got two nearly equal Sn2-N3/Sn2-N5 bonds (211.8 pm/208.2 pm). This describes a common hetero-leptic stannylene. This part of the molecule is very similar to the hetero-leptic bis(TMS)amidotin(II)N-(diisopropyl)(2-pyridylmethyl)amide. There we have found Sn-N bond length of 214.5 pm. And this compound comprises two possible conformations of a two and three coordinated tin center in one molecule. Besides that there is also the three coordinated Sn1 center, which is additionally stabilized by the pyridyl-nitrogen (N2) - having the typically long Sn1-N2 bond of 241.8 pm/236.1 pm. This bond is a σ -acceptor π -donor interaction.

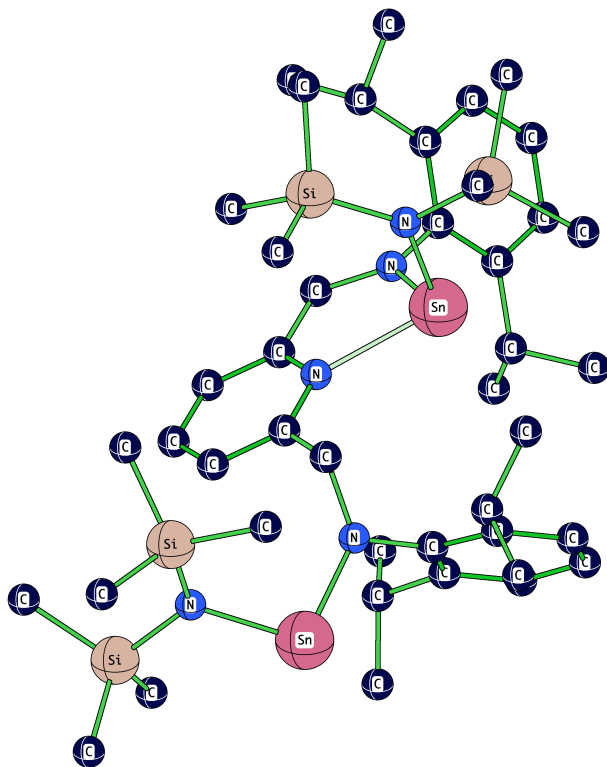


Figure 4.6: mPW1PW91/SDD optimized structure of N,N-tin(II)(NTMS)-N,N'-(pyridine-2,6-diylbis(methylene))bis(2,6-diisopropylaniline). Hydrogen atoms were omitted for clarity.

Table 4.1: Comparison of calculated (mPW1PW91/SDD) and experimental data of N,N-tin(II)(NTMS)-N,N'-(pyridine-2,6-diylbis(methylene))bis(2,6-diisopropylaniline)

distances [pm]	calculated	experimental
Sn1-N1	213.6	212.6
Sn1-N2	241.8	236.1
Sn1-N4	216.9	218.6
Sn2-N3	211.8	213.2
Sn2-N5	208.2	200.7
Σ angle- N1	359.19°	359.87°
Σ angle- N2	359.95°	360.00°
Σ angle- N3	359.91°	358.49°
Σ angle- N4	357.94°	357.72°
Σ angle- N5	358.18°	356.41°
¹¹⁹ Sn1 [ppm]	-157.57	120
¹¹⁹ Sn2 [ppm]	290.22	120

In Table 4.1 experimental and calculated data are summarized. The tin(II) centers Sn1 and Sn2 do not only differ in their Sn-N₍₁₋₅₎ bond distances, they also differ in their ¹¹⁹Sn chemical shift. The calculation predicts that the three coordinated Sn1 one center has a ¹¹⁹Sn chemical shift of -157.57 ppm and that the two coordinated Sn2 center will give a signal at 290.22 ppm in the spectra. The truth is, that in the experiment only one broad signal can be observed (120 ppm). Reason for this observation is, that these two Sn centers have the same chemical surrounding and the molecule is symmetric, so only one signal can be detected. (In solution the third coordination place switches between the two tin centers.)

The second attempt was to use the tin(II)-precursor in a 2:1 molar ratio with the ligand. The product was again a di-stannylene, but the ligand dimerized. Figure 4.7 displays the solid state structure of ethene-bistirmethylsilyl-diamine-tin(II).

In general base [HN(TMS)₂] is formed during the transamination reaction but additional access of base in the reaction mixture facilitates that the DAMPY ligand itself dimerizes. During the reaction a C=C double bond is formed and two ligand molecules are linked together. We determined this fact via analysis of the solid state structure. There we found the C1=C2 bond with 132.8 pm. In comparison the standard C-C single bond is at 150 pm [76].

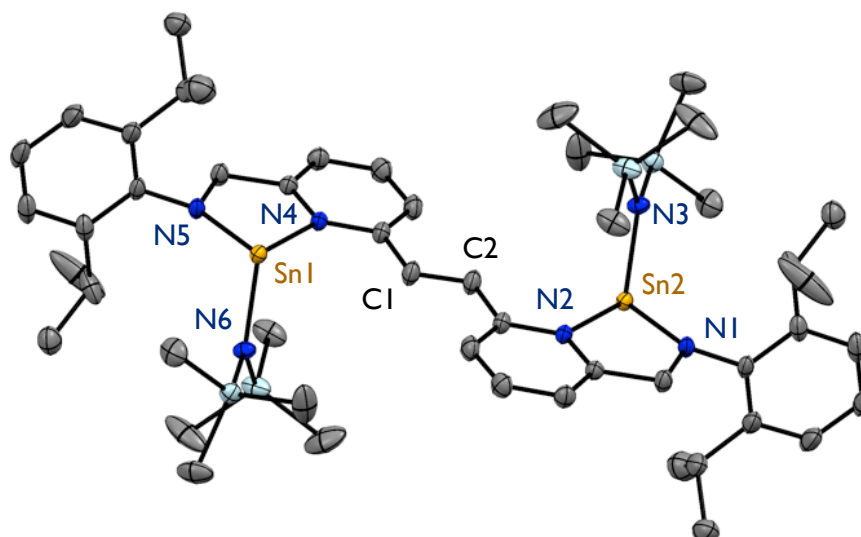


Figure 4.7: Solid state structure of ethene-bistrimethylsilyl-diamine-tin(II). Hydrogen atoms were omitted for clarity.

Table 4.2: Comparison of calculated (mPW1PW91/SDD) and experimental data of ethene-bistrimethylsilyl-diamine-tin(II)

distances [pm]	calculated	experimental
Sn2-N1	212.0	209.7
Sn2-N2	239.1	231.7
Sn2-N3	216.3	215.3
Sn1-N4	239.1	231.7
Sn1-N5	212.0	209.7
Sn1-N6	216.3	215.3
Σ angle- N1	357.65°	359.87°
Σ angle- N2	359.82°	360.00°
Σ angle- N3	359.97°	358.49°
Σ angle- N4	357.65°	357.72°
Σ angle- N5	358.18°	356.41°
Σ angle- Sn1	280.54°	275.73°
Σ angle- Sn2	280.54°	275.73°
$^{119}\text{Sn1}$ [ppm]	-162	-80
$^{119}\text{Sn2}$ [ppm]	-162	-80

Interesting about this molecule is that the two tin(II) centers (Sn1 and Sn2) are equal. They have the same chemical surrounding, because they show the same Sn-N distances and the same angular sums at the nitrogen and the tin atoms. Here we also can observe that always two nitrogen atoms are covalently bonded to the tin center and that a third pyridyl-nitrogen acts as a σ -acceptor π -donor. The Sn1-N4 and Sn2-N2 bonds are at 231.7 pm, they are longer than the Sn2-N3/Sn1-N6 bonds (215.3 pm). These long bonds correspond to the σ -acceptor π -donor interactions.

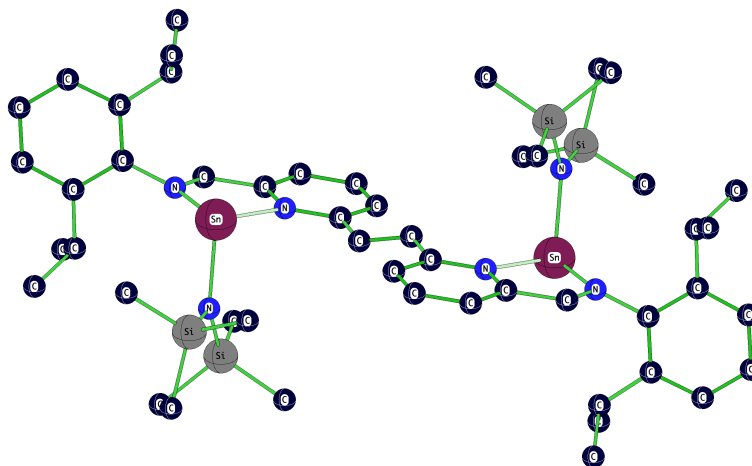


Figure 4.8: Optimized (mPW1PW91/SDD) structure of ethene-bistrimethylsilyl-diamine-tin(II). Hydrogen atoms were omitted for clarity.

The two tin centers are in a trigonal pyramidal surrounding, and have angular sums of 275.73° in the solid state and 280.54° in the geometry optimized structure. While these two tin centers are equal, they have the same ^{119}Sn chemical shift. According to the calculation -162 ppm and -80 ppm in the experiment.

These kind of compounds are already known. Hahn et.al. reported about bidentate benzimidazoline-2-germylenes. They described the reaction of a tetraamine ligand with the $\text{Ge}[\text{N}(\text{SiMe}_3)_2]_2$ precursor [77]. And they also worked with lutidine-bridged ligands bearing tin(II) and lead (II) as active metal centers [78].

Figure 4.9 displays the benzimidazoline-2-germylenes as chelating ligand for molybdenum as metal center. There the two germylene metal centers are also equal and have the same chemical surrounding.

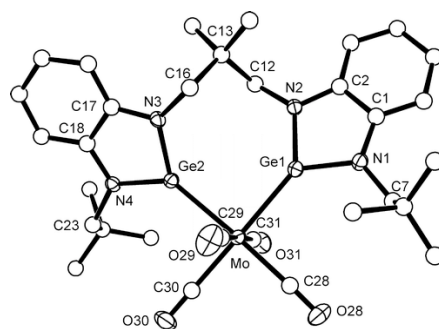


Figure 4.9: Solid state structure of [bis(N-neophenylbenzimidazoline-2-germylene)-2,2-dimethylpropane]-tetracarbonylmolybdenum(0). Hydrogen atoms were omitted for clarity [77].

And Figure 4.10 displays the lutidine-bridged bistannylene. There the two metal centers are equal and can form a three coordinated structure or they can trap a further tin atom in the center.

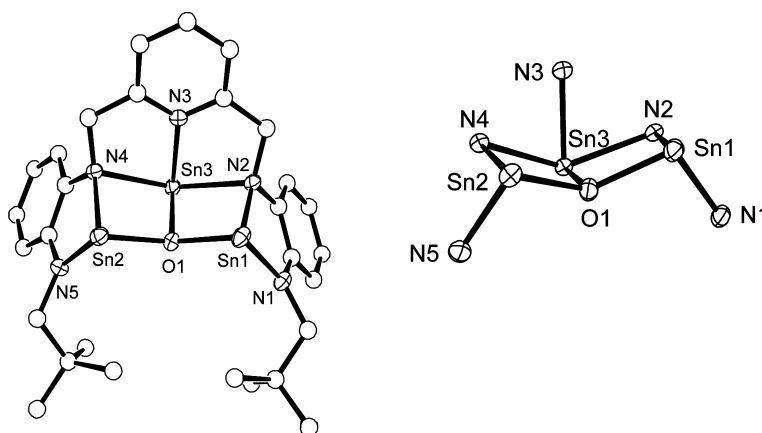


Figure 4.10: Solid state structure of bisstannylene. Hydrogen atoms were omitted for clarity [78].

The main difference between our tin(II) di-stannylene and the bisstannylene from Hahn is the ligand construction and the way of synthesis.

Hahn et.al. designed the ligand and afterwards they generated the bisstannylene. We produce our compound by only additional access of base in our ligand with tin-precursor reaction.

We assume that a ligand dimerization with a proton abstraction takes place, but the mechanistic background is not clear yet.

To determine the assumption that the basic tin(II)-precursor ($\text{Sn}[\text{N}(\text{TMS})_2]_2$) makes a proton abstraction at the ligand and induces maybe the formation of a C=N double bond or a C=C double bond, we used a modified ligand. As already mentioned the DIMPY - ligand is often used in transition metal chemistry, so we used it for our purposes. Figure 4.11 displays the reaction conditions and amounts of reactants, as well as the detected product.

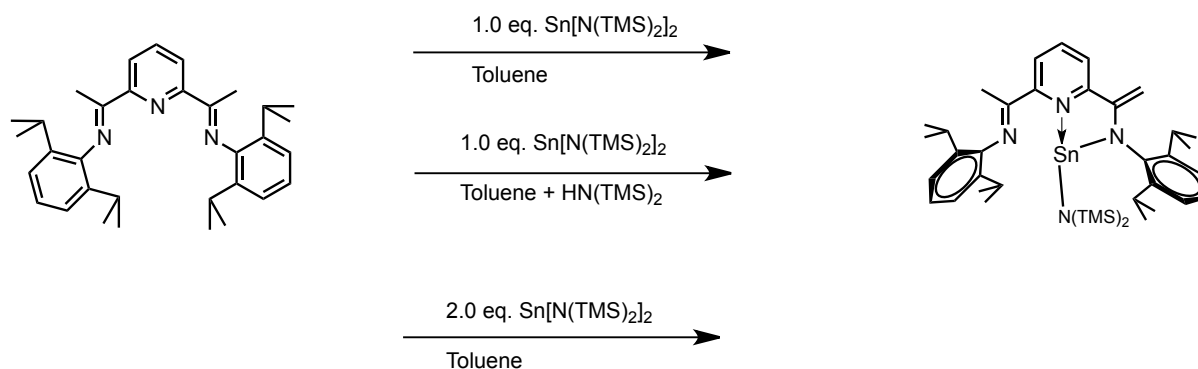


Figure 4.11: Reaction of the DIMPY-ligand with $\text{Sn}[\text{N}(\text{TMS})_2]_2$ in several molar ratios.

The product is a hetero-leptic three coordinated stannylene. Variation of the molar ratios always leads to the same product. Obvious is that one CH_3 -functionality turns into a CH_2 -functionality and forms a C=C double bond in the ligand system - a rearrangement reaction takes place. The structure was confirmed by single crystal-diffractometry and NMR measurements. Figure 4.12 displays the solid state and the geometry optimized structure.

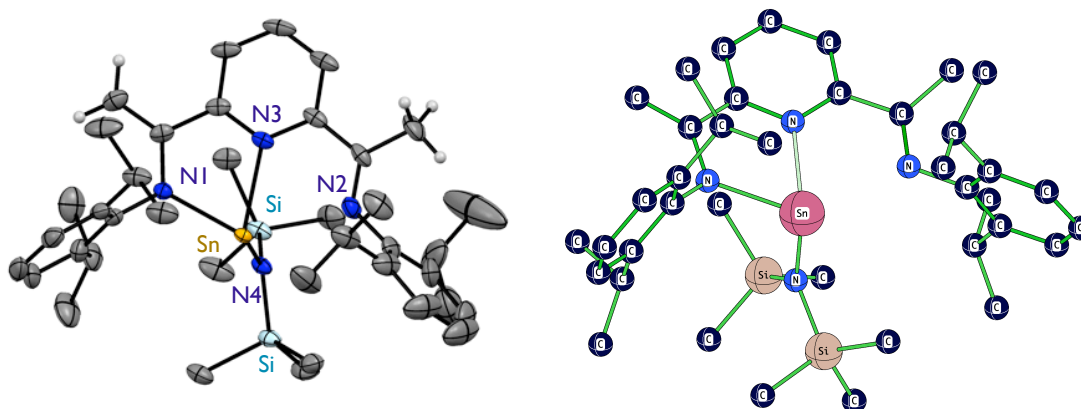


Figure 4.12: Solid state and optimized (mPW1PW91/SDD) structure of tin(II) 2,6-bis[1-(phenylimino)ethyl]pyridineTMS. Showing the CH_2 -group and the CH_3 - group all other hydrogen atoms were omitted for clarity.

Table 4.3 summarizes calculated and measured data. First of all, the Sn-N1 and Sn-N4 bond represent common Sn-N bonds. The Sn-N1 bond is long 223.6 pm/ 226.1 pm and the Sn-N4 bond has 215.2 pm/214.7 pm. Additionally, the tin metal center is stabilized by the pyridyl-nitrogen atom N3. We found a Sn-N3 bond length of 236.2 pm/240 pm. This range of the Sn-N bond corresponds to the already discussed tin(II) compounds. The NBO analysis gives more information about the donor/acceptor interaction.

Table 4.3: Comparison of calculated (mPW1PW91/SDD) and experimental data of tin(II) 2,6-bis[1-(phenylimino)ethyl]pyridineTMS

distances [pm]	calculated	experimental
Sn-N1	223.6	226.1
Sn-N2	280.9	281.1
Sn-N3	236.2	240.1
Sn-N4	215.2	214.7
Σ angle- N1	355.70°	352.82°
Σ angle- N2	360.00°	360.00°
Σ angle- N3	359.98°	360.00°
Σ angle- N4	359.82°	359.26°
¹¹⁹ Sn [ppm]	-190	-128
²⁹ Si1 [ppm]	-3.41	-2.26

Only the N1 nitrogen atom is in a slight trigonal pyramidal surrounding, with an angular sum of 355.70° / 352.82°. All other nitrogen atoms are in a planar surrounding with angular sums between 359 ° and 360°.

The ¹¹⁹Sn chemical shift is at -128 ppm in the experiment, giving a broad signal in the spectrum. This was confirmed by the calculated (mPW1PW91/IGLO-II) value of -190 ppm. Besides this NMR measurement we also did the ²⁹Si experiment and we have been able to assign the signal at -2.26 ppm/-3.41 ppm to the N(SiMe₃)₂ groups.

To get more information about the bonding situation we made some natural bond orbital calculations. Figure 4.13 displays the orbitals.

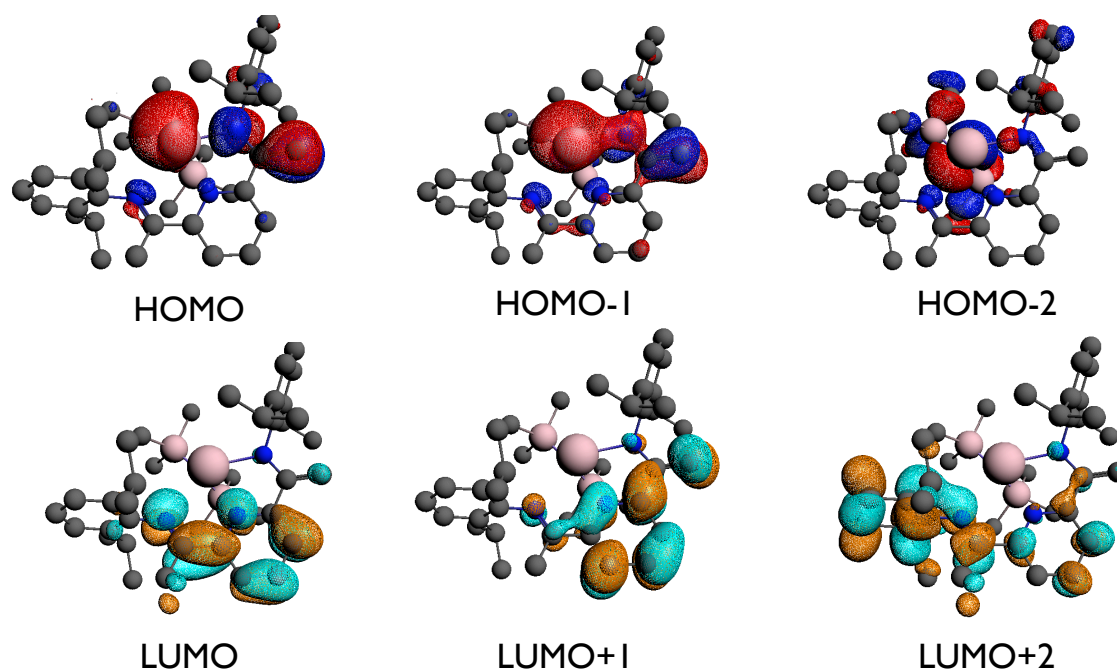


Figure 4.13: Calculated (mPW1PW91/IGLO-II) nuclear bond orbitals of tin(II) 2,6-bis[1-(phenylimino)ethyl]pyridineTMS

NBO analysis shows that the HOMO includes the electron lonepair from the pyridyl-nitrogen atom, which donates into the empty p-orbital of the tin center. The HOMO also displays the electron lone pair at the tin(II) metal center, the corresponding anti-bonding orbital is the LUMO +1. In the HOMO-1 orbital the π -bond between the tin and the N1 nitrogen atom is displayed as well as the π -bond between C and CH₂. The corresponding anti-bonding orbital is the LUMO. Last the HOMO-2 orbital allocates the σ -bond between the tin and the N(SiMe₃)₂ residue. The corresponding anti-bonding orbital is the LUMO+2. All occupied orbitals indicate that there must be an interaction between the N2 and the Sn-center, although the Sn-N2 distance is at 280.9 pm/281.1 pm.

Therefore the tin center is four coordinated. Geometry parameters are similar to the two compounds we already discussed before.

Further this reaction procedure shows, that the reaction is base catalyzed. The tin(II)-precursor and the base initiate that a CH₃ residue is transformed into a CH₂. But the base is not strong enough to provide a second proton abstraction step to form a symmetric stannylene. The other part of the ligand remains intact.

Deprotonation of the bis(imino)pyridine ligand and related complexes can occur. The capacity of bis(arylimino)pyridine ligands to undergo deprotonation reactions, alkylation, and participate in reduction chemistry has been the subject of a number of reports [73].

4.3 An aromatic Stannylene with special Geometry Features

As reported before we did the transamination reaction of the DAMPY ligand with the tin(II) precursor. We generated different types of di-stannylenes. Besides that, we also detected and analyzed a very unusual tin species - see Figure 4.14.

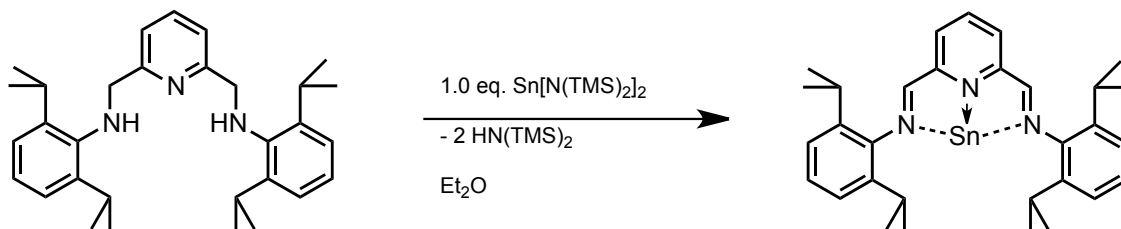


Figure 4.14: Transamination reaction of DAMPY with $\text{Sn}[\text{N}(\text{TMS})_2]_2$ displaying the unexpected stannylene

On the first glance it seemed to be the desired stannylene according to Figure 4.3. But solid state analysis showed that the product is something else - there is a tin atom in the ligand center but the ligand has changed during reaction.

Figure 4.15 displays the solid state and the geometry optimized structure.

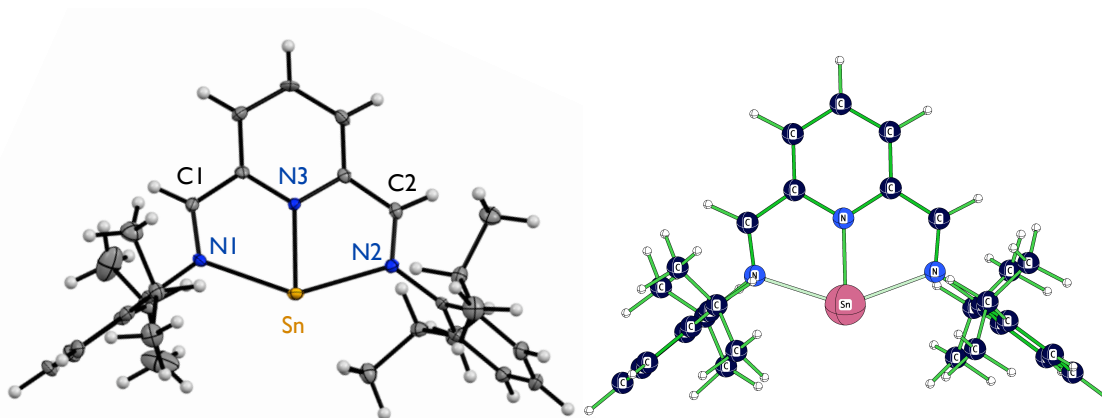


Figure 4.15: Solid state and optimized (mPW1PW91/SDD) structure of bisdiimino-Sn

According to the solid state structure double bonds were formed between N1-C1 and N2-C2. Via X-ray measurements we allocated the two single hydrogen atoms at the C1 and C2 atom centers. Therefore we geometry optimized the crystal structure and compared the data.

Table 4.4 summarizes bond distances and angles as well as measured and calculated (mPW1PW91/SDD; mPW1PW91/IGLO-II) parameters.

Table 4.4: Data from the solid state and optimized (mPW1PW91/SDD) structures of bis-imino-Sn and the DAMPY ligand

	bisdiimino-Sn		ligand alone	
	experimental	calculated	experimental	calculated
N3-C4 [pm]	139.0	140.3	134.2	134.7
N3-C3 [pm]	139.5	140.2	134.4	135.7
N1-C1 [pm]	132.1	132.8	145.9	146.4
N2-C2 [pm]	130.8	133.0	146.1	145.0
C3-C1 [pm]	140.7	141.9	150.0	152.0
C4-C2 [pm]	141.1	141.8	150.1	151.6
N1-Sn [pm]	239.7	237.7	-	-
N2-Sn [pm]	231.2	236.4	-	-
N3-Sn [pm]	212.2	215.2	-	-
N1-Sn-N3	70.54°	70.88°	-	-
N2-Sn-N3	72.18°	71.04°	-	-
N1-Sn-N2-N3	6.28°	6.54°	-	-
Σ angle- N1	359.87°	359.97°	-	349.68°
Σ angle- N2	357.85°	357.93°	-	348.36°
Σ angle- N3	359.98°	359.84°	-	36.00°
¹¹⁹ Sn shift [ppm]	64.45	-180	-	-

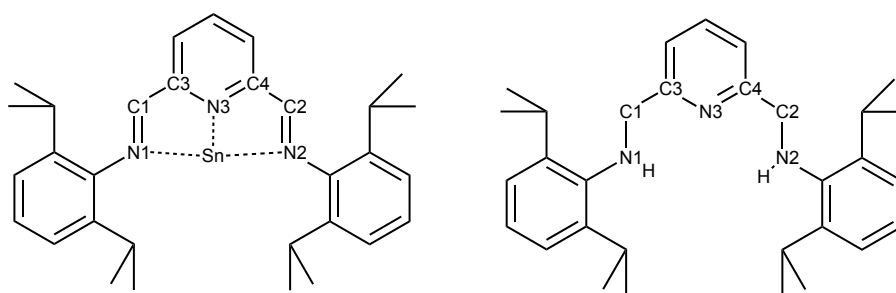


Figure 4.16: Substitution pattern of bisdiimino-Sn and the DAMPY ligand

Bond length analysis shows, that the C1-N1 bond is at 132.1 pm and the C2-N2 bond at 130.8 pm. Experimental common single bonds between nitrogen and carbon are usually 145-146 ppm [79].

In Table 4.4 DAMPY ligand parameters are displayed for comparison. It is obvious that the N1-C1/N2-C2 bonds are double bonds. The bond distance decreases from the original 145-146 pm to 132-130 pm. Also the C3-C1/C4-C2 bonds become smaller, from 150.1 pm to 140.7 pm. This circumstance indicates, that a conjugated π -system is formed. The bond distance between two double bonded carbon atoms is smaller (148 pm) than usual C-C single bonds (154 pm) [76].

The angular sum around the nitrogen atoms changed. In the free ligand N1 and N2 have a trigonal pyramidal surrounding (349.68° and 348.36°). In the tin-complex we found N1 and N2 are trigonal planar with bond angle sums of 359.97° and 357.93° . Planar nitrogen atoms usually appear if they are three-coordinated with electronegative substituents or if they have a double bond to the neighboring atom.

If there is a conjugated π -system formed in the ligand, than the compound should show aromaticity. To confirm this assumption we did NICS calculations. Figure 4.17 displays where dummy atoms (Bq) are placed in the molecule and Table 4.5 summarizes the values.

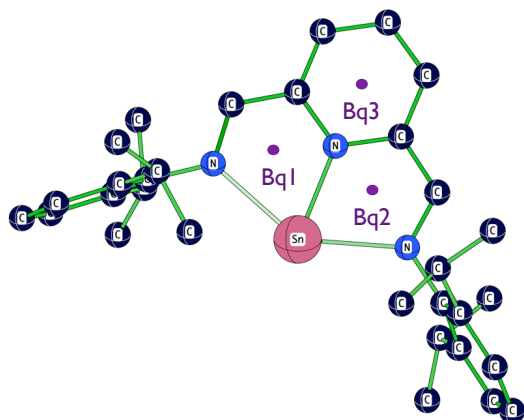


Table 4.5: Calculated (mPW1PW91/IGLO-II) NICS values for bisdiiminSn

Bq	NICS [ppm]
Bq1	-6.3
Bq2	-6.7
Bq3	-0.5

Figure 4.17: Optimized (mPW1PW91/SDD) structure bearing three dummy molecules (Bq1-Bq3) for the NICS calculation. Hydrogen atoms were omitted for clarity

The dummy atoms Bq1 and Bq2 have NICS values at -6.3 ppm and -6.7 ppm and that indicates that these parts of the molecule are aromatic. In contrast aromaticity at the pyridine ring system is nearly zero, having a NICS value of -0.5.

Besides these C=C double bonds we also detected that the Sn-N(1-3) bonds are not equal. The Sn-N1 and Sn-N2 bonds are at 239.7 pm/237.7 pm and 231.2 pm/236.4 pm. The Sn-N3 bond is shorter, with 212.2 pm. So a contraction of the whole ligand in this part happened.

This observation can be compared with the aromatic germylene and the bis(TMS)amido-tetrylenes. There we already found out, that an aromatic five membered ring with the metal center is built and that the pyridine backbone loses its aromaticity.

Two different metal center -nitrogen bonds we also observed in bis(TMS)amido-tetrylenes. Up to now we explained this circumstance with one shorter covalent bond and with one longer dative bond.

To gain a deeper insight into the orbital constitution NBO-analysis were carried out, using the the mPW1PW91 functional and IGLO-II basis sets for all atoms. Figure 4.18 displays the occupied and virtual orbitals of the bisdiimin-Sn derivative.

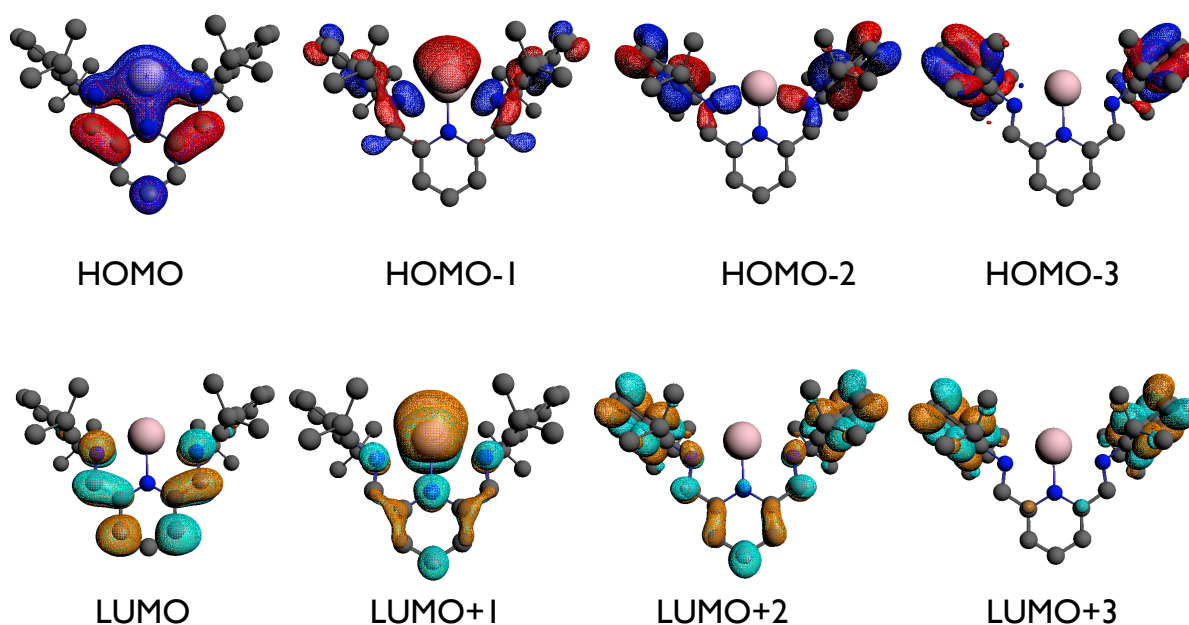


Figure 4.18: Natural Bond Orbitals for the bisdiimin-Sn.

The HOMO displays the π -interaction between the nitrogen atoms and the vacant p-orbital on the tin metal center. It seems that the interaction between the pyridyl-nitrogen is stronger than between the other two neighboring nitrogen atoms. This fits with the fact that the Sn-N3 distance is much shorter than the other two. The energy difference between the HOMO and the LUMO orbital is 2.34 eV.

The HOMO-1 displays the electron lone-pair at the tin center and the π -bond between the nitrogen and the carbon atom.

And the HOMO-2 shows the σ -bond between the neighboring nitrogen atoms and the tin center as well as the σ -bond between the nitrogen and carbon atoms. Further the π -orbitals of the diisopropyl groups are visible. The LUMO+2 is the corresponding anti-

bonding orbital.

Similar NBO orbitals were already discussed in the case of the aromatic germylene. There we also found that the metal center is embedded in a π -orbital between the nitrogen atoms. But there we have only one five membered ring. In contrast the bisdiimin-Sn has two five membered rings. The two rings are bridged by the Sn-N3 π -interaction.

All in all there is a conjugated π -system in the ligand-part, which bridges over the nitrogen atoms to the tin center and provides a π -interaction. NBO analysis confirms the NICS calculations. But besides these information, the NBO analysis also shows that there is still a conjugated π -system at the pyridine backbone - see HOMO, LUMO and LUMO +2 orbitals.

Conjugated π -systems tend to be colored. Our bisdiimin-Sn has a red-purple color in solution and the crystals are purple-brown. Figure 4.19 displays calculated and measured spectra.

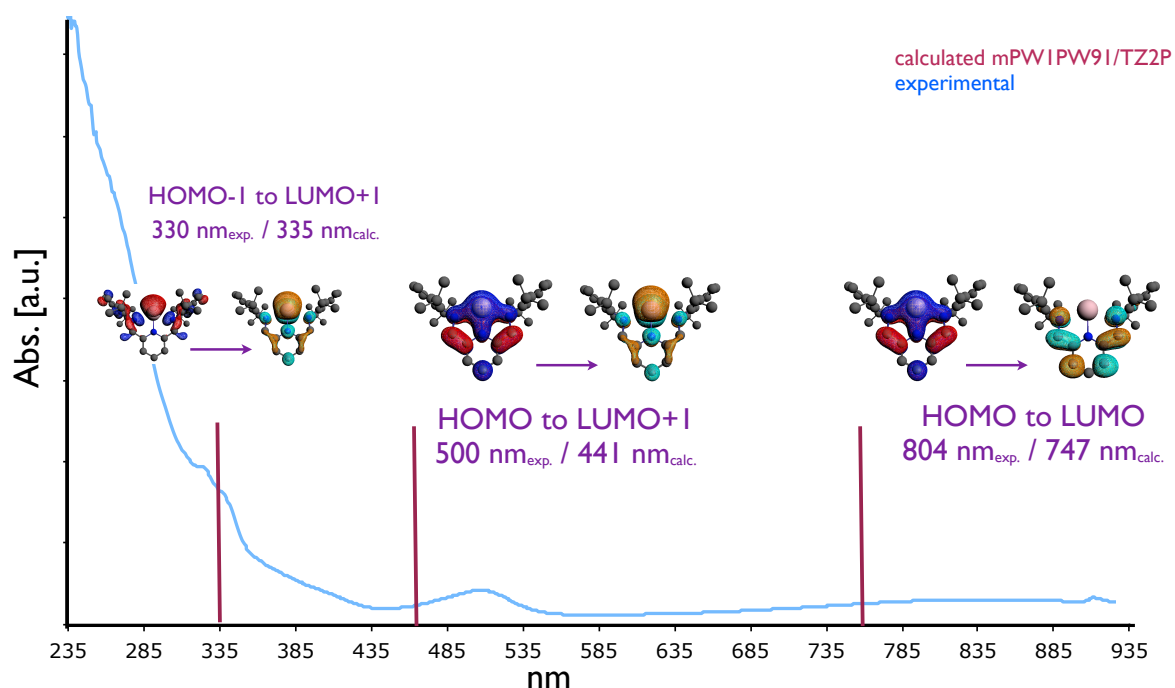


Figure 4.19: Experimental and simulated (mPW1PW91/ZORA/TZ2P) UV-VIS spectra, displaying the possible transitions.

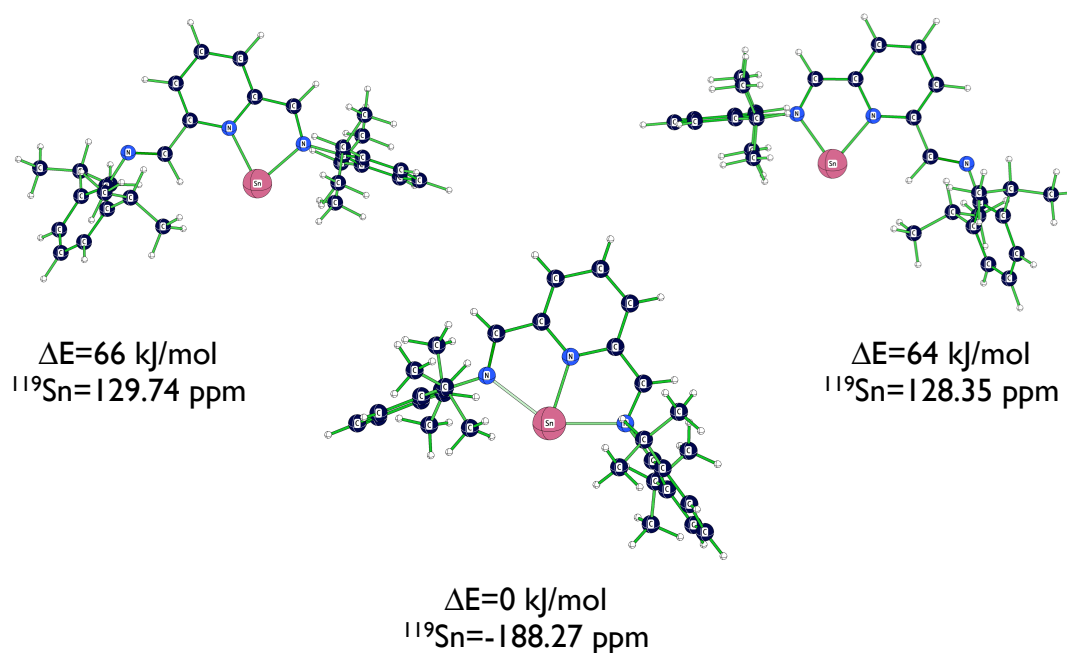
The experimental spectrum was recorded in heptane as solvent. Obvious are three transitions. First the HOMO -1 to LUMO+1 transition at 330nm/335nm, which is more in the ultraviolet region. The second important transition is at 500nm/441nm, and contributes a red-purple part in the color and at least the HOMO to LUMO transition at 804nm/747nm. Table 4.6 summarizes the calculated and experimental data.

Table 4.6: Comparison of calculated (mPW1PW91/ZORA/TZ2P) and experimental UV-VIS data of bisdiiminSn.

transition	experimental	calculated	ϵ exp.	type
HOMO-1 to LUMO	320 nm	335 nm	370	$n \rightarrow \pi^*$
HOMO to LUMO+1	500 nm	441 nm	82	$\pi \rightarrow \pi^*$
HOMO to LUMO	820 nm	747 nm	62	$\pi \rightarrow \pi^*$

Experimental and simulated data differ from each other. There is always a solvent interaction in the solution. We still have to be aware of the fact that the calculation assumes the molecule in the gas phase. In gas phase there are no molecule to solvent interactions involved. The data is not exact, but it confirms the trend.

Not only the UV-VIS spectra can be influenced by solvent interaction, also the chemical shift can be highly affected. For bisdiimin-Sn there are three possible conformations shown. Figure 4.20 displays three thermodynamically stable structures. Theoretically there can be more different thermodynamically stable structures.

**Figure 4.20:** Optimized (mPW1PW91/SDD) conformations of bisdiiminSn in gas phase. Calculated ^{119}Sn chemical shifts (mPW1PW91/IGLO-II).

The three-coordinated tin atom is the global minimum, as we found it in the solid state

structure. The two other conformations are possible, but the energy difference is 64/66 kJ/mol. This indicates that it is rather improbable to detect these species in the NMR measurement or to crystallize them. The Boltzmann weighted calculated ^{119}Sn chemical shift is at -180 ppm and the measured value is 64 ppm. This deviation may be contributed to the solvent to molecule interaction in solution. The simulated ^{119}Sn chemical shifts are in gas phase.

The broad ^{119}Sn signal in the experiment is similar to those we saw for the bis(TMS)amino-stannylene, indicating an anisotropy around the tin core.

According to the NMR-spectra it might be a stannylene because of its ^{119}Sn chemical shift anisotropy. Via the use of ^{119}Sn NMR spectroscopy it is possible to provide accurate, relatively easily obtainable information on the bonding to the tin atom [80]. Our compound shows these typical attributes of an tin(II)-species, giving one broad signal, 64 ppm +/- 5 ppm in the ^{119}Sn spectra.

We analyzed the bisdiiminSn and simulated an aromatic stannylene as product. Further to confirm our theory, we decided to simulate and compare also two other theoretically possible products. In the next chapter we will discuss a non-aromatic stannylene and a tin(II)dihydride as potential products.

4.3.1 Comparison of possible Products

To determine oxidation state of the tin metal center and to determine the bond order, quantum chemical calculations with the ADF[67] and AllAIM[81] programs were made. Alternative products for the transamination reaction of the DAMPY ligand, are a tin(II)dihydride species or a common stannylene. Figure 4.21 displays the possible products.

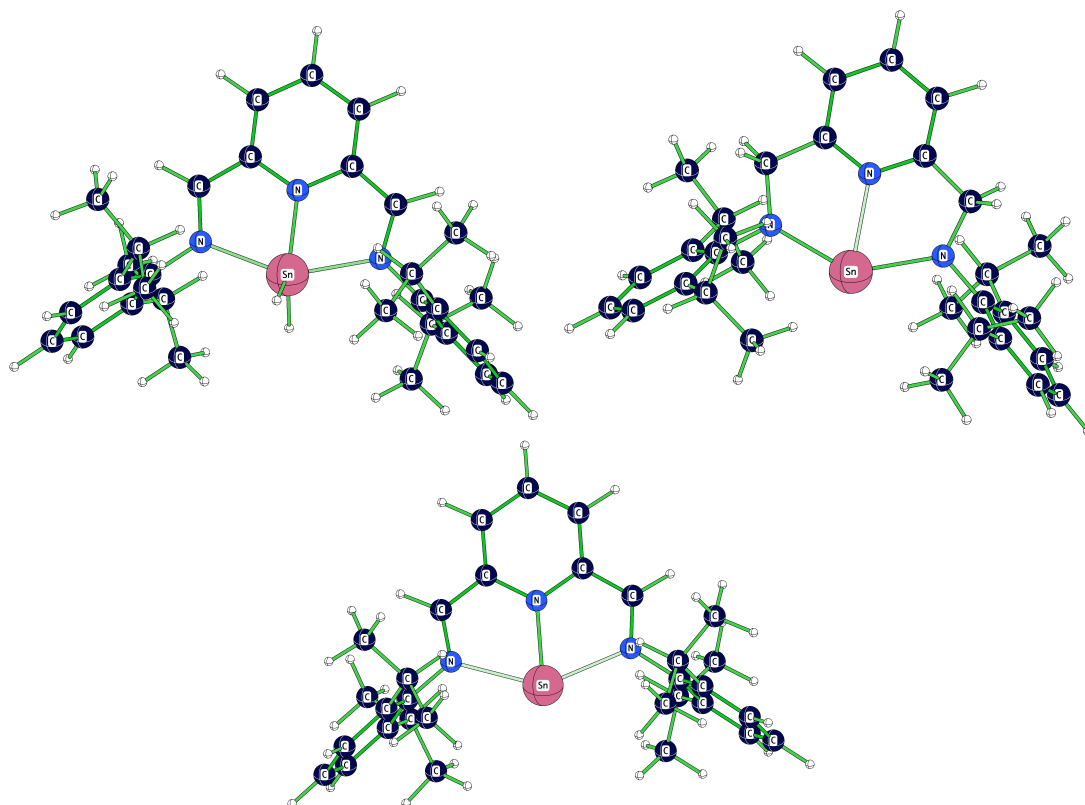


Figure 4.21: Geometry optimized (mPW1PW91/SDD) structures of the bisdiimini Sn(II)dihydride, bisdiaminSn(II) and bisdiiminiSn

Via comparison of Sn-N bond distances and angles it should be possible to exclude some of the possible products. Also the ^{119}Sn chemical shift will give information about the tin species in the ligand center. Calculated and measured data are compared in Table 4.7.

Table 4.7: Comparison of calculated (mPW1PW91/SDD and mPW1PW91/IGLO-II) data with the solid state parameters of the bisdiiminSn

distances [pm]	Sn(II)-dihydride	Sn(II)stannylene	bisdiiminSn	solid state
N1-Sn [pm]	224.2	219.2	237.7	239.7
N2-Sn [pm]	224.3	218.0	236.4	231.2
N3-Sn [pm]	206.3	239.0	215.2	212.2

On the first glance it is obvious that the proposed possible products, as a tin(II)dihydride or a stannylene are nearly impossible. Comparison of the calculated Sn-N distances with the solid state structure shows that in the case of the tin(II)dihydride they do not fit at all. The calculated values are too long - being at 224.2 pm for the Sn-N1/Sn-N2 bond and too short for the Sn-N3 value.

Via a ^{119}Sn NMR experiment, measuring a coupled Sn-H spectra we proofed there are no hydrogens attached to the tin center. The ^{119}Sn signal stays a broad singlet and does not split into two.

The comparison with the proposed non-aromatic stannylene species also shows an inaccurate fit with the solid state data. The Sn-N1/Sn-N2 distances are much shorter than in the solid state- being at a value of 219.2 pm and 218.0 pm. And in contrast the Sn-N3 distance is too long (239.0 pm) than measured in the solid state structure (212.3 pm).

Our experimental ^1H spectra confirm, that there is a nitrogen to carbon double bond. Additionally we assigned a singlet signal in the ^1H spectra to be buy to the hydrogen atoms at the double bonded carbon atoms. IR-measurements show us, that the C=N bond is there. We found the N=C vibration at 1647 cm^{-1} and 1506 cm^{-1} .

The only explanation is, that there is a N=C double bond in the ligand and that the tin center is embedded in a huge π -orbital, that bridges the three nitrogen atoms. We were able to exclude the tin(II)dihydride and the non-aromatic stannylene as potential products. Now the question comes up, how is the bond order in this unusual bisdiiminSn derivative and what kind of oxidation state can we propose.

Therefore we will make a BADER-analysis.

4.3.2 BADER Analysis

Via the BADER analysis we will be able to find bond critical points and to obtain the bond orders for our bisdiiminSn. For the BADER calculation we used a simplified model of our compound -see Figure 4.22.

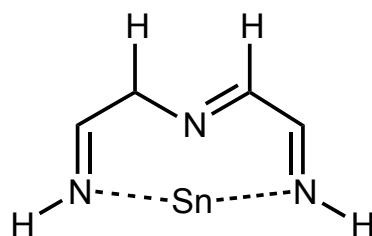


Figure 4.22: Simplified structure of bisdiiminSn

First of all in a molecule several kind of critical points can be found. Figure 4.23 displays calculated critical points in the model molecule.

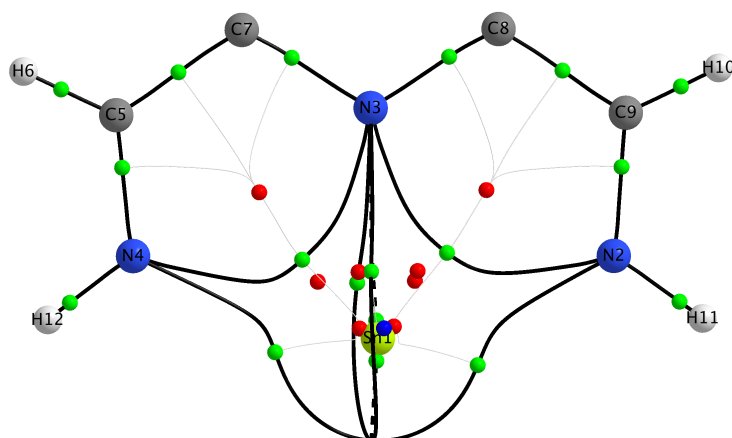


Figure 4.23: Critical points in the model molecule

- Green spheres: Bond Critical Points (BCPs).
- Red spheres: Ring Critical Points (RCPs).
- Blue sphere: Cage Critical Point (CCP).
- Black paths: Bond Paths, i.e., pairs of GradRho paths which originate at BCPs and terminate at nuclei (Nuclei Attractor Critical Points actually). Each BCP has a pair of GradRho paths which together define the Bond Path. Note that the C-C Bond Paths are significantly "bent", which is consistent with the notion of severe "bond strain" associated with Tetrahedrane.

Critical points are labeled: (rank, signature)

- Bond Critical Point (BCP): (3, -1)
- Ring Critical Point (RCP): (3, +1)
- Cage Critical Point (CCP): (3, +3)

A ring critical point will always be found in the interior of a ring of chemically bonded atoms. When several rings are connected in a manner which encloses an interstitial space, a cage critical point arises in the enclosed space [82].

We will take a look at the bond critical points, which are placed along the calculated bond paths. On the first glance it seems, that there is an interaction between the three nitrogen atoms and the tin metal center. Bond paths are calculated between the nitrogen atoms and a dashed line can be seen to the tin metal center. That indicates a weak interaction between these two nuclei (N3 to Sn) - see Figure 4.24.

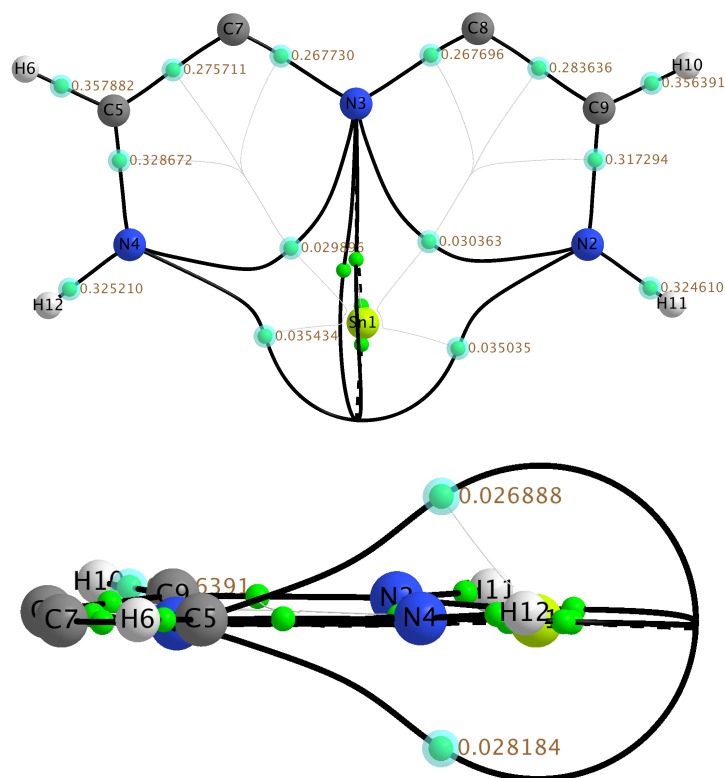


Figure 4.24: Bond critical points and bond paths.

The C=N double bonds have a value of $\rho=0.328$ au or smaller $\rho=0.267$ au at their BCP. For the C-C single bonds BCP values of $\rho=0.275$ au can be found. These figures fit with

the data Bader proposed in his work [83]. Values of $\rho=0.0298$ to $\rho=0.0354$ indicate that there is only a weak bonding interaction between the atoms, as we found for the N-N bonds. Further also the tin-nitrogen bonds are weak, BCS values of $\rho=0.0350$ au/ $\rho=0.0354$ au/ $\rho=0.000052$ were found. All the BCPs are along a bond path.

Firme and coworkers connected the charge density of atoms bonds with the bond order [84]. Values of $\rho=0.231$ au indicate a single bond (bond order is 1), values of $\rho=0.344$ au indicate a double bond (bond order is 2) and values of $\rho=0.412$ au indicate a triple bond (bond order is 3) according to their analysis.

This means, that in our case we have a nitrogen to carbon double bond ($\rho=0.328$) and nitrogen to carbon single bonds ($\rho=0.275$). This confirms the solid state structure and the geometry optimized structure. There we also ascertained that there is an conjugated π -system of short and longer N-C bonds. Values smaller than $\rho=0.231$ mean that there is less than a single bond, therefore the small $\rho=0.0350$ and $\rho=0.000052$ stand for only a weak interaction and a bond order small than one.

To allocate electron lone pairs and bonded charge concentrations, we did a relief map of $\nabla\rho$ - see Figure 4.25.

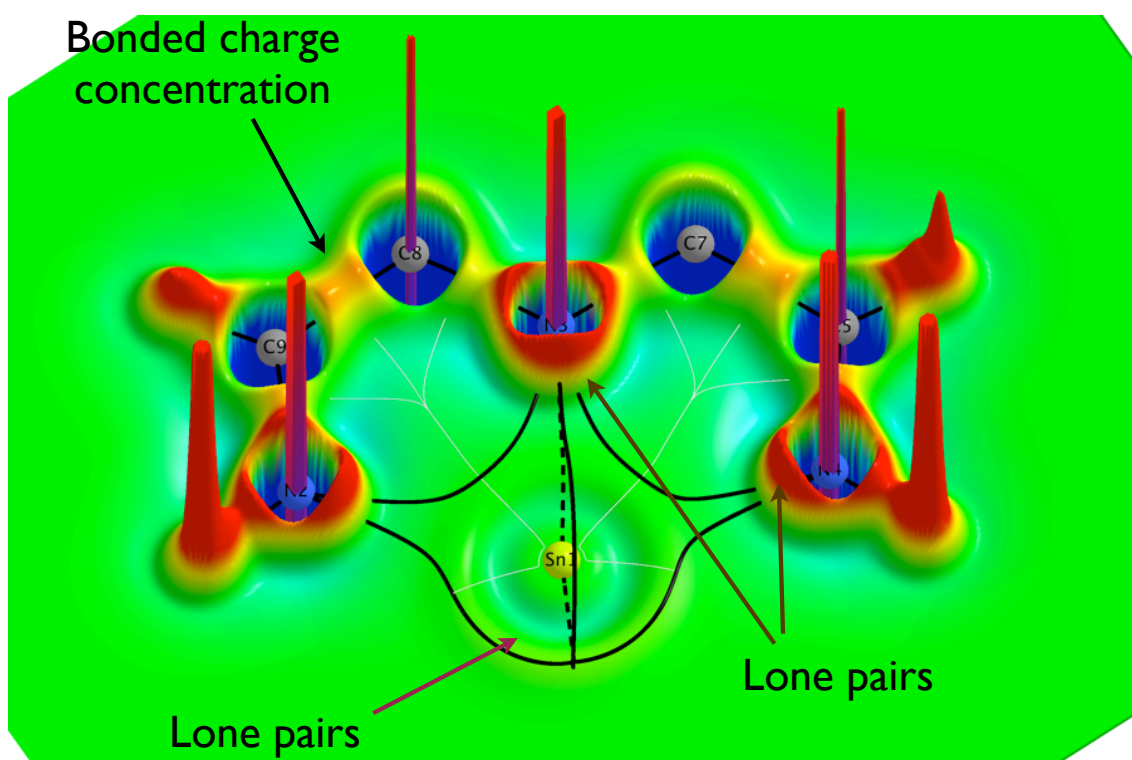


Figure 4.25: The laplacian surface of $\nabla\rho$, relief map

In the relief map we see the nitrogen carbon bonds (that is the bond charge concentration), the electron lone pairs at the nitrogen atoms (red regions), which are directed to the tin center. And we also see that there is a weak electron concentration at the tin center, indicating the electron lone pair. While we have a delocalized π -system around the tin center, it is possible that the non bonded electrons are distributed all over the molecule. Unfortunately there is no bonded charge concentration between the nitrogen atoms and the tin center- that confirms the assumption, that there is no covalent bond.

Besides that, as mentioned before, we found RCPs. The RCPs usually can be found if there are chemically bonded atoms or, in an aromatic system. We found the aromatic system in the bicyclic nitrogen, carbon and tin rings.

Analysis of the BADER charges showed that the tin is in an oxidation state of +II. There is no covalent bond between the tin center and the nitrogen atoms. The bonding situation indicates that there is aromaticity. The metal center is trapped between the nitrogen electron lone pairs. Via NBO analysis we assigned a π -bond at the Sn-N atoms. BADER analysis confirmed the assumption that the compound is an aromatic tetrylene.

The whole molecule is neutral, and no counter ions were detected. Therefore the tin metal center is formally seen a Sn(0) derivative.

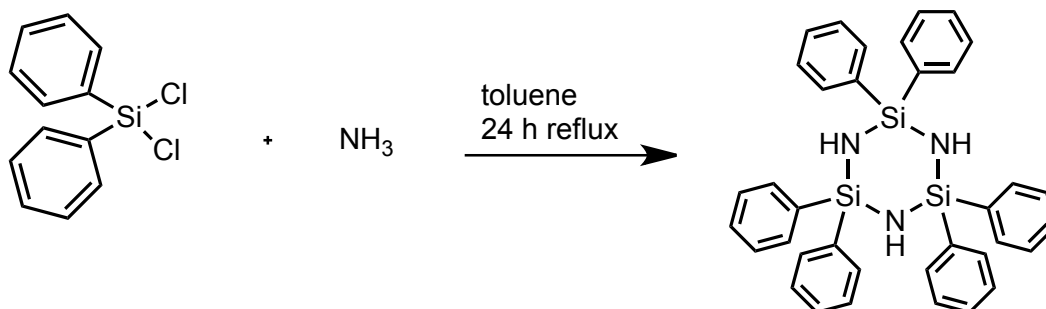
5 Experimental

5.1 General Procedure

All reactions were carried out under dry and inert nitrogen atmosphere using standard Schlenk, glove box, and syringe techniques. Chemicals were purchased from Sigma-Aldridge with further purification if necessary. Solvents were dried over molecular sieves or copper columns using an INNOVATIVE TECHNOLOGIES column solvent purification system. NMR spectra were recorded at 300.22 MHz (^1H NMR), 75.50 MHz (^{13}C NMR), 59.64 MHz (^{29}Si NMR), MHz (^{29}Al NMR), and 111.92 MHz (^{119}Sn NMR) on a Varian Mercury 300 instrument. Probes have been dissolved in THF and as an external standard a D_2O capillarity was used or CDCl_3 , C_6D_6 were used as internal standard.

5.2 Synthesis

5.2.1 Hexaphenylcyclotrisilazane



Dry ammonia gas was slowly purged through a boiling solution of diphenyldichlorosilane (150 ml, 0.713 mol) in 500 ml of toluene and refluxed for 3.5 hours. After 3.5 hours the heating was stopped and only ammonia gas was purged for 45 minutes through the reaction mixture. The solution was filtered and pentane was added so that the product crystallized. The colorless, powdery product was washed with cold pentane and dried under reduced pressure. Yield >90%.

^{13}C NMR (75 MHz, CDCl_3 , ppm): δ 138.77 (C ipso), 134.86 (C ortho), 129.71 (C para), 127.83 (C meta)

^1H NMR (300 MHz, CDCl_3 , ppm): δ 7.68 (m, 12H), 7.45 (m, 12H), 7.39 (m, 6H); NH 1.68 (s, 3H)

^{29}Si NMR (59 MHz, CDCl_3 , ppm): δ -20.14 (3Si)

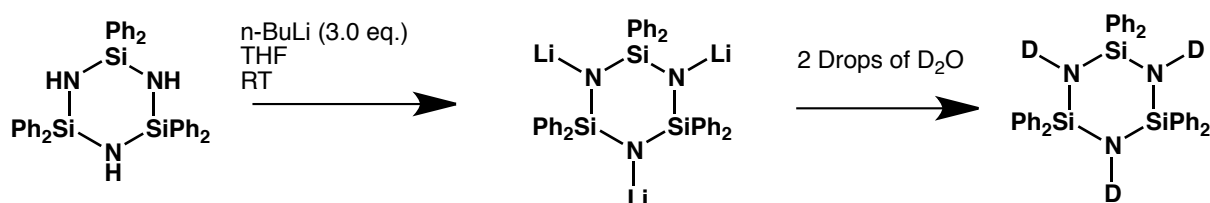
Elemental analysis (%) calcd for $\text{C}_{33}\text{H}_{33}\text{N}_3\text{Si}_3$: C 73.05, H 5.62, N 7.10; found: C 68.63, H 5.82, N 5.90

IR (cm^{-1}): (NH, sym. str) 3351.9, (NH asym. str.) 3368.6; (NH) 1366, 1208, 503; (Si-N-Si) 937, 949; (Si-Ph) 1183, 1115, 1107, (Si- Ph_2) 618; (Si-C, Ph) 527, 480, 470, 406, 393; (Ph, CH, C=C) 3071, 3054, 2933, 2855, 1585, 1430, 1463, 739, 728

Melting point: $>300^\circ\text{C}$

Crystallographic data: **1** and **1a**

5.2.2 1,3,5-deuterium-2,2,4,4,6,6-exaphenylcyclotrisilazane



To a stirred suspension of hexaphenylcyclotrisilazane (2.0 g, 3.38 mmol) in 50 ml of THF $n\text{-BuLi}$ (2.5 M in hexane, 4.05 ml) was added. The reaction mixture was stirred overnight at room temperature. Afterwards some drops of D_2 were added to the yellowish solution. The solvents were removed in vacuo to dryness. The product is a yellowish powder. Yield $>90\%$.

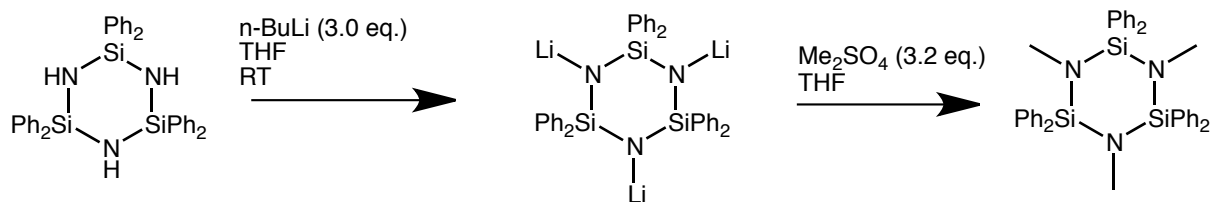
^{13}C NMR (75 MHz, CDCl_3 , ppm): δ 138.77 (C ipso), 134.86 (C ortho), 129.71 (C para), 127.83 (C meta)

^1H NMR (300 MHz, CDCl_3 , ppm): δ 7.65 (m, 12H), 7.36 (m, 12H), 7.39 (m, 6H)

^{29}Si NMR (59 MHz, CDCl_3 , ppm): δ -20.14 (3Si) IR (cm^{-1}): (ND, sym. str) 2494, (NH asym. str.) 2484; (NH) 366, 802; (Si-N-Si) 937, 949; (Si-Ph) 1183, 1115, 1107, (Si- Ph_2) 618; (Si-C, Ph) 527, 480, 470, 406, 393; (Ph, CH, C=C) 3071, 3054, 2933, 2855, 1585, 1430, 1463, 739, 728

Melting point: $>300^\circ\text{C}$

5.2.3 1,3,5-trimethyl-2,2,4,4,6,6-hexaphenylcyclotrisilazane



To a stirred solution of hexaphenylcyclotrisilazane (2.0 g, 0.00338 mol) in 50 ml of THF, butyl-lithium (7.3 ml, 0.011 mol, 2 M in hexane) was added at 0 °C. Afterwards the yellowish reaction mixture was treated with dimethyl sulfate (0.5 ml, 0.0152 mol) under cooling by slowly addition. The mixture was stirred over night at room temperature. Solvents was removed under reduced pressure and the product was obtained in >70% yield. For crystallization a small amount (500 mg) were dissolved in THF and a few drops of pentane were added. The mixture was stored at -30 °C.

^{13}C NMR (75 MHz, THF/ D_2O): δ 136.00, 134.76, 129.69, 127.96, 30.32 (Me)

^1H NMR (300 MHz, THF/ D_2O): δ 7.62 (d, 12 H), 7.45 (m, 12 H), 7.36 (m, 6 H), 2.30 (s, 9 H)

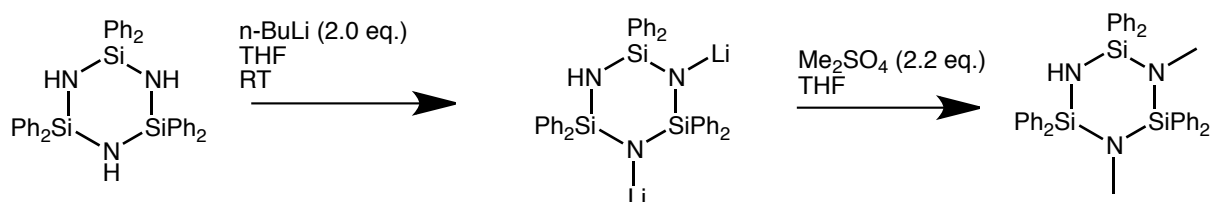
^{29}Si NMR (59 MHz THF/ D_2O): δ -15.25 (3Si)

Elemental analysis (%) calcd for $\text{C}_{39}\text{H}_{39}\text{N}_3\text{Si}_3$: C 73.88, H 6.20, N 6.63; found: C 64.54, H 5.77, N 1.38

IR (cm^{-1}): (Ph, C=C) 1585, 1430, 1463, 1376; (Ph, C-H) 3071, 3054, 2933, 2855, 739, 728; (Si-Ph) 1183, 1115, 1107, 617; (Ph, Si-C) 527, 480, 470, 456, 406, 396; (Si-N-Si) 949, 937, 933; (N-CH₃) 742, 658, 1042

Melting point: >300 °C Crystallographic data: 2

5.2.4 1,3,-dimethyl-2,2,4,4,6,6-hexaphenylcyclotrisilazane



To a solution of hexaphenylcyclotrisilazane (2.0 g, 3.38 mmol) in 50 ml of THF, butyl-lithium (2.7 ml, 0.007 mol, 2.5 M in hexane) was added under an ice bath and the mixture was stirred for 5 h at room temperature. Afterwards the yellowish reaction mixture was

treated with dimethyl sulfate (0.64 ml, 0,007 mol) under cooling by slowly addition. The mixture was stirred over night at room temperature. The suspension was filtered and the solvent was removed in vacuo to get the colorless product in >65% yield.

^{13}C NMR (75 MHz, THF/ D_2O , ppm): δ 136.00, 134.76, 129.69, 127.96, 30.32 (Me)

^1H NMR (300 MHz, CDCl_3 , ppm): δ 7.62 (d, 12H), 7.45(m, 12H), 7.36 (m, 6H), 2.42 (s, 6H)

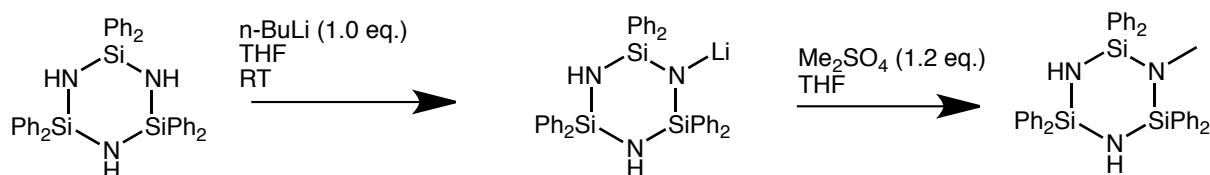
^{29}Si NMR (59 MHz THF/ D_2O , ppm): δ -18.03 (2Si), -20,01 (1Si)

Elemental analysis (%) calcd for $\text{C}_{39}\text{H}_{39}\text{N}_3\text{Si}_3$: C 73.88, H 6.20, N 6.63; found: C 64.54, H 5.77, N 1.38

IR (cm^{-1}):(NH) 3368.6; (Ph₂Si)1428.2; (NH) 1211.4, 1181.9; (PhSi) 1116.5, 1042.6, 1025.4, 995.7, 529.93, 479.23, 467.34; (SiN) 950.18, 939.08; (-C=C-; Ph) 739.8, 712.9, 697.8, 675.7; (N-CH₃) 1042.3, 655.99

Melting point: >300 °C

5.2.5 1-methyl-2,2,4,4,6,6-hexaphenylcyclotrisilazane



To a stirred solution of hexaphenylcyclotrisilazane (2.0 g, 3.38 mmol) in 10 ml of THF, methyl-lithium (2.7 ml, 3.6 mmol, 2.5 M in hexane) was added. The reaction mixture was warmed up for 2 h at 50 °C. Afterwards the yellowish reaction mixture was added slowly to an solution of dimethylesulfate (1.35 ml, 0,0036 mol) in 10 ml of THF under heating at 50 °C. After 6h the solvent was removed in vacuo. The white precipitate was treated with 10 ml of toluene. The suspension was filtered off and the solvent was removed in vacuo to dryness. The crude product was dissolved in THF and crystallized at -30 °C. Yield >65%.

^{13}C NMR (75 MHz, CDCl_3 , ppm): δ 138.82, 134.90, 134.75, 129.74, 129.30, 127.97, 127.86, 127.75, 30.63 (Me)

^1H NMR (300 MHz, CDCl_3 , ppm): δ 7.80 -7.30 (m, 30H), 2.51(s, 3H)

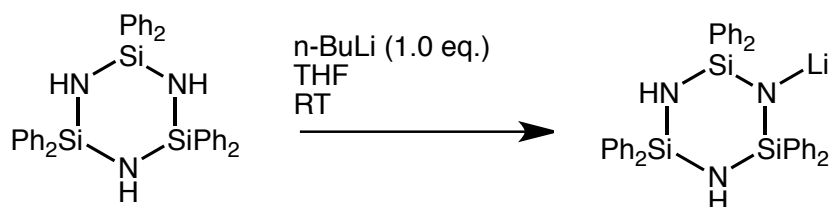
^{29}Si NMR (59 MHz, THF/ D_2O , ppm): δ -20.14(2Si), -17.30 (1Si)

Elemental analysis (%) calcd for $\text{C}_{37}\text{H}_{35}\text{N}_3\text{Si}_3$: C 73.34, H 5.82, N 6.93; found: C 72.49, H 5.81, N 5.97

IR(cm^{-1}): (NH) 3368.6; (Ph₂Si)1428.2; (NH) 1211.4, 1181.9; (PhSi) 1116.5, 1042.6, 1025.4, 995.7, 529.93, 479.23, 467.34; (SiN) 950.18, 939.08; (-C=C-; Ph) 739.8, 712.9, 697.8, 675.7; (N-CH₃) 1042.3, 655.99

Melting point: >300 °C

5.2.6 1-lithio-2,2,4,4,6,6-hexaphenylcyclotrisilazane



To a solution of hexaphenylcyclotrisilazane (0.250 g, 0.4223 mmol) in 10 ml of THF, $n\text{-BuLi}$ (2.5 M in hexane, 0.21 ml) was added drop-wise and stirred for 24h at room temperature. The solvents was removed in vacuo and the product was crystallized in pentane and diglyme to yield >65%.

^{13}C NMR (75 MHz, THF/ D_2O , ppm): δ 146.86, 143.36, 135.10, 134.66, 128.24, 127.18, 127.08, 126.84

^1H NMR (300 MHz, THF/ D_2O , ppm): δ 7.94 (m, 12H), 7.71 (m, 12H), 7.03 (m, 6H); NH 1.67(s, 2H)

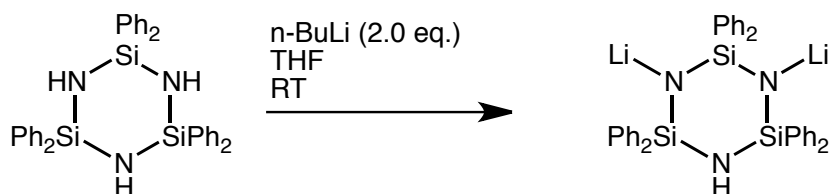
^{29}Si NMR (59 MHz, THF/ D_2O , ppm): δ -21.35 (2Si), -32.04(1Si)

Elemental analysis (%) calcd for $\text{C}_{37}\text{H}_{32}\text{N}_3\text{Si}_3\text{Li}_1$: C 72.32, H 5.39, N 7.03; found: C 68.01, H 4.64, N 7.14

IR(cm^{-1}): (NH) 3369, 1260, 502; (Si-Ph, C-H) 3071, 3054, 2933, 2855; (Ph, C=C) 1463, 1376, 1430, 1366; (Si-Ph) 1187, 1165, 1138, 1108, 1079, 1055, 1024; (Si-N-Si) 911; (Si-C) 803, 531, 485, 401

Crystallographic data: 3

5.2.7 1,3,-dilithio-2,2,4,4,6,6-hexaphenylcyclotrisilazane



To a stirred solution of hexaphenylcyclotrisilazane (0.250 g, 0.4223 mmol) in 20 ml of THF, *n*-BuLi (2.5 M in hexane, 0.34 ml) was added drop-wise and stirred for 24h at room temperature. The solvents was removed in vacuo and the product was crystallized in pentane and diglyme to yield >90%.

^{13}C NMR (75 MHz, THF/ D_2O , ppm): δ 153.36, 150.17, 134.97, 134.82, 127.07, 126.50, 126.32, 126.29, 125.50

^1H NMR (300 MHz, THF/ D_2O , ppm): δ 7.80 (m, 12H), 7.30 (m, 12H), 7.18 (m, 6H), NH 1.64(s, 1H)

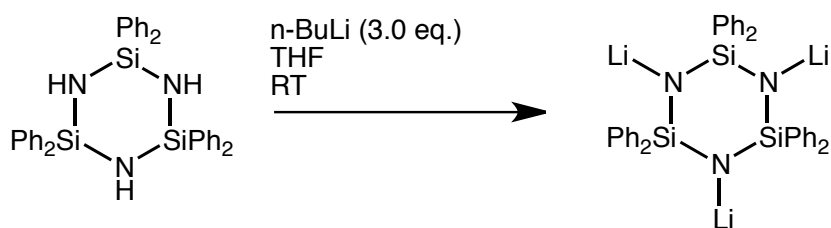
^{29}Si NMR (59 MHz, THF/ D_2O , ppm): δ -34.37(2Si), -21.35(1Si)

Elemental analysis (%) calc. for $\text{C}_{37}\text{H}_{32}\text{N}_3\text{Si}_3\text{Li}_2$: C 71.61, H 5.18, N 6.96; found: C 70.09, H 5.43, N 7.23

IR(cm^{-1}): (NH) 3369, 1260, 502; (Si-Ph, C-H) 3071, 3054, 2933, 2855; (Ph, C=C) 1463, 1376, 1430, 1366; (Si-Ph) 1187, 1165, 1138, 1108, 1079, 1055, 1024; (Si-N-Si) 911; (Si-C) 803, 531, 485, 401

Crystallographic data: 4

5.2.8 1,3,5-trilithio-2,2,4,4,6,6-hexaphenylcyclotrisilazane



To a suspension of hexaphenylcyclotrisilazane (2.0 g, 3.38 mmol) in 50 ml THF under ice cooling butyl-lithium (1.5 M in hexane, 7.3 ml) was added slowly. The reaction mixture was stirred over night at room temperature. The product crystallized out of the reaction mixture after storage at -30°C for one week, to yield >90%.

^{13}C NMR (75 MHz, THF/ D_2O , ppm): δ 154.31, 135.65, 126.26, 125.31

^1H NMR (300 MHz, THF/ D_2O , ppm): δ 8.11(m, 12H), 7.22 (m,12H), 7.16 (m, 6H)

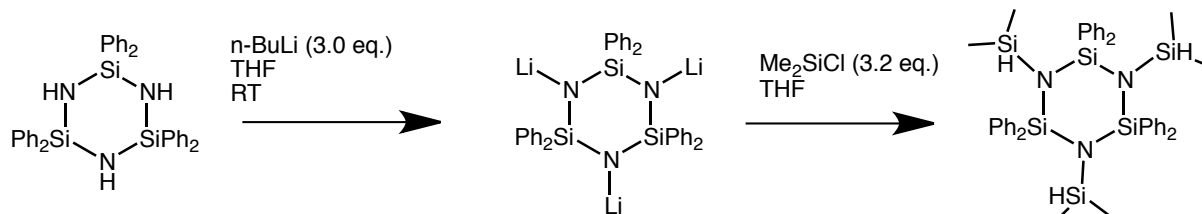
^{29}Si NMR (59 MHz, THF/ D_2O , ppm): δ -37.67(3Si)

IR(cm^{-1}): (Si-N-Si) 1013, 995; (Si-Ph) 1041, 1154, 1090; (Si-C) 803, 520, 339, 389, 490, 449; (Ph, C=C) 1366, 1376, 1463, 1430, 1585; (Si-Ph, C-H) 3054, 2933, 2855

Elemental analysis (%) calcd for $\text{C}_{37}\text{H}_{32}\text{N}_3\text{Si}_3\text{Li}_3$: C 70.92, H 4.96, N 6.89; found: C 70.45, H 7.03 N 4.99

Crystallographic data: 5

5.2.9 1,3,5-tris(dimethylsilyl)-2,2,4,4,6,6-hexaphenylcyclotrisilazane



To a suspension of hexaphenylcyclotrisilazane (2.0 g, 3.38 mmol) in 50 ml THF under ice cooling butyl lithium (1.5 M in hexane, 7.3 ml) was added slowly. The reaction mixture was stirred over night at room temperature. Next the yellowish solution was added to a stirred and cooled solution of dimethylsilylchloride (3.4 mmol) in 30 ml of THF. After 12h volatile substances were removed and the product was crystallized in THF at room temperature to yield >90%.

^{13}C NMR (75 MHz, THF/ D_2O , ppm): δ 138.42, 136.72, 129.74, 127.54, 1.20(CH₂)

^1H NMR (300 MHz, THF/ D_2O , ppm): δ 7.71(m, 12H), 7.38 (m, 12H), 7.24 (m, 6H), 4.30 (d, 12H), -0.47 (m, 3H)

^{29}Si NMR (59 MHz, THF/ D_2O , ppm): δ -10.90 (3SiH), -21.10(3Si)

IR(cm^{-1}): (Si-N-Si) 1002, 913; (Si-Ph, C-H) 3071, 3054, 2933, 2855; (SiMe₂H, Si-H) 2186, 2157, 2142, 2120, 976, 954; (SiMe₂H, SiCH₃) 1307, 1249; (SiMe₂H, Si-C) 881-849, 566, 553; (Ph, C=C) 1430, 1463, 1376; (Ph, C-H) 769, 739(Si-Ph) 1115, 1107

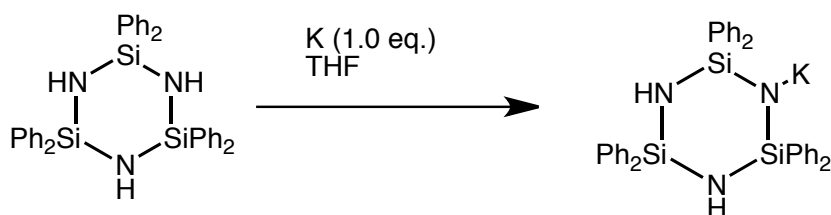
Elemental analysis (%) calcd for $\text{C}_{42}\text{H}_{51}\text{N}_3\text{Si}_3$: C 65.82, H 6.71, N 5.48;

found: C 65.34, H 6.74, N 5.46

Melting point: >300 °C

Crystallographic data: **6**

5.2.10 1-potassium-2,2,4,4,6,6-hexaphenylcyclotrisilazane



A suspension of hexaphenylcyclotrisilazane (0.5 g, 0.844mmol) in 10 ml of THF was stirred with elemental potassium (0.03 g, 0.844 mmol) over night at room temperature.

Hydrogen gas was observed. Out of the mother liquor (in this case the reaction mixture) the product was tried to crystallize. A few drops of pentane and diglyme were added to speed up the crystallization, but no crystals could be obtained. According to the ^1H spectra the reaction was quantitatively.

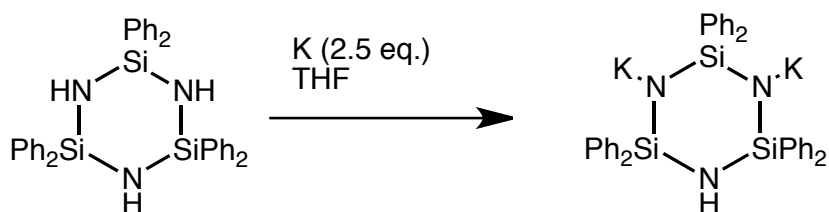
^{13}C NMR (75 MHz, THF/ D_2O , ppm): δ 152.60, 147.1, 135.11, 129.08, 127.96, 127.43, 127.00, 126.87

^1H NMR (300 MHz, THF/ D_2O , ppm): δ -7.78 (m, 12H), 7.29 (m, 12H), 7.20 (m, 6H), NH 1.64(s, 2H)

^{29}Si NMR (59 MHz, THF/ D_2O , ppm): δ -22.26 (2Si), -35.76(1Si)

IR(cm^{-1}): (NH) 3352, 1264; (Si-Ph, C-H) 3071, 3054, 2933, 2855, 769; (Ph, C=C) 1463, 1376, 1430; (Si-Ph) 1119, 1027; (Si-N-Si) 949, 937; (Si-C) 800, 524

5.2.11 1,3-di(potassium)-2,2,4,4,6,6-hexaphenylcyclotrisilazane



To a stirred suspension of hexaphenylcyclotrisilazane (0.5 g, 0.844 mmol) in 10 ml of THF, potassium hydride (0.1 g, 1.688 mol) was added and the mixture was stirred over night at room temperature. Hydrogen gas could be observed. Out of the reaction mixture the solid colorless product could be obtained in >90% yield. The probe was stored at -30°C for one week.

^{13}C NMR (75 MHz, THF/ D_2O , ppm): δ 146.86, 143.36, 135.10, 134.66, 128.24, 127.18, 127.08, 126.84

^1H NMR (300 MHz, THF/ D_2O , ppm): δ 8.05 (m, 12H) 7.94-7.44 (m, 18H), NH 1.63(s, 1H)

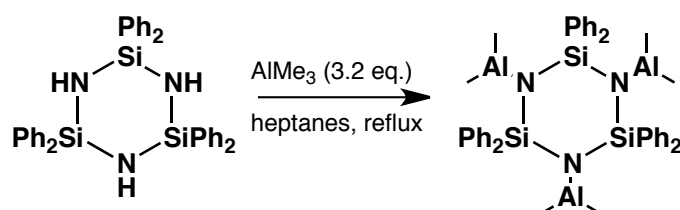
^{29}Si NMR (59 MHz, THF/ D_2O , ppm): δ -38.28(1Si) second signal is missing

IR(cm^{-1}): (NH) 3369, 1260, 502; (Si-Ph, C-H) 3071, 3054, 2933, 2855; (Ph, C=C) 1463, 1376, 1430, 1366; (Si-Ph) 1187, 1165, 1138, 1108, 1079, 1055, 1024; (Si-N-Si) 911; (Si-C) 803, 531, 485, 401

Melting point: $>300^\circ\text{C}$

Crystallographic data: 7

5.2.12 1,3,5-tris(Dimethylaluminum)-2,2,4,4,6,6-hexaphenylcyclotrisilazane



To a solution of hexaphenylcyclotrisilazane (0.49g, 0.834 mmol) in 15 ml of pentane, aluminum-trimethanide (2.5 M, 1.25ml, 2.5 mmol) was added slowly. The suspension was refluxed for 24 hours in an oil bath. After cooling to room temperature the product crystallizes as a colorless powder. The solvent was removed in vacuo and the product was re crystallized in THF to yield >95% colorless large crystals. The product is highly air and moisture sensitive.

^{13}C NMR (75 MHz, THF/ D_2O , ppm): δ -158.93, 146.73, 128.89, 130.22, 134.96, 141.11

^1H NMR (300 MHz, THF/ D_2O , ppm): δ 7.92, - 7.10 (m, 30H), -6.97 (s, 18H)

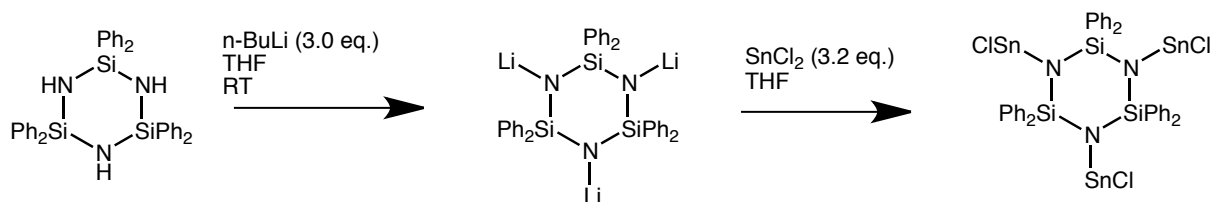
^{29}Si NMR (59 MHz, THF/ D_2O , ppm): δ -27.03 (3Si)

^{27}Al NMR (111.92 MHz, THF/ D_2O , ppm): δ 189.10 (3Al)

Melting point: >300 °C

Crystallographic data: 8

5.2.13 1,3,5-tris(SnCl)-2,2,4,4,6,6-hexaphenylcyclotrisilazane



To a solution of hexaphenylcyclotrisilazane (0.500 g, 0.844 mmol) in 20 ml of THF, n- BuLi (2.5 M in hexane, 1.01 ml) was added drop-wise and stirred for 24h at room temperature. Next to a suspension of tin(II)chloride (0.480 g, 2.534 mmol) in 50 ml of THF the lithiated reaction mixture was added slowly. An immediate reaction could be observe because the color changed to dark red- brown. The reaction mixture was stirred for 6 hours and the

product precipitated as dark green needles. The solution was filtered off and the product was dried in vacuo to yield >60%.

^{13}C NMR (75 MHz, THF/ D_2O , ppm): δ 142.60, 137.58, 127.84, 126.92

^1H NMR (300 MHz, THF/ D_2O , ppm): δ 8.16 (m, 12H), 7.14 (m, 12H), 7.11 (m, 6H)

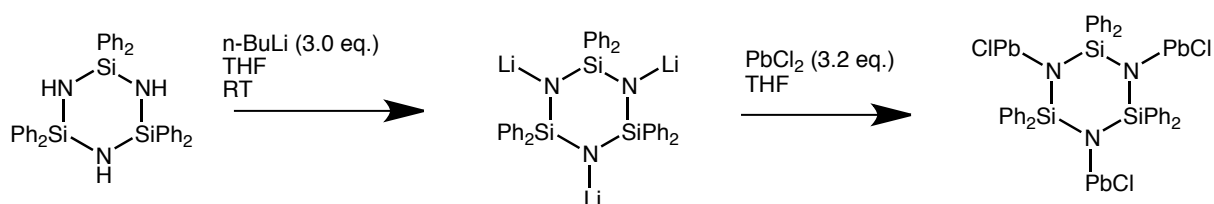
^{29}Si NMR (59 MHz, THF/ D_2O , ppm): δ -28.85 (3Si)

^{119}Sn NMR (111.92 MHz, THF/ D_2O , ppm): δ 94.98, broad signal

Melting point: >300 °C

Crystallographic data: **9**

5.2.14 1,3,5-tris(PbCl)-2,2,4,4,6,6-hexaphenylcyclotrisilazane



To a solution of hexaphenylcyclotrisilazane (0.500 g, 0.844 mmol) in 20 ml of THF, *n*-BuLi (2.5 M in hexane, 1.01 ml) was added drop-wise and stirred for 24h at room temperature. Next to a suspension of lead(II)chloride (0.704g, 2.534 mmol) in 50 ml of THF the lithiated reaction mixture was added slowly. An immediate reaction could be observe because the color changed to dark brown-black. The reaction mixture was stirred for 6 hours and the product precipitated as colorless needles. The solution was filtered off and the product was dried in vacuo to yield >60%. The product was recrystallized in THF to give large colorless needles.

^{13}C NMR (75 MHz, THF/ D_2O , ppm): δ 142.59, 137.07, 127.94, 127.14

^1H NMR (300 MHz, THF/ D_2O , ppm): δ 8.11 (m, 12H), 7.15 (m, 12H), 7.13 (m, 6H)

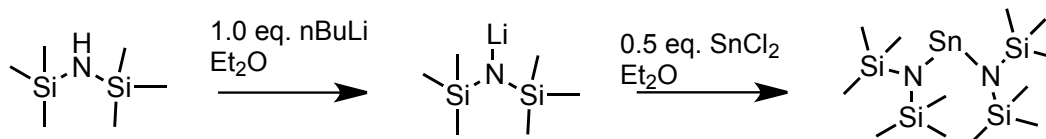
^{29}Si NMR (59 MHz, THF/ D_2O , ppm): δ -30.71 (3Si)

^{207}Pb NMR (111.92 MHz, THF/ D_2O , ppm): δ 2070 broad signal

Melting point: >300 °C

Crystallographic data: **10** and **10a**

5.2.15 Tin(II)bis[bis(trimethylsilyl)amide]



According to the literature the precursor was made [85]. Lithium bis (trimethylsilyl)amide-diethyl ether (prepared by the reaction of the parent amine and butyl lithium in diethyl-ether) was added slowly to a stirred suspension of tin(II)chloride in the same solvent in a 2:1 molar ratio. An immediate reaction was observed with precipitation of lithium chloride and the formation of an orange solution. After stirring at room temperature over night the solvent was removed in vacuo. The metal amide was extracted with pentane and filtered to give a yellow solution. Removal of volatiles in vacuo gave the tin(II) amide as a yellow oil in >80% yield.

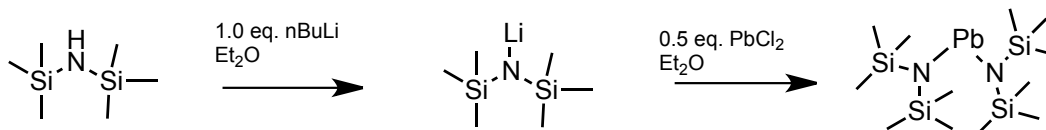
^{13}C NMR (75 MHz, C_6D_6 , ppm): δ 4.71

^1H NMR (300 MHz, C_6D_6 , ppm): δ 0.16

^{29}Si NMR (59 MHz, C_6D_6 , ppm): δ -2.32

^{119}Sn NMR (111.92 MHz, C_6D_6 , ppm): δ 767.5 broad signal

5.2.16 Lead(II)bis[bis(trimethylsilyl)amide]



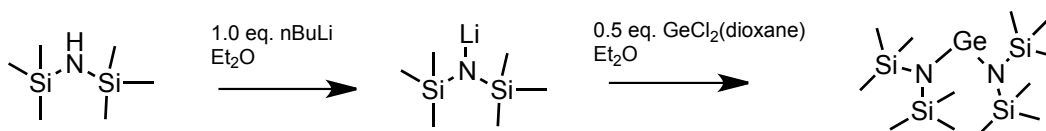
Literature: [85] Lithium bis (trimethylsilyl)amide in diethyl ether (prepared by the reaction of the parent amine and n-butyl lithium in diethyl-ether) was added slowly to a stirred suspension of lead(II)chloride in the same solvent in a 2:1 molar ratio. An immediate reaction was observed with precipitation of lithium chloride and the formation of an orange solution. After stirring at room temperature over night the solvent was removed in vacuo. The metal amide was extracted with pentane and filtered to give an orange solution. Removal of volatiles in vacuo gave the lead(II) amide as a yellow oil in >80% yield.

^{13}C NMR (75 MHz, THF/ D_2O , ppm): δ 5.21

^1H NMR (300 MHz, THF/ D_2O , ppm): δ 0.18 (s, 36H)

^{29}Si NMR (59 MHz, THF/ D_2O , ppm): δ -4.83 (2Si)

5.2.17 Germanium(II)bis[bis(trimethylsilyl)amide]



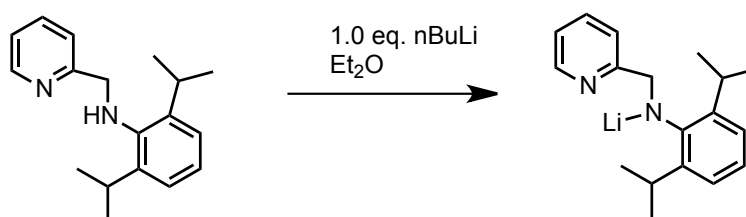
Literature: [85] Lithium bis (trimethylsilyl)amide-diethyl ether (prepared by the reaction of the parent amine and n-butyl lithium in diethyl-ether) was added slowly to a stirred suspension of germanium(II)chloride-dioxane adduct in the same solvent in a 2:1 molar ratio. An immediate reaction was observed with precipitation of lithium chloride and the formation of a light yellow solution. After stirring at room temperature overnight the solvent was removed in vacuo. The metal amide was extracted with pentane and filtered to give a bright yellow solution. Removal of volatiles in vacuo gave the germanium(II) amide as a bright yellow oil in >80% yield.

^{13}C NMR (75 MHz, THF/ D_2O , ppm): δ 5.21

^1H NMR (300 MHz, THF/ D_2O , ppm): δ -1.05 (s, 36H)

^{29}Si NMR (59 MHz, THF/ D_2O , ppm): δ -3.20 (2Si)

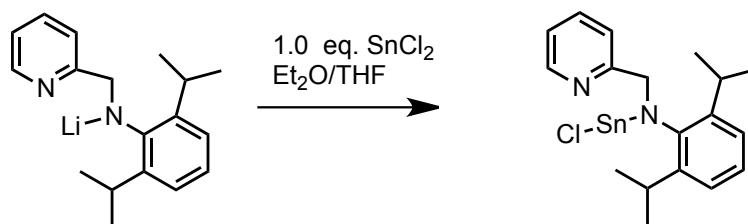
5.2.18 Lithium(I) N-(diisopropyl benzyl)(2-pyridylmethyl)amide



A solution of butyl lithium in hexane (2.5 M, 0.44 ml, 1.11 mmol) was added slowly to a cooled (-78°C) and stirred solution of N-(2,6-diisopropylphenyl)-2-pyridinylmethylamine (0.300 g, 1.11 mmol) in diethyl ether (10 ml). After complete addition the red solution was stored at -30°C . Colorless crystals formed after a few days. Yield is at >70%.

Crystallographic data: 11

5.2.19 Chloro-tin(II) N-(diisopropyl)(2-pyridylmethyl)amide



A cool -78°C solution of Lithium(I)N-(diisopropyl benzyl)(2-pyridylmethyl)amide (1.11 mmol) was added to a suspension of tin(II) chloride (0.212 g, 1.11 mmol) in THF and diethyl ether (50 ml, 1:1 ratio). The solution was warmed to room temperature and stirred over night. An immediate reaction was observed with precipitation of lithium chloride and the formation of a yellow-orange solution. The solution was filtered off and the solvent was removed in vacuo. The yellow chloro-tin(II) amide was dissolved in THF and stored at -30°C to yield $>90\%$ of yellow crystals.

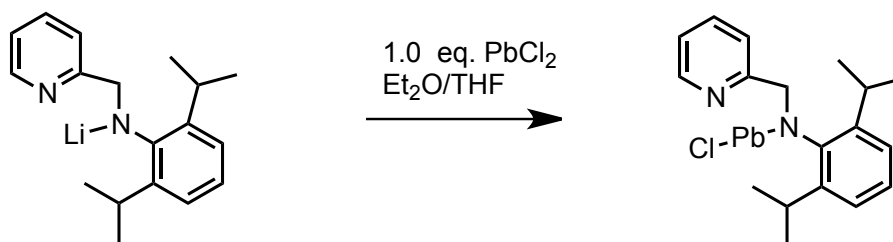
^{13}C NMR (75 MHz, THF/D₂O, ppm): δ 149.11, 142.37, 137.08, 125.55, 124.69, 123.37, 122.49, 122.00, 56.29, 28.11, 24.13, 23.63

^1H NMR (300 MHz, THF/D₂O, ppm): δ 1.11 (s, 12H), 3.27-3.04 (m, 2H), 4.03 (s, 2H), 6.52 (d, 2H), 6.83 (t, 1H), 7.20- 7.05 (m, 3H), 8.98 (1H)

^{119}Sn NMR (111.92 MHz, THF/D₂O, ppm): δ -30

UV Maxima: 432 nm $\epsilon=480$

5.2.20 Chloro -lead(II) N-(diisopropyl)(2-pyridylmethyl)amide



A cool -78°C solution of Lithium(I)N-(diisopropyl benzyl)(2-pyridylmethyl)amide (1.11 mmol) was added to a suspension of lead(II)chloride (0.311 g, 1.11 mmol) in THF and diethyl ether (50 ml, 1:1 ratio). The solution was warmed to room temperature and stirred over night. An immediate reaction was observed with precipitation of lithium chloride and the formation of a yellow-orange solution. The solution was filtered off and the solvent

was removed in vacuo. The yellow chlor-tin(II) amide was dissolved in THF and stored at -30°C to yield $>90\%$ orange crystals. (crystals were not measured)

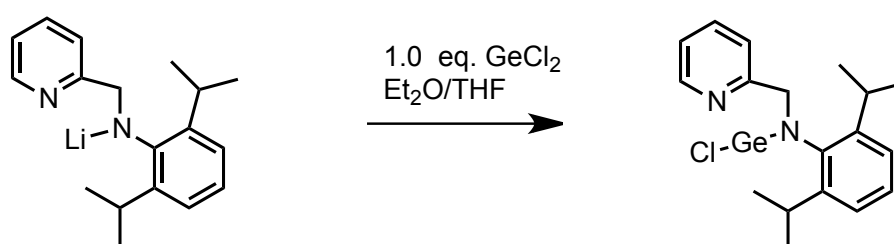
^{13}C NMR (75 MHz, THF/ D_2O , ppm): δ 159.25, 149.56, 143.56, 142.10, 135.51, 123.92, 123.20, 121.42, 57.03, 27.94, 24.05

^1H NMR (300 MHz, THF/ D_2O , ppm): δ 1.87 (s, 12H), 3.69-2.44 (m, 2H), 5.63 (s, 2H), 7.61-8.55 (m, 6H, aromatic region), 9.36 (1H)

^{207}Pb NMR (111.92 MHz, THF/ D_2O , ppm): δ -

UV Maxima at: 490 nm $\epsilon=380$, 389 nm $\epsilon=2000$

5.2.21 Chloro-Ge(II) N-(diisopropyl)(2-pyridylmethyl)amide



A cool -78°C solution of lithium(I)N-(diisopropyl benzyl)(2-pyridylmethyl)amide (1.11 mmol) was added to a suspension of germanium(II) chloride (dioxane complex 0.259 g, 1.11 mmol) in THF and diethyl ether (50 ml). The solution was warmed to room temperature and stirred over night. An immediate reaction was observed with precipitation of lithium chloride and the formation of a yellow-orange solution. The solution was filtered off and the solvent was removed in vacuo. The yellow chlor-germanium(II) amide was dissolved in THF and stored at -30°C to yield $>99\%$ orange-red crystals.

^{13}C NMR (75 MHz, THF/ D_2O , ppm): δ 159.25, 149.56, 143.56, 142.10, 135.51, 123.92, 123.20, 121.42, 57.03, 27.94, 24.05

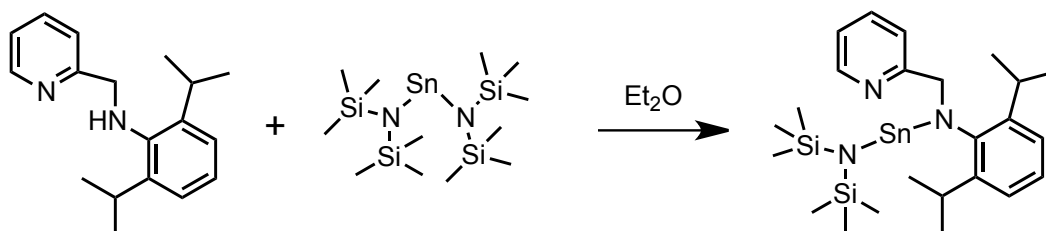
^1H NMR (300 MHz, THF/ D_2O , ppm): δ 1.37 (s, 12H), 3.69-2.44 (m, 2H), 5.41 (s, 2H), 7.53-8.60 (m, 6H, aromatic region), 9.12 (1H)

Melting Point: $\approx 53^{\circ}\text{C}$ -60°C

UV Maxima: 467 nm $\epsilon \approx 760$

Crystallographic data: **12**

5.2.22 Bis(TMS)amidotin(II) N-(diisopropyl)(2-pyridylmethyl)amide



A solution of tin(II)bis[bis(trimethylsilyl)amide] (0.49 g, 1.11 mmol) in was a added to a stirred solution of N-(2,6-diisopropylphenyl)-2-pyridinylmethylamine (0.300 g, 1.11 mmol) in 10 ml diethyl-ether. The color of the solution changed to olive green. After stirring over night at room temperature the solvent was removed in vacuo. The remaining green solid was dissolved in diethyl-ether and stored at -30°C yielding (>99%) the product as yellow crystals within several days.

^{13}C NMR (75 MHz, C_6D_6 , ppm): δ 166.2, 149.4, 148.0, 145.73, 139.8, 123.2, 123.6, 123.5, 122.5, 66.0, 28.0, 23.4, 2.1

^1H NMR (300 MHz, C_6D_6 , ppm): δ 8.82 (d, 1H), 8.13 (t, 2h), 7.69 (d, 1H), 7.20-7.11(m, 3H), 4.64 (s, 2H), 3.97-3.50 (m, 2H), 1.30 (d, 12H), 0.17 (s, 18H)

^{29}Si NMR (59 MHz, C_6D_6 , ppm): δ 1.89 (1Si), -2.97(1Si)

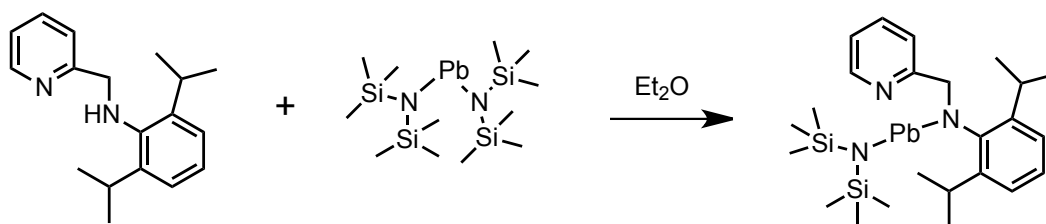
^{119}Sn NMR (111.92 MHz, C_6D_6 , ppm): δ 85 broad signal

Melting Point: $\approx 74^{\circ}\text{C}$ -78°C

UV Maxima: 320 nm $\epsilon=3024$, 440 nm $\epsilon=706$

Crystallographic data: 13

5.2.23 Bis(TMS)amidolead(II) N-(diisopropyl)(2-pyridylmethyl)amide



A solution of lead(II)bis[bis(trimethylsilyl)amide] (0.59 g , 1.11 mmol) in diethyl-ether was a added to a stirred solution of N-(2,6-diisopropylphenyl)-2-pyridinylmethylamine (0.300 g, 1.11 mmol) in diethyl-ether. The color of the solution changed to olive green.

After stirring over night at room temperature the solvent was removed in vacuo. The remaining green solid was dissolved in diethyl-ether and stored at -30°C yielding ($>70\%$) the product as yellow crystals within several days. (crystals were not measured)

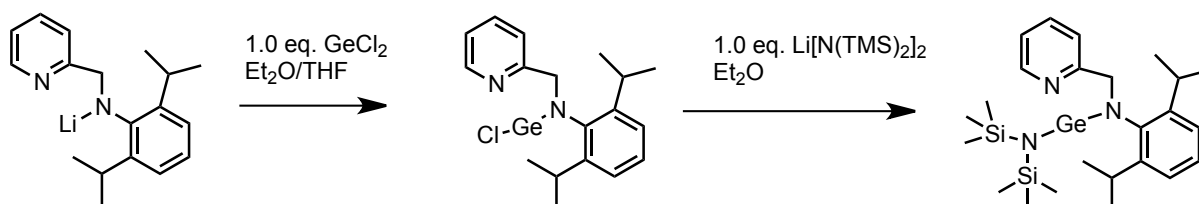
^{13}C NMR (75 MHz, THF/ D_2O , ppm): δ 166.2, 149.4, 148.0, 145.73, 139.8, 123.2, 123.6, 123.5, 122.5, 66.0, 28.0, 23.4, 2.1

^1H NMR (300 MHz, THF/ D_2O , ppm): δ 9.08 (d, 1H), 8.13 (t, 2h), 7.69 (d, 1H), 7.20-7.11(m, 3H), 4.64 (s, 2H), 3.97-3.50 (m, 2H), 1.30 (d, 12H), 0.20 (s, 18H)

^{29}Si NMR (59 MHz, THF/ D_2O , ppm): δ 2.06, -4.59

UV Maxima: 406 nm $\epsilon \approx 2500$

5.2.24 Bis(TMS)amidoGe(II) N-(diisopropyl)(2-pyridylmethyl)amide



A cool -78°C solution of lithium(I)N-(diisopropyl benzyl)(2-pyridylmethyl)amide (0.60 g, 1.11 mmol) was added to a suspension of germanium(II) chloride (dioxane complex 0.259 g, 1.11 mmol) in THF and diethyl ether (50 ml). The solution was warmed to room temperature and stirred over night. An immediate reaction was observed with precipitation of lithium chloride and the formation of a yellow-orange solution. Next a cool -78°C solution of lithium-hexamethyldisilazane was added to the chloro-germanium(II)amide reaction-mixture. The mixture was stirred over night. The orange-red solution was filtered off and the solvent was removed in vacuo. The red-orange solid was dissolved in THF and stored at -30°C to yield ($>70\%$) dark orange crystals. (crystals were not measured)

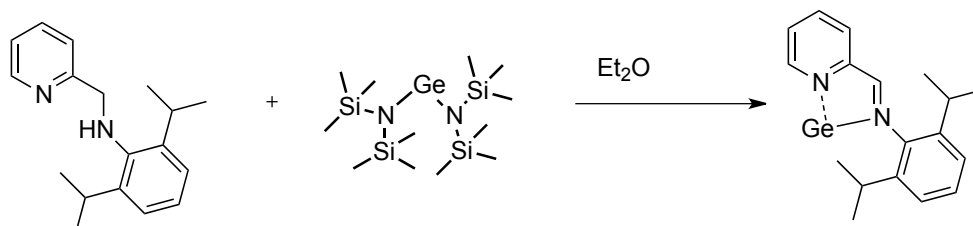
^{13}C NMR (75 MHz, C_6D_6 , ppm): δ 159.12, 149.4, 148.0, 145.73, 139.8, 123.2, 123.6, 123.5, 122.5, 56.74.0, 27.71, 23.4, 2.27

^1H NMR (300 MHz, C_6D_6 , ppm): δ 8.44 (d, 1H), 7.84 (t, 2h), 7.82 (d, 1H), 7.12-6.76 (m, 3H), 4.64 (s, 2H), 3.53-3.44 (m, 2H), 1.19 (d, 12H), 1.07 (s, 18H)

^{29}Si NMR (59 MHz, C_6D_6 , ppm): δ -2.46, 4.51

UV Maxima: 490 nm $\epsilon \approx 800$

5.2.25 Ge(II)bis[N-(2,6-diisopropylphenyl)(2-pyridylmethyl)imide]



To a stirred solution of N-(diisopropyl benzyl)(2-pyridylmethyl)amide (0.61g, 1.11 mmol) in 10 ml diethyl ether the Germanium(II)bis[bis(trimethylsilyl)amide] (1.11 mmol) was added. The reaction mixture was stirred at room temperature over night. The solvent was removed to dryness and the dark red oily crude product was dissolved in a small amount of pentane. The probe was stored at -30°C to yield (>40%) dark-red crystals.

^{13}C NMR (75 MHz, C_6D_6 , ppm): δ 159.12, 149.4, 148.0, 145.73, 139.8, 123.2, 123.6, 123.5, 122.5, 66.89, 27.71, 23.4

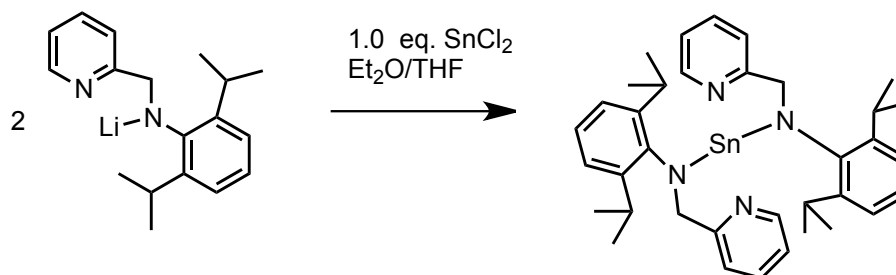
^1H NMR (300 MHz, C_6D_6 , ppm): δ 8.44 (s, 1H), 7.84 (t, 6h), 7.82 (d, 1H), 3.43-3.54 (m, 2H), 1.20 (d, 12H)

Melting Point: $\approx 45^{\circ}\text{C}$ - 53°C

UV Maxima: 540 nm $\epsilon \approx 600$

Crystallographic data: 14

5.2.26 Sn(II)bis[N-(2,6-diisopropylphenyl)(2-pyridylmethyl)amide]



A cool -78°C solution of lithium(I)N-(diisopropyl benzyl)(2-pyridylmethyl)amide (1.11 mmol) was added to a suspension of tin(II) chloride (0.106 g, 0.55 mmol) in THF and diethyl ether (50 ml, 1:1 ratio). The solution was warmed to room temperature and stirred over night. An immediate reaction was observed with precipitation of lithium chloride and the formation of a yellow-orange solution. The solution was filtered off an

the solvent was removed in vacuo. The yellow tin(II) diamide was dissolved in THF and stored at -30°C to yield (>50%) yellow crystals.

^{13}C NMR (75 MHz, C_6D_6 , ppm): δ 159.25, 149.13, 144.67, 142.61, 140.93, 135.74, 135.43, 134.98, 127.21, 124.67, 123.58, 122.98, 122.71, 121.61, 121.56, 129.37, 106.5, 57.03, 27.94, 24.68, 24.05

^1H NMR (300 MHz, C_6D_6 , ppm): δ 1.29 (s, 24H), 3.69-2.44 (m, 4H), 5.54 (s, 4H), 7.93-7.14 (m, 12H, aromatic region), 9.08 (2H)

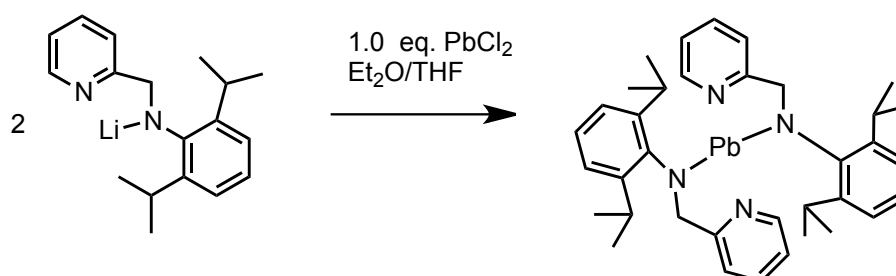
^{119}Sn NMR (111.92 MHz, THF/ C_6D_6 , ppm): δ -143 broad signal

Melting Point: $\approx 90^{\circ}\text{C}$ -114 $^{\circ}\text{C}$

UV Maxima: 296 nm, 337 nm $\epsilon = 5792$, 401 nm

Crystallographic data: 15

5.2.27 Pb(II)bis[N-(2,6-diisopropylphenyl)(2-pyridylmethyl)amide]



A cool -78°C solution of Lithium(I)N-(diisopropyl benzyl)(2-pyridylmethyl)amide (1.11 mmol) was added to a suspension of lead(II) chloride (0.150 g, 0.55 mmol) in THF and diethyl ether (50 ml, 1:1 ratio). The solution was warmed to room temperature and stirred over night. An immediate reaction was observed with precipitation of lithium chloride and the formation of a dark yellow solution. The solution was filtered off and the solvent was removed in vacuo. The yellow tin(II) diamide was dissolved in THF and stored at -30°C to yield (>50%) deep orange crystals.

^{13}C NMR (75 MHz, C_6D_6 , ppm): δ 159.25, 149.13, 144.67, 142.61, 140.93, 135.74, 135.43, 134.98, 127.21, 124.67, 123.58, 122.98, 122.71, 121.61, 121.56, 129.37, 106.5, 57.03, 27.94, 24.68, 24.05

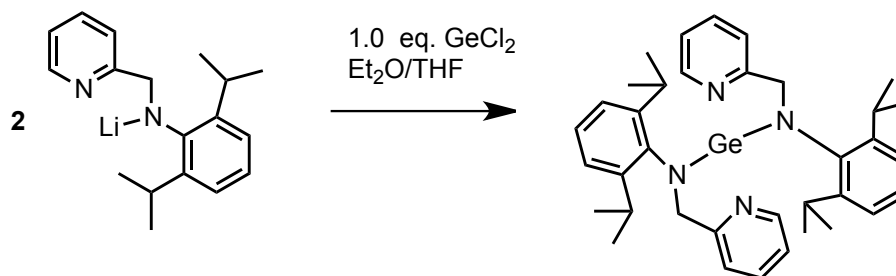
^1H NMR (300 MHz, C_6D_6 , ppm): δ 1.29 (s, 24H), 3.69-2.44 (m, 4H), 5.54 (s, 4H), 7.93-7.14 (m, 12H, aromatic region), 9.08 (2H)

UV Maxima: 309 nm $\epsilon = 6623$, 346 nm, 412 nm $\epsilon = 2268$

Melting Point: $\approx 98^{\circ}\text{C}$ -120 $^{\circ}\text{C}$

Crystallographic data: 16

5.2.28 Ge(II)bis[N-(2,6-diisopropylphenyl)(2-pyridylmethyl)amide]



A cool -78°C solution of lithium(I)N-(diisopropyl benzyl)(2-pyridylmethyl)amide (1.11 mmol) was added to a suspension of germanium(II) chloride (dioxane complex 0.129 g, 0.55 mmol) in THF and diethyl ether (50 ml). The solution was warmed to room temperature and stirred over night. An immediate reaction was observed with precipitation of lithium chloride and the formation of an orange solution. The solution was filtered off and the solvent was removed in vacuo. The orange germanium(II) diamide was dissolved in THF and stored at -30°C to yield red crystals.

^{13}C NMR (75 MHz, C_6D_6 , ppm): δ 159.25, 149.13, 144.67, 142.61, 140.93, 135.74, 135.43, 134.98, 127.21, 124.67, 123.58, 122.98, 122.71, 121.61, 121.56, 129.37, 106.5, 57.03, 27.94, 24.68, 24.05

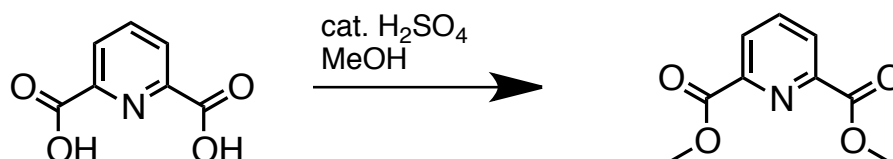
^1H NMR (300 MHz, C_6D_6 , ppm): δ 1.29 (s, 24H), 3.69-2.44 (m, 4H), 5.54 (s, 4H), 7.93-7.14 (m, 12H, aromatic region), 9.08 (2H)

Melting Point: $\approx 100^\circ\text{C} - 110^\circ\text{C}$

UV Maxima: 280 nm, 323 nm, 427 nm $\epsilon = 758$

Crystallographic data: 17

5.2.29 Dimethylpyridine-2,6-dicarboxylate

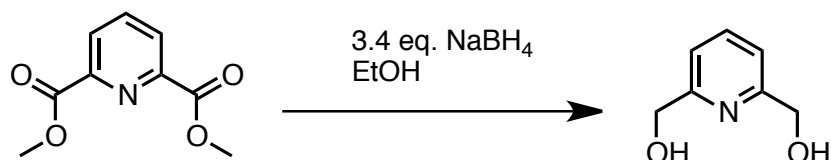


Literature: [86] In 200 ml of dry methanol the pyridine-2,6-dicarboxylic acid (15.4 g, 0.1 mol) was placed and 4 ml of concentrated Sulfuric-acid were added. The reaction mixture was re-fluxed for 48 hours to give the colorless crystalline product. The reaction

mixture was cooled down to 0 °C to precipitate the product. The product was filtered off and washed three times with cold methanol. Yield 90%.

^{13}C NMR (75 MHz, CDCl_3 , ppm): δ 165.22, 148.20, 138.77, 128.24, 53.25,
 ^1H NMR (300 MHz, CDCl_3 , ppm): δ 8.20 (d, 2H), 8.17 (t, 1H), 4.09 (s, 6H)

5.2.30 Pyridine-2,6-diylldimethanol



To a cooled solution (0 °C) of NaBH_4 (10.8 g, 0.28 mol) in 250 ml of dry ethanol the dimethyl pyridine-2,6-dicarboxylate (16g, 0.082 mol) was added in small portions. The reaction mixture was stirred over night at room temperature. The reaction was quenched slowly under cooling with acetone (100 ml). The acetone was added drop-wise, because the reaction mixture starts warming and cooking. Afterwards the reaction was stirred for 2 hours and finally a saturated solution of K_2CO_3 was added slowly via a dropping funnel. The quenched solution was heated for 4 hours and the clear solution was filtered off to get rid of the precipitate. The colorless solution was taken and the solvent was removed to obtain an colorless oil. The product was crystallized at $-30\text{ }^\circ\text{C}$ over night. Yield 85 % of colorless crystals.

^{13}C NMR (75 MHz, EtOH/ D_2O , ppm): δ 159.72, 139.69, 119.65, 64.59

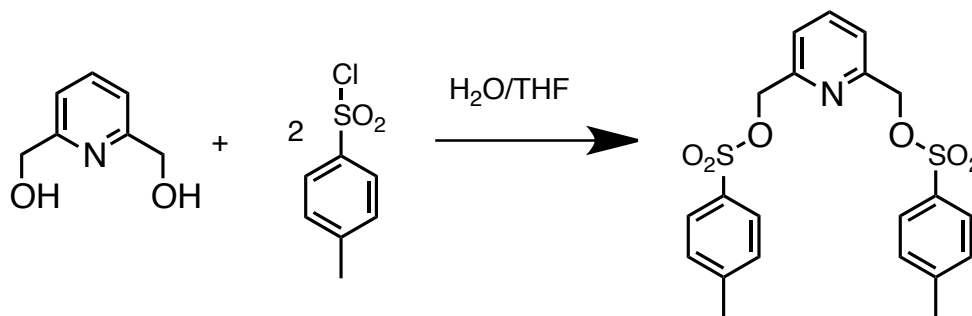
^1H NMR (300 MHz, EtOH/ D_2O , ppm): δ 7.89 (t, 1H), 7.41(d, 2H), 4.71 (d, 4H)

Elemental analysis (%) calcd for $\text{C}_7\text{H}_9\text{NO}_2$: C 60.42, H 6.52, N 10.67;

found: C 60.01, H 5.36, N 8.98

Mass (EI): m/z 140.1 (M^+) calcd for $\text{C}_7\text{H}_9\text{NO}_2$: 139.15

5.2.31 Pyridine-2,6-diylbis(methylene) bis(4-methylbenzenesulfonate)



To a cooled solution of pyridine-2,6-diyl dimethanol (12 g, 0.086 mol) in 45 ml of THF and 45 ml of water, the thioylchloride (38.0 g, 0.199 mol dissolved in 75 ml of THF) was added slowly via a dropping funnel. The ice bath was removed and the reaction mixture was stirred over night at room temperature. The reaction mixture was quenched with 150 ml of water and the two layers were separated from each other. The water phase was extracted several times with dichloro methane (150 ml). The organic phases were washed three times with a saturated sodium-sulfate solution. The solvent were removed and the crude product was re crystallized in ethanol to yield the powdery white product. Yiled 90%

^{13}C NMR (75 MHz, CDCl_3 , ppm): δ 153.52, 145.14, 140.37, 129.90, 128.03, 121.38, 75.40 21.64

^1H NMR (300 MHz, CDCl_3 , ppm): δ 7.83 (t, 1H), 7.77-7.25 (m, 14H), 2.43 (s, 6H)

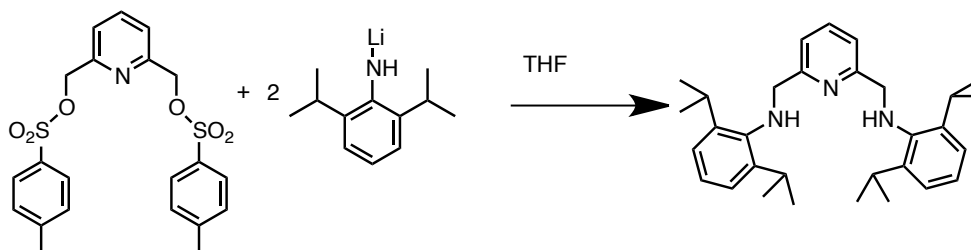
Melting Point: $\approx 187^\circ\text{C}$

Elemental analysis (%) calcd for $\text{C}_{21}\text{H}_{21}\text{N}_1\text{S}_2$: C 60.70, H 5.09, N 3.37;

found: C 58.26, H 4.56, N 0.02

Crystallographic data: **18**

5.2.32 N,N'-(pyridine-2,6-diylbis(methylene))bis(2,6-diisopropylaniline)



To a cooled solution (-78°C) of diisopropylaniline (4.19g, 0.0236 mol) in 20 ml of THF the $n\text{-BuLi}$ (9.44 ml, 0.0236 mol) slowly. After 30 minutes TMEDA (3.52 ml, 0.0236 mol) was added to the lithiated diisopropylaniline. In a second Schlenk the 2,6-bis(tosylmethyl)pyridine (5.3g, 0.0118 mol) was suspended in 20 ml of THF. The Li-diisopropylaniline was added drop-wise via a canula to the 2,6-bis(tosylmethyl)pyridine suspension. The deep red reaction mixture was warmed to room temperature and stirred over night. The reaction was quenched with a saturated aqueous solution of NaHCO_3 . The two layers were separated and the aqueous phase was extracted three times with dichloromethane. All volatile substances were removed in vacuo to give a red oil, the crude product. The yellow crystalline product was obtained by crystallized out of EtOH at -30°C . Yield 40%

^{13}C NMR (75 MHz, C_6D_6 , ppm): δ 145.7, 141.48, 130.14, 125.91, 123.93, 67.99, 28.224, 25.94, 25.41, 24.96

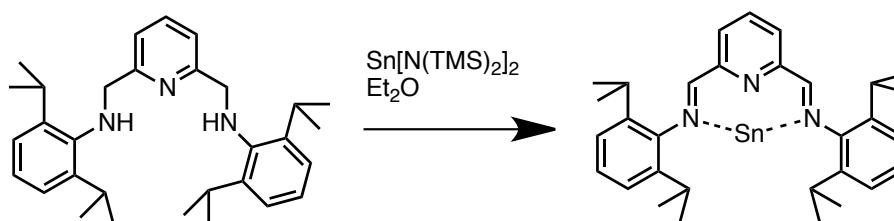
^1H NMR (300 MHz, THF/ D_2O , ppm): δ 7.13-6.78 (m, 9H), 4.43 (s, 2H), 4.18 (s, 4H), 3.54-3.42 (m, 4H), 1.21 (d, 24H)

Melting Point: $\approx 80^{\circ}\text{C}$

Elemental analysis (%) calcd for $\text{C}_{31}\text{H}_{43}\text{N}_3$: C 81.35, H 9.47, N 9.18; found: C 78.69, H 8.47, N 7.90 Mass (EI): m/z 457.4 (M^+) calcd for $\text{C}_{31}\text{H}_{43}\text{N}_3$: 457.35 IR (cm^{-1}): (NH) 3390, (CH₂) 1450, (Ph) 931, 864, 800; (Ph, CH) 752, 617 Crystallographic data: 19

5.2.33 Bisdiimino-Sn;

Sn-N,N-(pyridine-diylbis(ethene))bis(2,6-diisopropylaniline)



To a solution of $\text{N,N}'$ -(pyridine-2,6-diylbis(methylene))bis(2,6-diisopropylaniline) (0.100 g, 0.2 mmol) in diethyl ether (8 ml) the Tin(II)bis[bis(trimethylsilyl)amide] (0.02g, 0.6 mmol) was added. The reaction mixture was stirred for four days at ambient temperature. Afterwards the reaction mixture was stored at -30°C to crystallize brown small crystals.

^{13}C NMR (75 MHz, C_6D_6 , ppm): δ 145.7, 141.48, 130.14, 125.91, 123.93, 67.99, 28.224, 25.94, 25.41, 24.96

^1H NMR (300 MHz, THF/ D_2O , ppm): δ 8.08, 7.12, 7.07, 7.02, 6.88, 6.82, 6.79, 6.64,

6.47, 6.45, 6.41, 6.39, 3.53-3.44 (sep), 3.26-3.12(m), 3.02- 2.95 (sep), 2.77-2.71 (sep), 1.27

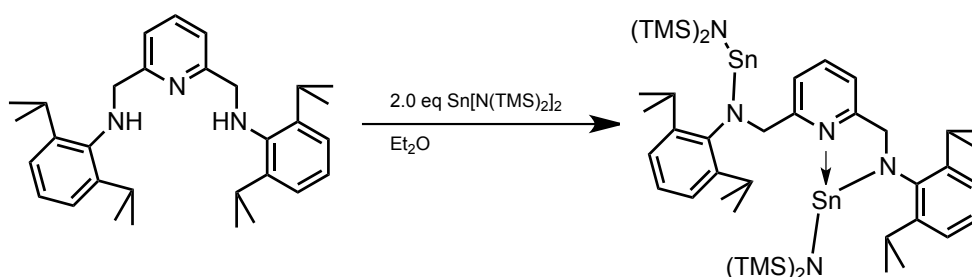
^{119}Sn NMR (111.92 MHz, C_6D_6 , ppm): δ 64 broad signal

IR(cm^{-1}): (C=N) 1647-1506, (CH) 1312; (CH₃) 1448; (Ph) 931, 864, 800; (Ph, CH) 752, 617

UV Maxima: 330 nm, 500 nm, 804 nm

Crystallographic data: 20

5.2.34 N,N-tin(II)(NTMS)-N,N'-(pyridine-2,6-diybis(methylene))bis(2,6-diisopropylaniline)



To a stirred solution of *N,N'*-(pyridine-2,6-diybis(methylene))bis(2,6-diisopropylaniline) (0.3 g, 0.6 mmol) in diethyl ether (5 ml) the Tin(II)bis[bis(trimethylsilyl)amide] (0.04g, 0,12 mmol) was added. An immediate color change happened from yellow to brown. The reaction mixture was stirred over night at room temperature and for further three days. Afterwards the reaction mixture was stored at -30°C to crystallize light yellow small crystals. A solid state measurement was done. Yield: 40%

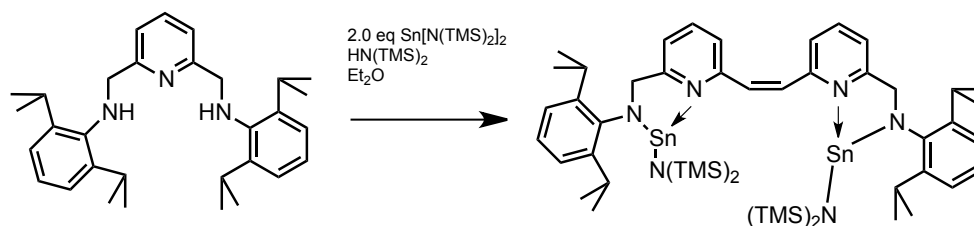
^{13}C NMR (75 MHz, C_6D_6 , ppm): δ 166.2, 149.4, 148.0, 145.73, 139.8, 123.2, 123.6, 123.5, 122.5, 66.0, 28.0, 23.4, 2.1

^1H NMR (300 MHz, THF/ D_2O , ppm): δ 7.22-7.03 (m, 6H), 6.47-6.39 (m, 3H), 3.67- 3.60 (m, 1H), 3.58-3.44 (m, 2H), 3.18-3.11 (m, 1H), 3.07 (s, 4H), 1.26 (d, 12H), 1.20 (d, 12H)

^{119}Sn NMR (111.92 MHz, C_6D_6 , ppm): δ 120 broad signal

Crystallographic data: 21

5.2.35 Ethene-bis(trimethylsilyl)-diamine-tin(II)



To a stirred solution of *N,N'*-(pyridine-2,6-diylbis(methylene))bis(2,6-diisopropylaniline) (0.3 g, 0.6 mmol) in diethyl ether (5 ml) the Tin(II)bis[bis(trimethylsilyl)amide] (0.04 g, 0.12 mmol) was added and additional base as HNTMS (2 drops). An immediate color change happened from yellow to dark-brown. The reaction mixture was stirred over night at room temperature and for further three days. Afterwards the reaction mixture was stored at -30°C to crystallize light yellow small crystals. A solid state measurement was done. Yield: 60%

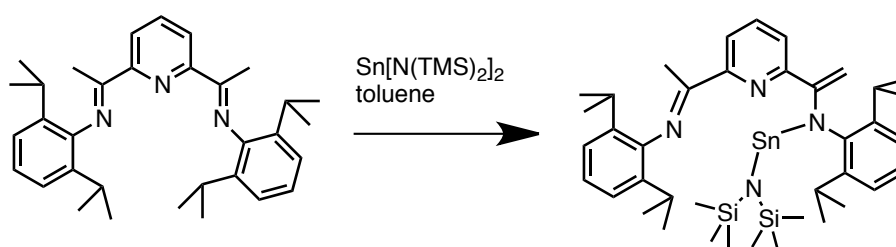
^{13}C NMR (75 MHz, C_6D_6 , ppm): δ 166.2, 149.4, 148.0, 145.73, 139.8, 123.2, 123.6, 123.5, 122.5, 66.0, 28.0, 23.4, 2.1

^1H NMR (300 MHz, THF/ D_2O , ppm): δ 7.22-7.03 (m, 6H), 6.47-6.39 (m, 3H), 3.67-3.60 (m, 1H), 3.58-3.44 (m, 2H), 3.18-3.11 (m, 1H), 3.07 (s, 4H), 1.26 (d, 12H), 1.20 (d, 12H)

^{119}Sn NMR (111.92 MHz, C_6D_6 , ppm): δ -80 broad signal

Crystallographic data: **22**

5.2.36 Tin(II) 2,6-Bis[1-(phenylimino)ethyl]pyridineTMS



To a solution of NNN-DippCH₃ Ligand (100 mg, 0.2 mmol) in toluene (10 ml) the Tin(II)bis[bis(trimethylsilyl)amide] (0.02 g, 0.6 mmol) was added. The reaction mixture was stirred for 2 days at room temperature. Afterwards the solution was stored at -30°C to crystallize in dark-brown-black crystals. Yield: 90%

^1H NMR (300 MHz, C_6D_6 , ppm): δ 7.58, 7.55, 7.25, 7.23, 7.11, 7.09, 7.08, 7.07, 7.05, 6.80, 6.78, 6.64, 6.62, 4.58, 4.15-4.08 (m), 3.26-3.19(m), 3.11-3.06 (m), 3.03-2.96 (m), 2.89- 2.82 (m) 2,07

^{13}C NMR (75 MHz, C_6D_6 , ppm): δ 164.51, 161.98, 152.30, 148.17, 143.61, 143.49, 138.43, 136.69, 127.96, 125.14, 124.61, 123.54, 123.40, 86.21, 29.83, 28.25, 26.88, 25.9, 24.20, 23.93, 23.48, 15.21

^{29}Si NMR (59 MHz, C_6D_6 , ppm): δ -2.26

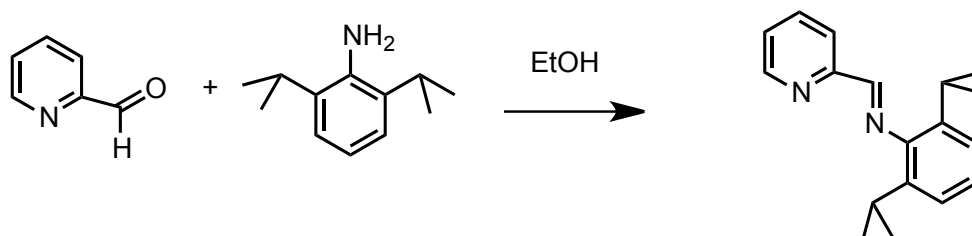
^{119}Sn NMR (111.92 MHz, C_6D_6 , ppm): δ -128 broad signal

Melting Point: \approx 97 °C -116 °C

IR(cm^{-1}): (C=N) 1645, 1570, (CH) 1312; (CH₃) 1459; (CH) 1364 (SiCH₃) 1256, 1249; (CH₃-C) 980 (Ph) 928, 856, 884, 815; (Ph, CH) 768, 723, 667, 619; (SiN) 2729

Crystallographic data: 23

5.2.37 2,6-diisopropyl-N-(pyridin-2-ylmethyl)aniline



Literature To a stirred solution of diisopropylaniline (45.5 ml, 0.241 mol) in ethanol the pyridinecarbaldehyde (23.08 ml, 0.241 mol) was added and the reaction mixture was refluxed for 6 hours. The solvents was removed in vacuum and the crude product was re-crystallized in pentane. Yield 73 %

^1H NMR (300 MHz, C_6D_6 , ppm): δ 8.54 (s, 1H), 8.43 (d, 1H), 8.25 (t, 1H), 8.22 (d, 1H), 7.11-7.05 (m, 3H), 6.64 (m, 1H), 3.14-3.05 (m, 1H), 1.11 (d, 12H).

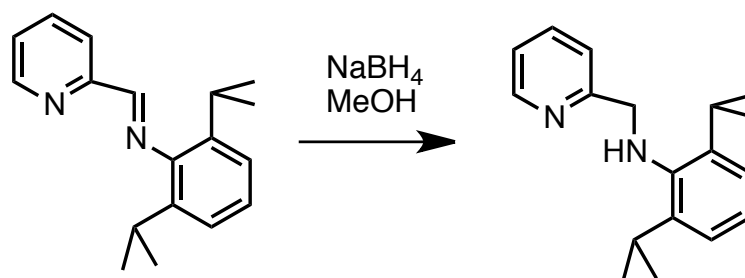
^{13}C NMR (75 MHz, C_6D_6 , ppm): δ 163.60, 154.78, 149.55, 148.88, 137.66, 135.93, 124.77, 124.60, 123.11, 120.52, 28.06, 23.19

Melting Point: \approx 53 °C

Elemental analysis (%) calcd for $\text{C}_{18}\text{H}_{22}\text{N}_2$: C 81.16, H 8.32, N 10.52;

found: C 80.89, H 8.14, N 10.37

5.2.38 (2,6-diisopropyl- benzyl)-pyridin-2-yl-amine



The 2,6-diisopropyl-N-(pyridin-2-ylmethyl)aniline (45.6 g, 0.171 mol) was dissolved in 250 ml of methanol and in small portions NaBH₄ (30 g, 0.891) was added. The reaction mixture was stirred over night and refluxed for further 3 hours. To remove the excess of NaBH₄ the mixture was quenched with 100 ml of water at 0 °C. The precipitate was dissolved in further 100 ml of water and the product was extracted several times with dichloromethane. The solvent was removed in vacuo and the oily crude product was recrystallized in cyclohexane at -30 °C. Yield 80%

¹H NMR (300 MHz, C₆D₆, ppm): δ 7.32- 7.12 (m, 7H), 4.78 (s, 1H), 4.20 (s, 2H), 3.75 (m, 2H), 1.24 (d, 12H)

¹³C NMR (75 MHz, C₆D₆, ppm): δ 159.25, 149.11, 143.70, 142.64, 135.64, 124.02, 123.58, 121.55, 56.74, 27.71, 24.07

Melting Point: ≈ 49 °C

Elemental analysis (%) calcd for C₄₂H₅₁N₃Si₃: C 65.82, H 6.71, N 5.48; found: C 65.34, H 6.74, N 5.46

IR(cm⁻¹): (NH) 3100, (CH₂-N) 1452, (Ph) 931, 864, 800; (Ph, CH) 752, 617

5.2.39 (N,N'E,N,N'E)-N,N'-(pyridine-2,6-diylbis(ethan-1-yl-1-ylidene))bis(2,6-diisopropylaniline)

This ligand was prepared according to the literature [87] and was a present from a former co-worker.

6 Materials and Methods

6.1 NMR, XRD-measurements and Elemental Analysis

NMR spectra were measured on a Varian Mercury 300 spectrometer.

XRD data collection was performed with a BRUKER-AXS KAPPA8 APEX II CCD diffractometer, using graphite monochromated Mo K α radiation (0.71073). Absorption corrections were performed using SADABS. The structures were solved with direct methods and the non-hydrogen atoms were refined anisotropically (full-matrix least squares on F²). All non-hydrogen atoms were refined employing anisotropic displacement parameters. Hydrogen atoms were located in calculated positions to correspond to standard bond lengths and angles. Crystallographic data for all compounds are given in the appendix chapter.

Elemental analyses were performed with a Heraeus VARIO ELEMENTAR EL analyzer.

6.2 Quantum chemical methods

In general we use two different quantum chemical software programs: Gaussian03 (Gaussian 03, Revision E.01) and ADF (Amsterdam Density Function; ADF2010.02).

6.2.1 Geometry optimization and Frequencies

Most of the structures were obtained from solid state data and pre optimized using the ADF program. Full geometry optimizations were performed on all molecules. All calculations (geometry optimization, frequencies and NMR) were performed with the Gaussian 03 (G03) suite of programs

Geometry optimizations were performed using Density-Functional Theory (DFT)[88] with the mPW1PW91 (Barone's Modified Perdew-Wang 1991 exchange functional and Perdew and Wang's 1991 correlation functional [89]).

For the silazanes we used the 6-31+G* Pople[90] basis sets and the mPW1PW91 functional.

Only the tin and lead substituted Si₃N₃ rings were optimized with the mPW1PW91 functional and the SDD basis sets. SDD is D95V up to Ar [91] and Stuttgart/Dresden ECPs [92] on the remainder of the periodic table.

Frequencies were calculated with Gaussian03, analytically using the same functional and basis sets as we used for the geometry optimization.

6.2.2 Nuclear Magnetic Resonance and NICS

The NMR calculations were carried out with the Gaussian03 program using the GIAO (Gauge-Independent Atomic Orbital [93]) method for most of the molecules. Table 6.1 displays reference molecules and the corresponding magnetic shieldings. The all electron IGLO-II [94] basis sets were used for all atoms.

Table 6.1: Calculated (mPW1PW91/IGLO-II) chemical shifts of the reference molecules

reference	magnetic shielding [ppm]		
SiMe₄	C=186.511	H=31.826	Si=349.660
SnMe₄	Sn=2553.33		

Only the lead and aluminum derivatives were calculated with the ADF program using ZORA (Zeroth Order Regular Approximation [95],[96]) for relativistic effects. Table 6.2 displays references and the corresponding magnetic shieldings. Here we also used the mPW1PW91 functional with TZ2P basis sets (valence triple zeta + 2 polarization functions).

Table 6.2: Calculated (mPW1PW91/IGLO-II) magnetic shieldings of the reference molecules

reference	magnetic shielding [ppm]
AlH₄	Al=529.592
PbMe₄	Pb=5037.628

6.2.3 Natural Bond Orbitals, UV-Spectra and BADER-Analysis

It should be noted that NBOs are intrinsic to the wave function, rather than to a particular choice of basis functions, and converge to well-defined limits as the quality wave function is improved [97]. They were carried out using the Gaussian03 package.

For simulation of the UV-VIS spectra we used the ADF program. And again we used the mPW1PW91 functional and the TZ2P basis sets in combination with ZORA.

Results are not perfect, but better than with the Gaussian03 program. The problem of missing and inaccurate basis sets for heavy atoms is solved by the ADF kit.

BADER analyses were carried out with the AIMALL program[81]. The atomic integration algorithms used in AIMAll is Proaim [98].

7 Appendix

7.1 Crystallographic Data

compound	1	1a	2
empirical formula	$C_{36}H_{33}N_3Si_3$	$C_{36}H_{33}N_3Si_3$	$C_{39}H_{39}N_3Si_3$
formula weight	591.92	371.86	633.20
temperature	100(2)K	283(5)K	283(5)K
wavelength	0.71073	1.54056	0.71073
crystal system	monoclinic	orthorhombic	orthorhombic
space group	C2/c	Pbca	Pbca
Unit cell dimensions	$a = 18.3949(9)$ $b = 9.4857(2)$ $c = 22.2341(6)$ $\alpha = 90^\circ$ $\beta = 90^\circ$ $\gamma = 90^\circ$	$a = 13.9559(5)$ $b = 13.6403(5)$ $c = 36.3836(13)$ $\alpha = 90^\circ$ $\beta = 90^\circ$ $\gamma = 90^\circ$	$a = 13.9559(5)$ $b = 13.6403(5)$ $c = 36.3836(13)$ $\alpha = 90^\circ$ $\beta = 90^\circ$ $\gamma = 90^\circ$
Volume	3076.59 ³	6926.08 ³	6926.08 ³
Z, Z'	4; 0	8; 0	8; 0

compound	3	4	5
empirical formula	$C_{36}H_{32}N_3Si_3Li_1$	$C_{36}H_{31}N_3Si_3Li_2$	$C_{36}H_{30}N_3Si_3Li_3$
formula weight	597.20	603.20	609.72
temperature	100(2)K	293(2)K	283(5)K
wavelength	0.71073	1.54056	1.54056
crystal system	monoclinic	monoclinic	monoclinic
space group	P 2(1)/c	P21/n	P21/n
Unit cell dimensions	$a = 13.5503(9)$ $b = 8.7844(6)$ $c = 13.0869(9)$ $\alpha = 90^\circ$ $\beta = 109.919(2)^\circ$ $\gamma = 90^\circ$	$a = 13.7367(6)$ $b = 13.4967(5)$ $c = 26.6564(12)$ $\alpha = 90^\circ$ $\beta = 101.898(2)^\circ$ $\gamma = 90^\circ$	$a = 21.1147(7)$ $b = 17.9439(5)$ $c = 29.4434(8)$ $\alpha = 90.00^\circ$ $\beta = 93.7690(1)^\circ$ $\gamma = 90.00^\circ$
Volume	$1464.56(17)^3$	$4835.9(2)^3$	$11131.4(0)^3$
Z, Z'	4; 0	2; 0	4; 0
compound	6	7	8
empirical formula	$C_{42}H_{51}N_3Si_6$	$C_{37}H_{33}N_3Si_3K_2$	$C_{42}H_{48}N_3Si_3Al_3$
formula weight	766.39	682.13	759.35
temperature	283(5)K	238(5)K	100(2)K
wavelength	0.71073	1.54056	1.54056
crystal system	triclinic	triclinic	monoclinic
space group	P-1	P-1	P2(1)/c
Unit cell dimensions	$a = 10.7005(3)$ $b = 10.7026(2)$ $c = 39.4421(9)$ $\alpha = 93.7620(1)^\circ$ $\beta = 93.7770(1)^\circ$ $\gamma = 113.8220(1)^\circ$	$a = 10.1528(13)$ $b = 13.0264(13)$ $c = 20.0542(16)$ $\alpha = 85.993(4)^\circ$ $\beta = 77.725(6)^\circ$ $\gamma = 71.324(4)^\circ$	$a = 19.6011(6)$ $b = 21.2494(7)$ $c = 13.8814(4)$ $\alpha = 90.00^\circ$ $\beta = 97.154(2)^\circ$ $\gamma = 90.00^\circ$
Volume	$4102.1(3)^3$	$2454.8(1)^3$	$5736.7(5)^3$
Z, Z'	0; 0	4; 0	4; 0

compound	9	10 (boat)	10a (chair)
empirical formula	$C_{36}H_{30}N_3Si_3Sn_3Cl_3$	$C_{36}H_{30}N_3Si_3Pb_3Cl_3$	$C_{36}H_{30}N_3Si_3Pb_3Cl_3$
formula weight	1052.87	1317.98	1317.98
temperature	293(2)K	100(2)K	238(5)K
wavelength	0.71073	1.54056	1.54056
crystal system	orthorhombic	monoclinic	triclinic
space group	Pbca	P 21/c	P-1
Unit cell dimensions	$a = 9.5456(6)$ $b = 9.2428(6)$ $c = 32.636(2)$ $\alpha = 90^\circ$ $\beta = 90^\circ$ $\gamma = 90^\circ$	$a = 23.8023$ $b = 16.0470(11)$ $c = 18.4861(14)$ $\alpha = 90^\circ$ $\beta = 90.322(3)^\circ$ $\gamma = 90^\circ$	$a = 10.1528(13)$ $b = 13.0264(13)$ $c = 20.0542(16)$ $\alpha = 85.993(4)^\circ$ $\beta = 77.725(6)^\circ$ $\gamma = 113.24(4)^\circ$
Volume	2879.4(3) ³	7060.7(6) ³	2454.8(1) ³
Z, Z'	8; 0	4; 0	4; 0
compound	11	12	13
empirical formula	$C_{36}H_{46}N_4Li_2$	$C_{18}H_{23}N_2GeCl$	$C_{24}H_{41}N_3Si_2Sn$
formula weight	548.66	219.51	546.48
temperature	100(2)K	100(2)K	100(2)K
wavelength	1.54056	1.54056	1.54056
crystal system	monoclinic	orthorhombic	monoclinic
space group	P 21/c	Pbca	P 21c
Unit cell dimensions	$a = 8.7290(4)$ $b = 17.2325(8)$ $c = 10.7703(5)$ $\alpha = 90.00^\circ$ $\beta = 104.175(2)^\circ$ $\gamma = 90.00^\circ$	$a = 16.1117(7)$ $b = 13.1965(5)$ $c = 16.9281(9)$ $\alpha = 90^\circ$ $\beta = 90^\circ$ $\gamma = 90^\circ$	$a = 14.5942(5)$ $b = 14.3277(5)$ $c = 16.2693(1)$ $\alpha = 90^\circ$ $\beta = 107.068(2)^\circ$ $\gamma = 90^\circ$
Volume	1570.7(7) ³	3599.2(2) ³	3274.3(8) ³
Z, Z'	2; 0	8; 0	8; 0

compound	14	15	16
empirical formula	$C_{34}H_{34}N_4Ge$	$C_{34}H_{34}N_4Sn$	$C_{34}H_{34}N_4Pb$
formula weight	388.30	668.87	388.30
temperature	100(2)K	100(2)K	100(2)K wave-length
1.54056	1.54056	1.54056	
crystal system	triclinic	monoclinic	triclinic
space group	P-1	P21/c	P-1
Unit cell dimensions	$a = 11.1937(4)$ $b = 12.3586(4)$ $c = 13.7658(4)$ $\alpha = 100.1840(1)^\circ$ $\beta = 96.8020(1)^\circ$ $\gamma = 90.5990(1)^\circ$	$a = 8.8320(15)$ $b = 9.1983(16)$ $c = 9.273(2)$ $\alpha = 100.374(8)^\circ$ $\beta = 91.560(6)^\circ$ $\gamma = 115.358(7)^\circ$	$a = 11.1937(4)$ $b = 12.3586(4)$ $c = 13.7658(4)$ $\alpha = 100.1840(1)^\circ$ $\beta = 96.8020(1)^\circ$ $\gamma = 90.5990(1)^\circ$
Volume	$1860.1(8)^3$	$664.99(1)^3$	$1860.1(8)^3$
Z, Z'	4; 0	2; 0	4;0
compound	17	18	19
empirical formula	$C_{18}H_{23}N_2GeCl$	$C_{21}H_{19}N_1O_6S_2$	$C_{34}H_{34}N_4Ge$
formula weight	219.51	546.48	388.30
temperature	100(2)K	100(2)K	100(2)K
wavelength	1.54056	1.54056	1.54056
crystal system	orthorhombic	orthorhombic	triclinic
space group	Pbca	Pbcn	P-1
Unit cell dimensions	$a = 16.1117(7)$ $b = 13.1965(5)$ $c = 16.9281(9)$ $\alpha = 90.00^\circ$ $\beta = 90.00^\circ$ $\gamma = 90.00^\circ$	$a = 21.084(18)$ $b = 6.251(5)$ $c = 15.435(13)$ $\alpha = 90.00^\circ$ $\beta = 90.00^\circ$ $\gamma = 90.00^\circ$	$a = 11.1937(4)$ $b = 12.3586(4)$ $c = 13.7658(4)$ $\alpha = 100.1840(1)^\circ$ $\beta = 96.8020(1)^\circ$ $\gamma = 90.5990(1)^\circ$
Volume	$3599.2(2)^3$	2034.27^3	$1860.1(8)^3$
Z, Z'	8; 0	4; 0	4;0

compound	20	21	22
empirical formula	$C_{34}H_{40}N_3Sn$	$C_{30}H_{40}N_4Si_8Sn_2$	$C_{21}H_{41}N_3Si_2Sn_2$
formula weight	572.37	548.66	388.30
temperature	100(2)K	100(2)K	100(2)K
wavelength	1.54056	1.54056	1.54056
crystal system	triclinic	triclinic	triclinic
space group	P-1	P-1	P 21/c
Unit cell dimensions	$a = 13.5293(4)$ $b = 8.6407(3)$ $c = 27.8602(8)$ $\alpha = 90.00^\circ$ $\beta = 95.1320(1)^\circ$ $\gamma = 90.00^\circ$	$a = 12.376(2)$ $b = 17.510(3)$ $c = 24.692(4)$ $\alpha = 102.684(5)^\circ$ $\beta = 92.234(6)^\circ$ $\gamma = 90.195(7)^\circ$	$a = 14.6942(5)$ $b = 14.3277(5)$ $c = 16.2693(1)$ $\alpha = 90.00^\circ$ $\beta = 107.068(2)^\circ$ $\gamma = 90.00^\circ$
Volume	$3243.8(7)^3$	5215.91^3	$1860.1(8)^3$
Z, Z'	4; 0	8; 0	8; 0
compound	23	24	
empirical formula	$C_{20}H_{35}N_3Si_2Sn$	$C_{34}H_{34}N_4Pb$	
formula weight	572.37	548.66	
temperature	100(2)K	100(2)K	
wavelength	1.54056	1.54056	
crystal system	monoclinic	triclinic	
space group	P 21/n	P-1	
Unit cell dimensions	$a = 8.9778(5)$ $b = 21.4516(12)$ $c = 22.0039(11)$ $\alpha = 90.00^\circ$ $\beta = 92.688(2)^\circ$ $\gamma = 90.00^\circ$	$a = 11.2628(4)$ $b = 12.40002(5)$ $c = 13.8070(5)$ $\alpha = 98.690(2)^\circ$ $\beta = 97.862(2)^\circ$ $\gamma = 93.711(2)^\circ$	
Volume	$4233.0(3)^3$	$1881.0(5)^3$	
Z, Z'	8; 0	4; 0	

7.2 Geometry optimized Structures

Hexaphenylcyclotrisilazane

planar conformation

mPW1PW91/6-31+G*

HF= -2424.350994

Si 0.00000 0.00000 0.00000 Si 3.13709 0.00000 0.00000 N 1.56304 0.68915 0.00000 N 0.18307
-1.70696 -0.04301 C 4.11089 0.52715 1.52190 C -1.00520 0.50650 1.49774 C 6.26275 0.76628
2.65980 C -0.95109 0.59851 -1.50697 C 5.50296 0.41658 1.52963 C -2.02215 -0.30898 2.00650
C 4.22635 1.35718 3.80520 C 3.47467 1.00745 2.67455 C -0.80471 1.75515 2.11195 C 5.59346
1.25246 3.78868 C -1.59750 2.16049 3.19057 C -2.58306 1.30885 3.69240 C -0.35852 0.42845 -
2.77269 C -2.22454 1.12782 -1.44967 C -2.80939 0.06270 3.08737 C -2.92334 1.50464 -2.60141
C -2.32093 1.31316 -3.85157 C -1.05337 0.75560 -3.96917 Si 1.57180 -2.71838 -0.06837 N
2.94892 -1.70858 -0.02556 C 4.11300 0.59948 -1.49351 C 1.54153 -3.82322 -1.58119 C 5.41953
2.35761 -2.58095 C 1.58265 -3.86020 1.42491 C 4.71270 1.85983 -1.47214 C 0.33864 -4.29045
-2.12227 C 4.93999 0.31289 -3.76298 C 4.23717 -0.17785 -2.65351 C 2.73666 -4.26542 -2.17508
C 5.53126 1.54925 -3.71795 C 2.71564 -5.14102 -3.26555 C 1.49694 -5.56309 -3.79948 C 1.70348
-3.27791 2.70102 C 1.40681 -5.22697 1.34650 C 0.29128 -5.14440 -3.21530 C 1.35931 -6.03504
2.48737 C 1.46683 -5.43333 3.74787 C 1.61394 -4.05832 3.88608 H 7.32776 0.66313 2.65687 H
6.00324 0.05721 0.65472 H -2.19998 -1.25716 1.54364 H 3.73035 1.70784 4.68606 H 2.40953
1.10779 2.69180 H -0.03518 2.40417 1.74933 H 6.15594 1.54629 4.65018 H -1.44844 3.12403
3.63134 H -3.16632 1.60614 4.53876 H 0.63805 0.04403 -2.83567 H -2.69146 1.25374 -0.49518
H -3.57519 -0.58907 3.45295 H -3.90161 1.93198 -2.52872 H -2.84877 1.60280 -4.73609 H -
0.61469 0.57832 -4.92888 H 5.86168 3.33166 -2.55608 H 4.63256 2.46144 -0.59092 H -0.58159
-3.97678 -1.67540 H 5.01542 -0.28079 -4.64997 H 3.79330 -1.15066 -2.69238 H 3.67506 -
3.92753 -1.78759 H 6.08535 1.90062 -4.56319 H 3.63433 -5.48756 -3.69077 H 1.48182 -6.20615
-4.65455 H 1.86650 -2.22342 2.78088 H 1.30368 -5.68229 0.38371 H -0.64757 -5.47765 -3.60570
H 1.24281 -7.09498 2.39874 H 1.43496 -6.04640 4.62424 H 1.65837 -3.60187 4.85281 H 3.81461
-2.20899 -0.01289 H 1.56175 1.68915 -0.00000 H -0.68276 -2.20713 -0.05571

Boat conformation

mPW1PW91/6-31+G*

HF=-2424.351124

Si -1.36767 -0.00827 -1.24145 N -1.47057 0.55107 0.40542 N 0.31233 -0.28742 -1.58296 Si
1.70235 -0.35591 -0.54217 Si -0.28407 0.73597 1.66886 N 1.26540 0.40079 0.96014 C -2.03917
1.23767 -2.48695 C -2.26195 0.85576 -3.82011 C -2.30676 2.56833 -2.13891 C -2.71742 1.76803
-4.76914 H -2.09196 -0.17525 -4.12392 C -2.76990 3.48626 -3.08027 H -2.15620 2.88807 -
1.11208 C -2.97248 3.08770 -4.39954 H -2.88093 1.44846 -5.79436 H -2.97443 4.51125 -2.78402
H -3.33296 3.80001 -5.13592 C -2.41276 -1.56896 -1.40621 C -3.77594 -1.50479 -1.73370 C
-1.86440 -2.83244 -1.13690 C -4.56369 -2.65387 -1.78424 H -4.23169 -0.54427 -1.96283 C -
2.64451 -3.98532 -1.18994 H -0.81106 -2.91799 -0.88350 C -3.99768 -3.89761 -1.51275 H -
5.61672 -2.57861 -2.04027 H -2.19673 -4.95212 -0.97786 H -4.60783 -4.79526 -1.55440 C -
0.72106 -0.44776 3.06989 C -1.63309 -0.08932 4.07500 C -0.19017 -1.74593 3.10198 C -2.00561
-0.99175 5.06999 H -2.05320 0.91393 4.09159 C -0.55539 -2.65200 4.09519 H 0.52334 -2.05296

2.34197 C -1.46583 -2.27625 5.08136 H -2.71263 -0.69108 5.83799 H -0.12927 -3.65129 4.09931
H -1.75181 -2.98085 5.85697 C -0.23471 2.47305 2.39815 C 0.36135 2.70384 3.64848 C -
0.73502 3.58189 1.70197 C 0.46282 3.98934 4.17674 H 0.74303 1.86625 4.22843 C -0.64494
4.86979 2.22618 H -1.20626 3.43307 0.73514 C -0.04237 5.07612 3.46551 H 0.92903 4.14194
5.14592 H -1.04479 5.71203 1.66856 H 0.02989 6.07860 3.87710 C 3.11365 0.60743 -1.32898 C
4.36131 0.03066 -1.60534 C 2.92577 1.95997 -1.66076 C 5.38626 0.77448 -2.18957 H 4.53617
-1.01397 -1.36176 C 3.94490 2.70740 -2.24430 H 1.96805 2.43438 -1.46052 C 5.17891 2.11379
-2.50969 H 6.34530 0.30766 -2.39497 H 3.77825 3.75150 -2.49304 H 5.97545 2.69478 -2.96546
C 2.27671 -2.13301 -0.27904 C 2.97212 -2.50465 0.88177 C 2.08370 -3.11415 -1.26311 C 3.45353
-3.80095 1.05642 H 3.13383 -1.77199 1.66918 C 2.56112 -4.41319 -1.09712 H 1.54324 -2.86325
-2.17279 C 3.24797 -4.75885 0.06506 H 3.98598 -4.06440 1.96595 H 2.39556 -5.15557 -1.87276
H 3.61970 -5.77056 0.19865 H 0.54096 -0.23085 -2.57052 H -2.39114 0.36057 0.79542 H
2.03160 0.88739 1.41450

1,3,5-triphenyl-2,2,4,4,6,6-cyclotrisilazane

mPW1PW91/6-31+G*

HF= -1731.2342731

Si -1.23761 -0.82955 -0.97166 N -1.43338 -0.35261 0.69258 N 0.44552 -0.69379 -1.39705 Si
1.70663 0.20679 -0.60467 Si -0.42612 0.68453 1.66165 N 1.00592 1.06027 0.74414 H 2.30737
1.20886 -1.52351 H 2.79305 -0.72240 -0.18386 H -2.08140 0.00064 -1.87846 H -1.67480 -
2.24113 -1.11851 H -1.10829 1.96214 1.99989 H -0.11703 -0.00790 2.94363 C 0.83625 -1.35113
-2.61157 C 1.33041 -2.65970 -2.58119 C 0.72674 -0.69208 -3.84083 C 1.70758 -3.29635 -3.76067
H 1.41202 -3.16792 -1.62529 C 1.10256 -1.33261 -5.01922 H 0.34597 0.32454 -3.85987 C
1.59411 -2.63584 -4.98261 H 2.08966 -4.31214 -3.72438 H 1.01078 -0.81082 -5.96699 H 1.88741
-3.13456 -5.90116 C -2.66202 -0.75791 1.31467 C -2.71363 -1.92868 2.07867 C -3.82112 0.01190
1.16846 C -3.90368 -2.32119 2.68510 H -1.81239 -2.52380 2.18832 C -5.01135 -0.38534 1.77389
H -3.77709 0.92313 0.57964 C -5.05620 -1.55217 2.53361 H -3.93039 -3.23190 3.27587 H -
5.90424 0.22026 1.65136 H -5.98370 -1.86059 3.00589 C 1.82532 2.10164 1.29885 C 2.80234
1.80767 2.25532 C 1.65473 3.42635 0.88288 C 3.59689 2.82276 2.78461 H 2.93215 0.77889
2.57801 C 2.44923 4.43814 1.41395 H 0.89567 3.64815 0.13918 C 3.42280 4.13969 2.36617 H
4.35274 2.58143 3.52588 H 2.30784 5.46243 1.08243 H 4.04199 4.92985 2.77928

1,3,5-tris(dimethylsilyl)-2,2,4,4,6,6-hexaphenylcyclotrisilazane

mPW1PW91/6-31+G*

HF=-3532.3557888

i 1.34255 -1.20323 0.19287 N -0.30823 -1.73901 -0.10738 N 1.40229 0.48361 0.70830 Si 0.32737
1.71154 0.02472 Si -1.59620 -0.57335 -0.31998 N -0.91487 0.93069 -0.95201 C 2.38669 -1.43167
-1.36898 C 3.79051 -1.41422 -1.32692 C 1.78413 -1.54965 -2.62958 C 4.55615 -1.51676 -2.48663
H 4.30499 -1.31834 -0.37458 C 2.53995 -1.64796 -3.79605 H 0.70112 -1.56291 -2.69710 C
3.93136 -1.63395 -3.72664 H 5.64035 -1.50217 -2.42164 H 2.04297 -1.73705 -4.75809 H 4.52526
-1.71460 -4.63248 C 2.02945 -2.29742 1.56790 C 2.91920 -3.35457 1.33815 C 1.55312 -2.12047
2.87672 C 3.32476 -4.19853 2.37223 H 3.30362 -3.53143 0.33745 C 1.94840 -2.95941 3.91300 H
0.85715 -1.31225 3.08786 C 2.83948 -4.00305 3.66213 H 4.01660 -5.01069 2.16779 H 1.56319 -
2.80218 4.91667 H 3.15110 -4.66055 4.46851 C -2.45973 -0.29607 1.33706 C -2.22849 -1.15648

2.41980 C -3.39730 0.73302 1.51968 C -2.90724 -1.00691 3.62864 H -1.50013 -1.95715 2.32572
C -4.08252 0.88815 2.72135 H -3.58821 1.43883 0.71716 C -3.84115 0.01437 3.78036 H -
2.70711 -1.69042 4.44927 H -4.79704 1.69823 2.83508 H -4.37355 0.13407 4.71964 C -2.86930
-1.26766 -1.53534 C -4.22971 -1.35197 -1.20552 C -2.47212 -1.78921 -2.77635 C -5.15530 -
1.92325 -2.07673 H -4.57408 -0.97996 -0.24451 C -3.38814 -2.36434 -3.65265 H -1.42664 -
1.75111 -3.06668 C -4.73621 -2.43162 -3.30385 H -6.20236 -1.97830 -1.79298 H -3.05117 -
2.75976 -4.60661 H -5.45411 -2.88149 -3.98342 C 1.38617 2.86045 -1.03916 C 1.51203 4.23881
-0.81858 C 2.13238 2.30082 -2.08931 C 2.33018 5.03172 -1.62166 H 0.96640 4.70955 -0.00550
C 2.95156 3.08507 -2.89630 H 2.07877 1.23267 -2.28101 C 3.04903 4.45656 -2.66662 H 2.40733
6.09803 -1.42889 H 3.51780 2.62347 -3.70005 H 3.68803 5.07172 -3.29359 C -0.50069 2.68181
1.41795 C -1.26171 3.82876 1.14164 C -0.43856 2.25652 2.75119 C -1.91055 4.53513 2.15246 H
-1.35799 4.18476 0.11848 C -1.08711 2.95204 3.76858 H 0.11780 1.35645 2.99462 C -1.81989
4.09900 3.47273 H -2.48623 5.42394 1.90927 H -1.02597 2.59425 4.79241 H -2.32328 4.64613
4.26466 Si 2.97542 1.14565 1.27446 Si -1.73857 1.69661 -2.33636 Si -0.62799 -3.49138 0.05749
H -0.15900 -3.92052 1.40209 H -1.67787 0.74816 -3.48021 H 3.84069 1.36989 0.08378 C -
3.54560 2.10915 -1.98332 C -1.02139 3.31103 -2.98133 C 2.81282 2.77888 2.19795 C 3.96699
0.06004 2.45064 C -2.43449 -4.01090 -0.00525 C 0.30170 -4.48587 -1.24120 H -4.13989 1.26621
-1.62670 H -4.00496 2.45834 -2.91630 H -3.62380 2.92476 -1.25489 H -1.01023 4.12432 -
2.25120 H -0.01626 3.21839 -3.39506 H -1.69390 3.61311 -3.79546 H 2.25711 3.55838 1.67673
H 3.83532 3.14827 2.34707 H 2.36050 2.64263 3.18463 H 3.43110 -0.15857 3.37815 H 4.85717
0.64903 2.70857 H 4.30708 -0.89051 2.03628 H -3.06722 -3.47315 0.70656 H -2.88822 -3.93394
-0.99485 H -2.44081 -5.06886 0.28907 H -0.08343 -4.28338 -2.24644 H 1.37605 -4.28465 -
1.25094 H 0.16243 -5.55459 -1.03876

1,3,5-trimethyl-2,2,4,4,6,6-hexaphenylcylotrisilazane

mPW1PW91/6-31+G*

HF=-2542.2222119

Si 0.00000 0.00000 0.00000 N 1.74161 0.00000 0.00000 N -0.56930 1.64795 0.00000 Si 0.29897
3.08974 0.44534 Si 2.81199 1.34935 -0.26358 N 2.00323 2.79674 0.25928 C -2.03556 1.76475
0.08024 H -2.51584 1.02826 -0.57389 H -2.36539 2.75148 -0.26078 H -2.41020 1.61422 1.10060
C 2.32200 -1.32717 -0.27133 H 3.35726 -1.37538 0.08231 H 2.30859 -1.57835 -1.33936 H
1.76767 -2.10747 0.26217 C 2.84076 3.99888 0.40028 H 2.86929 4.59587 -0.51963 H 3.86818
3.72884 0.66291 H 2.46826 4.64146 1.20638 C -0.61409 -0.94401 1.51701 C -1.93250 -1.41700
1.61622 C 0.22857 -1.14232 2.62041 C -2.39029 -2.05606 2.76700 H -2.61753 -1.29143 0.78115
C -0.21790 -1.78588 3.77235 H 1.25390 -0.78657 2.57035 C -1.53166 -2.24338 3.84830 H -
3.41591 -2.41033 2.81851 H 0.45784 -1.92950 4.61081 H -1.88471 -2.74447 4.74494 C -0.66045
-0.86350 -1.54491 C -1.03338 -2.21561 -1.56152 C -0.71017 -0.16141 -2.75960 C -1.44759
-2.83971 -2.73789 H -1.00174 -2.79551 -0.64266 C -1.12377 -0.77605 -3.93847 H -0.41284
0.88364 -2.78316 C -1.49670 -2.11929 -3.92880 H -1.73225 -3.88799 -2.72343 H -1.15126 -
0.20965 -4.86505 H -1.82052 -2.60237 -4.84618 C 3.32507 1.49862 -2.07346 C 4.23049 0.60667
-2.67124 C 2.75779 2.49032 -2.88781 C 4.55211 0.69693 -4.02385 H 4.69982 -0.17081 -2.07278
C 3.07837 2.59085 -4.24062 H 2.05313 3.19726 -2.45696 C 3.97658 1.69227 -4.81195 H 5.25378
-0.00687 -4.46258 H 2.62872 3.37229 -4.84692 H 4.22956 1.76780 -5.86557 C 4.36993 1.08724
0.77405 C 5.64601 1.46123 0.32765 C 4.26490 0.55901 2.07053 C 6.77088 1.31436 1.13912 H
5.76731 1.87416 -0.67047 C 5.38277 0.40559 2.88634 H 3.29021 0.25755 2.44594 C 6.64117

0.78444 2.42036 H 7.74784 1.61252 0.76949 H 5.27420 -0.00971 3.88436 H 7.51569 0.66596
3.05350 C -0.03910 3.60459 2.22932 C -1.20103 4.30232 2.59426 C 0.84602 3.23361 3.25278 C
-1.47243 4.61240 3.92570 H -1.90629 4.61702 1.82844 C 0.58536 3.54543 4.58529 H 1.75670
2.69705 2.99794 C -0.57738 4.23470 4.92457 H -2.37982 5.15147 4.18292 H 1.28927 3.25172
5.35895 H -0.78406 4.47861 5.96265 C -0.25984 4.49777 -0.68613 C -0.17184 5.84252 -0.29548
C -0.71296 4.22948 -1.98737 C -0.51468 6.87584 -1.16637 H 0.16504 6.09152 0.70778 C -
1.06351 5.25513 -2.86240 H -0.80039 3.19720 -2.31676 C -0.96250 6.58367 -2.45269 H -0.43587
7.90856 -0.83878 H -1.41734 5.01860 -3.86202 H -1.23484 7.38674 -3.13134

1,3,5-triphenyl-2,2,4,4,6,6-hexamethylcyclotrisilazane

mPW1PW91/6-31+G*

HF=-1967.1655156

Si 0.11335 0.65599 0.13782 N 0.02751 0.05059 1.79190 N 1.62889 0.07253 -0.53594 Si 3.05411
-0.16503 0.46118 Si 1.27695 0.37177 2.97944 N 2.71297 0.63666 1.99724 C 1.71963 -0.19649
-1.93254 C 1.59496 -1.50365 -2.42070 C 1.93265 0.83918 -2.85175 C 1.68298 -1.76742 -3.78554
H 1.41798 -2.30961 -1.71512 C 2.01353 0.57628 -4.21723 H 2.04271 1.85352 -2.48026 C 1.89093
-0.72857 -4.69079 H 1.58246 -2.78838 -4.14244 H 2.17871 1.39447 -4.91233 H 1.95681 -0.93372
-5.75479 C -1.15542 -0.61839 2.22834 C -1.28884 -2.00440 2.08255 C -2.20776 0.09497 2.81492
C -2.44181 -2.65758 2.50988 H -0.47427 -2.56211 1.63041 C -3.36107 -0.55868 3.24450 H -
2.11197 1.17105 2.92684 C -3.48329 -1.93813 3.09382 H -2.52606 -3.73350 2.38695 H -4.16611
0.01365 3.69628 H -4.38145 -2.44853 3.42747 C 3.79432 1.33009 2.62683 C 4.70082 0.65295
3.45155 C 3.96633 2.70579 2.43495 C 5.75044 1.33225 4.06737 H 4.57436 -0.41497 3.60325
C 5.01464 3.38491 3.04972 H 3.26607 3.23558 1.79669 C 5.91168 2.70145 3.86931 H 6.44306
0.78796 4.70275 H 5.13060 4.45267 2.88812 H 6.72863 3.23189 4.34859 C 1.42240 -1.09205
4.15055 C 0.94263 1.90573 4.01231 C 3.39922 -2.00010 0.70529 C 4.55336 0.62659 -0.33900 C
0.05256 2.53740 0.12005 C -1.32151 -0.01922 -0.85841 H 0.49515 -1.24391 4.71367 H 2.22276
-0.91507 4.87805 H 1.64681 -2.02243 3.61972 H -0.88606 2.90891 0.54710 H 0.87886 2.96360
0.69781 H 0.12699 2.92312 -0.90310 H 4.72615 0.18218 -1.32538 H 5.45700 0.47264 0.25976 H
4.42074 1.70412 -0.47525 H 2.53505 -2.51559 1.13745 H 4.25223 -2.15028 1.37711 H 3.64091
-2.48863 -0.24533 H -1.27788 0.35657 -1.88622 H -1.31535 -1.11217 -0.90100 H -2.27757
0.29424 -0.42632 H 0.81371 2.79620 3.38933 H 1.75474 2.10449 4.71967 H 0.02514 1.76631
4.59562

Hexatetbutylcyclotrisilazane

mPW1PW91/6-31+G*

HF=-1981.5933296

Si -1.43441 -0.66904 -1.00237 N -1.41640 -0.34945 0.72422 N 0.18318 -0.29924 -1.56124 Si
1.62615 0.35423 -0.81594 Si -0.23165 0.30121 1.84161 N 1.18599 0.62516 0.85791 H 0.30785 -
0.49951 -2.54927 H -2.31691 -0.52368 1.16163 H 1.95874 0.99095 1.40660 C -1.84517 -2.53326
-1.36755 C -2.74216 0.47987 -1.87436 C 2.13909 2.01144 -1.69975 C 3.08314 -0.92935 -0.93634
C -0.92476 1.93069 2.63668 C 0.28671 -0.95615 3.24707 C 4.22160 -0.57752 0.03491 C 3.65010
-1.04288 -2.36028 C 2.57200 -2.32133 -0.55205 C 3.59601 2.43217 -1.44554 C 1.92656 1.88187
-3.21845 C 1.26509 3.16764 -1.20105 C -2.25532 1.70561 3.37555 C -1.21425 2.96139 1.54111
C 0.09659 2.55353 3.60120 C -0.56416 -0.90967 4.52566 C 1.75009 -0.69274 3.64378 C 0.19242

-2.39309 2.72359 C -3.11032 0.02810 -3.29666 C -4.02458 0.56515 -1.02973 C -2.17547 1.89752
-2.00904 C -1.38994 -2.91394 -2.78709 C -3.33944 -2.86009 -1.21255 C -1.09746 -3.44304 -
0.38714 H 3.78075 3.40865 -1.91576 H 3.81331 2.55031 -0.37730 H 4.32709 1.73531 -1.86211
H 2.53153 1.08948 -3.66910 H 0.87797 1.68746 -3.46598 H 2.20603 2.82168 -3.71546 H 1.47982
4.07478 -1.78452 H 0.19926 2.95842 -1.29853 H 1.47027 3.39874 -0.15155 H -2.23360 -0.02127
-3.95357 H -3.79976 0.75746 -3.74558 H -3.60856 -0.94315 -3.32910 H -0.30593 -2.80272 -
2.90340 H -1.87637 -2.32735 -3.57099 H -1.62409 -3.97007 -2.98212 H -2.94020 2.56812 -
2.42715 H -1.86552 2.31312 -1.04953 H -1.31221 1.92350 -2.67955 H -0.02084 -3.26521 -
0.38938 H -1.25925 -4.49564 -0.66136 H -1.45503 -3.31025 0.63550 H -3.49739 -3.93816 -
1.35924 H -3.71003 -2.62129 -0.20828 H -3.97551 -2.34351 -1.93496 H -4.51421 -0.40393 -
0.89402 H -3.82556 0.98574 -0.03792 H -4.75293 1.22737 -1.51907 H 2.43288 -0.87490 2.80888
H 2.04387 -1.37184 4.45661 H 1.91920 0.32806 4.00456 H -1.62629 -1.09040 4.32704 H -
0.47587 0.03490 5.06857 H -0.22953 -1.70238 5.21011 H 0.69739 -2.52871 1.76647 H -0.84847
-2.70101 2.59140 H 0.65131 -3.08528 3.44430 H 4.68705 0.38763 -0.17605 H 3.87496 -0.56418
1.07408 H 5.01275 -1.33833 -0.02682 H 3.40104 -3.04343 -0.57041 H 2.15024 -2.33685 0.45573
H 1.80848 -2.67751 -1.24831 H 4.40612 -1.84044 -2.39487 H 2.87676 -1.30935 -3.09118 H
4.13634 -0.12776 -2.70665 H -2.65944 2.67408 3.70339 H -3.01301 1.25732 2.72098 H -2.16386
1.08008 4.26382 H -1.52466 3.91240 1.99779 H -0.34374 3.16136 0.91573 H -2.03191 2.63189
0.89575 H 0.32501 1.91289 4.45731 H -0.29555 3.49898 4.00217 H 1.04119 2.79089 3.09655

1,3-di(potassium)-2,2,4,4,6,6-hexaphenylcylotrisilazane

mPW1PW91/6-31+G*

HF=-3623.0558804

K -3.17964 -1.08694 -1.10983 Si 0.17509 -1.08595 -1.38956 Si -1.03619 1.60604 -1.40258 K
1.37416 4.03571 -1.28115 Si 1.17102 1.12130 0.51235 C -0.02535 2.14889 4.37383 H -0.60281
2.94850 4.81784 C 1.45220 0.11472 3.22368 H 2.03760 -0.69015 2.79733 C 0.51138 1.15377
5.17639 H 0.35446 1.17183 6.24563 C 0.17609 2.11499 3.00075 H -0.25581 2.88415 2.37397
C 0.91798 1.10062 2.39120 C 1.25100 0.13312 4.59577 H 1.67435 -0.64622 5.21452 N 1.17601 -
0.50894 -0.09199 N 0.07736 2.11657 -0.24679 N -0.99650 -0.00900 -1.87405 C -1.38151 4.04166
-3.00688 H -2.11388 4.34788 -2.26823 C -1.03710 4.93011 -4.02070 H -1.49954 5.90736 -
4.06167 C 0.10313 2.41585 -3.91734 H 0.55211 1.43173 -3.89361 C -0.81309 2.76607 -2.91950
C 0.45576 3.29451 -4.93180 H 1.16917 2.99042 -5.68584 C 5.00540 1.87059 -1.02606 H 5.61095
1.48119 -1.83296 C 3.45394 2.83367 1.04698 H 2.86840 3.19787 1.88556 C 2.95043 1.78254
0.27319 C 3.76088 1.31231 -0.76555 H 3.40962 0.49484 -1.38286 C -1.03498 -3.71429 -1.61213
H -0.82369 -3.61928 -2.67065 C -1.51019 -4.03038 1.09591 H -1.67961 -4.15232 2.15708 C
-1.67807 -4.85529 -1.14959 H -1.97577 -5.62566 -1.84762 C -1.91864 -5.01590 0.20802 H -
2.40996 -5.90736 0.57159 C -0.62145 -2.70031 -0.74089 C -3.90060 2.08789 -1.70469 H -
3.72313 1.96247 -2.76661 C -5.19169 2.35787 -1.26767 H -6.00030 2.43188 -1.98227 C -2.81990
2.00958 -0.81792 C 0.83666 -1.38941 -4.14614 H -0.08554 -0.84104 -4.28530 C 2.44550 -
2.36756 -2.68227 H 2.79849 -2.61441 -1.68872 C 1.25151 -1.66126 -2.84005 C -0.11091 4.56143
-4.98314 H 0.15927 5.24846 -5.77301 C 4.69310 3.40428 0.78893 H 5.05570 4.21306 1.40903 C
5.47217 2.92445 -0.25343 H 6.44052 3.35998 -0.45686 C -3.10144 2.20931 0.53666 H -2.28168
2.16956 1.24135 C 1.58137 -1.79321 -5.24562 H 1.23657 -1.56659 -6.24563 C 2.76743 -2.48723
-5.06087 H 3.35195 -2.80428 -5.91336 C 3.19848 -2.77476 -3.77318 H 4.12043 -3.31920 -
3.62106 C -4.38887 2.47547 0.98683 H -4.56969 2.63302 2.04157 C -5.43956 2.55356 0.08435 H

-6.44052 2.77412 0.42855 H 1.89168 -1.13125 0.24990 C -0.87196 -2.89063 0.62368 H -0.54375
-2.13332 1.32516

1-potassium-2,2,4,4,6,6-hexaphenylcyclotrisilazane

mPW1PW91/6-31+G*

HF=-3023.7122858

Si -0.14313 1.02887 -1.35899 Si 2.22177 -0.64522 -0.18632 Si -0.01479 0.59342 1.62459 N
1.50507 -0.24759 1.34441 N -0.76574 1.02640 0.19360 N 1.41472 0.22512 -1.45491 C -1.40077
0.07816 -2.45478 C 0.00490 2.73542 -2.16905 C -2.51117 0.72750 -3.02166 H -2.56238 1.81424
-2.99397 C -1.36514 -1.32441 -2.54747 H -0.51312 -1.86190 -2.13710 C -3.49796 -1.37766
-3.68767 H -4.29935 -1.93556 -4.16376 C -3.54949 0.01535 -3.62727 H -4.39161 0.54717 -
4.06269 C -2.39553 -2.04654 -3.15283 H -2.33453 -3.13009 -3.21449 C 0.60671 2.92318 -
3.42284 H 1.00829 2.06941 -3.96659 C 0.17857 5.29684 -3.34415 H 0.24904 6.28265 -3.79515
C -0.43421 5.13478 -2.10364 H -0.84519 5.99633 -1.58389 C -0.51719 3.86692 -1.52703 H -
0.99491 3.74398 -0.55793 C 0.69907 4.18517 -4.00596 H 1.17515 4.30303 -4.97560 C 2.12545
-2.51373 -0.49004 C 4.04799 -0.17189 -0.17399 C 2.13738 -3.42343 0.57805 H 2.16040 -3.04690
1.59827 C 6.75098 0.62535 -0.13839 H 7.79284 0.93268 -0.12426 C 4.40595 1.17351 0.01701
H 3.62805 1.92103 0.15380 C 2.11631 -4.80113 0.36384 H 2.12714 -5.48296 1.20998 C 5.08035
-1.10465 -0.34693 H 4.83733 -2.15329 -0.49780 C 5.74026 1.57079 0.03540 H 5.99276 2.61670
0.18547 C 6.41927 -0.71352 -0.32983 H 7.20220 -1.45442 -0.46588 C 2.08359 -5.30281 -0.93614
H 2.06750 -6.37536 -1.10775 C 2.09485 -3.04420 -1.78866 H 2.08105 -2.36920 -2.64162 C
2.07374 -4.41996 -2.01477 H 2.04999 -4.80323 -3.03135 C 0.34785 1.97855 2.86571 C -1.22180
-0.59798 2.52124 C -1.18744 -1.97822 2.25916 H -0.35478 -2.38467 1.68953 C 0.52427 1.72035
4.23391 H 0.39608 0.70813 4.61330 C 0.51343 3.30149 2.43086 H 0.38286 3.53154 1.37694 C
-3.27288 -2.32906 3.43261 H -4.05677 -2.99316 3.78566 C 0.85621 2.73501 5.13089 H 0.98774
2.50713 6.18529 C -2.30833 -0.11669 3.27303 H -2.36111 0.94333 3.51427 C 0.84268 4.32361
3.31970 H 0.96597 5.34026 2.95602 C -2.19556 -2.83594 2.70416 H -2.13747 -3.89971 2.48856
C 1.01542 4.04185 4.67391 H 1.27206 4.83613 5.36926 C -3.32305 -0.96484 3.72312 H -4.14627
-0.56454 4.30943 H 1.99869 0.43987 -2.25645 H 2.15579 -0.25218 2.12373 K -3.06551 -0.34572
0.07918

1-mono(lithio)-2,2,4,4,6,6-hexaphenylcyclotrisilazane

mPW1PW91/6-31+G*

HF=-2741.328249

Si 0.00000 0.00000 0.00000 Si 3.10031 0.00000 0.00000 Si 1.40132 2.58647 0.00000 N 2.89010
1.70024 -0.10064 N 0.11477 1.61290 0.43738 N 1.56185 -0.75347 -0.09805 C -1.02593 -0.94085
1.28303 C -0.89159 -0.30530 -1.64313 C -2.41766 -0.78799 1.33597 H -2.84028 -0.20584 0.71593
C -0.45234 -1.81038 2.22501 H 0.48918 -1.93279 2.22767 C -2.60696 -2.32915 3.17703 H -
3.13801 -2.80182 3.80748 C -3.20132 -1.46426 2.27043 H -4.14217 -1.33318 2.28525 C -1.23085
-2.49878 3.15730 H -0.81686 -3.08573 3.77953 C -0.61497 -1.43091 -2.43434 H 0.04263 -
2.05325 -2.14516 C -2.24053 -0.76417 -4.07885 H -2.69626 -0.91879 -4.89693 C -2.53271 0.35086
-3.32620 H -3.18491 0.96986 -3.63046 C -1.86962 0.57429 -2.11552 H -2.08900 1.34162 -
1.60125 C -1.28665 -1.65523 -3.64095 H -1.08432 -2.42552 -4.16003 C 4.02511 -0.46223 1.56567
C 4.20030 -0.63057 -1.38667 C 4.86811 0.43633 2.22767 H 4.90276 1.34056 1.93798 C 5.85365

-1.55951 -3.46798 H 6.40948 -1.87889 -4.16864 C 3.68433 -0.89686 -2.66296 H 2.75942 -0.75621 -2.82965 C 5.65781 0.03391 3.30360 H 6.22375 0.66094 3.73825 C 5.57438 -0.83731 -1.19554 H 5.95304 -0.66387 -0.34192 C 4.49915 -1.36236 -3.68959 H 4.12712 -1.54658 -4.54382 C 6.39579 -1.28755 -2.21901 H 7.32537 -1.40972 -2.06599 C 5.61729 -1.27649 3.73646 H 6.16226 -1.55470 4.46268 C 3.99662 -1.77694 2.03520 H 3.42931 -2.40895 1.60909 C 4.78052 -2.18335 3.11153 H 4.74059 -3.08263 3.41609 C 1.17272 3.46413 -1.66264 C 1.61603 3.95231 1.29462 C 2.85987 4.26578 1.85085 H 3.62773 3.78603 1.56459 C 2.24513 3.87895 -2.47022 H 3.13412 3.75102 -2.16159 C -0.11477 3.70428 -2.16006 H -0.86389 3.45159 -1.63325 C 1.90031 5.96101 3.26689 H 1.99788 6.63463 3.92925 C 2.03740 4.47649 -3.71818 H 2.78067 4.73811 -4.24867 C 0.51615 4.68376 1.76552 H -0.34492 4.50438 1.40623 C -0.33333 4.30063 -3.40226 H -1.22007 4.44143 -3.71283 C 3.00297 5.26339 2.81076 H 3.86503 5.46606 3.15595 C 0.74822 4.68673 -4.18232 H 0.60586 5.09346 -5.02954 C 0.64896 5.66794 2.74654 H -0.11682 6.13566 3.05673 Li -0.56718 1.92551 2.23489 H 1.60466 -1.54523 -0.28908 H 3.55034 2.09428 -0.29063

1,3-di(lithio)-2,2,4,4,6,6-hexaphenylcyclotrisilazane

mPW1PW91/6-31+G*

HF=-3058.2954189

Si 0.00000 0.00000 0.00000 Si 2.91458 0.00000 0.00000 Si 1.57979 2.59800 0.00000 N 0.07985 1.72946 0.09730 N 1.44014 -0.76280 0.34516 C 4.06529 -0.23715 1.50846 N 2.86065 1.63117 -0.46249 C 3.85037 -0.91517 -1.39298 C 4.47529 0.86098 2.28620 H 4.17400 1.73156 2.05549 Li 3.89064 1.99731 -2.03920 C 5.76608 -0.56303 3.74672 H 6.35011 -0.66969 4.48896 C 5.17818 -0.58435 -1.70105 H 5.62446 0.06890 -1.17617 C 3.24720 -1.90333 -2.18563 H 2.35083 -2.16019 -2.00351 C 5.35845 -1.67254 3.01199 H 5.64752 -2.54114 3.26101 C 5.31273 0.69982 3.38908 H 5.57488 1.45634 3.89855 C 4.52358 -1.50204 1.90799 H 4.25671 -2.26614 1.41141 C 5.23495 -2.15274 -3.53220 H 5.69451 -2.55844 -4.25772 C 5.86256 -1.18655 -2.75899 H 6.75933 -0.93492 -2.94947 C 3.93059 -2.51968 -3.23786 H 3.50037 -3.19274 -3.75240 C -1.38258 -0.58622 1.16918 C -0.69246 -0.42823 -1.72110 C -0.48889 -1.68842 -2.29899 H 0.00993 -2.34261 -1.82141 C -2.66240 -2.45519 2.10271 H -2.79630 -3.39265 2.18506 C -3.50313 -1.57474 2.75637 H -4.22793 -1.90347 3.27385 C -1.45648 0.48843 -2.45783 H -1.62000 1.34954 -2.09235 C -1.61803 -1.96432 1.32181 H -1.04659 -2.57941 0.87859 C -0.99955 -2.00908 -3.55732 H -0.83695 -2.86647 -3.93224 C -1.74362 -1.07613 -4.26181 H -2.08828 -1.29107 -5.12153 C -2.23569 0.26930 1.87211 H -2.09814 1.20728 1.81754 C -1.98347 0.17365 -3.70703 H -2.50570 0.81297 -4.17883 C -3.28637 -0.22229 2.65398 H -3.85421 0.38339 3.11725 C 0.10778 4.44517 -1.67740 H -0.66298 3.95890 -1.40782 C 1.85305 3.40026 1.69835 C 3.08111 4.94569 3.13039 H 3.71043 5.65117 3.21643 C 2.47284 4.78543 -1.64006 H 3.34108 4.53756 -1.34664 C 1.55891 3.39346 4.12015 H 1.13392 3.03192 4.88891 C 2.77116 4.44353 1.87273 H 3.19433 4.81842 1.10940 C 2.47626 4.41946 4.25933 H 2.68854 4.76026 5.11966 C 1.06932 6.24855 -2.94135 H 0.97052 6.99350 -3.52079 C 1.36573 4.04854 -1.19930 C 2.32983 5.87529 -2.49978 H 3.09523 6.36177 -2.78239 C 1.25508 2.88789 2.85768 H 0.62724 2.17846 2.78128 C -0.04140 5.53490 -2.53773 H -0.90456 5.78497 -2.84507 Li 1.56989 -1.79223 1.96121 H -0.57844 2.13200 0.24399

1,3,5 tri(lithio)-2,2,4,4,6,6-hexaphenylcyclotrisilazane

mPW1PW91/6-31+G*

HF=-2445.5096266

Si 0.00000 0.00000 0.00000 Si 2.89702 0.00000 0.00000 Si 1.46442 2.53673 0.00000 N 0.03196
1.66738 0.25696 N 1.44431 -0.79224 -0.37595 N 2.93163 1.68622 -0.06368 C 1.31984 3.57536
-1.60701 C 1.59337 3.88896 1.34917 C 0.59252 3.06644 -2.69336 C 2.81446 4.23422 1.96320
C 0.46497 4.59784 1.77698 C 0.52398 5.57847 2.77181 C 1.74441 5.87695 3.37105 C 1.95308
4.80336 -1.79969 C 0.52615 3.73751 -3.91793 C 2.88344 5.20380 2.93796 C 1.88786 5.50380 -
3.01375 C 1.18045 4.94631 -4.09751 C 3.53086 -0.59381 1.71319 C 3.69480 -1.95158 2.01373 C
4.22488 -0.66596 -1.22871 C 4.02794 -0.42896 -2.61219 C 3.74495 0.29480 2.75693 C 4.06272
-2.39010 3.29164 C 4.91807 -0.91085 -3.57375 C 5.36303 -1.37051 -0.87360 C 4.24750 -1.47602
4.31379 C 4.08016 -0.12275 4.03543 C 6.25897 -1.86707 -1.82154 C 6.03419 -1.63858 -3.16729
C -1.44754 -1.82880 -1.74997 C -0.81295 -0.71475 1.58202 C -0.03930 -0.97646 2.71868 C
-1.29505 -0.48710 -1.33215 C -0.62149 -1.36662 3.94130 C -2.00770 -1.49454 4.02871 C -
2.19831 -0.87589 1.71437 C -2.79320 -1.26253 2.93429 C -3.21017 -1.24692 -3.28206 C -2.14300
0.46038 -1.92750 C -2.38731 -2.20144 -2.71652 C -3.08728 0.08397 -2.88687 Li -0.87717 1.90165
1.91143 Li 4.36239 2.24908 -1.10090 Li 1.45718 -1.66985 -2.03048 H 3.17462 0.13409 -2.92796
H 4.74466 -0.72302 -4.61276 H 7.11769 -2.42319 -1.50815 H 5.56251 -1.54011 0.16387 H
6.71784 -2.02095 -3.89620 H 1.14892 5.44727 -5.04247 H -0.03516 3.31397 -4.72443 H 0.07344
2.13751 -2.58137 H 2.37107 6.45301 -3.11577 H 2.51000 5.22748 -0.99045 H -0.82531 -2.58205
-1.31368 H -2.46877 -3.22497 -3.01760 H -3.93559 -1.52682 -4.01713 H -3.72304 0.82602 -
3.32285 H -2.06502 1.48859 -1.64182 H -3.85523 -1.37368 3.00232 H -2.82444 -0.70047 0.86461
H -2.45864 -1.77577 4.95740 H -0.00607 -1.56283 4.79433 H 1.02436 -0.87749 2.65760 H
3.53399 -2.67633 1.24316 H 4.20129 -3.43457 3.47815 H 4.51342 -1.80267 5.29740 H 4.21113
0.60008 4.81341 H 3.64748 1.34339 2.56757 H -0.48020 4.38075 1.32485 H 3.70972 3.73023
1.66423 H 3.83153 5.44489 3.37145 H -0.36342 6.09627 3.07065 H 1.80585 6.60908 4.14894

1,3,5 tris(dimethylaluminum)-2,2,4,4,6,6-hexaphenylcyclotrisilazane

mPW1PW91/6-31+G*

HF=-3389.3905982

Si 0.01725 1.72619 0.02224 N 1.21786 0.67681 -0.67619 N -1.20252 0.68499 0.70006 Si -
1.47421 -0.87400 -0.02057 Si 1.45862 -0.90692 -0.00134 N -0.01832 -1.84086 -0.02216 C -
0.64190 2.88353 -1.32471 C -1.24011 4.11251 -0.99801 C -0.60818 2.52617 -2.68046 C -1.76508
4.95128 -1.97807 H -1.29205 4.42833 0.04106 C -1.12032 3.36423 -3.67015 H -0.19591 1.56535
-2.97262 C -1.69872 4.58145 -3.32090 H -2.22020 5.89630 -1.69498 H -1.07585 3.05912 -
4.71176 H -2.09947 5.23739 -4.08845 C 0.69713 2.84924 1.38745 C 1.31460 4.07384 1.08088
C 0.66335 2.46715 2.73636 C 1.85842 4.88490 2.07397 H 1.36740 4.40798 0.04763 C 1.19488
3.27715 3.73906 H 0.23416 1.50913 3.01215 C 1.79267 4.49061 3.40985 H 2.32841 5.82718
1.80647 H 1.14998 2.95322 4.77496 H 2.20872 5.12470 4.18756 C 2.21480 -0.83296 1.72790
C 3.15320 0.16406 2.03811 C 1.91960 -1.77288 2.72554 C 3.77806 0.21382 3.28239 H 3.38675
0.92899 1.30261 C 2.53502 -1.72932 3.97510 H 1.19595 -2.55867 2.52688 C 3.47117 -0.73550
4.25462 H 4.49502 1.00137 3.49583 H 2.28570 -2.47078 4.72913 H 3.95393 -0.69822 5.22696
C 2.74263 -1.71547 -1.15058 C 4.09571 -1.85657 -0.79501 C 2.34886 -2.21258 -2.40712 C
5.01127 -2.46457 -1.65187 H 4.43462 -1.49735 0.17291 C 3.25655 -2.82835 -3.26519 H 1.31381
-2.10438 -2.72286 C 4.59186 -2.95523 -2.88675 H 6.05053 -2.56266 -1.35201 H 2.92495 -
3.20217 -4.22960 H 5.30349 -3.43409 -3.55290 C -2.22131 -0.73722 -1.74990 C -3.15924 0.26968
-2.02771 C -1.91577 -1.63514 -2.78232 C -3.77357 0.36872 -3.27414 H -3.40053 1.00397 -
1.26417 C -2.52020 -1.54203 -4.03461 H -1.19122 -2.42606 -2.60909 C -3.45606 -0.53950 -

4.28167 H -4.49051 1.16288 -3.46153 H -2.26221 -2.25148 -4.81601 H -3.93025 -0.46325 -
5.25594 C -2.77463 -1.68655 1.10659 C -4.11854 -1.84748 0.72621 C -2.39832 -2.16870 2.37467
C -5.04219 -2.46119 1.56958 H -4.44308 -1.49781 -0.25004 C -3.31532 -2.78831 3.22074 H
-1.36965 -2.04972 2.70755 C -4.64087 -2.93574 2.81705 H -6.07402 -2.57561 1.25049 H -
2.99789 -3.14980 4.19455 H -5.35939 -3.41808 3.47323 Al 2.50588 1.09819 -1.93497 Al -0.05051
-3.66798 -0.02784 Al -2.49176 1.10037 1.95972 C 2.26433 0.82695 -3.86798 C 4.12249 2.04791
-1.33416 C -2.24757 0.83463 3.89353 C -4.11158 2.05090 1.36792 C -1.68968 -4.63752 -0.50546
C 1.54156 -4.70416 0.46811 H 1.82256 -5.37154 -0.35734 H 1.32042 -5.35509 1.32497 H 2.42306
-4.10860 0.72035 H -2.42972 -4.05122 -1.05765 H -2.18556 -4.99853 0.40558 H -1.44789 -
5.52681 -1.10172 H -4.57362 2.59866 2.19831 H -3.90782 2.76933 0.56474 H -4.87059 1.35449
0.98847 H -3.15169 0.38253 4.32089 H -1.39812 0.20160 4.16875 H -2.11379 1.80364 4.39301
H 4.58649 2.60362 -2.15807 H 4.88107 1.34852 -0.95910 H 3.91603 2.75785 -0.52423 H 1.40097
0.21173 -4.14037 H 3.15828 0.35020 -4.28983 H 2.15518 1.79536 -4.37450

1,3,5 tris(PbCl)2,2,4,4,6,6-hexaphaphenylcyclotrisilazane

Boat conformation

mPW1PW91/SDD

HF=-3813.3239727

Pb -0.68848 -0.12322 -3.51111 Pb -0.57255 -1.43590 3.13067 Pb 4.32156 1.32289 0.41386
Si 1.96856 -0.60671 -1.41610 Si -0.91010 -0.99176 -0.23038 Cl -1.90276 0.49173 4.28147 Cl
5.74374 0.18958 -1.39865 Cl -0.39801 -2.42288 -4.70914 Si 1.13499 0.82863 1.21526 N 2.38041
0.43224 -0.01431 N -0.15738 -0.36465 1.23787 N 0.20427 -0.70908 -1.55600 C 1.10477 3.53041
0.12437 C -0.52929 3.08165 1.85162 C 0.52656 2.62109 1.03217 C -0.98026 4.40677 1.76725 C
1.98732 0.65477 2.92385 C -1.38910 -2.77406 0.26417 C -2.58210 -2.98182 1.00061 C -0.88354
-5.15389 0.52950 C -0.54781 -3.88350 0.03848 C -2.53510 -0.17619 -0.81096 C -3.36843 -
0.86425 -1.72759 C -2.89673 1.13536 -0.44002 C -4.04650 1.74242 -0.96643 C 0.65694 4.85777
0.03516 C -0.38748 5.29940 0.85996 C -2.91562 -4.25199 1.50302 C 2.61290 1.46717 5.14914 C
1.99680 1.66848 3.90456 C -2.06363 -5.34053 1.26775 C -4.51574 -0.25478 -2.26431 C 2.36306
-3.31599 -2.23127 C 3.69763 -2.68729 -0.31535 C -4.85493 1.05173 -1.88373 C 2.75271 -2.33124
-1.29502 C 3.22920 0.24136 5.44372 C 2.90876 -4.60721 -2.18807 C 1.99249 1.55139 -3.32005
C 3.84990 -4.94298 -1.20251 C 4.24198 -3.97898 -0.26226 C 3.27326 -0.37734 -4.02969 C
2.46885 0.24283 -3.05249 C 3.58521 0.27637 -5.22984 C 2.62022 -0.57651 3.23914 C 3.23256
-0.78419 4.48611 C 2.30530 2.21176 -4.52076 C 3.10185 1.57026 -5.47964 H 2.60448 2.26041
5.88919 H 1.51564 2.61869 3.69792 H 3.70124 0.08711 6.40839 H 3.71083 -1.73363 4.70443
H 2.65865 -1.36571 2.49029 H 1.90332 3.19813 -0.53447 H 1.11658 5.53956 -0.67361 H -
0.73721 6.32486 0.79532 H -1.79066 4.73913 2.40812 H -1.00906 2.40299 2.55360 H 1.93592
3.21656 -4.70011 H 3.34901 2.07406 -6.40839 H 4.20862 -0.21987 -5.96594 H 3.67007 -1.36946
-3.84598 H 1.40708 2.07431 -2.56603 H 1.61813 -3.08592 -2.98960 H 4.02327 -1.94946 0.41155
H 4.97490 -4.22786 0.49883 H 4.27466 -5.94147 -1.17006 H 2.59776 -5.34471 -2.92105 H
-3.14489 -1.89552 -1.99502 H -5.14124 -0.80114 -2.96271 H -5.74374 1.52371 -2.28979 H -
4.31229 2.74926 -0.66072 H -2.28187 1.68014 0.26879 H -3.83758 -4.38911 2.05881 H -3.27961
-2.15839 1.14430 H -2.32009 -6.32486 1.64581 H -0.22740 -5.99581 0.33372 H 0.36763 -3.75822
-0.53003

Chair conformation

mPW1PW91/SDD
HF=-3813.3184357

Pb -0.46655 -0.57062 0.05947 Pb 0.30873 -0.58804 6.19203 Pb 5.22481 -0.60518 2.44455 Si
2.73812 -2.05469 4.36401 Si 2.41897 -2.05303 1.24969 Si -0.11861 -2.04067 3.08226 N 3.35072
-1.71950 2.73075 N 0.70175 -1.70615 1.53720 N 0.99157 -1.71226 4.42905 C 2.82942 -3.79137
0.60995 C 2.27550 -4.29719 -0.58695 C 3.71843 -4.61236 1.33417 C 4.04786 -5.89824 0.87990
C 4.21235 1.59979 5.85648 C 3.58697 -0.75125 5.48315 C 3.57601 0.61118 5.08931 C 4.24669 -
1.08150 6.68403 C -0.89082 -3.77273 3.03733 C -1.28901 -5.86597 1.83076 C -0.72265 -4.58400
1.89604 C -1.64609 -4.28315 4.11632 C -1.15069 0.63284 3.43701 C -1.50438 -0.72853 3.25527
C -2.12801 1.62711 3.60180 C -3.48718 1.27783 3.57937 C -3.85782 -0.06128 3.38862 C -
2.87599 -1.05206 3.22960 C 4.61181 -5.58616 5.69093 C 3.07780 -3.79174 5.04702 C 4.38852
-4.30349 5.17119 C 2.00094 -4.60580 5.45552 C 2.99743 1.60053 -0.76971 C 2.97111 -0.75141
-0.04395 C 2.64728 0.61354 0.16538 C 3.67347 -1.08601 -1.21918 C 2.60639 -5.58021 -1.04475
C 4.88003 -0.09632 7.45816 C 3.49377 -6.38457 -0.31240 C 4.86866 1.24380 7.04491 C 3.69052
1.24015 -1.93569 C 4.03105 -0.10260 -2.15507 C -2.21592 -5.56241 4.05164 C -2.03840 -6.35781
2.90853 C 2.22208 -5.89106 5.97281 C 3.52890 -6.38386 6.09321 H 1.58181 -3.69406 -1.16668
H 4.14748 -4.25066 2.26255 H 4.72675 -6.51570 1.45915 H 4.19160 2.63663 5.53550 H 3.03629
0.90288 4.18897 H 4.28388 -2.11746 7.00548 H -1.13791 -6.47624 0.94621 H -0.13917 -4.21721
1.05809 H -1.79172 -3.68633 5.01279 H -0.09972 0.91930 3.41811 H -1.83426 2.66300 3.74015
H -4.24782 2.04035 3.71057 H -4.90730 -0.33606 3.37709 H -3.17841 -2.08716 3.10664 H
5.62711 -5.95994 5.77919 H 5.24134 -3.70583 4.86065 H 0.98432 -4.23875 5.36064 H 2.73905
2.63928 -0.58883 H 2.14440 0.90870 1.08575 H 3.92412 -2.12378 -1.41440 H 2.17116 -5.94915
-1.96821 H 5.39148 -0.37627 8.37309 H 3.74677 -7.37951 -0.66563 H 5.36608 2.00200 7.64065
H 3.96067 1.99692 -2.66474 H 4.56151 -0.38585 -3.05807 H -2.79427 -5.93527 4.89119 H -
2.47680 -7.34988 2.86060 H 1.37720 -6.50296 6.27185 H 3.70237 -7.37841 6.49253 Cl 6.87125
-1.94225 3.94127 Cl -0.01409 -1.91644 -2.11474 Cl -1.81251 -1.91763 6.87968

1,3,5 tris(SnCl)2,2,4,4,6,6-hexaphenylcyclotrisilazane

mPW1PW91/SDD
HF=-3813.136873

C 0.00000 0.00000 0.00000 H 1.09347 0.00000 0.00000 C -0.15058 4.10571 0.00000 C -1.47587
4.37347 0.42548 H -2.27956 3.68286 0.17475 C -2.40067 3.60872 -6.28872 H -2.92000 2.65343 -
6.32347 C -1.07608 6.07090 -6.26516 H -0.54570 7.02308 -6.26020 C -1.30718 3.77252 -5.41831
C -0.64529 5.02417 -5.43678 H 0.26017 5.16576 -4.84379 Sn -1.59858 5.26871 -2.50937 Sn
3.45776 1.59372 -0.42663 Sn 1.78021 1.27906 -6.41279 Si 0.10822 2.65654 -1.22470 Si 2.21195
2.42053 -3.36344 Cl 2.70268 2.32572 1.83896 Si -0.71615 2.43617 -4.19160 Cl -4.04044 4.54162
-2.40289 C 3.73527 5.81955 -5.34966 N 0.96109 1.95182 -4.50557 N -0.69509 3.24353 -2.64913
C -3.65244 -1.25836 -4.24805 H -4.33840 -2.10612 -4.25368 C -2.27707 -1.46775 -4.37076
H -1.88616 -2.47933 -4.46769 C -0.65131 -1.11427 0.53549 H -0.07101 -1.94259 0.94095 C
-2.04843 -1.15892 0.55394 H -2.56384 -2.02358 0.97162 C -2.17563 5.88322 -7.10287 H -
2.51787 6.69203 -7.74715 C -2.83044 4.64693 -7.11781 H -3.68162 4.49162 -7.77997 C 0.84555
5.00965 0.41020 H 1.88169 4.83718 0.12504 C -1.78840 5.49903 1.19935 H -2.81922 5.67552
1.50093 C 0.54099 6.13182 1.18421 H 1.33598 6.81329 1.48509 C -0.77827 6.38486 1.57595 H
-1.01415 7.26272 2.17731 C -0.70803 1.08906 -0.53256 C -1.87095 0.94002 -4.24444 N 1.79225

2.31872 -1.65222 C -2.11534 1.01011 -0.51860 H -2.70774 1.80807 -0.96575 C -3.26176 1.12777
-4.10554 H -3.66621 2.13015 -3.96471 C -1.40164 -0.37892 -4.36881 H -0.33141 -0.56382 -
4.45871 C -4.14316 0.04390 -4.11095 H -5.21362 0.21707 -4.00407 C -2.77811 -0.09271 0.02413
H -3.86692 -0.12406 0.01856 Cl -0.30569 0.81516 -7.68574 H 3.94934 6.09931 -6.38013 C
2.90387 4.15817 -3.74875 C 3.69820 6.35198 -2.99525 H 3.87660 7.05109 -2.17922 C 4.96036
1.52222 -3.89820 H 5.22562 2.57704 -3.97666 C 3.62538 1.15942 -3.64140 C 3.16870 5.08587
-2.72400 H 2.93408 4.82101 -1.69485 C 3.20279 4.56147 -5.06499 H 3.00934 3.88717 -5.90284
C 5.64015 -0.80329 -3.95889 H 6.41615 -1.55765 -4.08081 C 5.95898 0.55277 -4.05472 H
6.98468 0.85856 -4.25177 C 3.32721 -0.22154 -3.55102 H 2.30333 -0.53741 -3.34454 C 3.98450
6.72245 -4.31024 H 4.39202 7.70932 -4.52766 C 4.31911 -1.19133 -3.70750 H 4.06497 -2.24798
-3.63213

Cyclotrisilazane

mPW1PW91/6-31+G*

HF=-1038.2427437

Si 0.00000 0.00000 0.00000 N 1.74514 0.00000 0.00000 N -0.61901 1.63164 0.00000 Si 0.02341
2.81192 -1.09606 Si 2.62073 1.01744 -1.09804 N 1.40613 2.03712 -1.82175 H -0.49322 -0.71492
-1.20208 H -0.46952 -0.67982 1.23504 H -1.12434 1.94762 0.81822 H 2.22055 -0.36162 0.81724
H 3.67782 1.73698 -0.33216 H 3.28668 0.31487 -2.22950 H 1.50202 2.17705 -2.82089 H -
0.86932 3.18893 -2.22661 H 0.32388 4.05356 -0.32808

1,3,5-trimethylcyclotrisilazane

mPW1PW91/6-31+G*

HF=-1156.1169954

Si 0.00000 0.00000 0.00000 N 1.74311 0.00000 0.00000 N -0.61292 1.63375 0.00000 Si -0.04124
2.70411 -1.23660 Si 2.54186 1.01449 -1.15755 N 1.28320 1.87251 -2.01389 H -0.53123 -0.75251
-1.16675 H -0.44616 -0.65038 1.26229 H 3.50994 1.88433 -0.42356 H 3.31783 0.27334 -2.19279
H -1.02122 3.00829 -2.31919 H 0.30909 4.00241 -0.58568 C 2.53451 -0.68776 1.01719 C 1.46970
2.09275 -3.45521 C -1.47382 2.14596 1.06440 H 3.02528 -1.58452 0.61775 H 3.31371 -0.03115
1.42556 H 1.90309 -1.00232 1.85396 H 2.00769 1.25361 -3.90617 H 2.03709 3.00787 -3.66842
H 0.50173 2.17390 -3.95945 H -1.38648 1.53269 1.96677 H -2.53097 2.15553 0.76979 H -
1.19251 3.17053 1.33758

Hexamethylcyclotrisilazane

boat conformation

mPW1PW91/6-31+G*

HF=-1274.1759801

Si -1.30225 0.77595 -0.92713 N -1.29704 0.73594 0.82270 N 0.34557 0.70038 -1.51248 Si
1.55134 -0.36334 -0.84892 Si -0.27704 -0.32039 1.75519 N 0.80347 -1.03374 0.58132 H 0.66374
1.47904 -2.07660 H -1.71413 1.52767 1.29703 H 1.00276 -2.01563 0.73756 C -2.28162 -0.68231
-1.59404 C -2.06359 2.40161 -1.48757 C 0.58772 0.68638 3.09202 C -1.20192 -1.73632 2.58241
C 1.98915 -1.81146 -1.96952 C 3.11985 0.62407 -0.51251 H -3.09829 2.49385 -1.13894 H -
2.08291 2.47218 -2.58086 H -1.50226 3.26129 -1.10514 H -1.83497 -1.62699 -1.26493 H -

2.29450 -0.68565 -2.68949 H -3.31700 -0.66310 -1.23654 H -1.91968 -1.35278 3.31636 H -
1.76312 -2.32242 1.84713 H -0.52388 -2.41434 3.11474 H 1.23832 0.05171 3.70422 H 1.20662
1.47678 2.65459 H -0.13385 1.16212 3.76748 H 2.70823 -2.49247 -1.49834 H 2.44182 -1.45594
-2.90206 H 1.09644 -2.38757 -2.23454 H 2.93306 1.43324 0.20128 H 3.51734 1.07343 -1.43083
H 3.90601 -0.01539 -0.09550

twist conformation

HF=-1274.1740566 Si 0.00000 0.00000 0.00000 Si 3.08177 0.00000 0.00000 Si 1.55876 2.63492
0.00000 N 1.53722 -0.51758 -0.57243 N 3.01020 1.71537 0.08903 N 0.27764 1.60990 0.52775
C -0.64160 -0.99964 1.43375 H -0.71710 -1.94082 1.16948 H -1.52283 -0.66285 1.69897 H
-0.02267 -0.92198 2.19002 C -1.22536 -0.11955 -1.39773 H -0.89699 0.39264 -2.16515 H -
2.08781 0.24311 -1.10769 H -1.33671 -1.05877 -1.65500 C 4.40638 -0.56693 -1.16715 H 4.15972
-0.32259 -2.08398 H 4.50390 -1.53927 -1.10342 H 5.25529 -0.13730 -0.93163 C 3.40034 -
0.71626 1.68832 H 4.25894 -0.38685 2.02567 H 3.42546 -1.69378 1.62877 H 2.68421 -0.44417
2.29863 C 1.64764 4.13391 1.09135 H 1.73599 3.85292 2.02566 H 0.82970 4.66365 0.98460 H
2.42350 4.67635 0.83850 C 1.24356 3.15954 -1.75833 H 2.02139 3.64959 -2.09703 H 0.45428
3.73933 -1.78951 H 1.09025 2.36734 -2.31387 H -0.11586 1.86411 1.09652 H 3.63137 2.05079
0.19084 H 1.57615 -0.97211 -1.18374

Nonamethylcyclotrisilazane

mPW1PW91/6-31+G*

HF=-1392.0407483

Si -1.30166 0.52560 -1.03515 N -1.37410 0.69675 0.70504 N 0.38130 0.56451 -1.52507 Si
1.58092 -0.39406 -0.70594 Si -0.31910 -0.20897 1.75353 N 0.78219 -1.07705 0.70038 C -2.19270
1.74075 1.31904 C 1.38943 -2.29430 1.25200 C 0.77185 1.23472 -2.76317 H -2.44086 1.48905
2.35725 H -1.69314 2.71967 1.33244 H -3.14788 1.86212 0.79828 H 0.67457 -2.84359 1.87128
H 2.27343 -2.08773 1.87370 H 1.70052 -2.97446 0.45358 H 0.40603 2.26706 -2.79721 H 0.40248
0.71784 -3.66081 H 1.86281 1.28803 -2.85388 C -1.29907 -1.43673 2.79667 C 2.21106 -1.78731
-1.81207 C 3.07083 0.66625 -0.23944 C 0.57004 0.95952 2.93988 H 1.31541 0.41482 3.53134
H 1.09152 1.75566 2.39818 H -0.11962 1.43404 3.64756 H -2.14551 -0.91619 3.26011 H -
1.71247 -2.24541 2.18465 H -0.71384 -1.88003 3.60959 H 3.09532 -2.29170 -1.40746 H 1.43702
-2.54015 -1.99577 H 2.49898 -1.37244 -2.78549 H 2.76745 1.54023 0.34580 H 3.62182 1.02545
-1.11619 H 3.77689 0.08620 0.36672 C -2.12236 -1.07973 -1.57947 H -1.64134 -1.93998 -
1.10263 H -2.05189 -1.21623 -2.66518 H -3.18395 -1.09643 -1.30666 C -2.20466 1.96539 -
1.84663 H -3.27129 1.94802 -1.59850 H -2.13260 1.90176 -2.93794 H -1.80441 2.93755 -1.54021

Chloro-germanium(II) N-(diisopropyl)(2-pyridylmethyl)amide

closed conformation

mPW1PW91/SDD

HF=-1273.0600873

N -0.06544 -0.02168 0.01988 N -0.06224 -0.02340 2.59893 C 3.22026 -0.06076 -2.35273 H
3.28850 -0.01461 -3.44596 H 4.14483 -0.50647 -1.97153 H 3.16240 0.96336 -1.97163 C 0.44002
-0.05552 -3.70027 H 1.18557 -0.36107 -4.42822 C 2.00463 -0.89091 -1.89499 H 2.02966 -
0.90820 -0.80149 C -0.28980 0.15426 -1.39026 C -3.95430 0.58724 -1.15466 H -4.67829 0.86377
-0.37933 H -3.90402 -0.50588 -1.20325 H -4.34565 0.94514 -2.11341 C -2.65936 2.73793 -

0.78639 H -1.69360 3.17567 -0.51283 H -3.40351 3.05875 -0.04795 H -2.94922 3.15023 -1.75953
C -1.71185 0.93207 -3.20585 H -2.63270 1.39172 -3.55239 C -1.50594 0.74604 -1.82827 C
0.69247 -0.25248 -2.33159 C 2.11660 -2.34348 -2.40352 H 2.14755 -2.38111 -3.49864 H 1.26430
-2.94935 -2.07549 H 3.03396 -2.80821 -2.02533 C -2.57435 1.19809 -0.84095 H -2.26656 0.84920
0.15037 C -0.74941 0.53354 -4.13883 H -0.92444 0.68359 -5.19948 C -0.54919 -0.75780 4.82401
H -0.54840 -0.55689 5.88736 C -0.39039 -1.32328 0.58647 H 0.37356 -2.09018 0.36412 H -
1.33869 -1.70179 0.17751 C -0.50036 -1.19728 2.08296 C -0.98500 -2.20399 2.92972 H -1.32716
-3.14083 2.50707 C -1.01385 -1.98065 4.30957 H -1.38801 -2.74699 4.97868 C -0.07089 0.20061
3.93335 H 0.32124 1.15229 4.26841 Cl 2.90282 0.17748 1.65517 Ge 0.78403 1.29099 1.11815

open conformation

HF=-1273.0342053

N -0.48863 0.68762 -0.50872 N 0.13202 -0.62855 2.59511 C 3.17313 0.32050 -1.93313 H 3.59015
-0.50292 -2.52345 H 4.00705 0.93341 -1.57297 H 2.56464 0.93363 -2.60826 C 1.40317 -2.28037
-1.84374 H 2.42669 -2.62270 -1.95812 C 2.34312 -0.21281 -0.74640 H 1.95413 0.64663 -0.19287
C -0.18890 -0.60835 -1.09800 C -3.56636 -1.95671 -0.65211 H -4.58856 -1.57896 -0.53862
H -3.14285 -2.10898 0.34578 H -3.62541 -2.93503 -1.14133 C -3.32444 -0.76824 -2.88303 H
-2.74612 -0.04398 -3.46733 H -4.35424 -0.40181 -2.80626 H -3.34344 -1.70830 -3.44477 C
-0.96441 -2.64982 -2.16013 H -1.77279 -3.27568 -2.52509 C -1.26254 -1.41331 -1.56709 C
1.15679 -1.03912 -1.22979 C 3.23635 -1.01081 0.22397 H 3.73077 -1.84877 -0.27959 H 2.65013
-1.41257 1.05475 H 4.01860 -0.36319 0.63520 C -2.71831 -0.96766 -1.47800 H -2.75228 0.00161
-0.97223 C 0.35721 -3.08421 -2.30033 H 0.56902 -4.04135 -2.76552 C 1.91868 0.24786 3.97347
H 2.62911 0.08322 4.77510 C -1.00556 0.68880 0.88193 H -1.68673 -0.15698 1.00809 H -
1.55878 1.62014 1.03152 C 0.06068 0.56118 1.95143 C 0.89877 1.64208 2.28481 H 0.79074
2.58626 1.76294 C 1.83975 1.48156 3.30864 H 2.49003 2.30281 3.59007 C 1.04363 -0.77409
3.58294 H 1.06194 -1.74193 4.07292 Ge -0.30149 2.10120 -1.70382 Cl -0.88605 3.86176 -
0.23765

Chloro-tin(II) N-(diisopropyl)(2-pyridylmethyl)amide

closed conformation

mPW1PW91/SDD

HF=-1272.6434056

Sn 0.00809 -0.43672 0.05955 N 0.02795 0.20194 2.04083 N 2.24870 -0.06836 0.58706 C -
2.83256 -2.52470 2.47410 H -3.81340 -2.44321 2.95694 H -2.58556 -3.58642 2.37241 H -2.92060
-2.10423 1.46637 C -3.15591 0.16541 4.03376 H -3.83563 -0.54944 4.48810 C -1.74381 -1.79926
3.29082 H -0.79535 -1.95131 2.76698 C -1.13361 0.64221 2.76489 C 0.00601 4.11463 3.24628
H 0.72157 4.79953 2.77639 H 0.49923 3.63438 4.09839 H -0.82019 4.71801 3.63857 C -1.18158
3.76395 1.03236 H -1.49686 3.03200 0.28106 H -0.50282 4.47884 0.55245 H -2.07329 4.31156
1.35772 C -2.56206 2.45705 3.54142 H -2.78399 3.51805 3.61225 C -1.40689 2.03509 2.86212
C -2.01064 -0.30126 3.36478 C -1.61345 -2.42505 4.69424 H -2.55246 -2.35407 5.25516 H -
0.83540 -1.92557 5.28192 H -1.35226 -3.48575 4.61099 C -0.49000 3.07155 2.22529 H 0.38094
2.53555 1.83431 C -3.43473 1.53214 4.12384 H -4.32491 1.87430 4.64215 C 4.60619 0.00003
0.14527 H 5.41488 -0.03516 -0.57312 C 1.25369 0.05939 2.81544 H 1.28086 -0.87947 3.40027
H 1.34932 0.87609 3.54701 C 2.46708 0.06594 1.91838 C 3.77695 0.17231 2.41234 H 3.93729
0.27328 3.47908 C 4.85283 0.14357 1.52160 H 5.86918 0.22800 1.88906 C 3.28577 -0.10946

-0.28388 H 3.03692 -0.24114 -1.32954 Cl 0.68317 -2.89157 0.45694

open conformation

HF=-1272.6143236

N -0.47936 0.72672 -0.55073 N 0.05167 -0.65186 2.52476 C 3.18986 0.32647 -1.96237 H 3.60852
-0.51108 -2.53116 H 4.02299 0.94729 -1.61374 H 2.58678 0.92258 -2.65885 C 1.41648 -2.26489
-1.82579 H 2.44170 -2.60401 -1.93594 C 2.35251 -0.17801 -0.76818 H 1.96264 0.69267 -0.23271
C -0.18215 -0.58047 -1.10600 C -3.52884 -1.92189 -0.56772 H -4.55409 -1.55191 -0.45445
H -3.08241 -2.01308 0.42749 H -3.58211 -2.92661 -1.00107 C -3.34915 -0.85952 -2.86537 H
-2.79170 -0.16668 -3.50582 H -4.38059 -0.49794 -2.78593 H -3.37333 -1.83080 -3.37094 C
-0.94864 -2.65408 -2.12168 H -1.75645 -3.29232 -2.46639 C -1.25094 -1.40631 -1.55448 C
1.16529 -1.01295 -1.23605 C 3.24264 -0.95500 0.22222 H 3.72707 -1.81213 -0.25836 H 2.65603
-1.32670 1.06652 H 4.03217 -0.30279 0.61205 C -2.70969 -0.97122 -1.46558 H -2.74264 0.02534
-1.01526 C 0.37419 -3.08515 -2.26040 H 0.58907 -4.05108 -2.70558 C 1.85404 0.11570 3.94732
H 2.54824 -0.09904 4.75137 C -1.01116 0.75722 0.83431 H -1.75066 -0.03967 0.95723 H -
1.50205 1.72308 0.98460 C 0.03253 0.55787 1.91520 C 0.90643 1.59612 2.29046 H 0.83782
2.55928 1.79691 C 1.82887 1.37065 3.31897 H 2.50520 2.15856 3.63268 C 0.94598 -0.86060
3.51709 H 0.92212 -1.84224 3.97868 Cl -0.79890 4.06846 -0.16468 Sn -0.25758 2.28506 -
1.85230

Chloro-lead(II) N-(diisopropyl)(2-pyridylmethyl)amide

closed conformation

mPW1PW91/SDD

HF=-1272.6892502

N -0.02667 0.08109 0.01122 N -0.00624 0.00172 2.73568 C 3.21321 -0.04860 -2.38182 H 3.28051
-0.01964 -3.47572 H 4.14131 -0.47924 -1.99227 H 3.14815 0.98418 -2.02285 C 0.41163 -0.09999
-3.71835 H 1.14607 -0.43064 -4.44690 C 2.00264 -0.88096 -1.91338 H 2.02913 -0.89636 -
0.81968 C -0.27844 0.19151 -1.39883 C -3.92201 0.54703 -1.08605 H -4.64194 0.85619 -0.31913
H -3.82367 -0.54308 -1.04493 H -4.34650 0.80504 -2.06266 C -2.72239 2.77365 -0.91464 H
-1.77004 3.27772 -0.71613 H -3.45281 3.11463 -0.17133 H -3.06944 3.09953 -1.90171 C -
1.73556 0.89426 -3.22533 H -2.66597 1.33540 -3.57166 C -1.50514 0.76057 -1.84570 C 0.68490
-0.25108 -2.34771 C 2.12345 -2.33609 -2.41137 H 2.15154 -2.38316 -3.50614 H 1.27630 -
2.94370 -2.07444 H 3.04477 -2.79108 -2.03116 C -2.56329 1.24000 -0.86011 H -2.20796 0.97734
0.14166 C -0.78653 0.46894 -4.16028 H -0.97925 0.57973 -5.22272 C -0.58481 -0.88568 4.89293
H -0.59603 -0.76796 5.96887 C -0.39007 -1.19164 0.61800 H 0.33580 -1.99779 0.39421 H -
1.35736 -1.54630 0.22633 C -0.49597 -1.10285 2.12210 C -1.05313 -2.14568 2.88287 H -1.43616
-3.02503 2.37860 C -1.10213 -2.03690 4.27401 H -1.53160 -2.83370 4.87055 C -0.03940 0.11023
4.08597 H 0.38914 1.00916 4.51169 Cl 3.22347 0.01979 1.72557 Pb 1.11830 1.51856 1.17973

open conformation

HF=-1272.6669934

N 0.02886 0.01275 -0.04932 N -0.01583 -0.04469 3.34796 C 3.92449 0.01229 -0.49401 H 4.58810
-0.84603 -0.64702 H 4.54647 0.88161 -0.25160 H 3.42486 0.20712 -1.45208 C 2.57610 -2.73905
0.27874 H 3.63266 -2.86036 0.49647 C 2.91124 -0.26529 0.63654 H 2.27242 0.61595 0.74718

C 0.62862 -1.30348 0.00613 C -2.52242 -3.09957 0.38478 H -3.58502 -2.95463 0.15940 H -2.33462 -2.74891 1.40442 H -2.31948 -4.17598 0.36160 C -1.92320 -2.85028 -2.06824 H -1.32950 -2.30070 -2.80803 H -2.98273 -2.72605 -2.31914 H -1.67700 -3.91253 -2.17080 C 0.43953 -3.71534 -0.27904 H -0.15951 -4.59345 -0.50084 C -0.16571 -2.44899 -0.28703 C 2.01267 -1.45050 0.30028 C 3.64853 -0.46320 1.97591 H 4.36985 -1.28627 1.92291 H 2.94262 -0.68294 2.78107 H 4.20089 0.44533 2.24097 C -1.64647 -2.34511 -0.63678 H -1.93051 -1.28923 -0.60697 C 1.80156 -3.86619 -0.00187 H 2.25364 -4.85264 -0.00533 C 1.20464 1.58744 4.65568 H 1.70032 1.83751 5.58648 C -0.84219 0.40093 1.08836 H -1.46726 -0.44872 1.38204 H -1.48903 1.21674 0.75150 C -0.09441 0.84625 2.32999 C 0.45916 2.13771 2.42491 H 0.35066 2.82864 1.59592 C 1.11681 2.51169 3.60264 H 1.54158 3.50480 3.70307 C 0.62249 0.32510 4.48109 H 0.65806 -0.41913 5.26999 Cl -0.90448 3.22297 -1.05753 Pb 0.34527 1.10908 -1.84938

Bis(TMS)amidogermanium(II) N-(diisopropyl)(2-pyridylmethyl)amide

closed conformation

mPW1PW91/SDD

HF=-1686.0012293

Si -3.21424 -0.29840 -1.36221 Si -3.04849 -0.27291 1.76290 N 0.77115 -0.30688 -1.02532 N -0.35082 2.04371 -0.95408 C -0.41613 -4.28317 -0.84671 H 0.20865 -5.18339 -0.83133 H -1.36878 -4.55435 -1.31641 H -0.61608 -3.99418 0.18984 C 2.53839 -3.60232 -0.64245 H 2.36791 -4.65360 -0.85462 C 0.25503 -3.13441 -1.62272 H -0.42741 -2.27992 -1.62150 C 1.77169 -1.28694 -0.69186 C 4.52408 1.11270 -0.43828 H 4.66682 2.17632 -0.21426 H 4.43754 0.99857 -1.52468 H 5.42958 0.58203 -0.12368 C 3.42699 0.74054 1.81705 H 2.52475 0.39975 2.33351 H 3.59128 1.79457 2.07091 H 4.27711 0.16564 2.20111 C 3.96207 -1.85650 0.22603 H 4.89361 -1.55381 0.69586 C 2.99318 -0.88470 -0.07518 C 1.54273 -2.66309 -0.96283 C 0.50909 -3.54550 -3.08867 H 1.19462 -4.39935 -3.14308 H 0.95563 -2.72374 -3.65896 H -0.42880 -3.83297 -3.57833 C 3.27821 0.56838 0.29127 H 2.41421 1.16730 -0.01500 C 3.74470 -3.20778 -0.05785 H 4.50401 -3.94569 0.18110 C -0.92852 4.26261 -1.65066 H -1.46528 5.18339 -1.46163 C 1.06321 0.51269 -2.19142 H 0.72521 0.06443 -3.14362 H 2.14946 0.66255 -2.30718 C 0.40638 1.86229 -2.06083 C 0.52536 2.88650 -3.01432 H 1.12750 2.72484 -3.90054 C -0.14079 4.09670 -2.80459 H -0.05644 4.89981 -3.52800 C -1.01292 3.20590 -0.74636 H -1.61348 3.25995 0.15300 C -4.61973 0.98370 -1.55229 H -5.42958 0.82879 -0.83442 H -5.04791 0.92328 -2.56077 H -4.22936 1.99860 -1.41237 C -2.17902 -0.13312 -2.94919 H -1.86432 0.89822 -3.13439 H -2.80599 -0.44184 -3.79509 H -1.29706 -0.77685 -2.93083 C -3.96492 -2.05393 -1.42573 H -3.16659 -2.80395 -1.41778 H -4.54567 -2.18673 -2.34703 H -4.62775 -2.26348 -0.58061 C -4.95602 -0.24982 1.71179 H -5.33397 0.74401 1.45118 H -5.32343 -0.49056 2.71742 H -5.39152 -0.97623 1.02019 C -2.49590 -1.92941 2.52194 H -2.78692 -2.76578 1.87666 H -2.94622 -2.08504 3.50971 H -1.40633 -1.95600 2.63752 C -2.57337 1.13457 2.96126 H -1.50520 1.13205 3.19601 H -3.13003 1.02520 3.90054 H -2.82981 2.11117 2.53311 N -2.28352 -0.03844 0.14252 Ge -0.37361 0.35668 0.43225

open conformation

HF=-1685.9928882

Si -3.25825 -0.41917 -1.39660 Si -3.24708 -0.41409 1.74734 N 0.53161 -0.37307 0.00334 N 0.11372 1.67711 -2.44916 C 1.51487 -2.99960 -2.64316 H 2.43340 -3.59445 -2.70860 H 0.95847 -3.12793 -3.57877 H 0.91182 -3.40930 -1.82548 C 3.90629 -1.72775 -0.97620 H 4.40350 -

2.14391 -1.84657 C 1.84075 -1.50908 -2.40793 H 0.89687 -0.96082 -2.35189 C 1.91959 -0.78669
0.06857 C 2.66122 1.05281 3.16033 H 2.12531 1.41575 4.04468 H 2.70154 1.86665 2.42795 H
3.68961 0.82791 3.46348 C 1.90208 -1.31999 3.63313 H 1.38726 -2.20159 3.23675 H 1.36694
-0.98081 4.52752 H 2.90661 -1.63172 3.93948 C 3.97116 -1.08536 1.34938 H 4.51593 -1.00959
2.28581 C 2.62673 -0.68156 1.29866 C 2.56386 -1.32122 -1.08001 C 2.63526 -0.94209 -3.59989
H 3.55848 -1.50475 -3.77845 H 2.90287 0.10597 -3.43621 H 2.03272 -1.00287 -4.51315 C
1.96183 -0.19318 2.58046 H 0.93031 0.07818 2.34331 C 4.61348 -1.60357 0.22154 H 5.65073
-1.91765 0.27932 C 1.77796 2.99769 -3.60964 H 2.09616 3.47768 -4.52752 C 0.28989 1.08286
-0.07770 H 0.71809 1.58047 0.80394 H -0.79544 1.22164 -0.06053 C 0.85599 1.74758 -1.31559
C 2.08614 2.42907 -1.28401 H 2.66157 2.45583 -0.36589 C 2.55278 3.06273 -2.44334 H 3.49806
3.59445 -2.43624 C 0.56894 2.28865 -3.56312 H -0.06217 2.20917 -4.44224 C -3.46318 1.41811
-1.83525 H -3.98933 1.97495 -1.05394 H -4.03787 1.51831 -2.76485 H -2.47848 1.86869 -
1.99473 C -2.23195 -1.24216 -2.77015 H -1.28044 -0.71658 -2.89885 H -2.77546 -1.17547 -
3.72074 H -2.04054 -2.30508 -2.57984 C -4.98095 -1.23993 -1.37246 H -4.89966 -2.30857 -
1.14547 H -5.45698 -1.13787 -2.35549 H -5.65073 -0.78520 -0.63438 C -4.37826 1.11553 1.70397
H -3.80664 2.01921 1.46842 H -4.84194 1.25497 2.68812 H -5.18432 1.02021 0.96944 C -
4.27877 -1.93503 2.25043 H -5.07937 -2.12949 1.52965 H -4.73609 -1.79089 3.23684 H -3.64723
-2.82967 2.29855 C -1.93722 -0.13182 3.10046 H -1.30050 -1.01056 3.25766 H -2.42929 0.08656
4.05588 H -1.29453 0.71904 2.85126 N -2.42300 -0.66944 0.17610 Ge -0.79187 -1.71044 0.21246

Bis(TMS)amidotin(II) N-(diisopropyl)(2-pyridylmethyl)amide

closed conformation

mPW1PW91/SDD

HF=-1685.5797566

Sn 0.92084 -0.43022 -0.71560 Si 0.79021 2.44797 1.40749 Si 2.42998 2.36721 -1.25143 N
0.42117 -1.72481 0.90951 N -1.39594 -0.20239 -0.34424 C 3.95490 -0.99455 2.74653 H 4.71240
-1.71494 3.07564 H 4.10478 -0.07079 3.31726 H 4.13757 -0.77560 1.68939 C 3.08724 -3.93125
2.38477 H 3.87202 -3.87866 3.13392 C 2.52888 -1.53875 2.96267 H 1.82188 -0.78767 2.59965
C 1.25266 -2.86937 1.17258 C -1.01315 -5.30218 -0.36677 H -1.78931 -5.32586 -1.14066 H -
1.49851 -5.14318 0.60262 H -0.54052 -6.29029 -0.33892 C 0.68601 -4.44513 -2.04133 H 1.39217
-3.64389 -2.28045 H -0.07014 -4.48499 -2.83444 H 1.23493 -5.39327 -2.05219 C 1.88899 -
5.18303 0.70569 H 1.74964 -6.10175 0.14276 C 1.06693 -4.07686 0.43395 C 2.28182 -2.80250
2.15153 C 2.25582 -1.77029 4.46319 H 2.95038 -2.50627 4.88441 H 1.23821 -2.14072 4.62733
H 2.37611 -0.83629 5.02445 C 0.02185 -4.19914 -0.67061 H -0.50751 -3.24277 -0.73759 C
2.89325 -5.11933 1.67631 H 3.52120 -5.98279 1.87159 C -3.57024 0.70383 -0.81388 H -4.18920
1.36662 -1.40494 C -0.93017 -1.81275 1.43898 H -1.00519 -1.50478 2.49950 H -1.29795 -
2.85266 1.41562 C -1.89992 -0.95887 0.65990 C -3.27205 -0.91168 0.96269 H -3.65849 -1.51756
1.77387 C -4.11335 -0.08157 0.21933 H -5.17399 -0.03816 0.43973 C -2.20242 0.61719 -1.06261
H -1.72266 1.20756 -1.83368 C -0.19366 4.04186 1.02183 H 0.43865 4.84614 0.63665 H -
0.68229 4.40674 1.93409 H -0.97450 3.83595 0.28033 C -0.36358 1.41399 2.51067 H -1.36475
1.31636 2.07974 H -0.46812 1.92647 3.47506 H 0.04053 0.41734 2.70075 C 2.28677 2.89701
2.50687 H 2.78294 1.98373 2.85333 H 1.96127 3.46218 3.38903 H 3.03151 3.50047 1.97859 C
2.63391 4.24974 -1.01177 H 1.71467 4.78630 -1.26688 H 3.42017 4.59475 -1.69505 H 2.93043
4.53583 0.00134 C 4.16142 1.57959 -1.13100 H 4.56177 1.68542 -0.11643 H 4.86253 2.05527
-1.82755 H 4.12442 0.51012 -1.36899 C 1.79378 2.15936 -3.04053 H 1.80076 1.11390 -3.36538

H 2.42438 2.73126 -3.73268 H 0.76898 2.54004 -3.12808 N 1.30001 1.59492 -0.07674

open conformation

HF=-1685.5679687

Sn 0.00039 0.00020 -0.00032 Si 0.00008 -0.00016 3.35859 Si 2.76471 0.00062 1.85579 N -0.42321 2.00754 -0.31090 N -1.87812 3.50524 2.13900 C -3.83480 0.32580 -1.01346 H -4.41964 0.32443 -1.94060 H -4.46535 -0.07750 -0.21259 H -2.98756 -0.35444 -1.15885 C -2.98962 2.66452 -2.98737 H -4.06101 2.57530 -3.13764 C -3.36015 1.75268 -0.66432 H -2.78548 1.70370 0.26478 C -1.02947 2.40472 -1.56279 C 1.84583 4.37465 -2.70433 H 2.93199 4.40053 -2.56034 H 1.39066 5.07080 -1.99144 H 1.63430 4.74752 -3.71258 C 1.98294 1.97544 -3.50962 H 1.61881 0.95124 -3.37479 H 3.06998 1.97556 -3.36909 H 1.77749 2.26666 -4.54563 C -0.80985 3.25066 -3.84109 H -0.18722 3.60916 -4.65561 C -0.20944 2.87639 -2.62773 C -2.43588 2.29441 -1.74854 C -4.57275 2.66862 -0.41021 H -5.24414 2.70431 -1.27556 H -4.25623 3.69099 -0.18427 H -5.15315 2.29434 0.44068 C 1.30949 2.94144 -2.51259 H 1.58263 2.60915 -1.50740 C -2.19169 3.14989 -4.02577 H -2.63951 3.43663 -4.97187 C -3.23923 5.50675 2.09159 H -4.05228 6.07762 2.52432 C -0.02039 3.10993 0.58822 H 0.70393 3.76634 0.08352 H 0.47478 2.65422 1.45144 C -1.16732 3.96980 1.08059 C -1.46861 5.20512 0.47885 H -0.89038 5.54144 -0.37393 C -2.51546 5.98378 0.99001 H -2.75995 6.93972 0.53969 C -2.88555 4.25975 2.62694 H -3.41950 3.84948 3.47791 C 0.10440 1.54521 4.45972 H 1.13739 1.79501 4.72064 H -0.44831 1.38081 5.39346 H -0.34915 2.39649 3.94225 C -1.82253 -0.23319 2.85233 H -2.19752 0.66275 2.34454 H -2.43628 -0.37287 3.75092 H -1.98208 -1.11441 2.21771 C 0.53241 -1.51526 4.39028 H 0.48342 -2.43194 3.79247 H -0.13350 -1.63598 5.25361 H 1.55366 -1.41400 4.77502 C 3.56112 0.93083 3.31314 H 3.26991 1.98636 3.31149 H 4.65379 0.87904 3.23330 H 3.28055 0.50201 4.28110 C 3.33768 -1.81716 1.90520 H 3.00551 -2.31432 2.82227 H 4.43121 -1.88828 1.85680 H 2.92485 -2.37462 1.05621 C 3.42919 0.76147 0.23732 H 3.11628 0.20077 -0.65322 H 4.52594 0.75630 0.24568 H 3.10177 1.80055 0.12458 N 0.98299 0.13438 1.86568

Bis(TMS)amidolead(II) N-(diisopropyl)(2-pyridylmethyl)amide

closed conformation

mPW1PW91/SDD

HF=-1685.6164317

Si -3.37250 -0.45597 -1.29636 Si -3.37334 -0.45488 1.83502 N 0.96745 -0.45647 -1.08001 N -0.22190 2.01366 -0.93486 C -0.29767 -4.26090 -0.77612 H 0.29989 -5.16745 -0.62661 H -1.26742 -4.56419 -1.18733 H -0.47193 -3.80959 0.20650 C 2.75520 -3.76075 -0.93450 H 2.56073 -4.80674 -1.15446 C 0.40818 -3.27275 -1.72582 H -0.21963 -2.38174 -1.81461 C 1.99436 -1.43822 -0.87734 C 4.76651 0.95165 -0.79006 H 4.93550 2.00647 -0.54340 H 4.58209 0.87561 -1.86727 H 5.69269 0.40653 -0.57647 C 3.87003 0.51443 1.53853 H 3.02642 0.14204 2.12908 H 4.04416 1.56244 1.81019 H 4.75760 -0.05913 1.82735 C 4.25362 -2.03908 -0.15269 H 5.22172 -1.74849 0.24604 C 3.26902 -1.05795 -0.35454 C 1.74485 -2.81048 -1.16393 C 0.56831 -3.88792 -3.13108 H 1.17799 -4.79836 -3.10147 H 1.05313 -3.18434 -3.81621 H -0.41041 -4.15371 -3.54735 C 3.58728 0.38441 0.02703 H 2.70005 0.98895 -0.18832 C 4.00656 -3.38511 -0.43966 H 4.77740 -4.13097 -0.27383 C -0.75995 4.22974 -1.69915 H -1.27407 5.16745 -1.53048 C 1.15887 0.42437 -2.21915 H 0.75793 0.00442 -3.16304 H 2.23171 0.59089 -2.41789 C 0.51209 1.78054 -2.04845 C 0.63656 2.77653 -3.03556 H 1.22082 2.57067 -3.92500 C 0.00474 4.00854 -2.85911 H 0.09757 4.78460 -3.61053 C -0.85099 3.20223 -0.76279 H -1.43972 3.30940 0.14023

C -4.81644 0.77808 -1.52355 H -5.67272 0.54554 -0.88419 H -5.16110 0.76136 -2.56525 H -4.48472 1.79760 -1.29414 C -2.22536 -0.16348 -2.78456 H -1.98442 0.89698 -2.90935 H -2.73811 -0.49660 -3.69532 H -1.29474 -0.72861 -2.69380 C -4.05637 -2.22954 -1.49771 H -3.23383 -2.95348 -1.48678 H -4.58887 -2.33408 -2.45122 H -4.75040 -2.50072 -0.69541 C -5.27673 -0.52052 1.71968 H -5.69269 0.44482 1.41454 H -5.67655 -0.75623 2.71395 H -5.64114 -1.28643 1.02839 C -2.79709 -2.06002 2.69317 H -3.00483 -2.92790 2.05694 H -3.31116 -2.20644 3.65097 H -1.71872 -2.04284 2.89336 C -2.98081 1.00950 3.00090 H -1.92281 1.05084 3.28382 H -3.56608 0.92762 3.92500 H -3.24434 1.95840 2.51866 N -2.53937 -0.24542 0.26350 Pb -0.32400 0.11434 0.65991

open conformation

HF=-1685.6086032

Si -3.42876 -0.57060 -1.40619 Si -3.38237 -0.48224 1.74325 N 0.67335 -0.54053 -0.00913 N 0.11316 1.50604 -2.43103 C 1.82417 -3.08249 -2.70235 H 2.78213 -3.60859 -2.78688 H 1.27403 -3.22590 -3.63962 H 1.25844 -3.56368 -1.89558 C 4.11277 -1.71556 -0.98717 H 4.63025 -2.10402 -1.85902 C 2.04262 -1.57986 -2.42394 H 1.06288 -1.09899 -2.35193 C 2.07613 -0.87169 0.05760 C 2.72037 1.00757 3.14362 H 2.17191 1.33709 4.03351 H 2.70263 1.82220 2.41149 H 3.76416 0.84716 3.43581 C 2.10036 -1.40080 3.62889 H 1.64414 -2.31699 3.23800 H 1.54073 -1.09107 4.51901 H 3.12114 -1.64716 3.94151 C 4.14623 -1.07153 1.33808 H 4.68631 -0.96670 2.27467 C 2.78408 -0.73350 1.28733 C 2.75271 -1.37283 -1.09108 C 2.79422 -0.92604 -3.59927 H 3.76308 -1.40528 -3.77974 H 2.97151 0.13688 -3.41162 H 2.20519 -1.01678 -4.51901 C 2.09436 -0.27926 2.56908 H 1.04872 -0.06970 2.32789 C 4.81401 -1.55875 0.21066 H 5.86550 -1.82132 0.26809 C 1.69022 2.92731 -3.59539 H 1.97193 3.43198 -4.51202 C 0.34777 0.90013 -0.06513 H 0.75329 1.42259 0.81491 H -0.74358 0.98552 -0.03939 C 0.86030 1.61034 -1.30305 C 2.05171 2.35812 -1.27771 H 2.63274 2.40910 -0.36420 C 2.47191 3.02561 -2.43591 H 3.38656 3.60859 -2.43334 C 0.52291 2.15167 -3.54358 H -0.11189 2.04563 -4.41734 C -3.47364 1.26704 -1.89085 H -3.96559 1.88097 -1.12980 H -4.02103 1.39727 -2.83319 H -2.45206 1.63295 -2.03589 C -2.43701 -1.49213 -2.75083 H -1.42837 -1.07193 -2.84417 H -2.92712 -1.36290 -3.72361 H -2.37322 -2.57305 -2.56899 C -5.21757 -1.23896 -1.42387 H -5.24347 -2.29727 -1.14175 H -5.64929 -1.14233 -2.42772 H -5.86550 -0.68726 -0.73288 C -4.20170 1.23753 1.75924 H -3.48818 2.01558 1.46815 H -4.56783 1.47005 2.76670 H -5.05760 1.28894 1.07727 C -4.69374 -1.76728 2.26464 H -5.52239 -1.80168 1.54991 H -5.10701 -1.52564 3.25170 H -4.25692 -2.77147 2.31804 C -2.02397 -0.50007 3.08514 H -1.57903 -1.49488 3.22322 H -2.45252 -0.21143 4.05247 H -1.22267 0.20927 2.85161 N -2.64176 -0.86684 0.17065 Pb -0.80325 -2.11526 0.18907

Ge(II)bis[N-(2,6-diisopropylphenyl)(2-pyridylmethyl)imide]

mPW1PW91/SDD

HF=-812.2201943

Ge -0.01709 0.00111 -0.03287 N 0.00561 0.00041 1.88244 N 1.92299 0.00021 0.24113 C -1.75611 -1.23470 3.09005 C -1.18104 0.00065 2.70300 C -1.75494 1.23625 3.09100 C -3.51937 0.00116 4.24110 H -4.42913 0.00136 4.83272 C 1.25296 -0.00031 2.48104 H 1.34613 -0.00074 3.55832 C -2.93103 1.21086 3.86035 H -3.38971 2.14722 4.16283 C -2.93217 -1.20880 3.85941 H -3.39173 -2.14496 4.16117 C -1.14217 2.57516 2.69779 H -0.21583 2.37635 2.15039 C 2.32114 -0.00044 1.60101 C -0.77749 3.41564 3.93821 H -0.28962 4.34867 3.63462 H -0.09333 2.87119

4.59710 H -1.66720 3.67863 4.52107 C -1.14463 -2.57388 2.69575 H -0.21790 -2.37552 2.14884
C 3.72032 -0.00114 1.92278 H 4.00663 -0.00164 2.96867 C -0.78125 -3.41602 3.93542 H -
0.09683 -2.87293 4.59516 H -0.29416 -4.34919 3.63102 H -1.67144 -3.67879 4.51765 C 4.23549
-0.00048 -0.45256 H 4.96097 -0.00048 -1.25621 C 2.89789 0.00018 -0.74548 H 2.53715 0.00070
-1.76788 C 4.66081 -0.00116 0.92442 H 5.71870 -0.00168 1.16098 C -2.07950 3.36159 1.75858
H -3.02701 3.60309 2.25322 H -2.30880 2.78395 0.85705 H -1.61050 4.30316 1.45147 C -
2.08252 -3.35835 1.75544 H -3.03048 -3.59921 2.24952 H -1.61450 -4.30017 1.44761 H -2.31083
-2.77960 0.85437

Ge(II)bis[N-(2,6-diisopropylphenyl)(2-pyridylmethyl)amide]

mPW1PW91/SDD

HF=-1621.7857156

N 0.00000 0.00000 0.00000 N 2.65975 0.00000 0.00000 N 3.50659 2.92665 0.00000 N 1.19370
2.51130 1.24571 C -1.33080 0.08801 -0.21859 H -1.70383 1.05473 -0.53368 C -2.18164 -1.00475
-0.03853 H -3.24374 -0.90155 -0.22166 C -1.62484 -2.22315 0.38469 H -2.25535 -3.09401 0.52700
C -0.24857 -2.30125 0.62322 H 0.20906 -3.22578 0.95600 C 0.54735 -1.16110 0.42001 C 2.03536
-1.13323 0.66979 H 2.17879 -1.13506 1.76957 H 2.46682 -2.08086 0.31291 C 3.98067 -0.20190 -
0.50443 C 4.19434 -0.40417 -1.90086 C 5.50933 -0.53837 -2.38448 H 5.67178 -0.68575 -3.44885
C 6.60776 -0.51539 -1.52097 H 7.61441 -0.62948 -1.91116 C 6.39646 -0.36080 -0.14630 H
7.24957 -0.35673 0.52599 C 5.10349 -0.19666 0.37571 C 3.03761 -0.54561 -2.88522 H 2.10957
-0.42725 -2.31758 C 3.02516 -1.95193 -3.52097 H 3.91710 -2.12185 -4.13503 H 2.14655 -
2.07192 -4.16573 H 2.99602 -2.73179 -2.75251 C 3.05787 0.54215 -3.97660 H 3.98588 0.51142
-4.55974 H 2.95948 1.53814 -3.53269 H 2.22060 0.40387 -4.67063 C 4.90946 -0.04179 1.87795
H 3.88772 0.32683 2.02292 C 5.04731 -1.40468 2.59291 H 6.06490 -1.79666 2.47890 H 4.35885
-2.14787 2.17927 H 4.84185 -1.30409 3.66557 C 5.87869 0.97453 2.51033 H 6.91415 0.61631
2.48235 H 5.62032 1.14020 3.56314 H 5.84227 1.93696 1.99185 C 4.54784 3.18551 -0.82180 H
4.57344 2.63503 -1.75416 C 5.54310 4.10518 -0.48399 H 6.36489 4.28985 -1.16430 C 5.44771
4.77078 0.74950 H 6.19896 5.49694 1.04019 C 4.37471 4.48557 1.60064 H 4.27722 4.97861
2.56103 C 3.40893 3.54897 1.19472 C 2.22743 3.15392 2.04637 H 2.61791 2.51580 2.86517 H
1.83324 4.05713 2.53664 C -0.15972 2.75217 1.63339 C -0.72489 2.07837 2.75677 C -2.06814
2.30276 3.09814 H -2.49591 1.78875 3.95405 C -2.87143 3.16711 2.34587 H -3.91176 3.32158
2.61504 C -2.31690 3.84217 1.25522 H -2.93354 4.53408 0.68775 C -0.96781 3.66707 0.89414 C
0.12310 1.13951 3.60400 H 1.02191 0.91816 3.01748 C -0.58252 -0.19282 3.91894 H -1.44008
-0.04772 4.58589 H 0.10929 -0.87811 4.42330 H -0.94413 -0.67825 3.00788 C 0.55107 1.82425
4.92143 H 1.07219 2.76800 4.73396 H 1.21639 1.17246 5.50063 H -0.32598 2.04779 5.54026
C -0.40065 4.51530 -0.23983 H 0.65378 4.24555 -0.35335 C -1.09912 4.24051 -1.58570 H
-0.96104 3.19726 -1.88784 H -0.67444 4.87333 -2.37374 H -2.17448 4.44761 -1.53191 C -
0.46800 6.01705 0.10981 H -1.50473 6.36039 0.20367 H 0.01299 6.61377 -0.67419 H 0.03887
6.22416 1.05837 Ge 1.61584 1.62813 -0.49383

Sn(II)bis[N-(2,6-diisopropylphenyl)(2-pyridylmethyl)amide]

four coordinated

mPW1PW91/SDD

HF=-1621.3699245

N -0.15753 0.01878 0.03559 N -0.09400 -0.10190 2.74956 N 3.03300 0.10717 3.50782 N 2.59091
1.31505 1.11433 C -0.08234 -0.00505 -1.31770 H 0.90016 -0.16732 -1.74297 C -1.20337 0.18349
-2.12504 H -1.10433 0.16205 -3.20283 C -2.44504 0.40543 -1.50452 H -3.33872 0.55177 -
2.10112 C -2.51319 0.44132 -0.11011 H -3.45354 0.61821 0.39952 C -1.34197 0.24476 0.64525
C -1.35927 0.29456 2.15150 H -1.66781 1.32219 2.43069 H -2.18574 -0.35508 2.49455 C -
0.17629 -0.41694 4.14284 C -0.33066 -1.77179 4.56569 C -0.34044 -2.07025 5.94100 H -0.45019
-3.10279 6.26195 C -0.23584 -1.06106 6.90260 H -0.25118 -1.30783 7.95977 C -0.13139 0.27217
6.49029 H -0.07013 1.05740 7.23850 C -0.09970 0.61189 5.12798 C -0.53610 -2.90436 3.56553
H -0.50503 -2.46021 2.56504 C -1.91963 -3.56330 3.75072 H -1.99601 -4.06492 4.72238 H -
2.09371 -4.31476 2.97157 H -2.72186 -2.81965 3.69662 C 0.57872 -3.96608 3.64199 H 0.62547
-4.42786 4.63533 H 1.55715 -3.52599 3.42120 H 0.40097 -4.76224 2.90969 C -0.02249 2.07584
4.71668 H 0.20319 2.08361 3.64437 C -1.37940 2.77907 4.94593 H -1.61918 2.81573 6.01542
H -2.19661 2.25209 4.44339 H -1.35091 3.80919 4.57054 C 1.08778 2.85178 5.44954 H 0.87682
2.94113 6.52161 H 1.16836 3.86863 5.04687 H 2.05892 2.36149 5.33943 C 3.21716 -0.61224
4.64190 H 2.59889 -1.49338 4.75938 C 4.14085 -0.23547 5.61601 H 4.25761 -0.83261 6.51138
C 4.89854 0.92953 5.40457 H 5.62922 1.25020 6.13893 C 4.69483 1.67280 4.23994 H 5.25682
2.58022 4.05010 C 3.74447 1.23652 3.29792 C 3.47266 2.01430 2.03588 H 3.07665 3.00068
2.35122 H 4.44911 2.23519 1.56639 C 2.60149 1.83570 -0.21831 C 1.77904 2.94587 -0.57327 C
1.76895 3.40603 -1.90009 H 1.13969 4.24996 -2.16832 C 2.55171 2.79396 -2.88552 H 2.52672
3.15674 -3.90851 C 3.38100 1.72415 -2.53643 H 4.00991 1.26751 -3.29613 C 3.43472 1.24333
-1.21485 C 0.94199 3.65950 0.47953 H 0.93909 3.01126 1.36306 C -0.51712 3.88444 0.04097 H
-0.58217 4.58789 -0.79732 H -1.10029 4.30723 0.86788 H -0.99087 2.94918 -0.26961 C 1.58073
5.01503 0.85743 H 2.62301 4.89645 1.16999 H 1.02703 5.49007 1.67635 H 1.56939 5.69918
0.00043 C 4.42229 0.13206 -0.87576 H 4.31093 -0.08300 0.19220 C 4.13164 -1.16931 -1.64897
H 3.13348 -1.55324 -1.41220 H 4.85738 -1.94557 -1.37982 H 4.19236 -1.01415 -2.73267 C
5.87632 0.58911 -1.11986 H 6.06191 0.77890 -2.18340 H 6.58136 -0.18289 -0.78968 H 6.09708
1.51257 -0.57397 Sn 1.66531 -0.58985 1.57932

three coordinated

HF=-1621.3573554

N 0.00000 0.00000 0.00000 N 2.69174 0.00000 0.00000 N 0.80909 5.55222 0.00000 N 1.28754
2.45981 -1.63653 C -1.34413 -0.10116 -0.14611 H -1.72380 -0.06435 -1.15917 C -2.19657 -
0.24573 0.94683 H -3.26501 -0.32798 0.79405 C -1.63430 -0.27362 2.23510 H -2.26871 -0.37885
3.10792 C -0.24889 -0.16921 2.37756 H 0.21510 -0.19037 3.35687 C 0.55774 -0.04467 1.23319
C 2.06525 0.03516 1.31500 H 2.31974 0.94149 1.89798 H 2.41150 -0.80994 1.93168 C 3.95565 -
0.68767 -0.04814 C 3.99520 -2.11072 -0.13096 C 5.23983 -2.76188 -0.17822 H 5.27255 -3.84560
-0.24738 C 6.43641 -2.04085 -0.14197 H 7.38903 -2.55967 -0.17931 C 6.39679 -0.64626 -
0.05764 H 7.32804 -0.08865 -0.02446 C 5.17424 0.04511 -0.00925 C 2.72577 -2.95397 -0.17430
H 1.87253 -2.26988 -0.12269 C 2.63675 -3.91579 1.02907 H 3.44745 -4.65262 1.00885 H 1.68751
-4.46406 1.01291 H 2.70512 -3.37566 1.97989 C 2.61213 -3.73546 -1.49936 H 3.43906 -4.44528
-1.61306 H 2.63169 -3.05704 -2.35815 H 1.67492 -4.30351 -1.53201 C 5.17280 1.56026 0.13173
H 4.14237 1.88717 -0.04415 C 5.56605 1.97653 1.56573 H 6.59489 1.67319 1.79209 H 4.91084
1.50850 2.30790 H 5.49838 3.06427 1.68608 C 6.08951 2.24895 -0.89648 H 7.14155 1.98751
-0.73768 H 6.01198 3.33942 -0.81144 H 5.82472 1.96322 -1.91951 C 1.22459 6.83666 0.06807
H 0.46485 7.56911 0.32115 C 2.54793 7.22804 -0.16838 H 2.83180 8.27167 -0.09950 C 3.48296
6.23366 -0.49462 H 4.51983 6.49166 -0.68329 C 3.05827 4.90368 -0.57264 H 3.74831 4.10982 -

0.82722 C 1.71082 4.59051 -0.31877 C 1.19959 3.16156 -0.33682 H 1.79740 2.57664 0.37260 H
0.17426 3.20895 0.05610 C 0.83898 3.17529 -2.80807 C -0.53633 3.50331 -2.99118 C -0.93219
4.23236 -4.12441 H -1.97879 4.49587 -4.24901 C -0.01087 4.60566 -5.10560 H -0.33337 5.16341
-5.97907 C 1.32719 4.23596 -4.95741 H 2.04073 4.50577 -5.73031 C 1.77508 3.53425 -3.82384
C -1.61800 3.04495 -2.01954 H -1.13588 2.41901 -1.26371 C -2.67278 2.17426 -2.73510 H
-3.22334 2.75120 -3.48551 H -3.40685 1.79045 -2.01489 H -2.20813 1.32619 -3.25207 C -
2.29038 4.23192 -1.30010 H -1.54871 4.83409 -0.76715 H -3.03591 3.87380 -0.57886 H -2.80631
4.87969 -2.01868 C 3.24906 3.15463 -3.74996 H 3.43293 2.77837 -2.73850 C 3.57795 2.02339
-4.74833 H 2.94935 1.14329 -4.57601 H 4.62769 1.71858 -4.65772 H 3.40897 2.35440 -5.77964
C 4.18417 4.35597 -3.99361 H 4.12111 4.71048 -5.02859 H 5.22648 4.06867 -3.81032 H 3.93274
5.19383 -3.33722 Sn 1.57996 0.36718 -1.78202

two coordinated

HF=-1621.3389758

N 0.00000 0.00000 0.00000 N 3.16807 0.00000 0.00000 N 0.04953 5.23188 0.00000 N 2.73440
3.23143 0.34450 C -1.19735 -0.51927 0.34021 H -1.86327 0.13604 0.89220 C -1.59100 -1.82279
0.00350 H -2.56730 -2.19190 0.29447 C -0.69026 -2.62250 -0.71277 H -0.95140 -3.63847 -
0.98839 C 0.55590 -2.08788 -1.06872 H 1.27806 -2.67851 -1.62049 C 0.87061 -0.76754 -0.70328
C 2.18995 -0.12886 -1.09793 H 2.62300 -0.72479 -1.91370 H 1.98359 0.86522 -1.50166 C
3.77686 -1.24889 0.40629 C 4.80517 -1.82605 -0.39433 C 5.39463 -3.03264 0.01709 H 6.18147
-3.47625 -0.58612 C 5.00226 -3.66280 1.20194 H 5.47314 -4.59141 1.50833 C 4.01025 -3.08203
1.99529 H 3.71713 -3.56844 2.92063 C 3.37911 -1.88341 1.61604 C 5.32638 -1.14726 -1.65697
H 4.74858 -0.23038 -1.80907 C 5.15444 -2.03476 -2.90652 H 5.75534 -2.94779 -2.83125 H
5.47676 -1.49741 -3.80570 H 4.11034 -2.33623 -3.04473 C 6.80280 -0.72959 -1.49011 H 7.44874
-1.60198 -1.34257 H 6.93040 -0.07133 -0.62419 H 7.15414 -0.19756 -2.38178 C 2.31284 -
1.28967 2.52984 H 1.83335 -0.47073 1.98550 C 1.21922 -2.31196 2.89629 H 1.61666 -3.12648
3.51240 H 0.77246 -2.75242 2.00026 H 0.42393 -1.82331 3.47077 C 2.94767 -0.71062 3.81248
H 3.44375 -1.49682 4.39302 H 2.18208 -0.25162 4.44907 H 3.70253 0.05033 3.58134 C -
0.88242 5.99628 0.61163 H -1.08057 6.96008 0.15396 C -1.57377 5.59063 1.76110 H -2.31933
6.23770 2.20846 C -1.27868 4.32994 2.30340 H -1.79761 3.97494 3.18761 C -0.30681 3.53774
1.68238 H -0.05633 2.55252 2.05924 C 0.34322 4.01867 0.52969 C 1.35926 3.17091 -0.20695
H 1.01767 2.13409 -0.16118 H 1.34132 3.50390 -1.25286 C 3.34782 4.54596 0.40021 C 3.86019
5.13632 -0.78973 C 4.48127 6.39322 -0.71941 H 4.86710 6.84878 -1.62669 C 4.62025 7.06437
0.49870 H 5.10859 8.03289 0.53741 C 4.13013 6.47600 1.66567 H 4.24419 6.99673 2.61172 C
3.48357 5.22693 1.64158 C 3.76055 4.44442 -2.14421 H 3.31160 3.45933 -1.98387 C 5.14934
4.21350 -2.77359 H 5.65672 5.16100 -2.98506 H 5.05386 3.66913 -3.72054 H 5.79644 3.63273
-2.10643 C 2.84634 5.23575 -3.10359 H 1.86885 5.42241 -2.64826 H 2.69965 4.68481 -4.04023
H 3.28953 6.20678 -3.35266 C 2.96894 4.65398 2.95741 H 2.40687 3.74505 2.72248 C 4.13142
4.27345 3.89858 H 4.81034 3.55388 3.42812 H 3.74766 3.82950 4.82498 H 4.72161 5.15667
4.16848 C 2.00829 5.62806 3.66816 H 2.52821 6.53450 3.99796 H 1.57558 5.15306 4.55650 H
1.19078 5.92924 3.00780 Sn 4.04283 1.69760 0.85122

second four coordinated conformation

HF=-1621.3424553

Sn 0.00000 0.00000 0.00000 N 2.19004 0.00000 0.00000 N 0.77837 2.29798 0.00000 C 3.83755
-2.51867 -2.95800 H 4.64683 -3.25158 -2.85723 H 3.89553 -2.09744 -3.96733 H 2.88358 -
3.04387 -2.87294 C 4.41295 -3.04068 -0.04859 H 5.03169 -3.59341 -0.74911 C 3.95353 -1.39730
-1.91036 H 3.16860 -0.66194 -2.11595 C 2.92014 -1.16101 0.43011 C 3.12226 -0.23879 3.90322
H 2.60403 0.39107 4.63636 H 3.89995 0.36314 3.42069 H 3.61996 -1.04873 4.44851 C 1.02211
-1.61549 3.56643 H 0.29000 -1.98285 2.84099 H 0.49373 -0.99771 4.30271 H 1.44153 -2.47918
4.09530 C 3.52399 -2.76775 2.17577 H 3.45631 -3.10473 3.20653 C 2.84914 -1.59530 1.78868
C 3.74287 -1.88547 -0.48348 C 5.33254 -0.71064 -2.04576 H 6.13819 -1.43759 -1.88776 H
5.46407 0.08994 -1.31066 H 5.45484 -0.28350 -3.04849 C 2.12282 -0.79633 2.86591 H 1.64435
0.05732 2.37462 C 4.29453 -3.49674 1.26772 H 4.80826 -4.39924 1.58401 C 0.48820 4.68988
0.07585 H -0.18683 5.53650 0.07841 C 2.97795 1.21617 -0.05062 H 3.58535 1.32102 -0.97127
H 3.70536 1.25214 0.78036 C 2.12395 2.45235 0.03406 C 2.70182 3.73329 0.10487 H 3.78174
3.82351 0.12856 C 1.88234 4.86149 0.13553 H 2.31379 5.85445 0.19574 C -0.02053 3.39532
0.00525 H -1.08066 3.20456 -0.06408 N -0.63700 0.04939 -2.11238 C -2.08174 0.10569 -2.39167
C -0.02017 -0.69185 -3.19465 C 0.59014 -0.02105 -4.29795 C -0.12306 -2.11756 -3.22666 C
1.08044 -0.78406 -5.37516 C 0.38288 -2.83343 -4.32550 C 0.97987 -2.17779 -5.40220 H 1.54365
-0.26661 -6.21152 H 0.30420 -3.91692 -4.33682 H 1.36200 -2.74000 -6.24828 C -2.92858 0.88537
-1.41931 C -4.28792 1.13703 -1.70291 C -3.16681 1.85662 0.69592 C -5.08756 1.76161 -0.74459
H -4.69891 0.83336 -2.65928 C -4.52136 2.12091 0.49260 H -2.67783 2.10733 1.63164 H -
6.13428 1.95928 -0.94796 H -5.11203 2.58940 1.27032 C 0.80414 1.48938 -4.40192 C -0.77573
-2.91644 -2.10072 C -0.45370 2.35994 -4.23535 C 1.90809 1.94673 -3.43277 H -0.81571 2.31067
-3.20650 H -1.25336 2.03918 -4.91269 H -0.21435 3.40423 -4.47239 H 1.17365 1.66837 -5.42140
H 1.59809 1.73092 -2.41047 H 2.84714 1.41875 -3.63023 H 2.08956 3.02443 -3.52883 N -
2.38788 1.26684 -0.24409 H -2.53484 -0.90640 -2.43134 H -2.25728 0.52247 -3.39620 C -
1.94942 -3.78000 -2.60914 C 0.25189 -3.79625 -1.35973 H -2.68200 -3.17966 -3.15981 H -
1.60018 -4.57312 -3.27990 H -2.46049 -4.26042 -1.76670 H -0.23030 -4.33820 -0.53783 H
0.69735 -4.53593 -2.03491 H 1.06521 -3.19738 -0.93813 H -1.17786 -2.20771 -1.36836

Pb(II)bis[N-(2,6-diisopropylphenyl)(2-pyridylmethyl)amide]

mPW1PW91/SDD

HF=-1621.4049765

N -0.19967 -0.00776 -0.04974 N -0.18820 -0.26035 2.70837 N 3.09577 0.07230 3.57544 N
2.76465 1.24465 1.08822 C -0.10853 0.15229 -1.39381 H 0.88130 0.06612 -1.82462 C -1.21875
0.43916 -2.18709 H -1.10276 0.56492 -3.25609 C -2.47042 0.57099 -1.56076 H -3.35675 0.79473
-2.14423 C -2.55576 0.42248 -0.17552 H -3.50317 0.53088 0.34064 C -1.39402 0.13237 0.56755
C -1.46872 -0.01901 2.06772 H -1.96532 0.89456 2.45040 H -2.19440 -0.83452 2.26962 C -
0.27500 -0.47692 4.11812 C -0.37422 -1.80140 4.64447 C -0.38399 -1.99717 6.03755 H -0.45196
-3.00666 6.43481 C -0.32988 -0.91500 6.92157 H -0.34428 -1.08218 7.99422 C -0.27627 0.38627
6.40964 H -0.25222 1.22813 7.09628 C -0.24970 0.62464 5.02576 C -0.50986 -3.01196 3.72793
H -0.48362 -2.63776 2.69891 C -1.86268 -3.72403 3.94093 H -1.93333 -4.15049 4.94824 H -
1.98530 -4.54234 3.22136 H -2.69893 -3.02816 3.81595 C 0.65132 -4.01173 3.89869 H 0.68288
-4.41600 4.91712 H 1.61852 -3.53869 3.69495 H 0.53865 -4.85514 3.20744 C -0.22237 2.05603
4.50880 H -0.04681 1.99061 3.42976 C -1.57779 2.75583 4.75340 H -1.77513 2.85785 5.82732
H -2.40751 2.18914 4.31810 H -1.57906 3.76034 4.31328 C 0.91263 2.89326 5.12815 H 0.76789
3.03435 6.20574 H 0.94519 3.88788 4.66737 H 1.88508 2.41591 4.97959 C 3.15970 -0.53162

4.78857 H 2.49170 -1.36912 4.94714 C 4.01678 -0.09087 5.79617 H 4.03373 -0.59728 6.75289
C 4.83447 1.02293 5.53699 H 5.51337 1.39560 6.29613 C 4.75225 1.65117 4.29330 H 5.35904
2.52040 4.06529 C 3.86432 1.15413 3.31835 C 3.75511 1.83096 1.97336 H 3.55671 2.90188
2.17705 H 4.77119 1.81718 1.52649 C 2.71938 1.83994 -0.20997 C 1.90957 2.98979 -0.45492 C
1.83323 3.52316 -1.75195 H 1.21179 4.39579 -1.93392 C 2.53955 2.95034 -2.81556 H 2.46521
3.37169 -3.81340 C 3.35708 1.84128 -2.57655 H 3.92610 1.41217 -3.39728 C 3.47313 1.28528
-1.28950 C 1.14969 3.66046 0.68074 H 1.22961 2.99020 1.54318 C -0.34510 3.85727 0.36511 H
-0.49324 4.55884 -0.46428 H -0.86668 4.26581 1.23900 H -0.82190 2.91134 0.09406 C 1.78796
5.01995 1.04295 H 2.85169 4.91452 1.28045 H 1.28441 5.46456 1.90985 H 1.70462 5.72430
0.20655 C 4.43558 0.12340 -1.07131 H 4.37384 -0.14748 -0.01187 C 4.05525 -1.11888 -1.90143
H 3.04421 -1.46584 -1.66026 H 4.74917 -1.94364 -1.70113 H 4.09005 -0.90616 -2.97623 C
5.89095 0.54078 -1.37166 H 6.02199 0.79269 -2.43038 H 6.58327 -0.27553 -1.13338 H 6.17906
1.41855 -0.78372 Pb 1.71338 -0.72910 1.53860

Sn-N,N-(pyridine-diylbis(ethene))bis(2,6-diisopropylaniline)

mPW1PW91/SDD
HF=-1371.9804672

Sn 0.03586 0.29211 0.02528 N 0.12627 0.32153 2.38760 N 2.09164 0.16033 0.64790 N 1.42684
0.18311 -1.89957 C 2.72929 0.09865 -1.64981 H 3.47060 0.04541 -2.44497 C 3.13301 0.08177
-0.28897 C 4.47022 -0.00395 0.11315 H 5.24057 -0.06229 -0.64862 C 2.43685 0.15360 2.00846
C 3.77212 0.06753 2.42029 H 3.98979 0.06505 3.48320 C 1.34681 0.24312 2.91129 H 1.51788
0.24664 3.98593 C 4.80761 -0.01330 1.47650 H 5.84125 -0.07983 1.79143 C -0.63424 -2.90097
4.50641 H 0.16601 -2.33617 4.99640 H -0.23322 -3.87773 4.21248 H -1.42530 -3.06981 5.24585
C -1.02863 0.42091 3.23470 C -2.67148 1.77362 4.39516 H -3.06017 2.74647 4.68024 C -
1.68573 -0.76220 3.65765 C -3.32304 0.61690 4.83352 H -4.20872 0.69272 5.45569 C -1.52078
1.70135 3.59215 C -0.84328 2.98542 3.12888 H 0.01911 2.71034 2.51369 C -2.83009 -0.63814
4.46323 H -3.34075 -1.53396 4.80264 C -2.26117 -2.97735 2.55940 H -1.84917 -3.93953 2.23428
H -2.64035 -2.45154 1.67747 H -3.11106 -3.18572 3.21884 C -1.17728 -2.14685 3.27450 H -
0.34821 -2.01850 2.57118 C -1.78521 3.82865 2.24568 H -2.13245 3.25152 1.38260 H -1.26520
4.71979 1.87581 H -2.66673 4.16268 2.80435 C -0.32138 3.81197 4.32165 H -1.14208 4.13728
4.97081 H 0.20015 4.70811 3.96663 H 0.37625 3.22884 4.93206 C 0.94152 0.21367 -3.25011 C
1.16528 2.77663 -3.23528 H 1.42984 2.56091 -2.19533 C 0.79299 1.46080 -3.90809 C 0.08067
-0.94158 -5.19912 H -0.19794 -1.86189 -5.70294 C 0.57527 -0.99951 -3.88533 C 0.72150 -
2.34830 -3.19143 H 1.02337 -2.16333 -2.15549 C 0.29431 1.46676 -5.22155 H 0.18004 2.41248
-5.74224 C -0.05811 0.27820 -5.86823 H -0.44071 0.30267 -6.88326 C 2.39654 3.41766 -3.90918
H 3.25627 2.73948 -3.89224 H 2.67948 4.34184 -3.39229 H 2.18792 3.66694 -4.95580 C 1.82522
-3.19797 -3.85577 H 1.57347 -3.42660 -4.89766 H 1.95166 -4.14739 -3.32302 H 2.78626 -
2.67276 -3.85166 C -0.01938 3.76259 -3.21200 H -0.31135 4.06711 -4.22335 H 0.25170 4.66835
-2.65761 H -0.89373 3.31447 -2.72961 C -0.61213 -3.11983 -3.15011 H -1.39435 -2.52580 -
2.66710 H -0.49334 -4.05286 -2.58744 H -0.95956 -3.38070 -4.15602

N,N-tin(II)(NTMS)-N,N(pyridine-2,6- diylbis(methylene))bis(2,6-diisopropylaniline)

mPW1PW91/SDD
HF=-3122.9565807

Sn 0.08743 -0.21437 -0.28551 Sn -0.11410 0.18534 6.32263 Si 2.85600 0.19709 7.73686 Si
1.89302 -2.57360 6.62374 Si -0.76307 -3.18529 -1.46911 Si 2.06695 -3.18583 -0.23685 C 1.77793
0.06803 2.67826 C 3.87158 1.52132 1.59987 H 4.67090 2.08950 1.13876 N 1.77939 0.35884
1.34470 C 3.89589 1.20521 2.95907 H 4.72541 1.51987 3.58275 C 2.80013 1.08291 0.80794 C
2.83526 0.47205 3.50282 H 2.80600 0.19131 4.54997 C -1.30993 0.76594 3.64209 C -1.24043
2.16393 3.39350 C -2.49670 0.04405 3.32967 C -3.49471 2.08976 2.45259 H -4.33038 2.59786
1.98268 C -3.56831 0.72183 2.72841 H -4.47321 0.17535 2.48105 C -2.34466 2.80115 2.79943
H -2.29975 3.86808 2.60345 C 1.95377 0.95400 -3.77004 C 0.41124 2.58818 -2.77003 C 0.15162
3.09155 -4.05781 H -0.54106 3.92033 -4.17495 C 1.67878 1.49962 -5.03444 H 2.17142 1.08978
-5.91129 C 1.31042 1.49139 -2.61650 C 0.77617 2.55656 -5.18664 H 0.56674 2.96057 -6.17212
C 2.54699 0.06145 9.61041 H 1.50707 0.31311 9.84827 H 3.19531 0.75335 10.16164 H 2.74021
-0.94993 9.98080 C 2.62670 2.03277 7.26088 H 2.67600 2.19214 6.17768 H 3.42673 2.62921
7.71674 H 1.67885 2.44582 7.62749 C 4.66219 -0.28213 7.37022 H 4.89524 -1.30084 7.69734
H 5.33960 0.39699 7.90210 H 4.88544 -0.21212 6.30023 C 0.21451 -3.32710 6.12688 H -
0.55362 -3.12387 6.88345 H 0.31143 -4.41669 6.05059 H -0.15060 -2.97282 5.15743 N -0.19072
0.06416 4.24550 N 1.70670 -0.79729 6.77843 N 0.58181 -2.29079 -0.67219 C 0.63349 -0.71729
3.29803 H 0.00184 -1.13443 2.50390 H 1.07376 -1.56170 3.83646 N 1.56225 0.93995 -1.31344
C -2.66574 -1.42787 3.68868 H -1.71687 -1.78266 4.10077 C -3.73452 -1.59671 4.78982 H
-3.49074 -0.99922 5.67567 H -3.81185 -2.64737 5.09219 H -4.71974 -1.27438 4.43545 C -
2.99995 -2.30397 2.46759 H -3.95430 -2.01541 2.01370 H -3.07809 -3.35612 2.76415 H -2.22606
-2.22267 1.69842 C 2.54719 -4.50560 -1.53379 H 1.76972 -5.26105 -1.68490 H 3.45316 -5.02605
-1.19830 H 2.76373 -4.04028 -2.50126 C 3.61643 -2.09427 -0.04151 H 3.71737 -1.37409 -
0.85764 H 4.49978 -2.74472 -0.05946 H 3.62919 -1.55243 0.90804 C -1.17352 -4.81174 -0.55345
H -0.34531 -5.52790 -0.58141 H -2.04163 -5.29117 -1.02264 H -1.42010 -4.61675 0.49587 C
-0.40829 -3.61662 -3.29391 H -0.32020 -2.70138 -3.88948 H -1.24431 -4.19960 -3.70118 H
0.50718 -4.19877 -3.42615 C 1.84930 -4.09929 1.42906 H 1.56462 -3.39937 2.22221 H 2.78513
-4.58801 1.72780 H 1.06977 -4.86480 1.36449 C 2.38133 -3.37014 8.28545 H 3.36808 -3.04465
8.63196 H 2.41599 -4.46097 8.17563 H 1.65027 -3.13319 9.06567 C -0.03191 3.00963 3.77901
H 0.75222 2.32901 4.12483 C -0.37825 3.96711 4.93941 H -1.15134 4.68308 4.63902 H 0.50679
4.53553 5.24800 H -0.75772 3.42034 5.81031 C 0.53569 3.80251 2.58613 H -0.17561 4.55529
2.22888 H 0.77166 3.14183 1.74743 H 1.45143 4.32775 2.88054 C 2.68172 -1.33863 -4.62153
H 1.67147 -1.73141 -4.48352 H 3.39210 -2.15627 -4.45128 H 2.78593 -1.02679 -5.66692 C
2.96420 -0.17804 -3.65021 H 2.87330 -0.56861 -2.63213 C 2.77158 1.40267 -0.66473 H 2.88229
2.49873 -0.76312 H 3.69840 0.98117 -1.10160 C 3.21466 -3.07257 5.34659 H 3.00898 -2.67217
4.34928 H 3.26162 -4.16498 5.26112 H 4.20535 -2.71845 5.64996 C -2.38197 -2.17370 -1.53847
H -2.73315 -1.83956 -0.55891 H -3.15519 -2.82204 -1.97217 H -2.29687 -1.29239 -2.18365 C -
0.25422 3.26636 -1.57833 H 0.06007 2.72857 -0.67807 C 0.21312 4.73114 -1.44177 H 1.30407
4.79443 -1.36567 H -0.22115 5.19132 -0.54638 H -0.09470 5.32726 -2.30820 C -1.79195 3.19551
-1.65402 H -2.17395 3.73662 -2.52744 H -2.24001 3.64043 -0.75803 H -2.13449 2.15832 -
1.72160 C 4.40225 0.34491 -3.86468 H 4.53237 0.70329 -4.89266 H 5.13547 -0.45149 -3.68999
H 4.63339 1.17972 -3.19469

Ethene-bis(trimethylsilyl)-diamine-tin(II)

mPW1PW91/SDD

HF=-3447.3416181

Sn 0.00802 -0.25358 -0.08465 N -0.00603 -0.24203 2.30676 C 1.23592 -0.26806 2.84922 C
0.30959 -0.06984 5.07120 H 0.42611 -0.00967 6.14707 C 1.42346 -0.18103 4.23845 H 2.42862 -
0.20978 4.64139 C -0.96936 -0.04574 4.50347 H -1.84520 0.00799 5.13421 C -1.11191 -0.12180
3.10988 C 3.39239 1.40986 -0.58916 C 3.09389 0.03229 -0.37431 C 2.62336 2.52304 0.11400 H
1.88423 2.05040 0.77005 C 4.42636 1.75762 -1.47547 H 4.65294 2.80631 -1.64600 C 3.85031
-0.96449 -1.05114 N -0.68381 -2.27729 -0.41336 Si -0.51361 -3.73606 0.60715 Si -1.57657
-2.32921 -1.97690 C 3.45261 -3.24037 -2.12375 H 2.65737 -2.82777 -2.75222 H 3.21263 -
4.28817 -1.91034 H 4.38085 -3.23052 -2.70609 C 3.59298 -2.44579 -0.81200 H 2.64602 -2.51816
-0.26744 C 4.87968 -0.57178 -1.92357 H 5.46238 -1.33047 -2.43729 C 3.55035 3.39222 0.98927
H 4.10081 2.78485 1.71615 H 2.96851 4.14189 1.53792 H 4.28759 3.92439 0.37790 C 1.85416
3.40236 -0.89310 H 2.54009 3.91173 -1.57925 H 1.27188 4.16904 -0.36856 H 1.16401 2.80009 -
1.49233 C 5.16950 0.77843 -2.14026 H 5.96647 1.06419 -2.81944 C 4.70650 -3.05906 0.06523 H
5.67313 -3.02434 -0.45088 H 4.48371 -4.10740 0.29620 H 4.81581 -2.51547 1.00978 C 2.41788
-0.39961 1.92335 H 3.12639 0.40991 2.17261 H 2.94372 -1.33553 2.19720 N 2.03677 -0.34425
0.52571 C 0.62095 -3.48341 2.11418 H 1.58781 -3.06226 1.82582 H 0.80795 -4.46516 2.56643
H 0.17119 -2.84995 2.88304 C -0.53935 -1.55637 -3.37860 H -0.41629 -0.47428 -3.25724 H
-1.02266 -1.72886 -4.34821 H 0.45785 -2.00821 -3.41284 C 0.24270 -5.22452 -0.32436 H -
0.47394 -5.71856 -0.98533 H 0.59432 -5.96905 0.40068 H 1.10104 -4.90734 -0.92576 C -2.04601
-4.08272 -2.56002 H -1.16619 -4.65811 -2.86198 H -2.69624 -3.98476 -3.43849 H -2.59332
-4.65805 -1.80701 C -2.21586 -4.26265 1.30035 H -2.62976 -3.47464 1.94051 H -2.12551 -
5.17393 1.90432 H -2.93974 -4.45994 0.50219 C -3.21122 -1.34529 -1.86582 H -3.85535 -
1.75523 -1.07932 H -3.75594 -1.39891 -2.81643 H -3.01314 -0.28807 -1.65248 C -2.42595 -
0.09908 2.45720 H -2.46612 -0.56061 1.47320 N -5.96507 0.56907 3.16327 C -7.20702 0.59510
2.62080 C -6.28069 0.39688 0.39883 H -6.39721 0.33671 -0.67704 C -7.39456 0.50807 1.23158
H -8.39972 0.53682 0.82864 C -5.00174 0.37278 0.96656 H -4.12590 0.31905 0.33581 C -
4.85919 0.44883 2.36015 C -9.36348 -1.08282 6.05918 C -9.06499 0.29475 5.84434 C -8.59446
-2.19600 5.35602 H -7.85533 -1.72336 4.69998 C -10.39746 -1.43059 6.94550 H -10.62404 -
2.47927 7.11603 C -9.82141 1.29153 6.52116 C -9.42370 3.56741 7.59377 H -8.62846 3.15481
8.22225 H -9.18373 4.61521 7.38037 H -10.35195 3.55755 8.17612 C -9.56408 2.77283 6.28202
H -8.61712 2.84520 5.73747 C -10.85078 0.89882 7.39360 H -11.43348 1.65751 7.90732 C
-9.52145 -3.06518 4.48075 H -10.07191 -2.45781 3.75387 H -8.93961 -3.81485 3.93211 H -
10.25869 -3.59735 5.09213 C -7.82526 -3.07532 6.36313 H -8.51119 -3.58469 7.04927 H -
7.24298 -3.84200 5.83859 H -7.13511 -2.47305 6.96236 C -11.14060 -0.45139 7.61029 H -
11.93757 -0.73715 8.28947 C -10.67760 3.38610 5.40480 H -11.64423 3.35138 5.92091 H
-10.45481 4.43444 5.17382 H -10.78691 2.84251 4.46025 C -8.38898 0.72665 3.54667 H -
9.09749 -0.08288 3.29742 H -8.91482 1.66257 3.27283 N -8.00787 0.67129 4.94432 C -3.54514
0.42612 3.01282 H -3.50498 0.88765 3.99683 Sn -5.97912 0.58061 5.55468 N -5.28728 2.60433
5.88339 Si -5.45749 4.06310 4.86287 Si -4.39453 2.65625 7.44693 C -6.59205 3.81045 3.35584
H -7.55891 3.38930 3.64421 H -6.77904 4.79220 2.90359 H -6.14229 3.17699 2.58698 C -
5.43175 1.88340 8.84863 H -5.55481 0.80132 8.72726 H -4.94844 2.05590 9.81824 H -6.42895
2.33525 8.88287 C -6.21380 5.55156 5.79439 H -5.49716 6.04560 6.45535 H -6.56542 6.29609
5.06934 H -7.07214 5.23438 6.39579 C -3.92509 4.40976 8.03004 H -4.80491 4.98515 8.33200
H -3.27486 4.31180 8.90852 H -3.37777 4.98509 7.27704 C -3.75524 4.58969 4.16968 H -
3.34134 3.80168 3.52952 H -3.84559 5.50097 3.56571 H -3.03135 4.78698 4.96784 C -2.75988
1.67233 7.33585 H -2.11575 2.08227 6.54935 H -2.21516 1.72595 8.28645 H -2.95796 0.61511
7.12251

Tin(II) 2,6-Bis[1-(phenylimino)ethyl]pyridineTMS

mPW1PW91/SDD

HF=-2323.1307675

Sn -0.03062 -0.03014 0.05467 Si -0.07608 -0.15680 3.31082 Si 2.82136 -0.06692 2.21324 C
3.46339 1.58353 2.93519 H 3.28214 2.40795 2.23678 H 4.54613 1.51717 3.10216 H 2.98968
1.83059 3.88980 C 1.85189 2.14547 -1.70380 C 2.29205 -0.13095 -2.17429 C 3.38056 0.23776
-2.99481 H 3.96803 -0.52981 -3.47626 C 2.90168 2.55245 -2.53323 H 3.10391 3.60271 -2.68798
C 3.69743 1.57987 -3.15840 H 4.53903 1.87440 -3.77443 N 1.59288 0.82014 -1.49648 N 0.89936
-1.73950 -1.04759 N 0.13631 2.77039 -0.15589 C 1.83465 -1.53638 -2.04034 C 0.92896 3.15169
-1.10502 C 2.29068 -2.47792 -2.93151 H 1.93563 -3.49909 -2.87928 H 2.97398 -2.24198 -
3.73512 C 0.93705 4.53661 -1.71661 H 0.17723 5.16464 -1.25239 H 0.74391 4.48441 -2.79275
H 1.90714 5.02436 -1.57865 C -0.87657 3.64310 0.37558 C -2.47148 2.92682 -1.53153 H -
1.63142 2.26350 -1.76325 C -2.71713 3.83173 -2.75694 H -3.58290 4.48393 -2.59801 H -2.91758
3.22302 -3.64565 H -1.85450 4.47207 -2.96834 C 0.70068 4.19075 2.32102 H 1.05236 3.16784
2.13839 C -0.62322 4.34726 1.58103 C 1.77131 5.16923 1.78969 H 1.98728 5.00562 0.73108 H
2.70705 5.04520 2.34593 H 1.43739 6.20609 1.91135 C -2.84968 5.34034 1.41127 H -3.60992
6.00492 1.80775 C -3.69457 2.02361 -1.27416 H -3.51477 1.35951 -0.42393 H -3.90119 1.40449
-2.15342 H -4.59170 2.61540 -1.06170 C -3.09498 4.60414 0.25081 H -4.05583 4.69372 -0.24586
C -1.62541 5.19791 2.07338 H -1.45023 5.74724 2.99098 C -2.12603 3.73917 -0.28688 C 0.56248
4.37980 3.84155 H 1.49263 4.08164 4.33632 H -0.25378 3.77826 4.25244 H 0.37956 5.42816
4.10385 C -1.30137 -2.04953 -2.98995 H -0.64906 -1.18685 -2.82231 C -0.90733 -3.13736 -
1.99599 C 0.16430 -2.97861 -1.07128 C -1.63267 -4.34142 -2.00262 H -2.45113 -4.46650 -
2.70563 C -0.27345 -5.21381 -0.20960 H -0.04334 -6.01858 0.47903 C -1.32204 -5.37710 -
1.11975 H -1.89223 -6.30059 -1.13548 C 0.48361 -4.03002 -0.16715 C 1.64390 -3.90344 0.81390
H 1.68870 -2.85273 1.12188 C -2.75599 -1.58727 -2.77164 H -3.46363 -2.40629 -2.94170 H -
3.00778 -0.77913 -3.46920 H -2.90194 -1.22034 -1.75118 C 2.98571 -4.25118 0.13062 H 2.97878
-5.29235 -0.21468 H 3.81587 -4.13464 0.83791 H 3.17688 -3.60865 -0.73235 C 1.47622 -4.77385
2.07174 H 0.50135 -4.62504 2.54512 H 2.25089 -4.52435 2.80518 H 1.58771 -5.83998 1.84185
C -1.09676 -2.51340 -4.44717 H -1.74679 -3.36246 -4.68785 H -0.05973 -2.81721 -4.61668 H -
1.33603 -1.70140 -5.14434 N 1.05822 -0.03905 1.91310 C 3.32342 -1.44902 3.43611 H 2.77468
-1.40842 4.38147 H 4.39261 -1.36298 3.66733 H 3.15447 -2.43423 2.99130 C 3.87315 -0.36425
0.65848 H 3.52195 -1.22114 0.07936 H 4.90080 -0.57451 0.98077 H 3.90848 0.51647 0.01029
C -1.72407 0.74147 2.96713 H -1.56702 1.75920 2.59543 H -2.28935 0.80866 3.90581 H -
2.35006 0.21080 2.24278 C -0.50135 -1.97283 3.69903 H -0.94600 -2.46242 2.82490 H -1.22116
-2.03536 4.52465 H 0.39294 -2.53730 3.98164 C 0.61267 0.61903 4.91404 H 1.55645 0.17440
5.24195 H -0.12152 0.46072 5.71422 H 0.76140 1.69657 4.80561

Bibliography

- (1) Colombo, P.; Mera, G.; Riedel, R.; Soraru, G. D. *Journal American Ceramic Society* **2010**, *93*, 1805–1837.
- (2) West, R.; Fink, M. J.; Michl, J. *Science* **1981**, *214*, 1343.
- (3) Hong, S. H.; S. I. Hyung, I. N. J.; Han, W.; Kim, M.; Yun, H.; Nam, S. W.; Kang, S. O. *Organometallics* **2010**, *29*.
- (4) Asay, M.; Jones, C.; Driess, M. *Chemical Reviews* **2011**, *111*, 354–396.
- (5) Kroke, E.; Li, Y.-L.; Konetschny, C.; Lecomte, E.; Fasel, C.; Riedel, R. *Materials Science and Engineering* **2000**, *26*, 97–199.
- (6) Ruhland-Senge, K.; Bartlett, R. A.; Olmstead, M. M.; Power, P. P. *Angewandte Chemie* **1993**, *105*, 459.
- (7) Sommer, L. H.; Tyler, L. J. *Journal American Chemical Society* **1954**, *76*, 1030–1033.
- (8) Metras, F. *Bulletin de la Societe Chimique de France* **1966**, 210–226.
- (9) Kliebisch, U.; Klingebiel, U.; Vater, N. *Chemische Berichte* **1985**, *118*, 4561.
- (10) Tekautz, G.; Binter, A.; Hassler, K.; Flock, M. *Chemical Physical Letters* **2006**, *7*, 421–429.
- (11) Rozsondai, B.; Hargittai, I.; Golubinskii, A.; Vilkov, L. V.; Mastryukov, V. S. *Journal of Molecular Structure* **1975**, *28*, 339–348.
- (12) Li, H.; Butler, I. S.; Gilson, D. F. R.; Harrod, J. F.; Morin, F. G. *Journal of Physical Chemistry* **1995**, *99*, 8490–8495.
- (13) Clegg, W.; Sheldrick, G. M.; Stalke, D. *Acta Crystallographica* **1984**, *C40*, 433–434.
- (14) Lippe, K.; Wagler, J.; Kroke, E.; Herkenhoff, S.; Ischenko, V.; Woltersdorf, J. *Chemistry of Materials* **2009**, *21*, 3941–3949.
- (15) Blake, A.; Ebsworth, E. A. *Acta Crystallographica* **1991**, *C47*, 1440–1442.
- (16) Lehnert, C.; Wagler, J.; Kroke, E.; Roewer, G. *Chemistry of Heterocyclic Compounds* **2006**, *42*, 1574–1584.
- (17) Klingebiel, U.; Noltemeyer, M.; Rackebrandt, H.-J. *Zeitschrift fuer Anorganische und Allgemeine Chemie* **1997**, *623*, 281.
- (18) Jaschke, B.; Helmold, N.; Mueller, I.; Pape, T.; Noltemeyer, M.; Herbst-Irmer, R.; Klingebiel, U. *Zeitschrift fuer Anorganische und Allgemeine Chemie* **2002**, *628*, 2071–2085.

- (19) Hesse, M.; Klingebiel, U. *Journal of Organometallic Chemistry* **1981**, *221*, C1–C6.
- (20) Fink, W. *Angewandte Chemie* **1961**, *73*, 467.
- (21) Hueckel IUPAC Gold Book. <http://goldbook.iupac.org>.
- (22) Frisch, M. J.; Trucks, G. W.; Schlegel, H. B.; Scuseria, G. E.; Robb, M. A.; Cheeseman, J. R.; Montgomery, J. A.; Vreven, J. T.; Kudin, K. N.; Burant, J. C.; Millam, J. M.; Iyengar, S. S.; Tomasi, J.; Barone, V.; Mennucci, B.; Cossi, M.; Scalmani, G.; Rega, N.; Petersson, G. A.; Nakatsuji, H.; Hada, M.; Ehara, M.; Toyota, K.; Fukuda, R.; Hasegawa, J.; Ishida, M.; Nakajima, T.; Honda, Y.; Kitao, O.; Nakai, H.; Klene, M.; Li, X.; Knox, J. E.; Hratchian, H. P.; Cross, J. B.; Bakken, V.; Adamo, C.; Jaramillo, J.; Gomperts, R.; Stratmann, R. E.; Yazyev, O.; Austin, A. J.; Cammi, R.; Pomelli, C.; Ochterski, J. W.; Ayala, P. Y.; Morokuma, K.; Voth, G. A.; Salvador, P.; Dannenberg, J. J.; Zakrzewski, V. G.; Dapprich, S.; Daniels, A. D.; Strain, M. C.; Farkas, O.; Malick, D. K.; Rabuck, A. D.; Raghavachari, K.; Foresman, J. B.; Ortiz, J. V.; Cui, Q.; Baboul, A. G.; Clifford, S.; Cioslowski, J.; Stefanov, B. B.; Liu, G.; Liashenko, A.; Piskorz, P.; Komaromi, I.; Martin, R. L.; Fox, D. J.; Keith, T.; Al-Laham, M. A.; Peng, C. Y.; Nanayakkara, A.; Challacombe, M.; Gill, P. M. W.; Johnson, B.; Chen, W.; Wong, M. W.; Gonzalez, C.; Pople, J. A. *Gaussian 93*; Gaussian Inc. Pittsburgh.
- (23) R. Schleyer, P. v.; Maerker, C.; Dransfeld, A.; Jiao, H.; Eikema Hommes, N. J. van *Journal American Chemical Society* **1996**, *118*, 6317–6318.
- (24) Smith, J.; Seshadri, K. S.; White, D. *Journal of Molecular Spectroscopy* **1973**, *45*, 327–337.
- (25) Breed, L. W.; Elliott, R. L. *Inorganic Chemistry* **1964**, *3*, 1622–1627.
- (26) Fink, W. *Helvetica Chimica Acta* **1962**, *XLV*, 1081–1089.
- (27) Fink, W. *Helvetica Chimica Acta* **1969**, *52*, 2261–2276.
- (28) Adamson, G.; Daly, J. J. *Journal of the Chemical Society (A)* **1970**, 2724–2728.
- (29) Schneider, J.; Popowski, E.; Reinke, H. *Zeitschrift fuer Anorganische und Allgemeine Chemie* **2003**, *629*, 55–64.
- (30) Fooker, U.; Khan, M. A.; Wehmschulte, R. *Inorganic Chemistry* **2001**, *40*, 1316–1322.
- (31) Brothers, P. J.; Power, P. P. *Advances in Organometallic Chemistry* **1996**, *39*, 1–69.
- (32) Gauss, J.; Schneider, U.; Ahlrichs, R.; Dohmeier, C.; Schnoekel, H. *Journal of the American Chemical Society* **1993**, *115*, 2402–2408.
- (33) Jolly, B.; Lappert, M. F.; Engelhardt, L. M.; White, A. H.; Raston, C. L. *Journal of the Chemical Society. Dalton Transactions*. **1993**, *16*, 2653–2663.
- (34) Engelhardt, L. M.; Jolly, B.; Lappert, M. F.; Raston, C. L.; White, A. H. *Journal of the Chemical Society, Chemical Communications* **1988**, 336–338.
- (35) Sen, S. S.; Kritzler-Kosch, M. P.; Nagendran, S.; Roesky, H. W.; Beck, T.; Pal, A.; Herbst-Irmer, R. *Eur. J. Inorg. Chem.* **2010**, 5304–5311.

- (36) Lacey, E.; Burks, P. *Journal of Applied Polymers* **1965**, *14*, 670–674.
- (37) Tokitoh, N.; Okazaki, R. *Coordination Chemistry Reviews* **2000**, *210*, 251–277.
- (38) Power, P. P. *Chemical Reviews* **1999**, *99*, 3463–3503.
- (39) Mizuhata, Y.; Sasamori, T.; Tokitoh, N. *Chemical Reviews* **2009**, *109*, 3479–3511.
- (40) Goldberg, D. E.; Harris, D. H.; Lappert, M. F.; Thomas, M. K. *J. C. S. Chem Comm.* **1976**, 261–262.
- (41) Kira, M.; Yauchibara, R.; Hirano, R.; Kabuto, C.; Sakurai, H. *Journal of the American Chemical Society* **1991**, *113*, 7785–7787.
- (42) Weidenbruch, M.; Schlaefke, J.; Schaefer, A.; Peters, K.; Schnering, H. G. von; Marsmann, H. *Angewandte Chemie. Int. Ed.* **1994**, *33*, 1846–1848.
- (43) Simons, R. S.; Pu, L.; Olmstead, M. M.; Power, P. P. *Organometallics* **1997**, *16*, 1920–1925.
- (44) Klinkhammer, K. W.; Schwarz, W. *Angewandte Chemie* **1995**, *107*, 1448.
- (45) Benet, S.; Cardin, C. J.; Cardin, D. J.; Constantine, S. P.; Heath, P.; Rashid, H.; Teixeira, S.; Thorpe, J. H.; Todd, A. K. *Organometallics* **1999**, *18*, 389–398.
- (46) Mehring, M.; Loew, C.; Schuermann, M.; Uhlig, F.; Jurkschat, K. *Organometallics* **2000**, *19*.
- (47) Ossig, G.; Meller, A.; Broenneke, C.; Mueller, O.; Schaefer, M.; Herbst-Irmer, R. *Organometallics* **1997**, *16*, 2116–2120.
- (48) Dias, H. V. R.; Jin, W. *Inorganic Chemistry* **1996**, *35*, 6546–6551.
- (49) Leites, L. A.; Bukalov, S. S.; Zabula, A. V.; Garbuzova, I. A.; Moser, D. F.; West, R. *Journal of the American Chemical Society* **2004**, *126*, 4114–4115.
- (50) Hahn, F. E.; Wittenbecher, L.; Van, D. L.; Zabula, A. V. *Inorganic Chemistry* **2007**, *46*, 7662–7667.
- (51) Gibson, V. C.; O'Reilly, R. K.; Wass, D. F.; Whitea, A. J. P.; Williams, D. J. *Dalton Transactions* **2003**, *14*, 2824–2830.
- (52) Cruz, C. A.; Emslie, D. J. H.; Harrington, L. E.; Britten, J. F.; Robertson, C. M. *Organometallics* **2007**, *26*, 692–701.
- (53) Zhang, S.; Katao, S.; Sun, W.-H.; Nomura, K. *Organometallics* **2009**, *28*, 5925–5933.
- (54) Nienkemper, K.; Kehr, G.; Kehr, S.; Froehlich, R.; Erker, G. *Journal of Organometallic Chemistry* **2008**, *693*, 1572–1589.
- (55) Laine, T. V.; Klinge, M.; Leskelae, M. *European Journal of Inorganic Chemistry* **1999**, 959–964.
- (56) Olbert, D.; Kalisch, A.; Görls, H.; Ondik, I. M.; Reiher, M.; Westerhausen, M. *Zeitschrift fuer Anorganische und Allgemeine Chemie* **2009**, *635*, 462–470.
- (57) Pauer, F.; Power, P. P. *Lithium Chemistry: A Theoretical and Experimental Overview*; Sapse, A.-M., R. Schleyer, P. v., Eds.; J. Wiley: New York, 1995, pp 295–392.

- (58) Mulvey, R. E. *Chemical Society Reviews* **1991**, *20*, 167–209.
- (59) Collum, D. B. *Accounts of Chemical Research* **1993**, *26*, 227–234.
- (60) Nagendran, S.; Roesky, H. W. *Organometallics* **2008**, *27*, 457–492.
- (61) Mcheik, A.; Katir, N.; Castel, A.; Gornitzka, H.; Massou, S.; Riviere, P.; Hamieh, T. *European Journal of Inorganic Chemistry* **2008**, *34*, 5397–5403.
- (62) Mansell, S. M.; Russel, C. A.; Waas, D. F. *Inorganic Chemistry* **2008**, *47*, 11367–11375.
- (63) Reger, D. L.; Wright, T. D.; Smith, M. D.; Rheingold, A. L.; Kassel, S.; Concolino, T.; Rhagitan, B. *Polyhedron* **2002**, *21*, 1795–1807.
- (64) Elschenbroich, C. *Organometallchemie*; Teubner Verlag, 2003; Vol. 4. Auflage.
- (65) Ahlrichs, R.; Baer, M.; Haeser, M.; Horn, H.; Koelmel, C. *Chemical Physical Letters* **1989**, *162*, 165–169.
- (66) Wang, B.; Dossey, A. T.; Walse, S. S.; Edison, A. S.; Kenneth M. Merz, J. *Journal of Natural Products* **2009**, *72*, 709–713.
- (67) Velde, G. te; Bickelhaupt, F. M.; Baerends, E. J.; Guerra, C. F.; Gisbergen, S. J. A. van; Snijders, J. G.; Ziegler, T. *Journal of Computational Chemistry* **2001**, *22*, 931–967.
- (68) Amsterdam Density Functional program. <http://www.scm.com>.
- (69) Gibbs, J. W. *The Collected Works of J. Willard Gibbs*; University Press: New Haven, 1948.
- (70) Hesse, M.; Meier, H.; Zeck, B. *Spektroskopische Methoden in der organischen Chemie*, 7 Auflage; Georg Thieme Verlag, 2005.
- (71) Guerin, F.; McConville, D. H.; Vittal, J. J. *Organometallics* **1995**, *14*, 3154–3156.
- (72) Martin, C. D.; Le, C. M.; Ragona, P. J. *Journal of the American Chemical Society* **2009**, 15126–15127.
- (73) Gibson, V. C.; Redshaw, C.; Solan, G. A. *Chemical Reviews* **2007**, 1745–1776.
- (74) Zhu, D.; Budzelaar, H. M. *Organometallics* **2008**, *27*, 2699–2705.
- (75) Harris, D.; Lappert, M. F. *Journal of the Chemical Society, Chemical Communications* **1974**, *21*, 895–896.
- (76) Hauptmann, S. *Organische Chemie*; VEB Deutscher Verlag für Grundstoffindustrie, 1985; Vol. 2. Auflage.
- (77) Zabula, A. V.; Hahn, F. E.; Pape, T.; Hepp, A. *Organometallics* **2007**, *26*, 1972–1980.
- (78) Zabula, A. V.; Pape, T.; Hepp, A.; Schappacher, F. M.; Rodewald, U. C.; Poeiigen, R.; Hahn, F. E. *Journal American Chemical Society* **2008**, *130*, 5648–5649.
- (79) Jie, S.; Diaconescu, P. L. *Organometallics* **2010**, *29*, 1222–1230.
- (80) Eichler, B. E.; Phillips, B. L.; Power, P. P.; Augustine, M. P. *Inorganic Chemistry* **2000**, *39*, 5450–5453.

- (81) Keith, T. A. AIMAll (Version 11.06.19). www.aim.tkgristmill.com.
- (82) Matta, C. F.; Boyd, R. J. *The Quantum Theory of Atoms in Molecules*; Matta, C. F., Boyd, R. J., Eds.; Wiley-VCH Verlag GmbH and Co. KGaA, Weinheim, 2007.
- (83) BADER, R. *Accounts of Chemical Research* **1985**, *18*, 9–15.
- (84) Firme, C. L.; Antunes, O. A. C.; Esteves, P. M. *Journal of the Brazilian Chemical Society* **2009**, *20*, S1–S6.
- (85) Lappert, M.; Protchenko, A.; Power, P.; Seeber, A. *Metal Amide Chemistry*; John Wiley and Sons, 2009; Vol. 1.
- (86) Desimoni, G.; Faita, G.; Quadrelli, P. *Chemical Reviews* **2003**, *103*, 3119–3154.
- (87) Wright, J. A.; Danopoulos, A. A.; Motherwell, W. B.; Carroll, R. J.; Ellwood, S.; Saßmannshausen, J. *European Journal of Inorganic Chemistry* **2006**, *23*, 4857–4865.
- (88) Parr, R.; Yang, W. *Density-Functional Theory of Atoms and Molecules*; Oxford University Press, 1994.
- (89) Adamo, C.; Barone, V. *Journal of Chemical Physics* **1998**, 664–667.
- (90) Ditchfield, R.; Hehre, W. J.; Pople, J. A. *Journal of Chemical Physics* **1971**, 724–726.
- (91) Jr., T. H. D.; Hay, P. J. in *Modern Theoretical Chemistry*; III, H. F. S., Ed.; Plenum, New York, 1976; Vol. 3.
- (92) Schleyer, R.; Stoll, H.; Preuss, H. *Journal of Chemical Physics* **1991**, 1360–1367.
- (93) Wolinski, K.; Hilton, J. F.; Pulay, P. *Journal of the American Chemical Society* **1990**, 8251–8257.
- (94) Huzinaga, S. *Journal of Chemical Physics* **1965**, 1293–1298.
- (95) Lenthe, E. van; Ehlers, A.; Baerends, E. *Journal of Chemical Physics* **1999**, 8943–8948.
- (96) Lenthe, E. van; Baerends, E.; Snijders, J. *Journal of Chemical Physics* **1993**, 4597–4583.
- (97) Tounen, H. M.; Roesler, R.; Dutton, J. L.; Ragona, P. J. *Inorganic Chemistry* **2007**, 10693–10706.
- (98) Biegler-Koenig, F.; Bader, R.; Tang, T. *Journal of Computational Chemistry* **1982**, 317–328.